INVESTIGATING VENOM SYNTHESIS: EXPLORING THE COMPOSITION, VARIATION AND GENE EXPRESSION DYNAMICS OF *BITIS ARIETANS* VENOM

Thesis submitted in accordance with the requirements of the University of Liverpool for the degree of Doctor of Philosophy

By Rachel Beth Currier

August 2012

ABSTRACT

Snake venom is a critical evolutionary innovation enabling venomous snakes to become successful limbless predators; it is therefore vital that snakes possess a highly efficient venom production system to maintain their predatory arsenal. The dynamics of venom synthesis and the regulatory mechanisms by which the expression of venom protein-encoding genes is controlled are little understood. The overarching aim of the work described in this thesis was to investigate the dynamics of venom synthesis in terms of the production of venom in juvenile snakes from birth and in the immediate replenishment of depleted venom stores using the African Puff Adder (*Bitis arietans*) as a model viperid species. We also aimed to investigate the underlying control mechanisms which regulate venom production

Initial studies revealed a remarkable degree of intra-species variation in the protein profile, immunoreactivity and enzyme activity of venom between *B. arietans* specimens originating from different geographical origins across sub-Saharan Africa and Arabia, and within the same geographical origin. Variation was most evident in the snake venom metalloproteinases (SVMPs); toxins with a primary role in the haemorrhagic and tissue-necrotic pathologies suffered by envenomed victims. Our findings are of therapeutic importance as observations could translate into variations in the clinical manifestation of *B. arietans* envenoming and affect the patient response to antivenom treatment.

To monitor the synthesis of venom proteins, we exploited the unusual stability of messenger RNA in lyophilised snake venoms as an alternative source of transcriptionally active mRNA to venom gland tissues, thus avoiding the requirement to sacrifice specimens for transcriptome analysis. Our optimised approach was used to quantitatively track changes in expression of venom protein-encoding genes. Our results showed that the gene expression, protein composition and functional activity of juvenile *B. arietans* venom did not appear to significantly change over time from birth to four years indicating that some aspects of venom are genetically hard-coded. We also showed that venom resynthesis triggered by venom expulsion peaked between days 3-7 following depletion of venom, with different protein families expressed in parallel. It appeared that venom production in both adult and juvenile specimens occurs very rapidly, presumably to ensure that venomous snakes retain their ability to efficiently predate and remain defended from predators.

Our findings suggest that highly regulated mechanisms may be in place to ensure the rapid synthesis of venom. As it appeared that different venom protein families shared similar expression levels during venom replenishment, we investigated whether venom genes also showed similarities in their genomic location, organisation and structure, and regulatory elements responsible for controlling expression levels. We have taken the first steps to begin to investigate the genomic structure and organisation of genes encoding venom protein families expressed in *B. arietans* venom.

Table of Contents

ABSTRACT .....

ACKNOWLEDGEMENTS I

AUTHOR DECLARATION I

PUBLICATIONS AND PRESENTATIONS ARISNG FROM THIS WORK ... II

ABBREVIATIONS III

LIST OF FIGURES V

LIST OF TABLES IX

1. INTRODUCTION 1

1.1. Taxonomy and global distribution of venomous snakes 1

1.2. Medical importance of snakebite 2

1.3. Origin and evolution of the venom arsenal 5

1.4. The venom delivery apparatus 8

1.4.1. Morphological adaptations of venomous snakes 8

1.4.2. Fang dentition 10

1.4.3. Cellular structure of the venom gland 11

1.4.4. The accessory gland 12

1.5. The venom arsenal: Protein families 13

1.5.1. Snake venom metalloproteinases (SVMPs) 13

1.5.2. Serine proteases 16

1.5.3. Phospholipase A_2s (PLA_2s) 18

1.5.4. L-amino acid oxidases (LAOs) 20

1.5.5. Hyaluronidase 21

1.5.6. Acetylcholinesterase (AChE) 23

1.5.7. Nucleases, nucleotidases and phosphomonoesterases 24

1.5.8. C-type lectins (CTLs) 25

1.5.9. Disintegrins 27

1.5.10. Bradykinin potentiating peptides (BPPs) 29

1.5.11. Inhibitory peptides (QKW tripeptides) 29

1.5.12. Kunitz serine proteinase inhibitors 31

1.5.13. Vascular endothelial growth factors (VEGFs) and nerve growth factor (NGFs) 31

1.5.14. Cysteine rich secretory proteins (CRISPs) 33

1.5.15. Purine and pyrimidine nucleosides 34

1.6. Venom protein synthesis and storage 35

1.7. The venom glandular environment; protecting against self-proteolysis 37

1.8. Analysis of venom composition; venomics and transcriptomics 39

1.9. Variation in venom composition 41

1.10. Aims of this work 43

2. MATERIALS AND METHODS 46

2.1. Venom extraction, preparation and storage 46

PROTEIN ANALYSIS 47

2.2. One dimensional sodium dodecyl sulphate polyacrylamide gel electrophoresis (1D SDS-PAGE) 47

2.2.1. Venom sample preparation for SDS-PAGE 47

2.2.2. SDS-PAGE gel preparation and electrophoresis 47

2.3. Immunoblotting 49

2.4. Substrate zymography 50

2.4.1. Venom sample preparation for substrate zymography 50

2.4.2. Zymogram gel preparation, electrophoresis and activation 51

2.5. Mass spectrometry: 51

2.5.1. In-gel trypsin digestion 51

2.5.2. HPLC – tandem mass spectrometry (HPLC-MS/MS) and protein identification using bioinformatics tools 52

MOLECULAR BIOLOGY 53

2.6. Extraction of Poly(A) mRNA from venom using oligo (dT) magnetic Dynabeads® 53

2.7. First strand complementary DNA (cDNA) synthesis 55

2.8. Plasmid purification of venom gland library cDNA for PCR positive control 56

2.9. Polymerase chain reaction (PCR) 57

2.9.1. PCR primer design 57

2.9.2. Conventional PCR 57

2.9.3. Purification of PCR products 59

2.9.4. Quantitative PCR (qPCR) 60

2.10. Isolation and characterisation of venom-encoding genes by genome walking protocols 61

2.10.1. Genomic DNA isolation 61

2.10.2. Quality assessment of genomic DNA 62

2.10.3. Genomic library construction using GenomeWalker™ Kit 62

2.10.4. Genome walking PCR primer design 64

2.10.5. Long range PCR amplification of genomic DNA and purification of PCR products 65

2.10.6. Sub-cloning and transformation of *E. coli* with purified genomic PCR products 67

2.10.7. Selection and amplification of recombinant *E. coli* colonies 68

2.10.8. Purification and analysis of recombinant plasmids by restriction enzyme digestion 68

2.10.9. Selection and submission of recombinant plasmids for DNA sequencing 69

2.10.10. Bioinformatics interrogation of genomic DNA sequences 69

2.11. Ethical declaration 70

3. INTRA-SPECIFIC VARIATION IN VENOM OF THE AFRICAN PUFF ADDER (*BITIS ARIETANS*); DIFFERENTIAL EXPRESSION AND ACTIVITY OF THE SNAKE VENOM METALLOPROTEINASES (SVMPs) 71

3.1. Abstract 71

3.2. Introduction 72

3.3. Materials and Methods: 75

3.3.1 Venom sample extraction and preparation 75

3.3.2. Venom protein composition profiling by 1D SDS-PAGE 76

3.3.3. Antibody cross-reactivity of venoms by immunoblotting 76

3.3.4. Venom enzyme activity profiling by substrate zymography 77

3.3.5. Identification of venom proteins by LC-MS/MS 77

3.4. Results: 78

3.4.1. Variation in venom composition between *B. arietans* specimens from different geographical origins: 78

3.4.2. Variation in venom between individual *B. arietans* specimens from the same geographical origin (Nigeria): 81

3.4.3. Comparison with variation in venom of Ghanaian *B. arietans* 92

3.4.4. Comparison with variation in venom of *B. arietans* with other species, *Echis ocellatus* and *Cerastes cerastes* 93

3.5. Discussion 97

4. OPTIMSATION OF QUANTITATIVE POLYMERASE CHAIN REACTION (PCR) PROTOCOLS; EXPLOITING VENOM AS A SOURCE OF MESSENGER RNA FOR GENE EXPRESSION ANALYSES 101

4.1. Abstract 101

4.2. Introduction 102

4.3. Materials and Methods: 105

4.3.1. Venom sample preparation 105

4.3.2. Extraction of Poly(A) mRNA from venom using Dynabeads® 105

4.3.3. Reverse transcription cDNA synthesis 106

4.3.4. Design of PCR primer pairs for conventional PCR and quantitative PCR reactions 106

4.3.5. Amplification of venom transcripts by conventional PCR 110

4.3.6. Experimental optimisation of annealing temperature for qPCR amplification 110

4.3.7. Optimising cDNA concentration for qPCR 112

4.3.8. Standard curve analysis to determine the amplification reaction efficiency in qPCR 112

4.3.9. Melt curve analysis to determine the specificity of primer pairs in qPCR 113

4.4. Results: 116

4.4.1. Quantity of mRNA recovered from venom 116

4.4.2. Testing the ability of primer pairs to specifically amplify a range of venom protein targets from venom gland and venom cDNA 117

4.4.3. Assessing DNA contamination of mRNA samples 120

4.4.4. Experimental optimisation of annealing temperature for qPCR amplification 122

4.4.5. Optimising cDNA concentration for qPCR amplification 123

4.4.6. Standard curve analysis to determine amplification reaction efficiency in qPCR 124

4.4.7. Melt curve analysis to determine qPCR primer specificity 129

4.6. Discussion 132

5. INVESTIGATION OF VENOM PRODUCTION IN JUVENILE *BITIS ARIETANS* SPECIMENS; ANALYSIS OF GENE EXPRESSION, PROTEIN

COMPOSITION AND ENZYME ACTIVITY OF VENOM FROM BIRTH TO MATURITY. 135

5.1. Abstract 135

5.2. Introduction 136

5.3. Materials and Methods: 139

5.3.1. Venom sample collection and preparation 139

5.3.2. Extraction of Poly(A) mRNA from venom using Dynabeads® 140

5.3.3. Monitoring gene expression levels using relative quantitative PCR (qPCR): 140

5.3.4. Venom protein composition profiling 1D SDS-PAGE: 142

5.3.5. Identification of venom proteins by LC-MS/MS 142

5.3.6. Venom enzyme activity profiling by substrate zymography: 142

5.4. Results: 142

5.4.1. Juvenile *Bitis arietans* survival, growth and venom yield rate 142

5.4.2. Quantitative PCR (qPCR) toxin expression profiles of juvenile *B. arietans* siblings from birth 145

5.4.3. Venom protein profiles of juvenile *B. arietans* siblings from birth 149

5.4.4. Mass spectrometry identification of proteins of interest from juvenile *B. arietans* samples 151

5.4.5. Enzyme activity of venom samples from juvenile *B. arietans* specimens 161

5.5. Discussion 161

6. UNUSUAL STABILITY OF MESSENGER RNA IN SNAKE VENOM REVEALS GENE EXPRESSION DYNAMICS OF VENOM REPLENISHMENT 166

6.1. Abstract 166

6.2. Introduction 167

6.3. Methods 169

6.3.1. Venom samples and standards: 169

6.3.2. Extraction of Poly(A) mRNA from venom using Dynabeads®: 170

6.3.3. cDNA synthesis: 170

6.3.4. Quantitative PCR (qPCR): 170

6.3.5. One-dimensional SDS-PAGE and gelatin zymography: 171

6.3.6. HPLC separation of venom and mass spectrometry protein identification 172

6.4. Results: 172

6.4.1. Quantity and quality of mRNA recovered from venom: 172

6.4.2. Venom protein expression profiles during venom re-synthesis: 172

6.4.3. Protein profiles and venom activity during venom re-synthesis: 179

6.5. Discussion 184

7. INVESTIGATION OF THE GENETIC ORGANISATION AND MECHANISMS RESPONSIBLE FOR REGULATING THE EXPRESSION OF VENOM PROTEIN-ENCODING GENES 189

7.1. Abstract 189

7.2. Introduction 190

7.3. Materials and methods 193

7.3.1. Isolation, quality control and PCR amplification of venom transcripts from *Bitis arietans* genomic DNA 193

7.3.2. Construction of 'Genome Walker libraries' 195

7.3.3. Genome walking by long-range PCR 195

7.3.4. Primer design 196

7.3.5. Sub-cloning and sequencing 197

7.3.6. Bioinformatics interrogation of sequences for promoter and transcription factors 197

7.4. Results: 198

7.4.1. Isolation and quality control of genomic DNA from *B. arietans* liver tissue 198

7.4.2. Amplification of venom protein targets from *B. arietans* genomic DNA using long-range PCR 199

7.4.3. Sub-cloning and sequencing of PCR products amplified from *B. arietans* genomic DNA 201

7.4.4. Sequence analysis of PCR products amplified from *B. arietans* genomic DNA 202

7.4.5. Amplification of gene targets from 'Genome walker' libraries 207

7.5. Discussion 213

8. GENERAL DISCUSSION 216

9. FUTURE WORK 223

APPENDICES 226

APPENDIX I: Recipes for buffers and stock solutions 226

APPENDIX II: The 'Minimum information for Publication of Quantitative Real-time PCR Experiments' (MIQE) guidelines. 230

APPENDIX III: Optimisation of annealing temperature for amplification by quantitative PCR. 233

APPENDIX IV: Optimisation of starting cDNA quantity for amplification by quantitative PCR. 235

APPENDIX V: Optimisation of quantitative PCR by standard and melt curve analysis. 236

APPENDIX VI: Juvenile *Bitis arietans* specimens 239

APPENDIX VII: Optimisation of relative real-time gene expression analysis with reference to the MIQE guidelines. 244

APPENDIX VIII: Sequence alignments of *Bitis arietans* serine protease and vascular endothelial growth factor gene sequences with homologous genes. 248

APPENDIX IX: Sequences and BLAST analysis of PCR products amplified and cloned from genome walker libraries. 252

REFERENCES 259

ACKNOWLEDGEMENTS

Firstly, I wish to thank my supervisors Dr Simon Wagstaff and Dr Rob Harrison for their consistent support, enthusiasm and encouragement throughout the course of this work. I would also like to thank Paul Rowley for imparting his expert knowledge of venomous snakes and for extracting venom samples used in this project. Without their help and guidance, none of this work would have been possible. I would like to thank students in the Alistair Reid Venom Research Unit, old and new; Darren, Nick, Camila, Maimonah and Fiona, for being great friends and making my time in the lab thoroughly enjoyable. Finally, I would like to thank my friends and family for their endless support and encouragement, and for always believing in me.

AUTHOR DECLARATION

The work presented in this thesis was performed entirely by myself with the exception of the high performance liquid chromatography (HPLC) separation and mass spectrometry identification of venom proteins described in Chapter 6 which was performed by Professor Juan J. Calvete (Laboratorio de Proteinomica Estructual at the Instituto de Biomedicina de Valencia, Valencia, Spain). All venom extractions were performed by Paul Rowley and Dr Robert Harrison in the Alistair Reid Venom Unit in the Liverpool School of Tropical Medicine.

PUBLICATIONS AND PRESENTATIONS ARISNG FROM THIS WORK

1. Currier, R.B., Calvete, J.J., Sanz, L., Harrison, R.A., Rowley, P.D., Wagstaff, S.C. (2012) Unusual stability of messenger RNA in snake venom reveals gene expression dynamics of venom replenishment. PLoS ONE 7(8): e41888. doi:10.1371/journal.pone.0041888.
2. Currier, R.B., Harrison, R.A., Rowley, P.D., Laing, G.D., Wagstaff, S.C. (2010) Intra-specific variation in venom of the African Puff Adder (*Bitis arietans*): Differential expression and activity of snake venom metalloproteinases (SVMPs). Toxicon 55: 864-873.

This work has been presented as oral and poster presentations at The International Society on Toxinology (IST) World Congress (Recife, Brazil) in 2009 and European Congress (Valencia, Spain) in 2011, the University of Bangor Herpetological Society Venom Day in 2010 and 2012 and the British Herpetological Society Annual Symposium in 2011.

ABBREVIATIONS

ADAM	A disintegrin and metalloproteinase
APS	Ammonium persulphate
bp	Base pairs
BLAST	Basic Local Alignment Search Tool
°C	Degrees centigrade
cDNA	Copy deoxyribonucleic acid
CTL	C-type lectin
CLP	CTL-like proteins
DAB	3, 3'-diaminobenzidine
dH_2O	Distilled water
DNA	Deoxyribonucleic acid
DTT	Dithiothreitol
E. coli	*Escherichia coli*
EDTA	Ethylenediaminetetraacetic acid
EST	Expressed sequence tag
HPLC	High performance liquid chromatography
IAN	Iodoacetamide
IPTG	Isopropyl-β-D-thio-galactoside
kb	Kilo base
kDa	Kilo dalton
KTI	Kunitz inhibitors
LAO	L-amino acid oxidase
LB	Luria-bertani
M	Molar concentration
mM	Millimolar concentration

MS	Mass spectrometry
Min	Minutes
MMP	Matrix metalloproteinase
ORF	Open reading frame
PAGE	Polyacrylamide gel electrophoresis
PBS	Phosphate buffered saline
PCR	Polymerase chain reaction
PDI	Protein disulphide isomerase
PLA_2	Phospholipase A_2
PLOB	Protein loading buffer
Poly(A)	Polyadenylated
qPCR	Quantitative PCR
RGD	Arginine-glycine-aspartate sequence
RNA	Ribonucleic acid
rpm	Revolutions per minute
RT-PCR	Reverse transcriptase PCR
SDS	Sodium dodecyl sulphate
SP	Serine protease
SVMP	Snake venom metalloproteinase
TBST	Tris-buffered saline-Tween 20
TEMED	Tetramethylethylenediamine
TGE	Tris-glycine-EDTA
UV	Ultraviolet
V	Voltage
VEGF	Vascular endothelial growth factor
X-gal	5-bromo-4-chloro-3-indolyl-β-galactoside

LIST OF FIGURES

Figure 1.1 Global medical importance of snakebite.

Figure 1.2 Cladogram of evolutionary relationships of the Toxicofera showing the recruitment timing of different protein-scaffold types for use as toxins.

Figure 1.3 The Viper venom delivery system.

Figure 1.4 Fine structure of the viperid venom gland.

Figure 1.5 Fang dentition of venomous snake families.

Figure 1.6 Structural classifications of the snake venom metalloproteinases.

Figure 1.7 Snake venom hyaluronidase sequence analysis.

Figure 1.8 Snake venom disintegrin sequence analysis.

Figure 1.9 Sequence analyses of QKW tripeptides from viper venoms.

Figure 1.10 The VEGF protein family and receptor selectivity.

Figure 1.11 Secretory cycle of the venom gland during venom synthesis.

Figure 2.1 Venom extracted from an adult *Bitis arietans* specimen.

Figure 2.2 Extraction of poly(A) mRNA from venom using Dynabeads®.

Figure 2.3 The GenomeWalker adaptor.

Figure 3.1 Adult *Bitis arietans* coloration and geographical distribution.

Figure 3.2 Analysis of pooled *B. arietans* venom samples from six different geographical origins.

Figure 3.3 Analysis of individual Nigerian *B. arietans* venom samples.

Figure 3.4 Reproducibility of venom protein profile of Nigerian *Bitis arietans* specimens.

Figure 3.5 Full and partial-length peptide sequences identified by LC-MS/MS from adult *Bitis arietans* specimens.

Figure 3.6 Analysis of individual Ghanaian *Bitis arietans* venom samples.

Figure 3.7 Analysis of other African viper venoms, Nigerian *E. ocellatus* (A) and Egyptian *C. cerastes* (B).

Figure 3.8 Immunoreactivity of *Bitis arietans* venoms to polyspecific antivenom.

Figure 3.9 Analysis of low molecular weight protein components of *Bitis arietans* venom.

Figure 4.1 qPCR plate and thermocycling for optimisation of annealing temperature.

Figure 4.2 qPCR plate and thermocycling for standard and melt curve validation.

Figure 4.3 Identifying the optimal venom quantity for mRNA and cDNA yield.

Figure 4.4 Amplification of venom targets from venom vs. venom gland cDNA.

Figure 4.5 Amplification of venom targets from different quantities of venom.

Figure 4.6 Assessing DNA contamination of mRNA samples using reverse transcriptase negative controls (conventional PCR primers).

Figure 4.7 Assessing DNA contamination of mRNA samples using reverse transcriptase negative controls and DNase treatment (qPCR primers).

Figure 4.8 Optimisation of annealing temperature for amplification by quantitative PCR.

Figure 4.9 Optimisation of initial cDNA concentration for amplification by quantitative PCR.

Figure 4.10 Standard curves generated by qPCR using purified PCR products as a standard cDNA sample.

Figure 4.11 Standard curves generated by qPCR using purified PCR products as a standard cDNA sample.

Figure 4.12 Melt curves generated by qPCR following amplification using purified PCR products as a standard cDNA sample.

Figure 4.13 Melt curves generated by qPCR following amplification using mature venom cDNA as a standard cDNA sample.

Figure 5.1 *Bitis arietans* juvenile specimen.

Figure 5.2 Juvenile *Bitis arietans* growth rate and venom production.

Figure 5.3 Juvenile *Bitis arietans* toxin gene expression profiles during venom production.

Figure 5.4 Juvenile *Bitis arietans* venom protein profile.

Figure 5.5 Mass spectrometry identification of protein bands from juvenile *Bitis arietans* venom.

Figure 5.6 Full and partial-length peptide sequences identified by LC-MS/MS from juvenile *Bitis arietans* specimens.

Figure 5.7 Juvenile *Bitis arietans* venom enzyme activity profiles.

Figure 6.1 Venom gene expression profiles during venom replenishment.

Figure 6.2 Reproducibility of venom gene expression profiles.

Figure 6.3 Average gene expression profiles of all *Bitis arietans* specimens.

Figure 6.4 HPLC-MS/MS protein profiling of Ghanaian and Nigerian *Bitis arietans* venoms.

Figure 6.5 Protein profiling of individual venom samples by HPLC and 1D SDS-PAGE.

Figure 6.6 Venom enzyme activity profiles during venom replenishment.

Figure 6.7 Stability of venom mRNA during long-term storage of lyophilised venom.

Figure 7.1 Genome walking protocol

Figure 7.2 Identification of DNA upstream of transcription start site by genome walking.

Figure 7.3 Analysis of genomic DNA extracted from *Bitis arietans* liver tissue.

Figure 7.4 PCR amplification of venom targets from *Bitis arietans* genomic DNA.

Figure 7.5 Analysis of venom target inserts following sub-cloning.

Figure 7.6 Genomic DNA sequences encoding *Bitis arietans* venom proteins.

Figure 7.7 Gene structures of venom protein-encoding genes.

Figure 7.8 Primary PCR amplification of targets from Genome Walker libraries.

Figure 7.9 Secondary PCR amplification of targets from Genome Walker libraries.

LIST OF TABLES

Table 2.1 Rapid silver staining protocol for staining SDS-PAGE protein gels.

Table 3.1 LC-MS/MS identification of venom proteins.

Table 4.1 Conventional PCR primer sequences.

Table 4.2 Quantitative PCR primer sequences.

Table 4.3 Quantitative PCR reaction efficiencies.

Table 5.1 Relative qPCR gene expression levels during venom production in juvenile *Bitis arietans* specimens.

Table 5.2 Statistical analysis of gene expression data from juvenile *Bitis arietans* venom samples.

Table 5.3 LC-MS/MS identification of venom proteins from juvenile *Bitis arietans* venom samples.

Table 6.1 Relative qPCR gene expression levels during venom replenishment individual adult *Bitis arietans* venom samples.

Table 6.3 Statistical significance of relative changes in gene expression during venom replenishment.

Table 7.1 PCR primer sequences for genome walking protocol.

Table 7.2 Identification of PCR products amplified from genome walker libraries.

1. INTRODUCTION

This PhD project aimed to explore and understand how the toxic array of proteins in snake venom are synthesised and regulated by the venom production system of venomous snakes. It is clearly important that this work is viewed in the context of our current knowledge of snakes and the biology of their venoms. The purpose of this introduction is to outline the taxonomy, medical importance, distribution/diversity of venomous snakes, evolution of the venom toxic arsenal, venom gland delivery system, structure/function of venom proteins, venom synthesis, the venom glandular microenvironment, the approaches used to analyse venom composition, reports of variation in venom composition and the aims of this work.

1.1. Taxonomy and global distribution of venomous snakes

The Serpentes (Ophidia) comprises approximately 2,800 snake species, categorised into three superfamilies and 16-20 families (O'Shea, 2005). All venomous snakes (advanced snakes) belong to the Colubroidea (or Caenophidia) superfamily. The Colubroidea has been traditionally subdivided into four families; Colubridae, Atractaspididae, Elapidae and Viperidae. The Colubridae are the largest and diverse family containing around 1,700 species distributed worldwide and the classification of this group is subsequently undergoing continual evaluation. The colubrids do not naturally form a monophyletic group, as many species are more closely related to other groups, such as elapids, than to each other (Lawson et al., 2005). While many are considered non-venomous, some colubrids such as the African Boomslang (*Dispholidus typus*) which produces hemotoxic venom, are medically important to

humans. The Atractaspididae contain around 30 species which are distributed across Africa and Arabia. Although venomous, atractaspidids (e.g. burrowing asps) are not associated with causing a significant number of human fatalities primarily due to their small size. The Elapidae consists of around 351 species which are widely distributed across the Americas, Africa, the Middle East, Asia and Australasia. There are two recognized sub-families; the Elapinae (coral snakes, cobras, mambas and kraits) and the Hydrophiinae (sea snakes). The elapids are front-fanged snakes, most of which produce highly potent neurotoxic venom, and are of significant medical importance to humans. The Viperidae contains around 311 species and have a worldwide distribution (except Australasia), occupying a range of terrestrial habitats across the Americas, Africa, Europe and Asia. The Viperidae contains two main sub-families; the Viperinae (pit-less vipers e.g. *Bitis*, *Cerastes*, *Echis* and *Vipera* genera) and the Crotalinae (pitvipers e.g. *Agkistrodon*, *Bothrops* and *Crotalus* genera). Viperids are also front-fanged snakes capable of producing highly potent hemotoxic venom and are responsible for a significant number or human fatalities worldwide (O'Shea, 2005).

1.2. Medical importance of snakebite

Envenoming following snakebite is largely a neglected threat to public health, yet causes considerable morbidity and mortality throughout the world. There are up to 1.8 million incidences of snakebite worldwide per year leading to up to 94,000 deaths, the majority of which occur in sub-Saharan Africa, South and Southeast Asia and Latin America (Kasturiratne et al., 2008). In Africa, a recent meta-analytical survey indicated that 95% of snakebites and 97% of deaths caused by snakebite

occurred in rural environments (Chippaux, 2011). Those most at risk of death/morbidity from snakebite are subsistence farmers, agricultural workers and children, where the threat of snakebite is a daily occupational hazard and access to health services is poor. In addition to the risk of mortality, many victims of snakebite are also left with permanent disabilities and sequelae due to severe tissue necrosis. The morbidity of snakebite in Africa is reflected in the high incidence of amputations of the affected limb (5,900-14,600 per year) (Chippaux, 2011) demonstrating that snakebite may also have a considerable economic impact. A strong correlation between snakebite-induced mortality and poverty has been demonstrated through mapping the global distribution of snakebite with economic factors such as gross domestic product (GDP) and per capita government expenditure on health, illustrating that snakebite is a significant health issue of the rural poor (Figure 1.1) (Harrison et al., 2009).

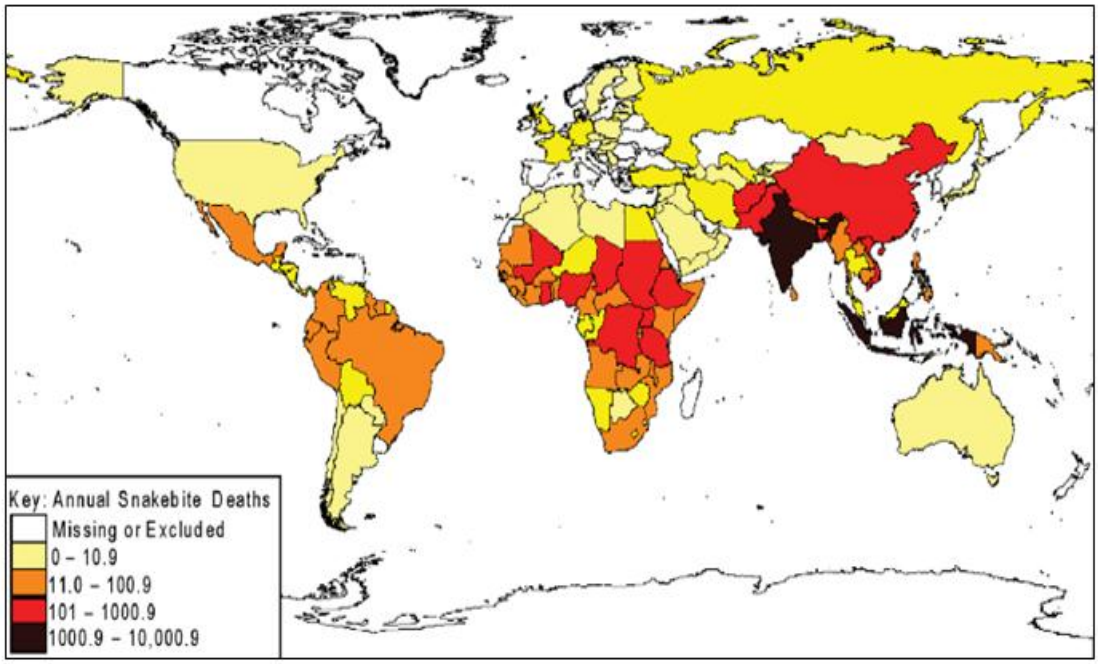

Figure 1.1 Global medical importance of snakebite: The global distribution of the annual estimates of snakebite-induced deaths. Darker colours denote the highest numbers of snakebite mortality (Kasturiratne et al., 2008).

Antivenom is the only effective treatment for snakebite. Antivenoms are produced by immunising animals (most commonly horses) with either a single venom to produce monospecific antivenoms, or a mixture of venoms to produce polyspecific antivenoms, with increasing doses over several months. The venom-neutralising antibodies (IgG) produced by the immunised animal are collected and purified, resulting in antivenom (Lalloo and Theakston, 2003). Although effective, safe and affordable antivenoms are available, the lack of a coordinated and constructive strategy for the delivery of antivenoms in the developing world has resulted in a global antivenom crisis (Williams et al., 2011). The Global Snakebite initiative is a worldwide, rational approach developed by toxinologists which aims to reduce the incidence of death and morbidity due to snakebite through a combination of community education, surveillance of snakebite, clinical research, medical management, rehabilitation and implementation of government health policies (Williams et al., 2010). In current research, there are several strategies which aim to improve the efficiency and specificity of antivenom treatment and to address the safety issues with some current antivenoms by improving the dose, purity and geographic/species efficacy of antivenom (Harrison et al., 2011). One strategy includes the use of IgGs from alternative venom-immunised animals (e.g. camelids). Camelid IgGs are less immunogenic and therefore lower the risk of activating complement, thus reducing the incidence of adverse effects and improving the safety of antivenom treatment (Herrera et al., 2005). Current research has provided encouraging support for the potential use of camelid IgG in antivenom production (Cook et al., 2010a, Cook et al., 2010b, Cook et al., 2010c). Another strategy involves the research into the design of toxin-specific epitopes, directed to target only venom components causing the most severe venom-induced pathologies and

thus improving the dose-efficacy of antivenom is also providing promising results (Wagstaff et al., 2006). In combination, these approaches aim to significantly improve the treatment and management of snakebite worldwide.

1.3. Origin and evolution of the venom arsenal

Venom delivery systems have evolved independently several times throughout nature, including in the Cnidaria (jellyfish and anemones) (Bloom et al., 1998), Gastropoda (cone snails) (Olivera et al., 2002), Hymenoptera (bees and wasps), Arachnida (spiders and scorpions) (Escoubas et al., 2006), Chordata (fish), Reptilia (snakes and lizards) (Fry et al., 2006) and Mammalia (platypus) (Whittington et al., 2009). Arguably, one of the most sophisticated, diverse and efficient venom systems exist among the venomous snakes.

The Colubroidea encompass around 80% of the ~2,900 species of snakes (Vidal et al., 2007). The Colubroids form a clade with the closely related Iguania and Anguimorphs, known collectively as the Toxicofera. Members of this group share a number of basal protein families that were recruited into the venom delivery system prior to the divergence of these lineages (Fry et al., 2009). Although evidence supports the presence of venom as a basal evolutionary characteristic in the Serpentes (Fry et al., 2006), it is currently thought that only ~450 venomous species of medical importance exist, which are found exclusively within the Colubroidea, thus, venomous dependency appears to have been lost over time. The families of venomous snakes which are the most medically important to humans are the Viperidae, Elapidae and to a lesser extent, the Atractaspididae, each of which represent an independent, monophyletic lineage within the Colubroidea.

Snake venom has evolved into a highly complex mixture of several hundred unique constituents including enzymatic and non-enzymatic proteins and peptides, carbohydrates, lipids, metal ions and organic compounds (Aird, 2002).While the composition and toxicity of venoms can vary widely between snake taxa, the primary evolutionary function of venom is to ensure the rapid and efficient immobilisation and killing of a diverse range of prey species (Kordiš et al., 2002). Venoms may also serve in a defensive role as a deterrent to predators/aggressors.

Venom toxins have been recruited into the venom arsenal from normal, non-toxic physiological proteins by adaptive evolution (Fry, 2005). The rapid explosion of multiple gene duplication and diversification, selective expression in the venom gland and subsequent structural and functional divergence from non-toxin homologues has resulted in the formation of multi-isoform, multi-domain protein families in snake venoms (Fry, 2005, Fry et al., 2009). The first protein families recruited into a venomous role prior to the divergence of the Colubroidea include the cysteine-rich secretory proteins, hyaluronidase, kallikrein enzymes and nerve growth factor (Figure 1.2). Newly recruited toxin groups have evolved to form large, multi-gene families via the 'birth-and-death' model (Fry et al., 2003). This involves the creation of gene families as a result of repeated gene duplication events and rapid structural and functional diversifications of genes to form evolutionarily related but functionally distinct genes; a key process in the process of adaptive evolution. Where some genes are retained in the genome, over time, other genes are subsequently deleted from the genome or become non-functional giving rise to pseudogenes (Nei et al., 1997).

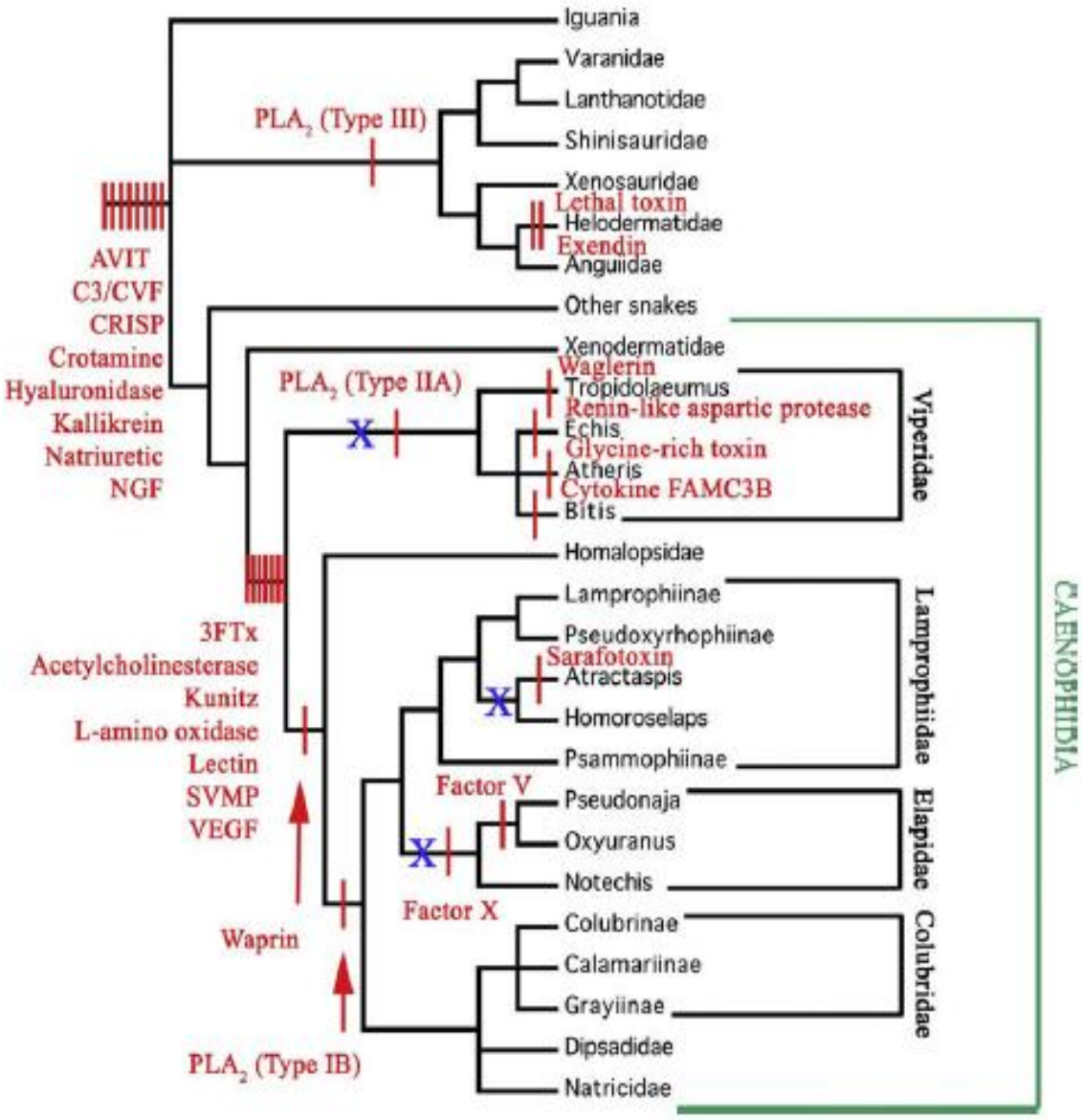

Figure 1.2 Cladogram of evolutionary relationships of the Toxicofera showing the recruitment timing of different protein-scaffold types for use as toxins: Blue X shows independent evolution of hollow front-fanged, high-pressure venom delivery systems and red lines indicate a toxin recruitment event. 3FTX = three finger toxin, C3/CVF=ComplementC3/Cobra Venom Factor, CRISP=Cysteine-rich secretory protein, NGF=Nerve Growth Factor, SVMP = snake venom metalloproteinase, VEGF = vascular endothelial growth factor (Fry et al., 2009).

Snake venom toxins are continually subjected to adaptive evolutionary pressures, resulting in the rapid evolutionary explosion of very diverse venoms. The distinct

substrate specificities and consequent diverse pathologies of venoms generate great interest in both biological and therapeutic research.

1.4. The venom delivery apparatus

1.4.1. Morphological adaptations of venomous snakes

The highly complex and functionally diverse mixture of proteins present in venom is synthesised by venom glands which are modified parotid glands with an elongated and specialised structure. Front-fanged venomous snakes (viperids, elapids and atractaspidids) possess a large post-orbital venom-producing apparatus lying along the upper jaw, whereas the venom glands of venomous lizards run along the lower jaw and glands along the upper jaw have been apparently lost. The venom delivery system of venomous snakes comprises of the specialised secretory glands, a toxic venom arsenal, compressor muscles, fangs and a predatory behaviour (Kardong, 1980, Kochva, 1987, Jackson, 2003) (Figure 1.3).

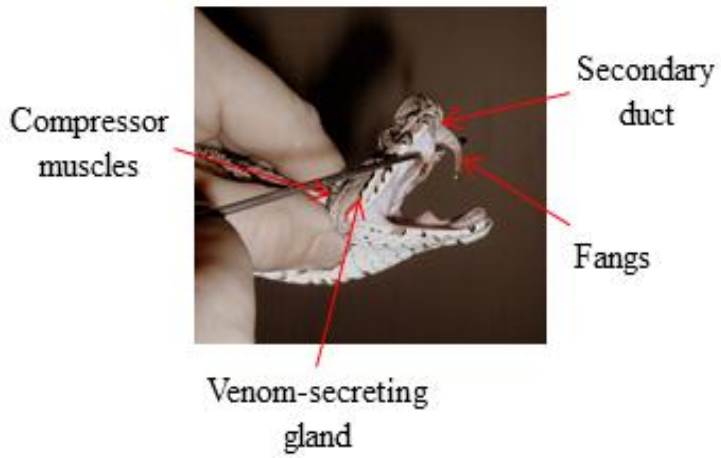

Figure 1.3 The viper venom delivery system.

In front-fanged venomous snakes, the venom gland apparatus is a highly pressurized, closed system which employs extremely efficient mechanisms to result in the rapid expulsion and injection of venom into the envenomed prey tissues. The venom gland structure consists of four discrete regions; the main glandular lumen, the accessory gland, the primary duct and the secondary duct. Venom is synthesised and stored in the main glandular lumen. During expulsion, venom is transported, via the ducts, from the lumen to the tubular fangs which inject venom into the envenomed prey. However, the structural features of glands can vary between different families of snakes (Kardong, 1980, Kochva, 1987, Weinstein et al., 2010). The Viperidae family possess the most morphologically specialised and efficient venom delivery systems of all venomous snakes. Figure 1.4 shows the detailed structure of the viperid venom glands. Viperid venom glands have a complex tubular structure with a highly folded glandular secretory epithelium divided into several ductules enabling maximal venom synthesis and storage (Jackson, 2003). Viper venom glands also have capacious glandular lumen enabling storage of significant volumes of venom resulting in the accumulation of potentially large quantities of venom that can be injected into the victim following snakebite. The glandular lumen is connected, via the primary duct, to the accessory gland, a separate region of the apparatus which may contribute to venom composition. The secondary duct connects the accessory gland to the fangs which inject the venom. Venom glands of elapid snakes share similarities to those of viperids but have a more simplified structure with a smaller lumen consisting of branching tubules converging into the accessory gland and primary/secondary ducts. The venom glands of atractaspidid snakes differ from those of both vipers and elapids in that their glands have an elongated, cylindrical structure

with characteristic unbranched tubules and do not possess a distinct, discrete accessory gland (Kochva, 1987).

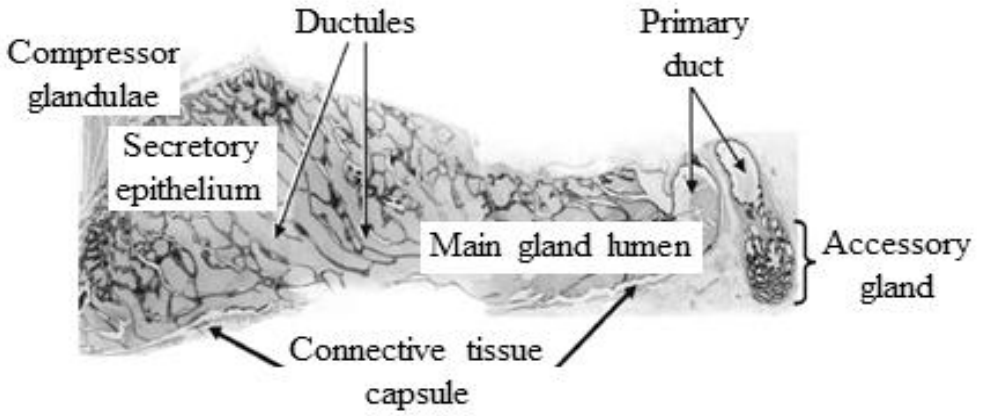

Figure 1.4 Fine structure of the viperid venom gland: Venom glandular structure showing compartmental sections and features of the glands including the secretory epithelium, main lumen, ducts and accessory gland. Figure adapted from Mackessey and Baxter (Mackessy and Baxter, 2006).

1.4.2. Fang dentition

The dentition of fangs/teeth in non-venomous and venomous snakes varies greatly between different families of snakes (Jackson, 2002, Jackson, 2003, Jackson, 2007). Aglyphous snakes, such as pythons, are mostly non-venomous and have teeth lacking any specialisation (e.g. grooves). Opisthoglyphous snakes (Colubridae) are rear-fanged snakes possessing rear-grooved elongate fangs at the back of the mouth. Most opisthoglyphous snakes are considered non-venomous or weakly venomous and therefore harmless to humans due to their inefficient venom delivery systems, with exceptions including the Boomslang (*Dispholidus typus*) which are capable of delivering haemotoxic venom following snakebite. Proteroglyphous snakes (Elapidae) are front-fanged snakes possessing deeply grooved fangs forming a

channel through which venom is directed. Proteroglyphous fangs are relatively short, and therefore elapids are required to maintain contact with their prey during injection of venom. Solenoglyphous snakes (Viperidae) are front-fanged snakes with hollow, tubular hyperextendable fangs resembling hypodermic needles. Solenoglyphs possess the most efficient venom delivery systems as the fangs are connected to a moveable maxillary bone allowing for maximal fang length. Their incredibly long fangs are indicative of the manner by which they predate, typically adopting a 'strike and release' behaviour whereby large quantities of venom can be injected deep into the prey tissues to exert rapid pharmacological effects. Figure 1.5 shows variation in fang dentition between the most clinically important families of venomous snakes, the viperids and elapids, in comparison to the predominantly non-venomous family, the colubrids, of lesser medical importance.

Figure 1.5 Fang dentition of venomous snake families: Variation in fang dentition of the most medically important front-fanged venomous snakes A) Viperidae and B) Elapidae in comparison to the rear-fanged Colubridae (C). (Photographs courtesy of Juan M. Renjifo).

1.4.3. Cellular structure of the venom gland

Venom glands comprise of a highly folded secretory epithelium consisting of several distinct cell types including secretory, mitochondria-rich, horizontal and 'dark' cells

(Oron and Bdolah, 1978, Mackessy, 1991, Mackessy and Baxter, 2006). An abundance of glandular secretory cells (79% of the proportion of cells in the epithelium) are required to synthesise and secrete venom proteins and other components including physiological proteins, mucus and saliva into the glandular lumen. In lower abundance (10%) are horizontal cells, interdigitating between the basement membrane and base of the secretory cells, which function to phagocytose cellular debris and replace dead secretory cells. 'Dark' cells (9%) possess long dendritic processes which interdigitate between secretory cells and may play a role in cellular communication between cells. Mitochondria-rich cells (2%), which are densely packed with mitochondria, are thought to sustain the high energetic costs of venom production by the venom gland (Mackessy, 1991). The venom gland epithelium is basally supported by a connective tissue capsule through which pass a network of capillaries and nerves processes. The venom gland is surrounded by compressor muscle tissue which contracts during venom extraction in order to expel the venom glandular contents in a highly pressurized system.

1.4.4. The accessory gland

Currently, very little is known about the characteristics and function of the accessory glands in the venom delivery system. In viperids, the accessory glands are separate from but connected to the main gland via the primary duct. In contrast, in elapids, the accessory gland surrounds the duct. There is currently little understanding of the input of accessory gland secretions to the main venom bolus. Although there have been no significant biochemical or toxic contribution detected, it is thought that accessory gland secretions may play a role in activating latent venom enzymes

expelled from the main gland before release into the secondary duct and fang to be injected into prey tissue during envenomation (Mackessy and Baxter, 2006), but this is yet to be confirmed by experimental data.

1.5. The venom arsenal: Protein families

Snake venom proteins have been extensively studied and characterised. Studies have shown significant structural and functional diversity among proteins, but the majority of toxin isoforms belong to a few key protein groups. A description of the structure, biological function and pathological role of the key components of snake venoms (categorised as enzymatic or non-enzymatic) are outlined as follows:

Enzymatic components:

1.5.1. Snake venom metalloproteinases (SVMPs)

Zinc-dependent metalloproteinases in snake venom are members of the M12 reprolysin subfamily of metalloproteinases, which also contains the ADAMs (a disintegrin and metalloproteinase) group of proteins which share some structural features such as the homologous metalloproteinase domain (Takeda et al., 2012). The snake venom metalloproteinases (SVMPs) are a group of enzymes which demonstrate relatively broad proteolytic specificity and have been the focus of much research due to their association with severe pathologies including local and systemic haemorrhage (Gutiérrez et al., 2005b). The structure and function of the SVMPs shows a significant level of diversity resulting in a complex, multi-isoform family. The SVMPs can be sub-divided into four classes based on their domain structure and

function, ranging from PI class to the more complex and multi domain-containing PIV SVMPs shown in Figure 1.6 (Fox and Serrano, 2008). The domain structure of SVMPs is described in detail by Fox and Serrano (Fox and Serrano, 2008).

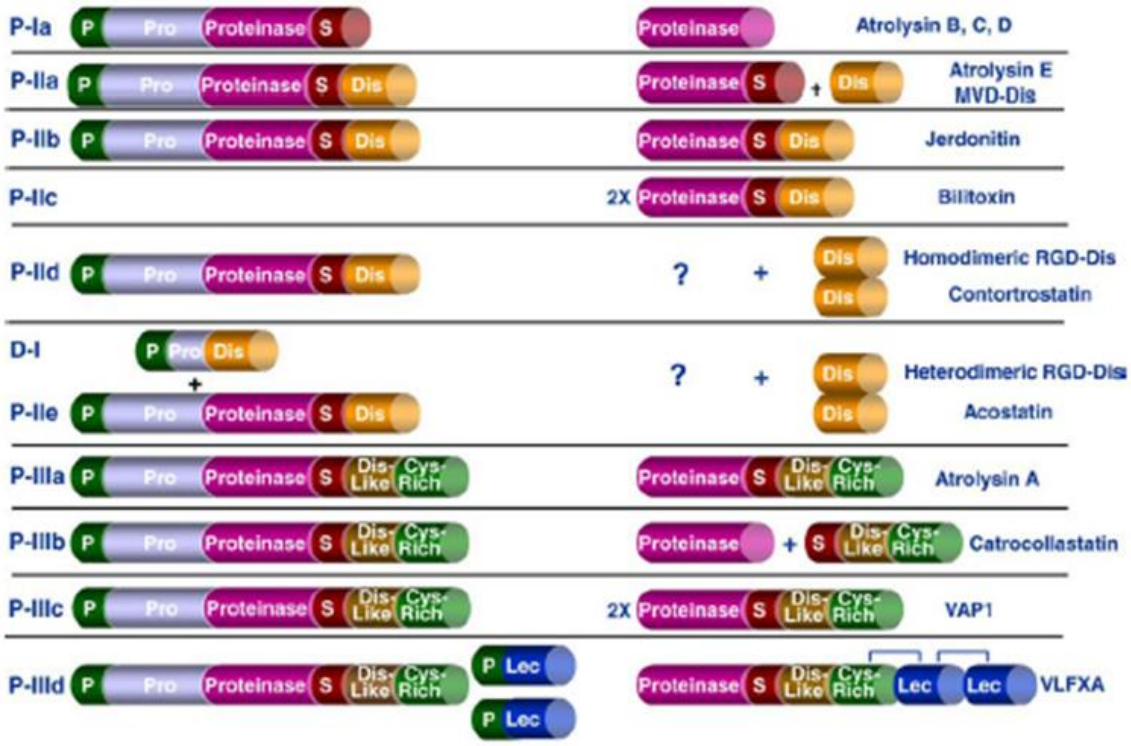

Figure 1.6 Structural classifications of the snake venom metalloproteinases: Schematic diagram to show the domain structure of each class of SVMPs ranging from PI to PIIID/PIV with examples of SVMPs purified from snake venoms (right). Figure taken from Fox and Serrano (Fox and Serrano, 2008). P = signal peptide, Pro = prodomain, S = spacer domain.

The PI class SVMPs represent the structurally simplest form and consist only of the propeptide and metalloproteinase domains in the nascent form. In the mature enzyme, the propeptide is proteolytically processed. All SVMPs share the highly conserved metalloproteinase domain characterized by a canonical zinc-binding motif (HEX box). The PII class SVMPs contain an additional disintegrin domain. There are five sub-classifications of PII SVMPs. Firstly, the PIIa class in which the

disintegrin domain (usually characterised by the presence of an RGD motif) is proteolytically cleaved from the metalloproteinase domain, giving rise to a 'free' disintegrin. In the PIIb class, the disintegrin domain is also proteolytically processed but remains part of the enzyme structure. The PIIc SVMPs represent a dimeric form of the PIIb class. The PIId and PIIe classes are precursor enzyme forms which give rise to homodimeric and heterodimeric RGD-containing disintegrins.

The sub-classifications of PIII SVMPs all contain additional disintegrin-like and cysteine-rich domains in their nascent form (Fox and Serrano, 2005, Fox and Serrano, 2008). The disintegrin domain here shares some sequence homology to the disintegrin domains of PII SVMPs but is said to be structurally distinct due to differences in the sequence homology of the RGD integrin-binding site. In the PIIIa subclass, the disintegrin-like and cysteine-rich domains are not proteolytically processed from the metalloproteinase domain, whereas in the PIIIb subclass, proteolytic processing occurs. The PIIIc subclass represents a dimeric form of the PIIIa. The PIV (recently classified as PIIId) SVMPs contain, in addition to the domains described for PIII SVMPs, disulphide-bonded CTL-like domains (Fox and Serrano, 2005, Fox and Serrano, 2008).

SVMPs have been shown to exhibit a diverse array of biological activities. The proteolytic activities of the SVMPs are largely associated with the metalloproteinase domain and characteristically include haemorrhage, apoptosis, myonecrosis, proteolysis, fibrinolysis, inhibition of platelet aggregation and activation of coagulation factors such as prothrombin, extensive tissue necrosis, oedema and inflammation (Baramova et al., 1989, Gutiérrez and Rucavado, 2000, Gutiérrez et al., 2005b, Kamiguti et al., 1996). This is due to the wide range of cellular targets of SVMPs including extracellular matrix proteins, connective tissue, platelets and

coagulation factors (Escalante et al., 2006, Franceschi et al., 2000, Rucavado et al., 1998). The non-proteolytic activities of the SVMPs are mostly associated with the disintegrin and cysteine-rich domains contained in the PII and PIII classes.

SVMPs are one of the most abundant enzyme families in viper venoms. Recent transcriptomic and proteomic investigations have estimated that the SVMP composition of most viperid venoms is at least 32%, (Bazaa et al., 2005, Juárez et al., 2006, Sanz et al., 2008), with the most SVMP-rich venom identified from the saw-scaled viper, *Echis ocellatus* of which SVMPs account for approximately 67% of the total protein composition (Wagstaff et al., 2009), whereas SVMPs constitute very little of the composition of elapid venoms (Li et al., 2004a, Nawarak et al., 2003). The high proportion of SVMPs in venoms, and their broad range of highly destructive toxic properties, gives an indication of the functional and pathological importance of this group of enzymes during viper envenomation.

1.5.2. Serine proteases

Snake venom serine proteases (SPs) are a group of enzymes present in snake venoms which affect reactions involved in the blood coagulation cascade. SPs can be categorised into thrombin-like or kallikrein-like proteases. The thrombin-like subgroup contains enzymes functionally related to thrombin, defined by their ability to cleave fibrinogen, releasing fibrinopeptides following cleavage the Arg-Lys bonds on the α- and β-chains of fibrinogen, and subsequently converting fibrinogen to fibrin (Pirkle, 1998). Many thrombin-like SPs in venoms mimic other catalytic properties of thrombin such as activating several components of the blood

coagulation cascade involved in platelet aggregation (e.g. factor V) (Siigur et al., 1999).

Kallikrein-like SPs in snake venoms are similar to the mammalian kallikrein enzymes which initiate the release of bradykinin through the proteolytic cleavage of kininogen (Matsui et al., 2000). Bradykinin is a potent vasodilator which increases vascular permeability, resulting in hypotensive symptoms in victims following envenomation with venom containing kallikrein-like SPs (Warrell, 2010). Some SPs in venom show both kallikrein-like and thrombin-like protease activities such as the SPs halytase isolated from *Agkistrodon halys blomhoffii* (Matsui et al., 1998). Halytase showed sequence homology to thrombin-like snake venom SPs (66-72%), mammalian tissue kallikrein enzymes (42%) and thrombin (26%) and was shown to specifically cleave both fibrinogen and kininogen, although this enzyme appeared to be devoid of coagulant activity (Matsui et al., 1998). Other enzymes such as crotalase, also show both kinin-releasing and coagulant activities (Markland, 1976).

In addition to the SVMPs, SPs are also highly pathologically important in viper envenoming. The abundance of SPs in viper venom ranges from 2 to 31% of the total protein composition of venom (Gutiérrez et al., 2009). Although SPs in snake venom exert a wide range of biological activities affecting the coagulation cascade and haemostatic system, individual SPs usually catalyse a specific reaction in the coagulation cascade with macromolecular specificity to their protein target (Markland, 1998).

1.5.3. Phospholipase A_2s (PLA_2s)

Phospholipase A_2s (PLA_2s) are esterolytic enzymes and are occur abundantly in nature. Snake venoms are also a rich source of PLA_2s. The primary action of these enzymes is in the hydrolysis glycerophospholipids at the *sn*-2 position of the glycerol backbone. Snake venom PLA_2s can be classified into two groups based on amino acid sequence, three-dimensional structure and disulphide bond patterns. Group I PLA_2s are found in the mammalian pancreas and in the venoms of elapid and colubrid snakes. Group I PLA_2s are typically 115-120 amino acid residues in length with 7 disulphide bridges. Elapid venom PLA_2s contain a characteristic loop that connects the catalytic α-helix and the β-wing known as the elapid loop, whereas mammalian PLA_2s contain an additional extension of 5 amino acids, called the pancreatic loop. Group II PLA_2s enzymes are present in viper venoms and typically contain 120-125 amino acid residues with 7 disulphide bridges. This group lack the pancreatic or elapid loop which is characteristic of group I PLA_2s, but contain an additional C-terminal extension. Group II PLA_2s can be further divided into groups based on the amino acid residue at the 49^{th} position. Those with an aspartic acid residue are known as D49 enzymes; aspartic acid plays an important role in catalysis and is therefore conserved in most group II PLA_2s (Scott et al., 1990). Amino acid substitutions at the 49^{th} position can occur; where the amino acid residue is replaced by lysine, serine, asparagine or arginine, enzymes are identified as K49 (Maraganore et al., 1984), S49 (Polgár et al., 1996), N49 (Tsai et al., 2004) or R49 (Chijiwa et al., 2006). Enzymes in which the aspartic acid residue has been substituted show low or no hydrolytic activity as substitution interrupts the binding of cofactor Ca^{2+} to the Ca^{2+} binding loop (Maraganore and Heinrikson, 1985). Neurotoxic PLA_2s produced

by elapids predominantly responsible for the cause of death by paralysis of prey and are therefore vital for the envenomation strategy of this family of venomous snakes.

Snake venom PLA_2s show remarkable functional diversity and can exert a wide variety of pharmacological effects including pre- and post-synaptic neurotoxicity, myotoxicity, cardiotoxicity, coagulopathy, hypotension, haemolysis and proinflammatory, in addition to the potential role they play in digestion of prey (Kini, 2003, Kini, 2006, Montecucco et al., 2008). Some PLA_2s exhibit pre- or post-synaptic neurotoxicity. These enzymes belong to the group I PLA_2s and are abundant components of elapid venoms. Pre-synaptic PLA_2s disrupt neurotransmitter release at the neuromuscular junction, the effects of which are irreversible. Pre-synaptic neurotoxins have been shown to specifically target voltage-sensitive K^+ channels (e.g. β-bungarotoxin (Black et al., 1988)), brain synaptic membrane proteins (e.g. ammodytin (Križaj et al., 1995)) and neuronal Ca^{2+} binding proteins (e.g. taipoxin (Kirkpatrick et al., 2000)). Post-synaptic neurotoxins extracellularly target the neuromuscular junction by competitively blocking acetylcholine receptors, the effects of which can be reversed by antivenom treatment.

Viper venoms primarily contain group II PLA_2s. Some group II PLA_2s such as crotoxin and notexin have myotoxic properties and can induce myonecrosis or system myotoxicity (Gopalakrishnakone et al., 1984, Mebs and Ownby, 1990). Others have been demonstrated to evoke inflammatory events such the PLA_2 isolated from *Naja naja atra* venom which promotes inflammatory cell infiltration (Zhang and Gopalakrishnakone, 1999) and Asp49 and Lys49 PLA_2s from *Bothrops asper* venom which stimulate the phagocytic activity of macrophages (Zuliani et al., 2005).

1.5.4. L-amino acid oxidases (LAOs)

L-amino acid oxidases (LAOs) are homodimeric flavoenzymes which catalyse the oxidative deamination of L-amino acids to form α-ketoacids, in addition to the production of ammonia and hydrogen peroxidase. LAOs occur frequently in nature and are present in the venom of most snakes, occurring most abundantly in the venom of Crotaline snakes. The proportion of LAO in venoms as a percentage of the total weight of dried venoms ranges from 1-4% up to 30% in venom from the Malayan pitviper, *Calloselasma rhodostoma* (Ponnudurai et al., 1994). The venoms from mambas and sea kraits contain trace amounts of LAO and colubrid venoms also appear to be devoid of LAO activity (Mackessy, 2002).

Several LAOs have been shown to affect platelet aggregation. LAOs purified from the venoms of *Naja naja kaouthia* (Tan and Swaminathan, 1992) and *Agkistrodon halys blomhoffii* (Takatsuka et al., 2001) demonstrated platelet aggregating inhibiting properties, whereas LAOs from the venoms of *Ophiophagus hannah* (Ahn et al., 1997) and *Eristocophis macmahoni* (Ali et al., 2000) cause an induction of platelet aggregation. Other LAOs show additional effects including haemolysis and oedema-induction (e.g. *Trimeresurus flavoviridis* (Abe et al., 1998) and *E. macmahoni* venom LAOs (Ali et al., 2000)). Other venom LAOs have been reported to demonstrate cytotoxic effects (e.g. *O. hannah* (Ahn et al., 1997)) or antibacterial properties (Stiles et al., 1991, Stábeli et al., 2004, Izidoro et al., 2006). LAOs from snake venoms have been reported to show moderate lethal toxicity and are therefore not thought to be a major pathological component of snake venom (Tan and Saifuddin, 1989).

1.5.5. Hyaluronidase

Hyaluronidase is an enzyme which specifically degrades hyaluronan, a ubiquitous component of the extracellular matrix which is essential in maintaining the structure and viscosity of the extracellular matrix. Hyaluronan has also been implicated in many biological processes such as wound healing and inflammation (Kreil, 1995, Stern and Jedrzejas, 2006). Although hyaluronidases are not thought to be toxic themselves, the resultant effect of hyaluronidase activity leads to an increased permeability of the extracellular matrix (Kudo and Tu, 2001). This facilitates the diffusion of toxins into tissues of the envenomed prey and assists the entry of more destructive venom enzymes such as proteases into the haemostatic system, therefore contributing to the local and systemic effects of envenomation (Pukrittayakamee et al., 1988). Thus, hyaluronidase has been termed the 'venom spreading factor'.

Hyaluronidase is a highly conserved constituent component which is ubiquitously expressed in all snake venoms. Despite its important role in snake envenomation, hyaluronidase remains a relatively unstudied venom toxin as the rapid autolysis of this protein has inhibited its chromatographic isolation preliminary to functional studies. Hyaluronidases have been isolated and purified from the venoms of *Deinagkistrodon acutus* (Xu et al., 1982), *Agkistrodon contortrix* (Kudo and Tu, 2001) and the Indian Cobra, *Naja naja* (Girish et al., 2004). A study by Harrison *et al* determined the nucleotide sequence of hyaluronidase from several viperid species (*Echis ocellatus*, *Echis pyramidum leakeyi*, *Cerastes cerastes cerastes* and *Bitis arietans*), demonstrating a high level of sequence homology between species (over 95%) (Figure 1.7) (Harrison et al., 2007). This study, for the first time, determined the sequence structure of a snake venom hyaluronidase which has five conserved N-linked glycosylation sites and conserved residues in the catalytic, positional and

cysteine scaffold regions with a predicted molecular mass of over 50 kDa (Harrison et al., 2007).

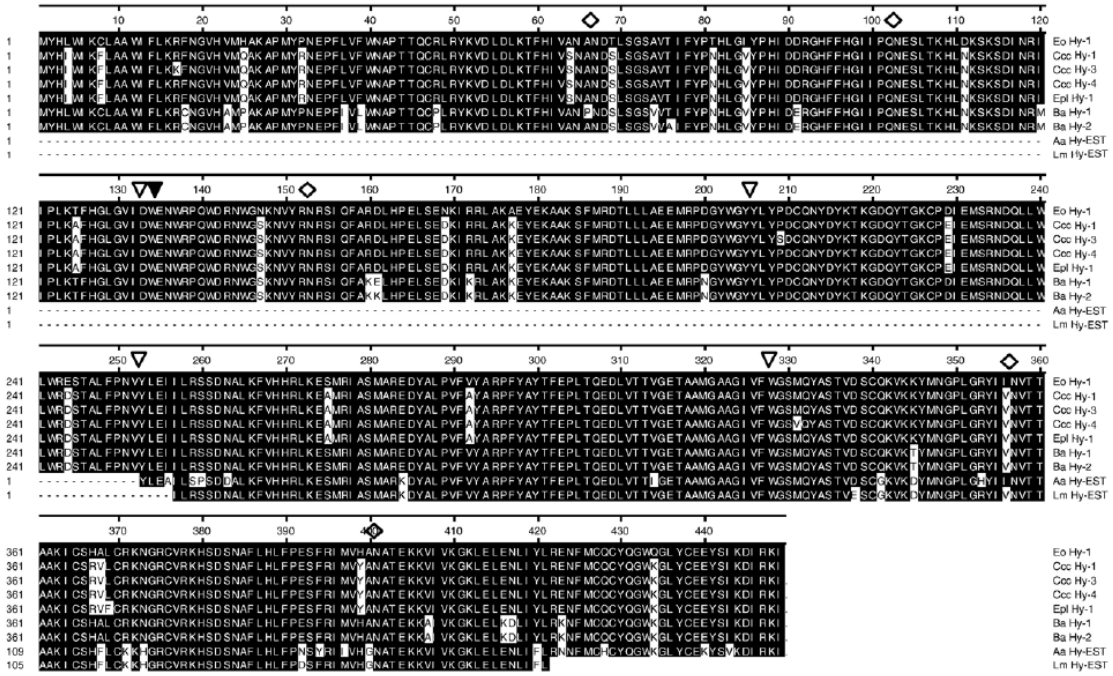

Figure 1.7 Snake venom hyaluronidase sequence analysis: Alignment of inferred full length hyaluronidase venom gland cDNA sequences from *Echis ocellatus*, *Cerastes cerastes*, *Echis pyramidum leakeyi*, *Bitis arietans*, *Echis carinatus sochureki* with EST sequences from *Agkistrodon acutus* and *Lachesis muta* from Harrison *et al* 2007 (Harrison et al., 2007). The conserved catalytic and positional residues are identified by the solid and open triangles respectively.

Hyaluronidase activity facilitates the diffusion of venom proteins into prey tissues and therefore results in the rapid influx of target-specific venom toxins into the circulating blood system and thus, is an essential component of all snake venoms. It is also thought that hyaluronidase is also involved in the symptoms of extensive local tissue destruction observed following snakebite. Current antivenoms are unable to neutralise the local symptoms and so the resultant uncontrollable tissue destruction remains a complex and unresolved clinical issue. As hyaluronidase degrades

hyaluronan, a key structural component of the extracellular matrix, it is thought that hyaluronidase may be one of several factors involved in causing severe tissue damage as it has been demonstrated that the inhibition of hyaluronidase presents local tissue destruction (Yingprasertchai et al., 2003). In addition, the inhibition of hyaluronidase by injection of inhibitors following envenomation can delay the time to death (Girish and Kemparaju, 2006) which also implicates the potential therapeutic use of hyaluronidase inhibitors in the treatment of snakebite.

1.5.6. Acetylcholinesterase (AChE)

Acetylcholinesterase (AChE) is present in all vertebrates and plays a functional role in the cholinergic system in the rapid hydrolysis and subsequent inactivation of the neurotransmitter, acetylcholine at the neuromuscular junction (Tougu, 2001). AChE has been detected at high levels in most elapid venoms, with the exception of the genus *Dendroaspis* which instead contains fasciculins, potent inhibitors of AChE (Karlsson et al., 1984, Cousin and Bon, 1997, Frobert et al., 1997). Studies analysed the AChE activity of 45 snake venoms and detected an absence of AChE activity in viperid and crotalid venoms (Frobert et al., 1997). In this study, a variation in the stability of AChEs among elapid venoms was apparent; AChE isolated from *Bungarus* venoms was much more stable than AChE isolated from venoms of *Hemachatus*, *Ophiophagus* and *Naja* species (Frobert et al., 1997). Venoms from *Bungarus* species were also shown to have the richest source of AChE activity with over twice as much activity as *Naja* venoms (Frobert et al., 1997). Despite the common occurrence of AChE in venoms, the biological function of AChE during envenomation remains unclear.

1.5.7. Nucleases, nucleotidases and phosphomonoesterases

Hydrolytic enzymes, such as nucleases (DNase, RNase and phosphodiesterase), nucleotidases (5' nucleotidase, ATPase and ADPase) and phosphomonoesterases (acid and alkaline phosphomonoesterases) have been found in venoms.

Nucleases are enzymes which act on nucleic acids (DNA/RNA). Venoms have been shown to contain both endonucleases which degrade either DNA or RNA specifically, and exonucleases which degrade both DNA and RNA. Currently, there have been very few studies investigating venom nucleases and so the occurrence, distribution and function are not fully understood. RNases have been identified from the venoms of *Naja naja oxiana* (Vasilenko and Ryte, 1975) and *Naja naja* (Mahalakshmi and Pandit, 1987, Mahalakshmi et al., 2000), and DNases have only been identified from *Bothrops atrox* venom (Georgatsos and Laskowski, 1962). Phosphodiesterases (PDEs) catalyse the phosphodiester bonds in polynucleotides acting on DNA, rRNA and tRNA. Unlike DNases/RNases, PDEs have been found ubiquitously in snake venoms across a wide range of taxa including colubrids, elapids and viperids (Aird, 2002, Aird, 2005, Mackessy, 2002) although few studies have attributed a biological function to this enzyme group.

Nucleotidases act upon nucleic acid derivative and nucleic acid-related substrates (e.g. ATP and ADP). 5' nucleotidases catalyse the hydrolysis of phosphate from the sugar moiety. These enzymes have also been found ubiquitously in snake venoms with viper venoms showing a greater 5' nucleotidase activity than elapids (Aird, 2005). There is, again, a lack of information about the biological role of 5' nucleotidases in snake venoms, although 5' nucleotidases in the venoms from *Deinagkistrodon acutus* (Ouyang and Huang, 1986) and *Trimeresurus gramineus*

(Ouyang and Huang, 1983) were shown to inhibit platelet aggregation either induced by ADP, collagen, sodium arachidonate, ionophore A-23187 in platelet-rich plasma and thrombin in platelet poor plasma. More recently, 5' nucleotidases in the venom of *Naja naja* have been shown to be involved in the anticoagulant effect of this venom by interacting with anticoagulant factors (Dhananjaya et al., 2006).

ATPases and ADPases catalyse the hydrolysis of ATP and ADP respectively. ATPase and ADPase activity have been observed in several snake venoms (Kini and Gouda, 1982a, Kini and Gouda, 1982b, Sales and Santoro, 2008). As the ATPases from venoms have not been purified, little is known about their biological role in venom. The ADPases, for example in *D. acutus* venom, have been shown to have platelet aggregation inhibiting properties (Ouyang and Huang, 1986).

Phosphomonoesterases catalyse non-specific hydrolysis of phosphate esters. Acid phosphomonoesterases are most active at pH 5.0 whereas alkaline phosphomonoesterases are most active at pH 9.5. Both acid and alkaline phosphomonoesterases have been found in venoms, although the alkaline enzymes appear more widespread and abundant, appearing in venoms from a range of snake taxa (Mackessy, 2002, Aird, 2002). However, phosphomonoesterases in venoms are yet to be characterised or assigned a biological role.

Non-enzymatic components:

1.5.8. C-type lectins (CTLs)

C-type lectins (CTLs) are non-enzymatic proteins found in many animals which bind in a Ca^{2+}-dependent fashion to mono- and oligosaccharides. In snake venoms, there

are two types of CTLs; CTL-like proteins (CLPs) and the classic sugar binding snake lectins. CLPs are found only in snake venoms and show a level of sequence homology with classic CTLs, but lack the Ca^{2+} binding loop which recognises carbohydrates (Ogawa et al., 2005). The basic structure of snake CTLs is a homodimeric form, whereas CLPs are heterodimers composed of homologous α- and β-subunits, interacting with a loop linked by a disulphide bond.

Sugar binding CTLs are not highly toxic components of snake venoms. They have been shown to initiate various immunological processes including adhesion, endocytosis and pathogen neutralisation (Weis et al., 1998). They have also demonstrated the ability to inhibit tumour cell lines and endothelial cell growth (de Carvalho et al., 2001), thus their role in snake venom is currently not fully understood. CLPs, on the other hand, show a diverse array of pharmacological activities affecting coagulation factors, platelets, haemostasis and thrombosis and can be divided into three subgroups based on biological activity; these are coagulant proteins, platelet aggregation agonists and platelet aggregation antagonists (Morita, 2005, Ogawa et al., 2005).

Firstly, anticoagulant proteins, which target the coagulation factors X and factor IX, have been isolated from several venoms. These bind to the γ-carboxyglutamic acid (Gla) domain of factor X and IX in the presence of Ca^{2+} (Atoda et al., 1994). Anticoagulant CTLs have been identified from the venoms of *Bothrops jararaca* (Sekiya et al., 1993), *Trimeresurus flavoviridis* (Atoda et al., 1994), *Echis carinatus leucogaster* (Chen and Tsai, 1996), *Deinagkistrodon acutus* (Atoda et al., 1998) and *Agkistrodon halys brevicaudus* (Koo et al., 2002). Secondly, platelet aggregation agonists, which have been isolated from the venoms of *Trimeresurus albolabris* (Andrews et al., 1996), *Crotalus durissus terrificus* (Polgár et al., 1997),

Calloselasma rhodostoma (Shin and Morita, 1998) and *Ophiophagus hannah* (Du et al., 2002). These activate platelet aggregation by binding to the platelet glycoproteins (GP) which facilitate the binding of fibrinogen to integrin αIIbβ3 and mediate the adherence of platelets to collagen. Other platelet aggregation agonists bind directly to von Willibrand Factor (vWF), forming an active complex which induces platelet aggregation by interacting with GPIb receptor. These include botrocetin from *B. jararaca* venom (Read et al., 1989) and bitiscetin from *B. arietans* venom (Hamako et al., 1996). In contrast, several CLPs act as platelet aggregation antagonists by interacting directly with GPIb receptor, thus blocking the binding of vWF and inhibiting platelet aggregation. These include agkicetin from *Agkistrodon acutus* venom (Chen and Tsai, 1995), mamushigin from *Agkistrodon halys blomhoffii* (Sakurai et al., 1998), CHH-A/B from *Crotalus horridus horridus* venom (Andrews et al., 1996) and echicetin from *Echis carinatus* venom (Peng et al., 1993).

1.5.9. Disintegrins

Disintegrins are present in snake venoms as a result of the proteolytic processing of multi-domain class II or class III venom metalloproteinases. Disintegrins are a family of small (40-100 amino acids), cysteine-rich polypeptides which can be divided into five different groups based on their length and number of disulphide bonds in the polypeptide (Calvete, 2005, Calvete et al., 2005). The sequence alignments of several different venom disintegrins from each group are shown in Figure 1.8. Short disintegrins are composed of 41-51 residues and four disulphide bonds, medium disintegrins contain around 70 residues with six disulphide bonds and long disintegrins are composed of an 84 residue polypeptides cross-linked by seven

disulphide bonds (Calvete et al., 2005, Calvete et al., 2003). Short, medium and long disintegrins contain an RGD tripeptide, the binding motif of RGD-dependent integrins. The fourth group of disintegrins are derived from PIII SVMPs and contain 100 amino acids with 16 residues involved in the formation of eight disulphide bonds and the fifth group is composed of homo- and hetero-dimeric disintegrins (Calvete et al., 2003).

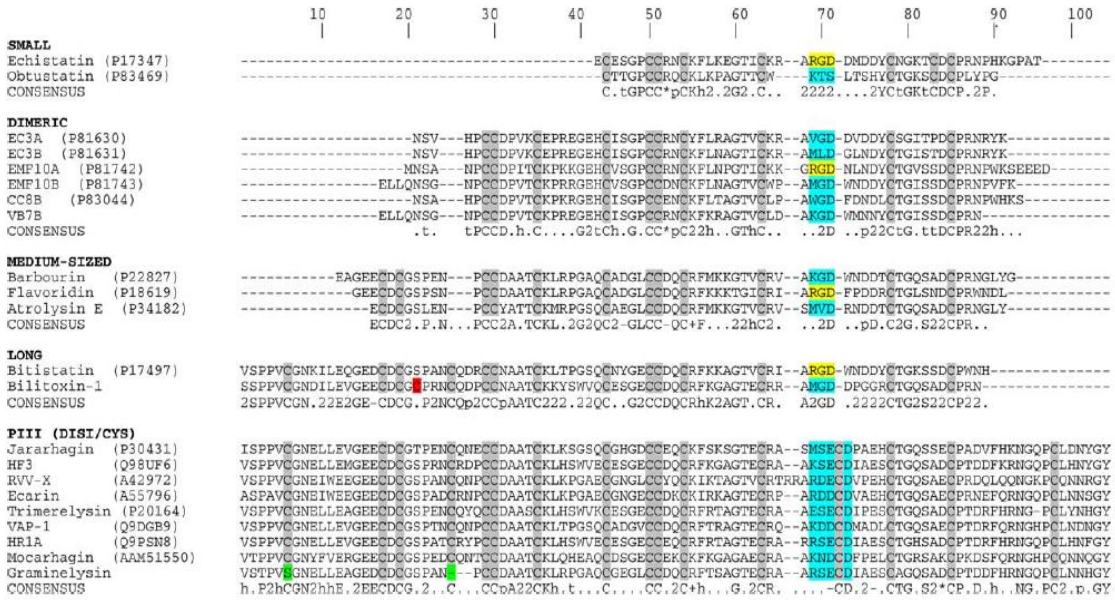

Figure 1.8 Snake venom disintegrin sequence analysis: Alignment of selected polypeptide sequences of the different disintegrin subfamilies including short, dimeric, medium, long and PIII-derived disintegrins. Cysteine residues are highlighted in grey, missing cysteines are highlighted in green, the extra cysteine in bilitoxin is shown in red, the RGD tripeptide is shown in yellow and non-RGD integrin binding tripeptides in blue (Calvete et al., 2005).

Snake venom disintegrins were first described as potent inhibitors of platelet aggregation by Huang *et al* in 1987 and were shown to act through selectively blocking the binding of fibrinogen to the integrin $\alpha_{IIb}\beta_3$ receptor (Huang et al., 1987). The disintegrins have evolved numerous integrin-binding motifs including RGD

which blocks the $\alpha_8\beta_1$, $\alpha_5\beta_1$, $\alpha_v\beta_1$, $\alpha_v\beta_3$ and $\alpha_{IIb}\beta_3$ integrins, MLD blocks the $\alpha_4\beta_1$, $\alpha_4\beta_7$, $\alpha_3\beta_1$, $\alpha_6\beta_1$, $\alpha_7\beta_1$ and $\alpha_9\beta_1$ integrins, VGD and MGD block the $\alpha_5\beta_1$ integrin, KGD block the $\alpha_{IIb}\beta_3$ integrin, WGD $\alpha_5\beta_1$, $\alpha_v\beta_3$ and $\alpha_{IIb}\beta_3$ (and is as potent in its inhibitory action as the RGD motif) and KTS/RTS block $\alpha_1\beta_1$ integrins (Calvete, 2005, Calvete et al., 2005).

1.5.10. Bradykinin potentiating peptides (BPPs)

BPPs are short chain pyroglutamyl proline-rich oligopeptides expressed from within larger precursor components, typically encoding numerous distinct BPPs flanked by conserved spacer regions and C-terminal C-type natriuretic peptides (CNP). BPPs, were originally isolated and characterised from *B. jararaca* venom (Ferreira et al., 1970a, Ferreira et al., 1970b) and can have profound effects on the cardiovascular system of the envenomed victim. They act through inhibiting angiotensin-converting enzyme and potentiating the action of bradykinin and are therefore thought to contribute to the symptoms of hypotension experienced as a consequence of envenoming by some viperid species (Hayashi and Camargo, 2005).

1.5.11. Inhibitory peptides (QKW tripeptides)

Following a transcriptomic survey of the venom gland from *E. ocellatus*, a group of endogenous inhibitors of the SVMPs was discovered (Wagstaff and Harrison, 2006). Proline-rich, C-type natriuretic peptide-containing transcripts characterised by a QKW tripeptide repeat were identified in the transcriptome, which were highly homologous to the bradykinin potentiating peptides in *B. jararaca* venom (Figure

1.9)(Wagstaff et al., 2008). As previously described, BPPs in venom induce hypotension in the envenomed victim; as *E. ocellatus* venom rarely causes symptoms of hypotensive in victims following envenoming, the presence of this unusual cluster of transcripts was examined in further detail. The findings of this study provided the first characterisation of novel genes encoding QKW tri-peptides with inhibitory properties including the inhibition of SVMP catalytic activity and venom-induced haemorrhagic activity (Wagstaff et al., 2008).

Figure 1.9 Sequence analyses of QKW tripeptides from viper venoms: Comparison of polypeptides encoded by novel transcripts isolated from the venom glands of two viperids, *Echis ocellatus* and *Cerastes cerastes* venom glands. QKW tripeptide repeats are indicated by open square brackets. The pHpG tract and CNP precursors in *E. ocellatus* sequences are denoted by solid bars (Wagstaff et al., 2008).

1.5.12. Kunitz serine proteinase inhibitors

Snake venom kunitz serine proteinase inhibitors (KTI) belong to the bovine pancreatic trypsin inhibitor (BPTI) gene family. KTI/BPTI inhibitors can be divided into two groups; the non-neurotoxic trypsin and chymotrypsin inhibitors, and the neurotoxic KTI/BPTI group. The latter group are homologs of trypsin/chymotrypsin inhibitors which have lost their proteinase inhibitory function and act as K^+ and Ca^{2+} channel blockers such as dendrotoxin, a neurotoxic KTI/BPTI which has been isolated and characterised from mamba (*Dendroaspis*) venoms (Harvey and Karlsson, 1980, Smith et al., 1993). Snake venom KTI/BPTI proteinase inhibitors belong to a functionally diverse, multi-gene family and have been isolated from the venoms of several viper and elapid species (Župunski et al., 2003).

1.5.13. Vascular endothelial growth factors (VEGFs) and nerve growth factor (NGFs)

The protein family of vascular endothelial growth factors (VEGFs) are regulators of neovascularization and angiogenesis (Olsson et al., 2006). There are currently seven members of this protein family including tissue type VEGF (VEGF-A), VEGF-B, placenta growth factor (PlGF), VEGF-C, VEGF-D, viral VEGF (VEGF-E) and snake venom VEGF (svVEGF) and, although diversity within sub-types exists, all members of the family are structurally homologous (Olsson et al., 2006) (Yamazaki and Morita, 2006) (Figure 1.10). VEGF was first characterised from the venom of *Vipera aspis aspis* following the isolation and purification of a heparin-binding dimeric hypotensive factor with 45% sequence homology to tissue type VEGF (Komori et al., 1999). VEGFs have also been characterised from *Bothrops insularis*

(de Azevedo et al., 2001), *Trimeresurus flavoviridis* (Takahashi et al., 2004), *Agkistrodon piscivorus piscivorus* (Yamazaki et al., 2005) and *Bitis arietans* (Yamazaki et al., 2009) venom glands. Although tissue type VEGFs are highly conserved throughout vertebrates, including snakes, svVEGFs expressed are highly diversified in structure, particularly in the functionally important regions including receptor-binding loops and C-terminal co-receptor binding regions (Yamazaki et al., 2009). Some svVEGFs have been shown to induce strong vascular permeability with similar activity to VEGF-A (Takahashi et al., 2004), but the receptor selectivity of svVEGFs has not yet been fully explored and therefore the specific functions of svVEGFs in envenoming are not completely understood.

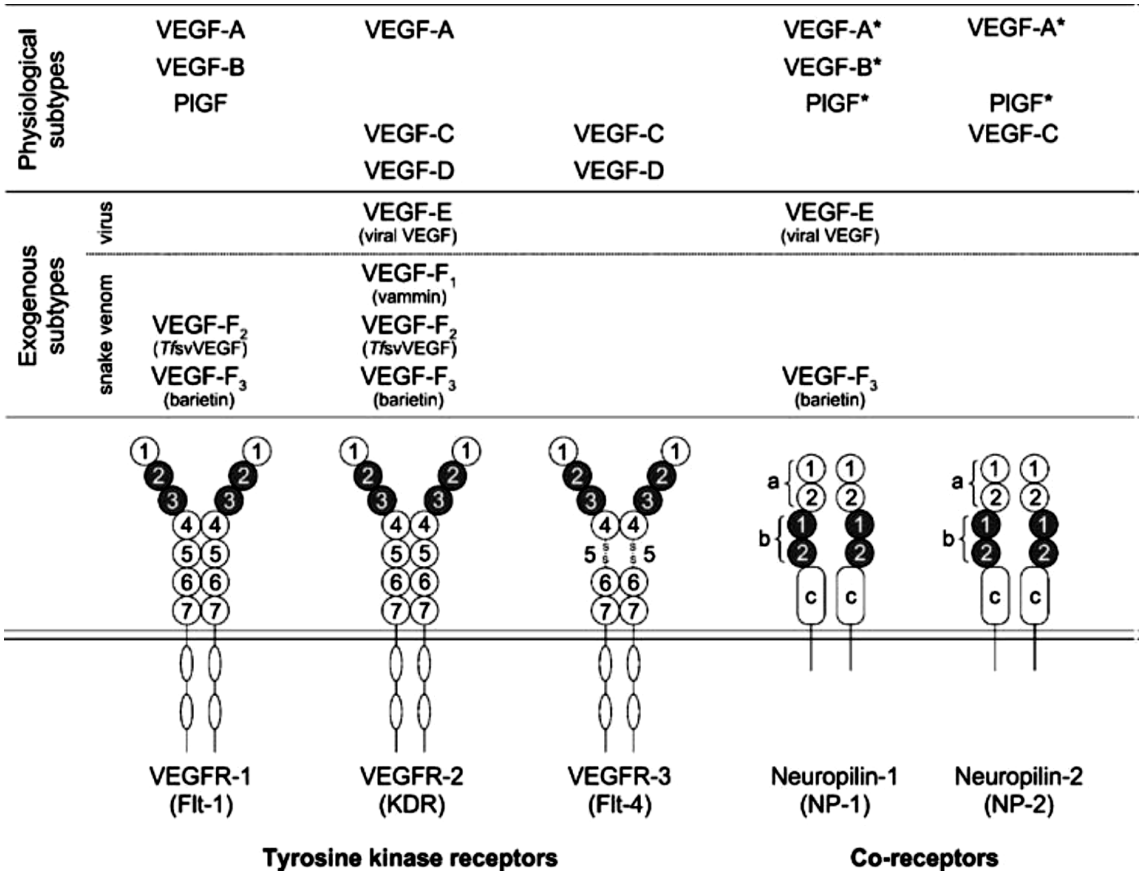

Figure 1.10 The VEGF protein family and receptor selectivity: Interaction of several VEGF ligands with their receptors. The ligand binding domain for each receptor is shaded black (Yamazaki and Morita, 2006).

Nerve growth factors (NGFs) are members of the neurotrophin family of proteins which are responsible for the maintenance and survival of neuronal cells and the stimulation of nerve growth. NGFs were first isolated from the venom of *Agkistrodon piscivorus* and *Crotalus adamanteus* (Cohen and Levi-Montalcini, 1956) and have since been isolated from venoms of several species of vipers and elapids including *Daboia russellii* (Koyama et al., 1992), *Vipera lebetina* (Siigur et al., 1985), *Vipera berus berus* (Siigur et al., 1986), *Echis carinatus* (Siigur et al., 1987), *Naja naja* (Hogue-Angeletti et al., 1976) and *Gloydius halys* (Siigur et al., 1987). Snake venom NGFs have been shown to display around 65% sequence homology to mammalian NGFs and may have similar biological activities (Kostiza and Meier, 1996) but the relevance of NGFs in envenoming is currently little understood.

1.5.14. Cysteine rich secretory proteins (CRISPs)

Cysteine rich secretory proteins (CRISPs) have been isolated and characterized from most reptile venoms, including all three families of venomous snakes (colubrids, viperids and elapids) (Fry et al., 2006, Hill and Mackessy, 2000, Yamazaki and Morita, 2004). Venom CRISPs have been shown to demonstrate a wide range of biological effects including blockage of cyclic nucleotide-gated ion channels in elapid venom (Yamazaki et al., 2002a), blockage of calcium-activated potassium channels in elapid venom (Wang et al., 2005), blockage of smooth muscle contraction in viper venom (Yamazaki et al., 2002b) and proteolysis in cone snail venom (Milne et al., 2003). The CRISP isolated from the venomous lizard species, *Heloderma horridum*, (helothermine) is of particular interest as it exhibits a diversity

of functions including the blockage of potassium currents (Nobile et al., 1994) and calcium channels in neurons (Nobile et al., 1996) and the potential induction of hypothermia in prey (Mochca-Morales et al., 1990).

1.5.15. Purine and pyrimidine nucleosides

Purine and pyrimidine nucleosides are present in most elapid and viperid venoms, although appear to be absent from crotalid venoms (Aird, 2005). Nucleosides are multifunctional toxins acting on all cell types. It has been suggested that purines (adenosine, inosine and guanosine) contribute to the immobilization (through hypotension or paralysis) and digestion of prey (Aird, 2002). Adenosine has been shown to assist in the immobilization of prey by activating neuronal adenosine A_1 receptors leading to the induction of sedative effects (Dunwiddie and Worth, 1982) and alterations in cognitive functioning (Winksy and Harvey, 1986). Adenoside and inosine have been shown to promote inflammation (Walker et al., 1997, Fan and Jamal Mustafa, 2006), the activation of mast cell A_2 receptors (Ramkumar et al., 1993) and, at high concentrations, induce apoptosis (Tanaka et al., 1994, Abbracchio et al., 1995) (Saitoh et al., 2004). Pyrimidine nucleosides (cytidine and uridine) have also been found in most elapid and viperid snake venoms (Aird, 2005). The function of purines and pyrimidines in envenomation is currently unclear but is has suggested that these components play a role in the envenomation strategies of advanced snakes, such as the ‘strike and release’ (viper) and the ‘seize and grasp’ (elapid) approaches, in enabling the rapid immobilization of prey (Aird, 2005).

1.6. Venom protein synthesis and storage

The cycle of transcriptional activity of secretory cells is thought to be initiated through the act of venom expulsion either by snake bite or manual extraction (Mackessy, 1991). Morphological observations of the venom gland epithelium following manual extraction of venom showed that the secretory cells change from a short, cuboidal shape during the inactive (atrophic) state to a long columnar shape (hypertrophic) following activation initiated by depletion of the venom gland contents (Oron and Bdolah, 1978) (Figure 1.11). Newly synthesised venom proteins are secreted into the large central lumen and smaller tubular ductules of the venom gland via exocrine transportation, or can be stored in microvesicles (Carneiro et al., 2007), or granules within the secretory cells of the glandular epithelium (Oron and Bdolah, 1978).

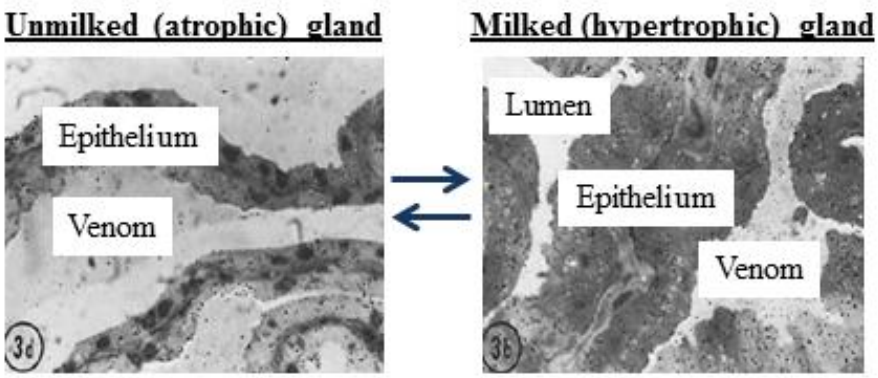

Figure 1.11 Secretory cycle of the venom gland during venom synthesis: Microscopic examination of the venom glandular secretory epithelium during the cycle of venom synthesis to show changes in the size of secretory cells with levels of activity. Figure modified from Oron, U. and Bdoloh (Oron and Bdolah, 1978).

The activity of mRNA and the rate of protein accumulation in the venom gland are thought to change throughout the course of venom synthesis as cells cycle. Previous

literature using immunohistochemistry methodologies indicates that total RNA activity occurs at day 3 post venom extraction and translation of amino acids incorporated into proteins reaches maximal levels following a short lag period between 4 to 8 days post venom extraction (Paine et al., 1992). Protein synthesis is thought to be maintained at a high rate until completion on day 16 but studies have suggested that secretory cells can remain active for up to 30 to 60 days post venom extraction indicating that the complete cycle of venom synthesis may be longer than expected (Carneiro et al., 2002). The organization and regulation of venom protein production is not yet fully understood. There is some evidence to suggest that the regeneration of depleted venom proteins following venom gland expulsion may be asynchronous (Oron and Bdolah, 1973, Oron et al., 1978). Although secretory cells have the capacity to synthesise and secrete the complete range of venom proteins, it is thought that each toxin group has a rate of production independent of other components synthesised by the glands. A study on *Vipera ammodytes* venom glands demonstrated that the glands may synthesise a greater proportion of molecules without an obvious predatory function immediately after venom extraction and a higher percentage of toxic components are synthesised later in the cycle on day 8 post-milking (Oron and Bdolah, 1973). This study noted that on the first day following venom extraction, only 25% of newly synthesised proteins could be precipitated by antivenom in comparison to venom synthesised at 8 days post-venom extraction where 80% of proteins were precipitated by antivenom (Oron and Bdolah, 1973). These results could be interpreted to suggest that the venom gland may synthesise non-toxic venom proteins, such as structural or inhibitory/stabilising components, prior to the synthesis of toxic venom proteins. It could be suggested that the physiological proteins with inhibitory functions may function to prepare and

protect the glandular epithelium for the storage of toxins. Asynchrony in venom synthesis was further investigated in a study by Oron *et al* (Oron et al., 1978) whereby venom of *Vipera palaestinae* was analysed following injection of animals with [^{3}H] Leucine. The incorporation of [^{3}H] Leucine into venom components in the venom glands was compared between snakes injected 2 and 4 days after milking. Considerable variability in the incorporation of several proteins was evident, however, more stability and less variability were observed in the synthesis of neurotoxins: enzymes which are essential enabling prey immobilisation. It has been suggested that non-parallel synthesis of some venom proteins may be related to the importance of their toxic or physiological role in venom in that the expression of components most vital in envenoming is more stable and less variable than those less fundamentally important in the pathology of snakebite (Oron et al., 1978).

1.7. The venom glandular environment; protecting against self-proteolysis

The venom gland provides a unique natural microenvironment which synthesises and stores a highly biologically active and volatile combination of toxic components. Despite the presence of potent enzymes, the venom gland provides conditions that stabilise these and other proteins during long-term storage of venom. Several biological, chemical and physical properties have been shown to influence venom protein stability and may contribute to the maintenance of a stable glandular environment.

Biochemical factors such as pH, metal ions chelators and endogenous inhibitors may act to ensure stabilisation of venom components and prevent self-autolysis of venom constituents. Previous studies have demonstrated that the venom gland contents are

acidic (Mackessy and Baxter, 2006). The acidic pH is thought to be achieved by the mitochondria-rich cells in the glandular epithelium which are morphologically similar to the parietal cells of the gastric pits in mammalian stomach lining. In the stomach, parietal cells function to activate digestive enzymes following the acidification of stomach contents. However, in venom, the acidic environment may serve to inhibit the function of venom enzymes (Mackessy and Baxter, 2006). Studies have shown that the pH of the venom gland may influence the activity of venom enzymes. Sousa *et al* (Sousa et al., 2001) investigated the stability of venom under different pH conditions. Thus, following incubation at room temperature for 48 hours, the naturally occurring proteolytic action of venom upon its own components was seen to be significantly reduced or absent in venom incubated in the acidic environment (pH 5.0) when compared to venom maintained at in alkaline conditions (pH 8.5) illustrating the proteolytic-inhibiting properties of an acidic environment. In addition, some biological properties of venom such as haemagglutinating activity was drastically decreased and many high molecular weight proteins degraded under alkaline conditions, supporting evidence that that venom is significantly more stable at a weakly acidic pH (Sousa et al., 2001).

There may also be non-proteinaceous components of venom that specifically inhibit venom toxicity during glandular storage. Studies have demonstrated that citrate is present in snake venoms and is thought to chelate divalent metal cations resulting in the inactivation of cation-reliant enzymes such as Zn^{2+}-dependent SVMPs and Ca^{2+}-dependent PLA_2s. Studies therefore suggest that citrate may act as a complete (Francis and Kaiser, 1993) or partial inhibitor of snake venom enzymes (Odell et al., 1998). The presence of citrate as a major component of venom has been documented in the study of the venom of several Vipers including *Bothrops asper*, *Crotalus*

atrox, *Crotalus viridis viridis*, *Crotalus adamanteus*, *Sistrurus miliarius barbouri*, *Crotalus horridus horridus*, *Agkistrodon contortrix mokasen*, *Agkistrodon contortrix contortrix*, *Agkistrodon piscivorus piscivorus* (Frietas et al., 1992). Francis *et al* found citrate levels ranged from 95 to 150mM across venom from four different species; *Agkistrodon contortrix contortrix*, *Bothrops asper*, *Bitis caudalis* and *Vipera ammodytes* (Francis et al., 1992). The potential function of citrate as an enzyme inhibitor may explain the high levels of citrate reported in these venoms.

Toxic-specific inhibitory peptides may be present in abundance in venom which could be responsible for subduing the toxic effects of venom components. A study by Wagstaff *et al* (Wagstaff et al., 2008) identified and characterised a group of tri-peptides present in abundance in the venom of the saw-scaled viper, *E. ocellatus*, and the puff adder, *B. arietans*. These peptides were shown to act to specifically to inhibit the *in vitro* and *in vivo* activity of SVMPs. It is currently unknown as to whether peptides acting to specifically inhibit the activity of other venom toxins are synthesised by the venom glands.

1.8. Analysis of venom composition; venomics and transcriptomics

Studies of snake venom gland transcriptomes aim to examine the expression levels of all mRNAs encoding venom proteins in cells of the venom glandular epithelium. The resultant transcriptome reflects all of the genes which are actively expressed by the venom gland at any given time and provides a comprehensive picture of the abundance and diversity of all of the transcripts encoding venom proteins. The venom gland transcriptome has been produced and extensively studied for several medically important species of vipers including *Bitis gabonica* (Francischetti et al.,

2004), *E. ocellatus* (Wagstaff et al., 2009, Casewell et al., 2009), *Bothrops* species (Cidade et al., 2006, Kashima et al., 2004, Neiva et al., 2009), *Sistrurus catenatus edwardsii* (Pahari et al., 2007) and *Deinagkistrodon acutus* (Zhang et al., 2006) and elapids including *Bungarus flaviceps* (Siang et al., 2010), *Bungarus multicinctus* and *Naja atra* (Jiang et al., 2011) and *Micrurus altirostris* and *M. corallinus* (Corrêa-Netto et al., 2011). The ability to generate an accurate representation of all venom proteins transcribed by the venom glands of snakes through transcriptomic surveys is vital for venom research. From a clinical perspective, transcriptomic studies have improved our understanding of the toxic composition of venom and thus greatly aided in our ability to characterise envenomation profiles and in the strategies to improve the treatment of snakebite such as in the design of toxin-specific antivenoms. From a biological view, transcriptomic studies aiming to generate a full catalogue of transcripts encoded by snake venom glands could reveal novel or unusual components of snake venom of interest for drug discovery and in addressing unanswered fundamental biological questions. However, it is also vital that venom gland transcriptomes are analysed in combination with the venom proteome or 'venome'. Although the transcriptome can be viewed as a precursor of the proteome, small transcriptional and post-translational processes may significantly influence the overall protein composition of venom. A study by Wagstaff *et al* revealed differences between the transcriptome and proteome of *E. ocellatus* venom glands and demonstrated that some venom proteins such as hyaluronidase and nerve growth factors which were predicted by the transcriptome, could not be detected in the proteome (Wagstaff et al., 2009). Such studies emphasise the importance of combined transcriptomic and proteomic approaches to analysing venom composition.

1.9. Variation in venom composition

Variation in venom has been well documented on several taxonomic levels including inter-family, inter-genus and inter- or intra-species variation in venom (Chippaux et al., 1991). Many studies investigating the levels of venom variation have attributed their findings to factors such as dietary, geographical, ontogenetic and gender associated changes.

Diet has been demonstrated as one of the most important factors influencing variation in venom composition. Intra-species variation in venom composition was first correlated with diet by Daltry *et al* who investigated variation in venom from the Malayan pitviper, *Calloselasma rhodostoma*. Studies provided evidence that variation in venom protein composition and biological activity was most strongly associated with diet, rather than geographic proximity or phylogenetic relationships between populations of *C. rhodostoma* across Southeast Asia (Daltry et al., 1996a, Daltry et al., 1996b). These studies suggested that natural selection of venom toxins most adapted to immobilize, kill and digest local prey items has resulted in variable venom protein patterns in this species (Daltry et al., 1996b). Variation in the venom protein composition between closely related subspecies of *Sistrurus* rattlesnakes (Sanz et al., 2006) and *Echis* species (Barlow et al., 2009) have been correlated with the recruitment of different toxins into the proteome of species with predominantly mammalian or varied diets. In a transcriptomic approach, findings of a recent study demonstrated significant intra-family variation in the venom transcriptomes of *Echis* species (Casewell et al., 2009) where changes in toxin isoform diversity and expression levels could be correlated with prey specificity.

Ontogenetic variation in the composition and activity of venom has been

demonstrated in several species. It is thought that ontogenetic shifts in venom composition and function are related to dietary and habitat shifts from juvenile to adult snakes. The first observations of ontogenetic variation in venom were demonstrated by Reid and Theakston who identified changes in the coagulant activity of *Crotalus atrox* venom as snakes age (Reid and Theakston, 1978). This study concluded that the venom of juvenile snakes was more lethal (indicated by LD_{50}) and showed greater ability to induce platelet aggregation (indicated by *in vitro* platelet aggregation assays) and emphasises the importance of understanding ontogenetic variation in venom from a clinical perspective as different venom activities could explain conflicting reports of snakebite envenoming symptoms. Further studies illustrating ontogenetic variation in venom composition and toxicity are described in detail in Chapter 5, however, the general consensus conclusions for the majority these studies indicate that juvenile venoms, overall, exert a distinct pathology to adult venoms, particularly in the coagulant activity of venom. Gender associated variations in venom composition and activity have also been demonstrated in *B. jararaca* (Furtado et al., 2006, Menezes et al., 2006, Pimenta et al., 2007), *Boiga irregularis* (Mackessy et al., 2006) and *Deinagkistrodon acutus* (Gao et al., 2011). These studies indicated that differences in the protein composition and various toxic properties of venom between males and females could be observed.

The study of variation in venom composition and function is important for therapeutic, biological and evolutionary purposes. Variation in venom could affect the clinical presentation of venom-induced pathology following envenomation. This could subsequently lead to variations in the efficacy of antivenom treatment in patients, particularly in those treated with antivenoms which are in use over wide geographical areas. Such antivenoms may not incorporate the complete species

diversity of venom composition and therefore vary in their ability to neutralise venom toxicity.

1.10. Aims of this work

Presently, there are several aspects of fundamental venom biology which are yet to be resolved. These include the dynamics of venom protein synthesis and the mechanisms by which protein synthesis by the venom gland is controlled and regulated. In past years, many areas of venom research have experienced significant benefit from the recent advances in proteomic and transcriptomic technologies leading to a greater understanding of snake venoms. However, we currently still have little understanding of how venom is synthesised, regulated and maintained by snake venom glands. The major aim of this work was to elucidate the real-time time scale for the replenishment of venom proteins during venom synthesis and to investigate how venom synthesis is controlled and coordinated using advanced high throughput techniques.

The initial aim of this thesis was to gain a greater understanding of the composition of venom of the African Puff Adder, *B. arietans*. This viperid species is a member of the sub-family Viperinae and is the most medically important species of the genus *Bitis*. The genus also incorporates other species of lesser medical importance including the Gaboon viper (*B. gabonica*), the Horned Puff adder (*B. caudalis*), the Rhinoceros viper (*B. nasicornis*) and the Dwarf adder (*B. schneideri*). With an average size of around 1m in length, this stout and powerful snake is one of the most common venomous snakes in Africa. There are currently two recognised sub-species of *B. arietans*. These are the pan-African sub-species *B. arietans arietans* and the

Somali Puff Adder (*B. arietans somalica*) which is found exclusively in Somalia and Northern Kenya. *B. arietans* exhibits a diverse and extensive pan-African geographical distribution occupying a range of varied habitats throughout sub-Saharan Africa and the Arabian Peninsula. The venom from *B. arietans* is highly toxic, containing an abundance of haemotoxic proteases and other enzymes. Toxins in *B. arietans* venom typically interfere with the haemostatic system and are responsible for causing the characteristic symptoms of *B. arietans* envenoming such as severe local and systemic effects including swelling, haemorrhage and tissue necrosis (Warrell et al., 1975). Without antivenom treatment, *B. arietans* envenoming can have fatal consequences (Warrell et al., 1975). Due to (i) its extensive co-distribution in areas of high human density, (ii) highly potent venom and (iii) potentially large quantities of venom which can be injected per bite, *B. arietans* is considered one of the most medically important species of venomous snake in Africa. In addition to the saw-scaled viper (*E. ocellatus*) and the spitting cobra (*Naja nigricollis*), the Puff Adder is therefore thought to be responsible for a high proportion deaths resulting from snakebite in sub-Saharan Africa. These characteristics also make this species an ideal candidate to investigate occurrence of intra-species variation in venom. In a study including proteomics, immunological and venom enzyme activity analyses, we aimed to evaluate the levels of intra-species variation in the venom proteome, immunoreactivity and enzyme function of this species. Specifically, we aimed to determine the degree of variation between *B. arietans* specimens from both different and the same geographical origins across sub-Saharan African and Arabia. The overall outcome of this work aimed to gain a greater understanding of the venom of this clinically and biologically important

species of venomous snake; the resultant findings of this study could therefore have both biological and therapeutic implications.

The second aim of this work was to develop and optimise novel protocols to efficiently and quantitatively track changes in the gene expression of specific venom proteins, including venom toxins and less toxic physiological proteins, during the course of venom production. The experimental limitations of current methodologies render the study of real-time gene expression analyses extremely difficult as they rely upon the extraction of transcriptionally active messenger RNA from venom gland tissues, therefore requiring the sacrifice of snakes. Consequently, we elected to conduct a novel approach enabling the analysis of venom gene expression using non-invasive experimental techniques, circumventing the requirement to sacrifice snakes for venom glandular dissection. This unique approach aimed to utilise and exploit the unusual presence and stability of messenger RNA in lyophilised venom samples in a stringently optimised quantitative PCR protocol, as an alternative source of messenger RNA for gene expression and transcription analyses.

Our fully optimised experimental approach would be applied to quantitatively monitor the levels of expression of venom protein-encoding genes using quantitative PCR. We aimed to track changes in gene expression during venom synthesis, both in terms of the production of venom in juvenile snakes from birth to maturity, and in the replenishment of depletion venom stores by adult specimens, using *B. arietans* as a model species. After gaining a greater understanding of the dynamics of venom protein expression during venom synthesis, we subsequently aimed to investigate and characterise the genomic structure and organisation of venom protein-encoding genes and subsequently identify gene regulatory regions (e.g. promoters and transcription factors) responsible for controlling venom synthesis.

2. MATERIALS AND METHODS

Recipes for buffers and stock solutions used during the course of this experimental work can be found in appendix I.

2.1. Venom extraction, preparation and storage

All venoms used in this work were extracted by Paul Rowley and Dr Rob Harrison from snakes maintained under identical climatic and dietary conditions in the herpetarium at the Alistair Reid Venom Research Unit in the Liverpool School of Tropical Medicine. During venom extraction, venom glands were massaged to ensure maximal quantities of venom were obtained (Figure 2.1). Following extraction, venom samples were immediately transferred into glass bijoux bottles using a sterile pipette, weighed and frozen at -20°C for 24 hours. Venoms were then freeze-dried using a mini Lyotrap lyophilizer (LTE Scientific Ltd, UK) for 3-4 hours before storage at 4°C until analysis. Following reconstitution of lyophilised venom, samples were stored at -80°C.

Figure 2.1. Venom extracted from an adult *Bitis arietans* specimen.

PROTEIN ANALYSIS

2.2. One dimensional sodium dodecyl sulphate polyacrylamide gel electrophoresis (1D SDS-PAGE)

2.2.1. Venom sample preparation for SDS-PAGE

Unless otherwise stated, lyophilised venom samples were reconstituted in 1X phosphate-buffered saline (1X PBS) at a concentration of 10mg/ml. Venom samples were diluted to a final concentration of 1mg/ml in 2X protein loading buffer (2X PLOB). To prepare reduced 2X PLOB, a reducing agent, β-mercaptoethanol, was added to non-reduced loading buffer at a proportion of 15% v/v (e.g. 150µl β-mercaptoethanol per 850µl non-reduced 2X PLOB). For non-reduced 2X PLOB, the reducing agent was substituted for the same volume of distilled water (dH_2O). Venom samples for both non-reduced and reduced SDS-PAGE were heated to 95°C for 5 min prior to electrophoretic analysis to promote protein denaturation. The addition of the reducing agent, β-mercaptoethanol, acted to further denature proteins by disrupting intra and inter molecular disulphide bridges.

2.2.2. SDS-PAGE gel preparation and electrophoresis

1D SDS-PAGE was used to separate venom samples into their constituent protein components based on molecular mass. 1mm glass plates were assembled using the mini-Protean electrophoresis system (BioRad, UK) according to the manufacturer's instructions. 1mm or 7.5mm 15% polyacrylamide resolving gels (for 4 gels: 7.5ml dH_2O, 5ml 1.5M Tris pH 8.8, 7.5ml 40% Bis Acrylamide, 200µl 10% SDS, 120µl 10% ammonium persulphate (APS) and 14µl TEMED) were prepared, poured into the glass plates, overlaid with dH_2O to remove bubbles and prevent drying and

allowed to polymerize for 45 min. Acrylamide concentration was adapted to prepare 10 or 12% gels if further separation of proteins was required. Following polymerisation, dH_2O was removed and the stacking gel mixture (for 4 gels: 5ml dH_2O, 2ml 0.5 M Tris pH 6.8, 350µl 40% Bis Acrylamide, 30µl 10% APS and 5µl TEMED) was poured on top of the polymerised resolving gel and a 15-well 1mm comb was inserted into the plate. The stacking gel was allowed to polymerise for a further 45 min. Electrophoresis was carried out using a mini-Protean cell (BioRad, UK) at 200V for 45 min to 1 hour in 1X Tris-glycine-SDS (TGS) running buffer. A standard broad range molecular weight protein marker ranging from 10 to 225kDa (Promega, UK) (7µl) was run alongside 10µl venom samples in order to give an indication of the molecular weight of venom proteins in the sample. Gels were then stained with Coomassie Blue R-250 overnight and destained with coomassie destain solution until clear. Where increased sensitivity in gel-staining was required, for example when analysing venom samples of a low protein concentration or to visualise proteins of low abundance in venom samples, a silver staining kit (PageSilver™ silver staining kit, Fermentas, UK) or the rapid staining protocol adapted from Nesterenko *et al* (Nesterenko et al., 1994) which is described in table 2.1 was used.

	Step:	Solution/per gel:	Incubation time:
1	***Fixation***	60ml 50% acetone, 1.5ml 50% trichloroacetic acid, 25 µl 37% formaldehyde (HCHO).	5 min
2	***Rinse***	dH_2O	3 x 5 sec
3	***Wash***	dH_2O	5 min
4	***Rinse***	dH_2O	3 x 5 sec
5	***Pre-treat***	60ml 50% acetone	5 min
6	***Pre-treat***	100µl 10% $Na_2S_2O_3 \cdot 5H_2O$ in 60ml dH_2O	1 min
7	***Rinse***	dH_2O	3 x 5 sec
8	***Impregnate***	0.8ml 20% $AgNO_3$, 0.6ml 37% HCHO in 60ml dH_2O	12-15 min
9	***Rinse***	dH_2O	2 x 5 sec
10	***Develop***	1.2g Na_2CO_3, 25µl 37% HCHO, 25µl 10% $Na_2S_2O_3 \cdot 5H_2O$ in 60 ml dH_2O	10-20 sec
11	***Stop***	1% glacial acetic acid in 60ml dH_2O	
12	***Rinse/store***	dH_2O	

Table 2.1. Rapid silver staining protocol for staining SDS-PAGE protein gels: Protocol adapted from Nesterenko et al (Nesterenko et al., 1994). Volumes of solutions used are suitable for staining one 7.5mm mini gel.

2.3. Immunoblotting

Immunoblotting was used to detect specific venom proteins which were immunoreactive to antivenoms or toxin-specific antibodies. 1D SDS-PAGE separation of venom samples was conducted as previously described in section 2.2.2. Following electrophoresis, the polyacrylamide gel was sandwiched together with a 0.45µm nitrocellulose membrane (BioRad, UK) between two double layers of filter paper and foam padding. The sandwich was inserted into a cassette and placed into an immunoblotting transfer tank (BioRad, UK) containing immunotransfer buffer. Electro-transfer of proteins from the SDS-PAGE gel onto the nitrocellulose membrane was achieved following electrophoresis of proteins for 1 hour at 100V, mixing continually with a magnetic stirrer. An ice block was inserted into the

transfer tank to prevent the buffer from overheating during electro-transfer. Once complete, transferred proteins were temporarily visualised using 1X Ponceau S dye to check the efficiency of electro-transfer and to enable labelling of markers and sample well lanes. Membranes were thoroughly rinsed in 1X Tris-buffered saline Tween-20 (TBST) to remove the Ponceau S dye. Membrane protein binding sites were blocked overnight in 5% non-fat milk (Marvel) in TBST to reduce non-specific protein binding. Primary antibodies were diluted in 5% non-fat milk at a concentration ranging from 1/1000 for antivenoms to 1/200 for toxin-specific antibodies. For negative controls, normal animal sera (e.g. horse or mouse sera) were used. Membranes were incubated with the primary antibodies for 5 hours. Membranes were washed by conducting three 10 min washes in TBST. Horseradish peroxidase-conjugated secondary antibodies (e.g. anti-horse or anti-mouse) (Sigma, UK) were diluted in 5% non-fat milk at a concentration of 1/1000. Membranes were incubated with the secondary antibody for 2 hours followed by a final three 10 min TBST washes. Blots were developed using a 3,3'-Diaminobenzidine peroxidase (DAB) solution for approximately 2 min.

2.4. Substrate zymography

2.4.1. Venom sample preparation for substrate zymography

The proteolytic activity of venom proteins was assessed by addition of substrates into SDS-PAGE gels and subsequent examination of lysis. Reconstituted venom samples were prepared at a concentration of 1mg/ml in non-reduced 2X PLOB as described in section 2.2.1. For zymography, samples were not denatured by heating to 95°C.

2.4.2. Zymogram gel preparation, electrophoresis and activation

0.75mm gels were prepared using BioRad equipment. The resolving gel was prepared by co-polymerising molten gelatin or fibrinogen with polyacrylamide (for 4 gels 5ml dH_2O, 5ml 1.5M Tris pH 8.8, 5ml 40% Bis Acrylamide, 5ml of 10mg/ml molten gelatin or fibrinogen in dH_2O, 100µl 10% SDS, 300µl 10% APS and 15µl TEMED), poured into the glass plates and overlaid with dH_2O before allowing to polymerise for 45 min. The stacking gel was prepared as previously described for 1D SDS-PAGE, poured with a 15-well 0.75mm comb and left to polymerise for a further 45 min. Electrophoresis of venom samples was carried out at 200V for 45 min in 1X TGE running buffer. Following electrophoresis, gels were incubated at room temperature for 30 min in enzyme re-naturing buffer (2.5% Triton X-100 solution) with gentle agitation. Gels were then washed three times with dH_2O before incubating overnight at 37°C in developing buffer. Gels were then stained with Coomassie Blue R-250 for 2-3 hours and destained briefly for 1-2 min until clear areas indicating degradation of substrate by venom enzymes were visible.

2.5. Mass spectrometry:

2.5.1. In-gel trypsin digestion

In-gel trypsin digestion of protein bands was performed using protocols adapted from Hayter *et al* (Hayter et al., 2003). Coomassie stained protein bands which were clearly distinguishable as single bands on 1D SDS-PAGE gels were excised using a clean scalpel and transferred into a 1.5ml eppendorf tube. Gel bands were destained to remove all traces of Coomassie Blue by incubating at 37°C for 10 min in 20-50µl destaining solution containing 50mM Ammonium bicarbonate/50% acetonitrile

(AmBic/ACN). Destaining was repeated at least three times by replacing the solution with fresh destain solution each time in order to remove all traces of Coomassie Blue. Once destained, proteins were reduced by incubating with 20µl DTT at 37°C for 30 min and alkylated by incubating with 20µl IAN at 37°C for 30 min in the dark. The gel bands were then dehydrated by adding 10µl of 100% ACN and incubating at 37°C for 15 min – after which time the gel band turned white. The solvent was carefully removed and the remaining acetonitrile was left to evaporate at 37°C for 10 min. The trypsin solution required to digest proteins was prepared by re-suspending 25µg proteomics grade trypsin (Sigma, UK) in 250µl of 50mM acetic acid. The trypsin stock solution was diluted 1:10 in 50mM AmBic/50%ACN (giving a final concentration of 0.1µg/µl) and 10µl of the final solution was added to the gel band and incubated for 1 hour at 37°C. A further 10µl of the trypsin solution was added and incubated overnight at 37°C. Enzymatic digestion was terminated by adding 2µl 2.6M formic acid. Digests were dried using a Speed Vac and could be stored at -20°C until mass spectrometry analysis. Prior to LC-MS, 50µl high performance liquid chromatography (HPLC)-grade water was added to each gel band, sonicated for 10 min and centrifuged for 20 min at 13,000rpm.

2.5.2. HPLC – tandem mass spectrometry (HPLC-MS/MS) and protein identification using bioinformatics tools

In order to analyse the protein composition of venom fractions, whole venom samples (5mg/ml solution in 0.1% formic acid mobile phase buffer) were centrifuged at 13,000rpm for 20 min. Samples were fractionated in the first dimension via an ion-exchange 2mm x 50mm ProPac ® SCX-10G column over a gradient (600-900mM

NaCl in 0.1% formic acid, pH 2.3) at a flow rate of 60µl/min using an Ultimate 3000 system (Dionex, UK). Following this, the fractions generated (20 per sample) were subjected to second dimension fractionation over a gradient (2-90% acetonitrile in 0.1% formic acid over 50 min) at a flow rate of 300nl/min using a 300µm I.D. x 15cm capillary LC ion exchange column packed with 3µm PepMap™ C18 stationary phase. Eluted peptides were analysed on a LCQ Deca XP Plus Mass Spectrometer (ThermoFisher, UK), operating on a 'triple play' mode (zoom scan followed by MS/MS). Proteins were identified by screening LC-MS sequence data against Uniprot databases and a *B. arietans* venom gland EST database using Proteome Discoverer 1.0.0 (ThermoScientific) software incorporating both Sequest (ThermoScientific (Yates et al., 1996) and Mascot (Matrix Science Ltd, UK (Perkins et al., 1999) search algorithms. A parent mass tolerance of 1.5Da and fragment mass tolerance of 1Da were used, allowing for 1 missed cleavage. Carbamidomethylation of cysteine and oxidation of methionine were the fixed and variable modifications respectively. For Sequest, high confidence peptide matches were filtered with an XCorr cut-off (+1>1.5, +2>2 and +3>2.5) and for Mascot, an Exp value of less than 0.01 indicated a confident peptide match.

MOLECULAR BIOLOGY

2.6. Extraction of Poly(A) mRNA from venom using oligo (dT) magnetic Dynabeads®

Poly adenylated messenger RNA (poly(A) mRNA) was extracted from lyophilised venom samples using Dynabeads® mRNA DIRECT™ Kit (Dynal, Invitrogen) following a protocol adapted from Chen *et al* (Chen et al., 2002)(Figure 2.2).

Messenger RNA was isolated from venom following hybridization and capture by magnetic oligo $(dT)_{25}$ coated beads. 2mg lyophilised venom was reconstituted in 300µl lysis/binding buffer (100mM Tris-HCl, pH 7.5, 500mM LiCl, 10mM EDTA, pH 8, 1% LiDS and 5mM DTT). 50µl Dynabeads were washed in an equal volume of lysis/binding buffer before removing buffer after separation of beads on a magnet. Washed beads were incubated with the lysed venom sample by inverting at room temperature for 10 min. Unbound material was removed by placing on the magnet for 2 min. Beads were then washed twice using 600µl washing buffer A (10mM Tris-HCl pH 7.5, 0.15 M LiCl, 1mM EDTA and 1% LiDS) and once with 300µl washing buffer B (10mM Tris-HCl pH 7.5, 0.15M LiCl, 1mM EDTA). Poly(A) mRNA was eluted in 10µl Tris-HCl (10mM, pH 7.5) at 65-80°C for 2 min. Following the first elution of mRNA, unbound material was transferred back to the pre-washed magnetic beads and the mRNA isolation protocol was repeated once to ensure complete capture of mRNA from venom. Absorbance at 260/280nm and concentration of eluted mRNA was determined using the Nanodrop 1000 (ND-1000) Spectrophotometer and software (version 3.2.1). Messenger RNA was placed on ice and used immediately in first strand cDNA synthesis.

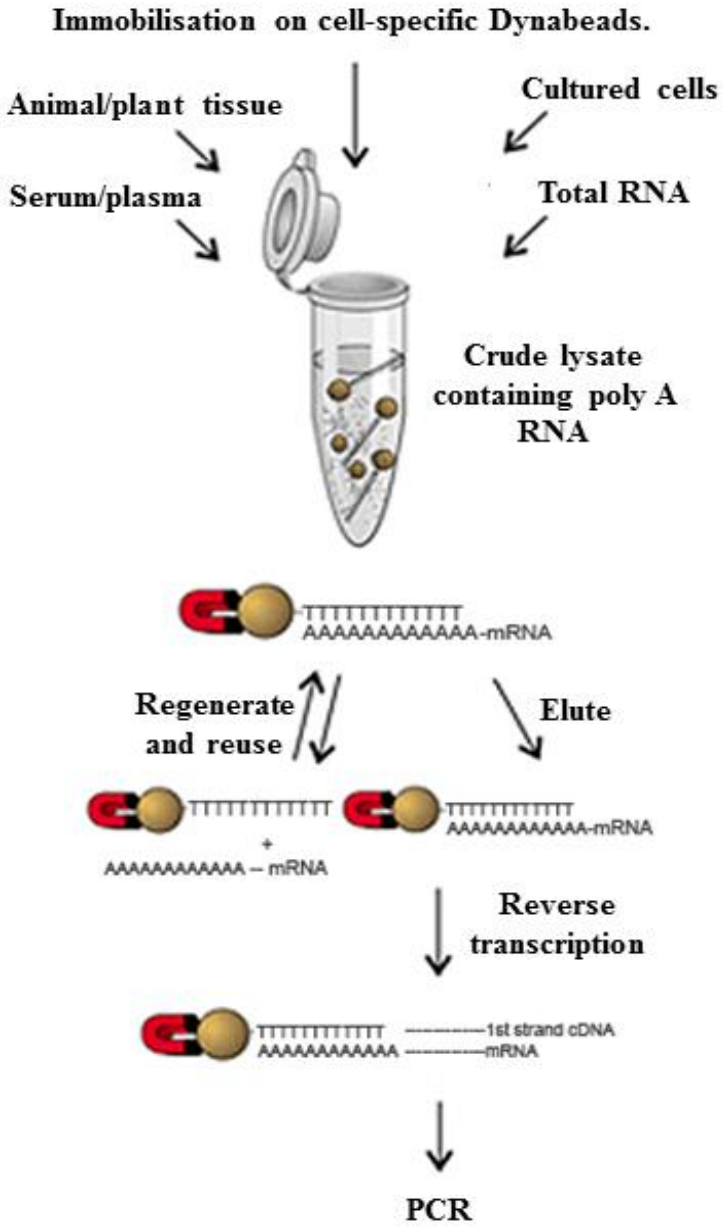

Figure 2.2 Extraction of poly(A) mRNA from venom using Dynabeads®: Flow diagram to show a direct approach for the extraction and PCR-amplification of mRNAs from snake venom and other biological materials.

2.7. First strand complementary DNA (cDNA) synthesis

cDNA synthesis was performed from mRNA previously extracted from venom using first strand Superscript III cDNA synthesis kit (Invitrogen, UK). 8µl 2-5ng/µl mRNA was added to each reaction tube containing 1µl primer (50µM oligo dT) and 1µl

10mM dNTP mix. Samples were incubated for 5 min at 65°C and placed on ice for 1 min. The cDNA synthesis master mix was prepared as follows (per reaction): 2µl 10x RT buffer, 4µl 25mM $MgCl_2$, 2µl 0.1M DTT, 1µl RNaseOUT (40U/µl), 1µl Superscript III RT (200U/µl). 10µl of the master mix was added to each reaction, gently mixed and incubated for 50 min at 50°C. The reaction was terminated following incubation at 85°C for 5 min. 1µl RNase H was added to each reaction and incubated at 37°C for 20 min. Confirmation and concentration of cDNA was performed using the ND-1000 Spectrophotometer. cDNA was used immediately in PCR or was stored at -20°C until required.

2.8. Plasmid purification of venom gland library cDNA for PCR positive control

A previously constructed *B. arietans* venom gland cDNA library using methods described in Wagstaff *et al* (Wagstaff and Harrison, 2006) was used as a positive control in polymerase chain reaction (PCR) experiments. 3ml sterile LB broth was inoculated with 2 x 200µl aliquots of the *B. arietans* venom gland cDNA library and incubated overnight at 37°C with vigorous agitation. Venom gland plasmid DNA was purified using the QIAprep Spin Miniprep kit (Qiagen, UK). All buffers were provided in the kit. 1.5ml of each culture was transferred to a 1.5ml eppendorf tube and centrifuged at 13,000rpm at 22°C for 1 min. Supernatant was discarded and 250µl *E. coli* resuspension buffer (P1 and RNase A) was added to re-suspend the bacterial pellet. 250µl *E. coli* lysis buffer (P2) was added and mixed well by inversion for 5 min to lyse bacterial cells. 350µl neutralisation buffer (N3) was added and mixed immediately by inverting the tube for 2 min. The mixture was centrifuged at 13,000rpm at 22°C for 10 min to pellet protein and genomic DNA. The

supernatant was applied to the QIA prep spin column, incubated at room temperature for 1 min and centrifuged at 13,000rpm at 22°C for 1 min. The flow-through was discarded. The column was washed with 0.5ml wash buffer PB and centrifuged for 30-60 seconds. Flow-though was discarded. A second wash with 750µl wash buffer PE was carried out, centrifuged for 1 min and the flow-through was discarded before repeating the wash with buffer PE. A dry spin was performed in order to remove any residual wash buffer and dry the column. To elute DNA, the spin column was inserted into a new 1.5ml eppendorf tube. 50µl MilliQ ultrapure water (Merck Millipore, UK) was pipetted directly onto the surface of the spin column and incubated at room temperature for 1 min. The column was centrifuged at 13,000rpm at 22°C for 1 min and plasmid DNA was placed on ice or stored at -20°C until use for PCR.

2.9. Polymerase chain reaction (PCR)

2.9.1. PCR primer design

PCR primers were designed to amplify a range of venom protein-encoding gene targets with varied representation in the *Bitis arietans* venom gland EST database. Primer design is discussed in greater detail in Section 4.3.4 in Chapter 4.

2.9.2. Conventional PCR

The GoTaq® PCR Core system I (Promega, UK) was used to perform conventional PCR. PCR master mixes were prepared per reaction as follows: 10µl 5 x PCR buffer, 4µl $MgCl_2$, 1µl dNTPs, 2.5µl 5' primer, 2.5µl 3' primer, 0.25µl *Taq* polymerase,

28.75µl MilliQ ultrapure water (Merck Millipore, UK). 49µl of the master mix was added to 1µl venom gland cDNA in 0.2ml thin-walled eppendorf tubes. Following successful amplification of gene targets from venom gland cDNA, identical reactions were performed from venom cDNA. In this instance, 2µl of venom cDNA per PCR reaction was used (volume of MilliQ ultrapure water per reaction was adjusted to 27.75µl). Samples were mixed thoroughly before initially undergoing the following amplification programme:

- Step 1: Denaturation 94°C, 5 min.
- Step 2: Denaturation 94°C, 1 min; annealing step 55°C, 1 min; extension 72°C, 1 min. Repeat for 35 cycles.
- Step 3: Final extension 72°C, 7 min. Maintained at 4°C.

As all primer pairs were designed with similar melting and annealing temperatures, PCR amplification was carried out using an annealing temperature of 55°C. Following initial PCR amplification as described above, we observed several non-specific PCR products. To optimise the PCR amplification and improve specificity, we elected to perform a touch-down PCR programme. Touch-down PCR was used to facilitate the binding of primers to specific sequences and avoid non-specific binding. A touch-down PCR programme was designed, beginning with a high annealing temperature (i.e. near to the primer melting temperature) to ensure highly specific annealing of primers sequences. The temperature was gradually decreased to a lower temperature which would be more tolerable to non-specific binding and therefore increase the overall yield of the amplicon.

A touch-down programme was employed as follows:

- Step 1: Denaturation 94°C, 5 min.

- Step 2: Denaturation 94°C, 1 min; annealing step 66-55 °C, 1 min; extension 72°C, 1 min. Repeat for 35 cycles.
- Step 3: Final extension 72°C, 7 min. Maintained at 4°C.

Agarose-ethidium bromide (Agarose-EtBr) gels were prepared by melting a solution of 1% agarose in 1X Tris-Acetate-EDTA (TAE) buffer for 2-3 min or until agarose was completely dissolved. The molten agarose was cooled to ~50-55°C and 10-20µl ethidium bromide was added. The solution was gently mixed and poured into the gel casing containing the appropriate size well comb and left to solidify for 1 hour. To analyse the amplicon, 5µl of the PCR reaction was added to 5µl dH_2O and 2µl 6X DNA loading buffer. The PCR reaction mixture was run on the 1% agarose-EtBr gel for 1 hour-90 min at 100V alongside 5µl marker (Benchtop DNA ladder, Promega, UK) in an electrophoresis tank filled with 1X TAE buffer. PCR products were visualised on the gel using a UV light box or transilluminator.

2.9.3. Purification of PCR products

Amplicons from conventional PCR experiments were purified and tested as a standard for subsequent quantitative PCR (qPCR) experiments. Firstly, 45µl of each product was run on a 1% agarose-EtBr gel for 1 hour. Bands were visualised using the UV transilluminator and excised using a clean scalpel blade. Excised bands were cut into small pieces and transferred into an eppendorf tube and weighed. The Wizard PCR clean-up system (Promega, UK) was used to purify products and all solutions/reagents used were provided in the kit. Firstly, 10µl of the membrane binding solution was added per 10mg gel slice. The gel band was dissolved by incubating at 60°C for 2 min and mixing by vortex for a few seconds; this process

was repeated until the gel band was completely dissolved. A mini-column was inserted into a collection tube and the molten gel solution was transferred onto the column. Following incubation at room temperature for 1 min, the mixture was centrifuged for 1 min at 16,000 x *g*. The flow-through was discarded and the mini-column was re-inserted into the collection tube. To wash the column, 700µl membrane wash solution was added, centrifuged for 1 min at 16,000 x *g* and the flow-through discarded. A further 500µl membrane wash solution was added and centrifuged for 5 min at 16,000 x *g*. The collection tube was emptied and re-centrifuged for 1 min with the inner centrifuge lid removed to allow evaporation of excess ethanol in the membrane wash solution which could affect subsequent analysis of DNA. Following the final wash, the mini-column was transferred into a clean 1.5ml eppendorf tube, 50µl nuclease-free water was added directly onto the mini-column filter surface and incubated at room temperature for 1 min. A final centrifuge at 16,000 x *g* for 1 min was carried out. The mini-column was then discarded and DNA collected in the eppendorf tube was stored at -20°C until further use.

2.9.4. Quantitative PCR (qPCR)

The KAPA SYBR® FAST qPCR Kit (KAPA Biosystems, AnaChem) containing 2X qPCR master mix (DNA polymerase, SYBR green fluorescent dye, $MgCl_2$, dNTPs and stabilisers) was used for all qPCR experiments. Briefly, 11µl PCR reactions were prepared by adding 10µl master mix (containing 0.22µl forward primer (10µM), 0.22µl reverse primer (10µM), 5.5µl KAPA SYBR green dye and 4.06µl ultrapure water) to 1µg of each cDNA sample in a 1µl volume. QPCR reactions were

performed using the BioRad CFX 384 real-time PCR system using a two-step PCR program and data was analysed using the CFX manager software. Detailed descriptions of the optimisation and standardisation of qPCR experiments can be found in Chapter 4.

2.10. Isolation and characterisation of venom-encoding genes by genome walking protocols

2.10.1. Genomic DNA isolation

Liver tissue was harvested from an adult *B. arietans* specimen in 2006 and immediately frozen in liquid nitrogen. 25mg frozen tissue was gently ground in liquid nitrogen and transferred to a 1.5ml eppendorf tube. Genomic DNA was isolated according to the DNeasy Blood and tissue Kit (Qiagen, UK). 180µl of buffer ATL and 20µl Proteinase K was added to the tissue sample, mixed thoroughly by vortexing and incubated at 56°C until tissue was completely lysed. 200µl buffer AL was added to the sample and mixed thoroughly by vortexing. 200µl absolute ethanol was added to the sample and immediately mixed thoroughly by vortexing in order to yield a homogenous solution. The solution (including any precipitate) was pipetted onto the DNeasy Mini Spin column placed in a 2ml collection tube and centrifuged at 8000rpm for 1 min. The spin column was placed in a new collection tube, 500µl buffer AW1 was added and centrifuged 8000rpm for 1 min. The spin column was placed in a new collection tube and 500µl buffer AW2 was added and centrifuged at 13,000rpm for 3 min to dry the membrane to ensure that no residual ethanol remained on the membrane. The spin column was placed into a clean 1.5ml eppendorf tube, 200µl buffer AE was pipetted directly onto the surface of the

membrane and incubated at room temperature for 1 min then centrifuged at 8000rpm for 1 min for elute genomic DNA. Elution of DNA was repeated for a second time using a new eppendorf tube to increase the overall yield of DNA. Genomic DNA at a concentration of approximately 0.1µg/µl was eluted and stored at -20°C until further use.

2.10.2. Quality assessment of genomic DNA

0.1-10µg genomic DNA isolated from *B. arietans* liver tissue was analysed on a 0.6% agarose-EtBr gel alongside 1µg human control genomic DNA to assess the quality of genomic DNA. Genomic DNA purity was assessed by performing *DraI* digestion. 0.1µg-10µg *B. arietans* genomic DNA was added to 1.6µl *DraI* (10units/µl), 2µl 10X *DraI* restriction buffer and 11.4µl MilliQ ultrapure water (Merck Millipore, UK). An identical reaction was also prepared using 1µg human control genomic DNA and negative controls where *DraI* enzyme was substituted for water. Reactions were gently mixed and incubated overnight at 37°C. 5µl of each reaction was analysed on a 0.6% agarose-EtBr gel alongside undigested genomic DNA to visualise DNA smearing following digestion.

2.10.3. Genomic library construction using GenomeWalker^{TM} Kit

Genome walking experiments were performed using the GenomeWalker^{TM} Universal kit (ClonTech, UK). Four digestion reactions containing *B. arietans* genomic DNA were set up – one for each of the restriction digestion enzymes included in the library construction kit; *DraI*, *EcoRV*, *PvuII* and *StuI* creating four DNA libraries (DL1-4).

Additionally, one *PvuII* digestion of human genomic DNA was set up as a positive control. 25µl of genomic DNA at a concentration of 0.1µg/µl was transferred to a labelled eppendorf tube. 8µl of restriction enzyme (10 units/µl), 10µl 10X restriction buffer and 57µl dH_2O was added and mixed gently. Digestion reactions were incubated at 37°C for 2 hours. Each reaction was gently vortexed for 5-10 seconds and returned to 37°C for overnight incubation. Following digestion, 5µl of each reaction was removed and analysed on a 0.6% agarose-EtBr gel to determine whether digestion was complete. Digested genomic DNA was then purified. Firstly, 95µl of phenol was added to each DNA digest and mixed by gently vortexing for 5-10 seconds. The mixture was briefly centrifuged to separate aqueous and organic phases. The upper aqueous phase was transferred into a new 1.5ml eppendorf tube and the lower organic layer was discarded. To each tube 95µl chloroform was added and mixed by gently vortexing for 5-10 seconds. The mixture was briefly centrifuged to separate aqueous and organic phases. The upper aqueous phase was transferred into a new 1.5ml eppendorf tube and the lower organic layer was discarded. To each tube, 190µl ice cold 95% ethanol, 9.5µl 3M NaOAc (pH 4.5) and 20µg glycogen was added and mixed by gently vortexing for 5-10 seconds. The mixture was centrifuged at 13,000rpm for 15 min at 4°C. The supernatant was discarded and the pellet was washed in 100µl of ice cold 80% ethanol. The mixture was centrifuged at 13,000rpm for 10 min. The supernatant was discarded and the pellet was air dried. The pellet was dissolved in 20µl TE 10/0.1 (10mM Tris, 0.1mM EDTA pH 7.5) by gently vortexing for 5-10 seconds. From each reaction, 1µl was removed and visualised on a 0.6% agarose-EtBr gel to confirm DNA. The GenomeWalker^{TM} adaptor (shown in Figure 2.3) was ligated onto the four blunt-end digestions of *B. arietans* genomic DNA and one positive control (restriction-digested human genomic DNA). 4 µl

digested and purified DNA was transferred into a fresh 0.5ml eppendorf tube into which 1.9µl GenomeWalker adaptor (25µM), 1.6µl 10X ligation buffer and 0.5µl T4 DNA ligase buffer (6 units/µl) was added and incubated at 16°C overnight. To stop the reactions, tubes were incubated at 70°C for 5 min. To each tube 72µl TE 10/1 (10mM Tris, 1mM EDTA pH 7.5) and mixed by gently vortexing for 10-15 seconds.

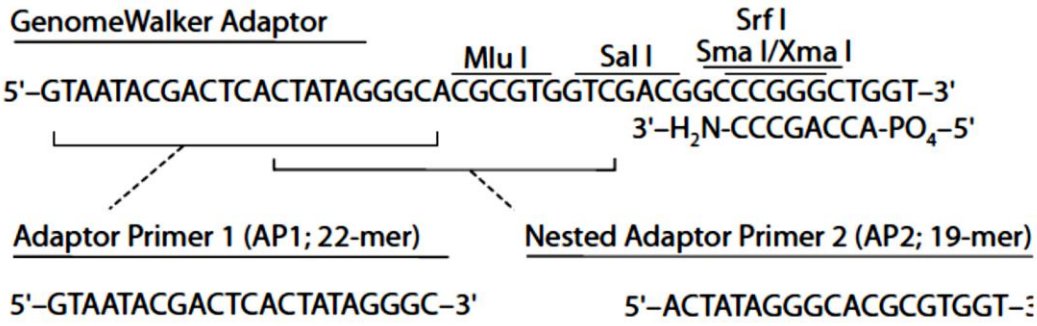

Figure 2.3 The GenomeWalker adaptor: Structure of the GenomeWalker™ adaptor which was ligated to both ends of the genomic DNA fragments to create genome walker libraries. The amine group on the lower strand of the adaptor blocks extension of the 3' end of the adaptor-ligated genomic fragments, thus preventing formation of an adaptor primer 1 (AP1) binding site of the general population of fragments.

2.10.4. Genome walking PCR primer design

PCR primers were designed to amplify a region of genomic DNA upstream of the transcription start site with the aim of obtaining sequences containing regulatory elements. For each gene of interest, two gene-specific reverse primers were designed; one for primary PCR and one for secondary (nested) PCR. The primary gene-specific primer was designed to be positioned as close to the 5' end of the coding region of the gene as possible. Primer pairs were designed to anneal to the highly conserved regions of the signal peptide of each venom protein group target including SVMP,

SP, CTL, LAO, VEGF, KTI, QKW and PDI. Primers were 28 nucleotides in length, aimed to have a GC% content of approximately 40% and similar melt temperatures of 65-70°C. The secondary gene-specific primer was designed to anneal to sequences beyond the 3' end of the primary primer and avoid overlapping of primary and secondary sequences. Forward primers, which were designed specifically to bind to the adaptor sequence ligated onto genomic DNA during genome library construction, were provided in the GenomeWalker^{TM} Universal kit (ClonTech, UK). Primer sequences are shown in Table 7.1 in Section 7.3.4 of Chapter 7.

2.10.5. Long range PCR amplification of genomic DNA and purification of PCR products

Amplification from genome walker libraries was carried out using the Advantage 2 PCR kit (ClonTech, UK). Positive controls included amplification of human tissue-type plasminogen activator (tPA) from a human *PvuII* genome walker library and a pre-constructed human genome walker library provided in the kit A master mix containing 5µl 10X Advantage 2 PCR buffer, 1µl GSP1 (10µM), 1µl AP1 (10µM), 1µl 50X dNTP mix (10mM), 1µl 50X Advantage 2 Polymerase mix and 40µl PCR grade water per reaction was added to 1µl of each genomic DNA library (DL1-4). The following thermocycling protocol was conducted: 7 cycles; 94°C 25 seconds, 72°C for 3 min, 32 cycles; 94°C for 25 seconds, 67°C for 3 min followed by extension for 7 min at 67°C. 5µl of the PCR reaction was visualised on a 1% agarose-EtBr gel. For secondary PCR, 1µl primary PCR amplicon was diluted in 49µl PCR-grade water and 1µl was added to a master mix (containing 5µl 10X Advantage 2 PCR buffer, 1µl GSP2 (10µM), 1µl AP2 (10µM), 1µl 50X dNTP mix

(10mM), 1µl 50X Advantage 2 Polymerase mix and 40µl PCR grade water per reaction). The following thermocycling protocol was conducted: 5 cycles; 94°C for 25 seconds, 72°C for 3 min, 20 cycles; 94°C for 25 seconds, 67°C for 3 min, followed by extension at 67°C for 7 min. 5µl of the PCR reaction was visualised on a 1% agarose-EtBr gel.

For cloning, PCR products were purified according to recommendations from the TOPO XL PCR cloning kit (Invitrogen) using the S.N.A.P^{TM} purification columns provided in the kit. 40µl of selected products was added to 8µl 6 x crystal violet loading buffer and separated on a 0.8% agarose gel containing 80µg crystal violet dye at 80V until the dye had migrated approximately ¼ of the way towards the negative terminal and thin blue bands of PCR product are visible. The gel was placed on a light box and single-band products were excised. The gel band was placed on parafilm, chopped up into small pieces and transferred into a 1.5ml eppendorf tube. The volume of the gel was estimated by weight (1mg = approx. 1µl). 2.5 times the gel volume of 6.6M sodium iodine was added to the gel and mixed well by vortexing. The gel was incubated at 42-50°C and mixed periodically by vortexing until completely dissolved. At room temperature, 1.5 times volume of binding buffer was added and mixed well by vortexing. The S.N.A.P^{TM} column was assembled in the collection tube. All of the dissolved gel mixture was added onto the column and centrifuged at 5600rpm for 30 seconds. The liquid collected in the tube was poured back onto the column and centrifuged again. The liquid from the collection tube was transferred back onto the column and centrifuged for a third and final time. The liquid in the collection tube was discarded. 400µl 1 x final wash buffer was added to the column and centrifuged at 5600rpm for 30 seconds. The liquid from the collection tube was transferred back onto the column and centrifuged. Liquid was

discarded and the column was centrifuged at 10,000rpm for 1 min to dry the column. The column was transferred to a clean 1.5ml eppendorf tube. 40µl TE buffer was added directly onto the column and incubated at room temperature for 1 min. To elute DNA bound to the column, the column was centrifuged at 10,000rpm for 1 min. DNA concentration was measured using the ND-1000 spectrophotometer, in addition, 10µl DNA was run on a 1% agarose-EtBr gel to visualise DNA.

2.10.6. Sub-cloning and transformation of *E. coli* with purified genomic PCR products

Sub-cloning of PCR products was performed using the TOPO® XL PCR cloning kit (Invitrogen, UK). Two cloning reactions for each PCR product were set up in order to optimise the efficiency of cloning. The first reaction contained 2µl purified PCR product, 1µl pCR XL TOPO vector and 2µl MilliQ ultrapure water (Merck Millipore, UK). The second reaction contained 4µl purified PCR product and 1µl pCR XL TOPO vector. Ligation reactions were mixed gently and incubated at room temperature. The incubation time was increased to 1 hour in order to improve the efficiency of cloning long PCR products. Following incubation, ligation reactions were terminated by adding 1µl 6X TOPO cloning stop solution and mixed at room temperature. Reactions were placed on ice. One vial of OneShot TOP 10 chemically competent *E. coli* cells (50µl) per ligation reaction was gently thawed on ice. 5µl TOPO cloning reaction was added to the vial of *E. coli* cells and mixed gently by inverting the tube. Tubes were incubated for 30 min on ice. This was followed by a heat shock at 42°C for 30 seconds, after which tubes were immediately placed on ice for 2 min. 250µl of SOC medium was added to each transformation tube and

incubated at 37°C for 1 hour while shaking horizontally. Two volumes of transformed cells (75µl and 230µl) of each transformation reaction was spread onto an IPTG/Xgal/Kanamycin impregnated agar plate and incubated overnight at 37°C to optimise bacterial growth.

2.10.7. Selection and amplification of recombinant *E. coli* colonies

Following overnight incubation, the ratio of blue: white (non-recombinant: recombinant) colonies of *E. coli* was recorded to assess the efficiency of ligation. For each plate, a sample of 5 white colonies was taken and transferred into a falcon tube containing 2ml of LB Kanamycin medium. Recombinant colonies were cultured overnight at 37°C with agitation.

2.10.8. Purification and analysis of recombinant plasmids by restriction enzyme digestion

Plasmid DNA from overnight *E. coli* cultures was purified using the QIAprep Spin Miniprep plasmid purification kit (Qiagen, UK). 1.5ml of each culture was transferred to a 1.5ml eppendorf tube and centrifuged at 13,000rpm at 22°C for 1 min. Supernatant was discarded and the pellet was resuspended in 250µl *E. coli* resuspension buffer. 250µl *E. coli* lysis buffer was added and mixed well for 5 min to lyse bacterial cells. 350µl neutralisation buffer was added and mixed well for 2 min. The mixture was centrifuged at 13,000rpm at 22°C for 10 min to pellet genomic DNA and protein. The spin column and collection tube was assembled. The supernatant was recovered and applied to the spin column, incubated at room

temperature for 1 min and centrifuged at 22°C for 1 min. The flow-though was discarded. 750µl wash buffer was added onto the spin column and centrifuged at 13,000 rpm at 22°C for 1 min and the flow-through was discarded before repeating the wash. A dry spin was performed in order to remove any residual wash buffer and dry the column. The spin column was inserted into a new 1.5ml eppendorf tube. 50µl MilliQ ultrapure water (Merck Millipore, UK) was pipetted directly onto the surface of the spin column and incubated at room temperature for 1 min. To elute DNA, the column was centrifuged at 13,000rpm at 22°C for 1 min and plasmid DNA was placed on ice. To determine the presence of inserts in plasmid constructs, restriction digestion of DNA was performed. 5µl plasmid DNA was mixed with 0.5µl *EcoRI*, 2µl Buffer H, 0.2µl BSA (10µg/µl) and 12.3µl MilliQ ultrapure water (Merck Millipore, UK) and incubated at 37°C for 4 hours to overnight. 4µl digests were analysed on a 1% agarose-EtBr gel to detect the presence of PCR product inserts.

2.10.9. Selection and submission of recombinant plasmids for DNA sequencing

A selection of plasmids containing inserts were submitted to Beckman Coulter Genomics for Sanger DNA sequencing in both directions using M13 forward and M13 reverse sequencing primers.

2.10.10. Bioinformatics interrogation of genomic DNA sequences

A bioinformatics pipeline was employed to describe the upstream region of genomic DNA and identify and characterise promoters and regulatory sequences of the gene.

Sequence data was analysed using DNASTAR. To assemble contigs from multiple fragments of the same gene, the forward and reverse sequences for each clone were assembled in SeqMan to create a single construct or contig from the sequences. The alignments were examined to identify any discrepancies and the nucleotide consensus nucleotide sequences were translated. Firstly, the est2genome (Mott, 1997) program was used to identify the specific gene sequence obtained following sub-cloning by screening the genomic sequence against the *B. arietans* EST database. The open reading frame for each contig was identified using the ORF finder tool from NCBI (NCBI, 2012b) and analysing each translation to identify the correct reading frame. Signal peptides were identified using SignalP server (version 4.0 (Bendtsen et al., 2004). Sequences were identified by performing a BLAST similarity search (NCBI, 2012a) against the nucleotide database. To map intron-exon boundaries in gene sequences, Wise2 algorithm (NCBI, 2012c) was used to compare translated protein sequences and genomic DNA sequences, allowing for frameshifting errors.

2.11. Ethical declaration

All animal experimentation involving snakes conducted during the course of this work was undertaken using protocols approved by The Liverpool School of Tropical Medicine Animal Welfare Committee and performed with licenced approval of the UK Home Office.

3. INTRA-SPECIFIC VARIATION IN VENOM OF THE AFRICAN PUFF ADDER (*BITIS ARIETANS*); DIFFERENTIAL EXPRESSION AND ACTIVITY OF THE SNAKE VENOM METALLOPROTEINASES (SVMPs)

The results of most of the work performed in this chapter have been published in Toxicon (Currier et al., 2010).

3.1. Abstract

Bitis arietans is considered one of the most medically significant snakes in Africa, primarily due to a combination of its extensive geographical distribution, common occurrence throughout sub-Saharan Africa and highly potent haemorrhagic and cytotoxic venom.

Our investigation has revealed a remarkable degree of intra-species variation between pooled venom samples from different geographical origins across sub-Saharan Africa and Arabia, and within a group of individual specimens from the same origin in Nigeria as determined by a combination of immunological, biochemical and proteomic assays. We demonstrate significant qualitative and quantitative differences between *B. arietans* venom in terms of protein expression, immunogenicity and activity of the snake venom metalloproteinases (SVMPs); toxins with a primary role in the haemorrhagic and tissue-necrotic pathologies suffered by envenomed victims. Specifically, we have identified a processed PII SVMP that exhibits striking inter-specimen variability. The findings of this chapter illustrate the degree of variation in venom composition from *B. arietans*, a venomous

snake of significant medical importance. These results are therefore important to therapeutic, biological and evolutionary venom research.

3.2. Introduction

The Puff adder, *B. arietans*, occupies a diverse range of habitats throughout the savannah areas of sub-Saharan Africa and parts of the Arabian Peninsula, regions which are also densely populated with people and livestock (Figure 3.1).

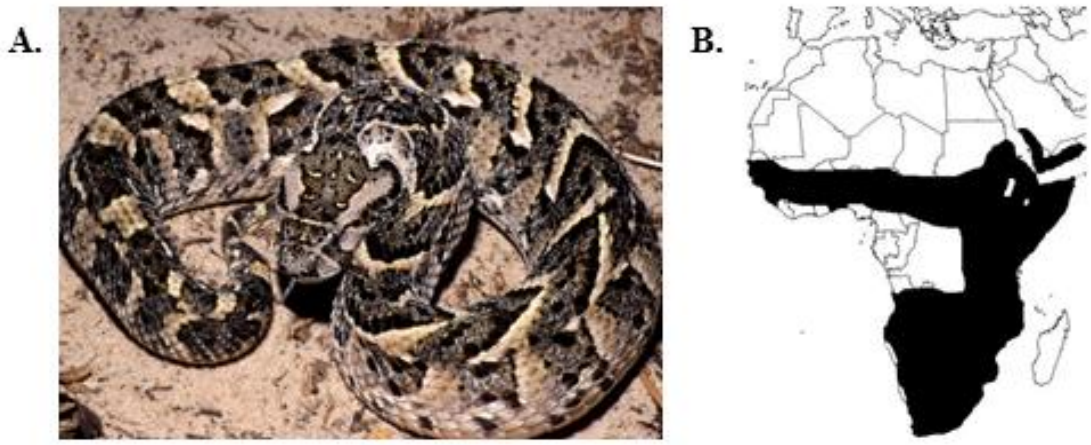

Figure 3.1 Adult *Bitis arietans* coloration and geographical distribution: A) An adult *B. arietans* specimen originating from Ghana (photograph courtesy of Wolfgang Wuster) and B) the widespread geographical distribution of *B. arietans* throughout sub-Saharan Africa.

The venom of this species is highly potent and typically interferes with the haemostatic system to cause severe local and systemic effects such as swelling, haemorrhage and necrosis (Warrell et al., 1975). Without antivenom treatment, *B. arietans* envenoming can have fatal consequences (Warrell et al., 1975). In Africa, it is estimated that snakebite accounts for up to 32,000 deaths per year, with many

more victims left with permanent disabilities and sequelae (Kasturiratne et al., 2008). The Puff Adder (*B. arietans*), the saw-scaled viper (*Echis ocellatus*) and the spitting cobra (*Naja nigricollis*) are responsible for the majority of these fatalities in Africa. The medical importance of *B. arietans* and its unusually extensive pan-African distribution for a single species make this species an ideal subject to investigate intra-species venom variation, not only from a biological and evolutionary standpoint, but also from the perspective of the possible consequences venom variation may have on the clinical symptoms of envenoming and patient response to antivenom.

Viper venom is a highly complex biologically active mixture typically containing numerous enzymatic and non-enzymatic components (Serrano et al., 2005), most of which are proteins and peptides enabling the rapid immobilisation, killing and digestion of envenomed prey. Variation in venom protein composition has been well documented on several taxonomic levels and particularly within species occupying wide geographical distributions. Several studies investigating inter-species venom variation have attributed their findings to factors such as specimen age, dietary and gender associated changes. Firstly, diet has been strongly linked to variation in venom protein composition and biological function. Daltry *et al* correlated variation in the protein composition and biological activity of *Calloselasma rhodostoma* venom to geographic location and phylogenetic relationships. Studies presented strong evidence for the association between variation in the venom of this species and its diet (Daltry et al., 1996a, Daltry et al., 1996b). Variation in venom protein composition between closely related subspecies of *Sistrurus* rattlesnakes determined by proteomics (Sanz et al., 2006) and in the venom toxicity of *Echis* species determined by LD_{50} assays (Barlow et al., 2009) have also been correlated with the selection of different toxins into the proteome of species with predominantly

mammalian or varied diets. Ontogenetic shifts related to specimen age (and dietary shifts in venom-specificity) will be described further in Chapter 5. Differences in venom between adult and juvenile venoms with respect to (i) coagulant activity of *Bothrops atrox* and *Crotalus atrox* venom (Lopez-Lozano et al., 2002) (Reid and Theakston, 1978) (ii) PIII to PI SVMPs in *B. asper* (Alape-Giron et al., 2008), and (iii) haemorrhagic and oedema-forming activities both in *B. atrox* and *B. asper* (Saldarriaga et al., 2003) have been demonstrated. Finally, examples of gender-specific differences in *B. jararaca* venom have also been demonstrated (Menezes et al., 2006) in respect of fibrinogenolytic and amidolytic properties, differential processing of bradykinin-potentiating peptides (Pimenta et al., 2007), and differential hyaluronidasic, haemorrhagic, coagulant, phospholipasic and myotoxic properties (Furtado et al., 2006).

While variation in venom composition has been described for members of the *Bitis* genus of less medical significance (e.g. *B gabonica gabonica*, *B. g. rhinoceros*, *B. nasicornis* and *B. caudalis*) (Calvete et al., 2007a, Calvete et al., 2007b), there have been no such studies on *B. arietans*, the most clinically important member of the genus. A previous investigation of *B. arietans* venom demonstrated that the proteome may be less complicated than originally predicted, containing proteins belonging to only a few major toxin families, the majority of which are SVMPs and to a lesser extent, SPs, disintegrins and CTLs (Juárez et al., 2006). The latter proteomic studies, in conjunction with our own venom gland transcriptomic results (Wagstaff and Harrison, unpublished) indicate that the composition of *Bitis* venom exhibits extensive isoform diversity, potentially within one of the most toxic groups of venom proteins, the SVMPs.

The primary aim of this study was to explore the *B. arietans* venom proteome and

determine the extent of variation between specimens from different or the same geographical origins, particularly within the major toxin groups responsible for the most significant clinical pathology. As much of the pathology of viper envenoming is caused by enzymes and venom is the immunogen used for antivenom preparation, we therefore elected to use biochemical assays of enzyme function and immunological assays, in addition to the standard proteomic techniques used to characterise venom proteome diversity, to produce a more comprehensive understanding of variation in *B. arietans* venom. The results of this work aimed to provide detailed analyses of the protein composition of *B. arietans* venom and gaining an insight into the levels of variability in the venom from this species, which we could later correlate with gene expression and transcriptomic analyses.

3.3. Materials and Methods:

3.3.1 Venom sample extraction and preparation

Individual venom samples extracted from 12 Nigerian and 6 Ghanaian wild-caught adult specimens were analysed. Individual snakes were maintained in the herpetarium at the Alistair Reid Venom Unit under identical climatic conditions where they were fed the same diet and the technique and frequency of venom extraction was identical for all animals. Following manual extraction, venom was frozen at -20°C, lyophilised and stored at 4°C until analysis. Following analysis, venom extractions from the same specimens were repeated to ensure reproducibility of observations. Pooled venom samples from *B. arietans* specimens originating from six different geographical origins across Africa and Western Arabia (Ghana, Nigeria, Zimbabwe, Malawi, Tanzania and Saudi Arabia) typically comprised multiple

extractions from larger pools (usually tens) of individual specimens had been reconstituted in phosphate-buffered saline (PBS) at 10mg/ml and stored at -80°C. To compare the levels of intra-species venom variation within groups of different viperid species, the protein composition of venom from individual Saw-scaled vipers (20 *Echis ocellatus*, Nigeria) and Desert horned vipers (18 *Cerastes cerastes*, Egypt) specimens was analysed.

3.3.2. Venom protein composition profiling by 1D SDS-PAGE

Lyophilised venom samples were reconstituted at 10mg/ml in PBS and diluted to 1mg/ml in reducing or non-reducing SDS-PAGE sample buffer and separated on 1mm 15% SDS-PAGE gels as described in Section 2.2 of Chapter 2.

3.3.3. Antibody cross-reactivity of venoms by immunoblotting

Gels were electro-blotted to 0.45µm nitrocellulose membranes using the manufacturer's protocols (BioRad) under reducing conditions as described in Section 2.3 of Chapter 2. Following blocking and washing, blots were incubated for 5 hours with the following primary antibodies diluted in blocking buffer; EchiTAb-Plus-ICP (an equine IgG polyspecific antivenom prepared against *E. ocellatus*, *B. arietans* and *N. nigricollis* venoms; Instituto Clodomiro, University of Costa Rica (Gutiérrez et al., 2005a) (1/1000 dilution), rabbits immunised with recombinant *E. ocellatus* SVMP epitope string [E. o α-SVMP-string] (Wagstaff et al., 2006) or sera from mice immunised with a DNA-encoding expression plasmid pVaxSec (Wagstaff et al., 2006) containing *E. ocellatus* VEGF clone Eo_venom_02G03 (Accession number:

DW360875) [E. o α-VEGF] (1/200 dilution). We elected to investigate the immunoreactivity of the SVMPs due to their abundance, toxicity and important pathological role in viperid envenoming. We also selected to analyse the immunoreactivity of VEGF. VEGFs are of interest due to the variation in structure and function that exists between different species of venomous snakes. A recent publication showed that barietin, a VEGF isolated from *B. arietans* venom, may be unique among the snake venom VEGFs as it is able to bind to heparin with a high affinity, despite apparently lacking the heparin binding sites in the C-terminal region present in other snake venom VEGFs (Yamazaki et al., 2009). It is therefore thought that barietin may demonstrate unique biological properties which require further investigation. Although the toxin-specific antibodies used were specific to *E. ocellatus* venom, previous investigation has demonstrated varying degrees of cross-reactivity with venoms of other viperid species, including *B. arietans* (Wagstaff et al., 2006). Blots were incubated with secondary antibodies, washed and developed as described in Section 2.3 of Chapter 2.

3.3.4. Venom enzyme activity profiling by substrate zymography

Zymography was carried out using gelatin and fibrinogen substrates to visualise the degradative activity of the enzymes present in viper venoms as described in Section 2.4 of Chapter 2.

3.3.5. Identification of venom proteins by LC-MS/MS

In-gel trypsin digestion, LC-MS/MS and protein identification protocols are

described in Section 2.5 of Chapter 2. Several protein bands of interest from SDS-PAGE profiles of individual Nigerian venom samples were excised from the gel as a discrete entity (see Figure 3.2 and Table 3.1). Protein bands of interest which were expressed in more than one individual viper were excised from all those individuals to ensure reproducibility and accuracy of the identification.

3.4. Results:

3.4.1. Variation in venom composition between *B. arietans* specimens from different geographical origins:

Protein profile

We observed variation in venom protein profiles separated by reducing and non-reducing SDS-PAGE of pooled venom from *B. arietans* specimens originating in Ghana, Saudi Arabia, Nigeria, Zimbabwe Malawi and Tanzania (Figure 3.2Ai and ii). Saudi Arabian venom had the most distinct venom protein profile in comparison with the African samples; this was most evident under reducing SDS-PAGE conditions as a distinct protein of approximately 22kDa (Figure 3.2Aii[1]) present in the African venoms was clearly lacking in the Saudi Arabian venom. The variation between *B. arietans* venoms from within Africa was less striking. The Ghanaian, Nigerian, Zimbabwean and Malawian venoms showed a relatively similar protein profiles but the Tanzanian venom was markedly different; the 22kDa protein present in all other African venoms was at a much lower level in Tanzanian venom and this venom also contained a highly expressed protein of approximately 12kDa (Figure 3.2Aii[2]) which was either absent or present at a significantly lower level in other venoms.

Antibody cross-reactivity

We used toxin-specific antibodies to SVMPs (Wagstaff et al., 2006) and VEGF, (Figure 3.2Bi and ii) to further investigate toxin-class specific changes in expression between pooled venom samples. With respect to SVMP composition, immunoblot analysis, like the SDS-PAGE result, revealed that the Saudi Arabian *B. arietans* venom was substantially different from the African venoms as this sample presented very little SVMP reactivity to the antisera. Tanzanian venom also showed a unique, intense immunoreactivity with the SVMP antibody to proteins in the lower molecular mass region, approximately 14kDa (Figure 3.2Bi[A]) – possibly corresponding to a fragment of a metalloproteinase domain that underwent autolysis. This was a similar molecular mass to the uniquely expressed 12kDa protein (Figure 3.2Aii[2]) observed in this sample, suggesting that the protein may be a member of this enzyme family, although we were unable to obtain a confident LC-MS/MS identification to confirm this. The remaining African venoms showed similar SVMP immunoreactivity and all venom samples exhibited the same reactivity to the VEGF antibody. However, as the antisera used in these experiments were raised against *E. ocellatus* venom proteins, it is possible that some variation in immunoreactivity of venoms may be due to differences in antibody specificity, although cross-reactivity between African viper venoms has been observed.

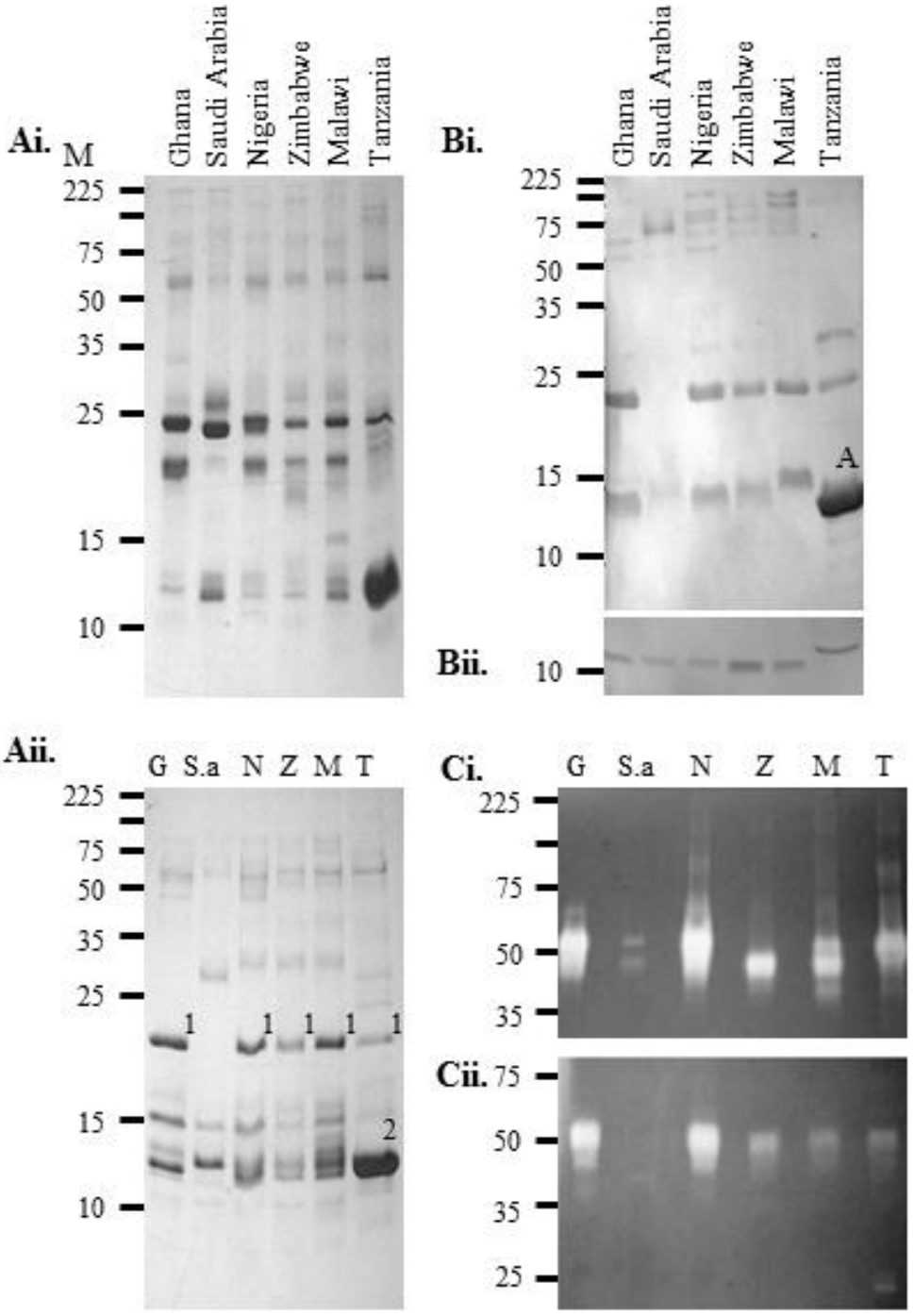

Figure 3.2 Analysis of pooled *B. arietans* venom samples from six different geographical origins: A) SDS-PAGE under i) non-reducing and ii) reducing conditions, B) reduced immunoblotting against i) *E. o* α-SVMP epitope string and ii) *E. o* α-VEGF antibodies and C) substrate zymography using i) gelatin and ii) fibrinogen substrates. Molecular weight markers (kDa) are shown on the left of each image. Note that migration on zymograms does not necessarily correspond with migration on SDS-PAGE or immunoblots due to differences in sample preparation conditions and the presence of substrate in the gels.

Enzyme activity

The substrate-degrading activity of SVMPs present in the *B. arietans* venoms varied significantly between samples from different geographical origins. With gelatin and fibrinogen zymography, the extent of substrate degradation by venom enzyme activity followed a general pattern of decreasing lytic activity as follows; Nigeria > Ghana > Malawi > Tanzania > Zimbabwe > Saudi Arabia (Figure 3.2Ci and ii). These activities do not display an obvious geographical trend. For example, *B. arietans* venom from the relatively closely neighbouring countries of Malawi, Tanzania and Zimbabwe exhibit varied fibrinogen- and gelatin-degrading activities. Similarly, Nigerian venom showed significantly greater gelatin and fibrinogen substrate-degrading ability compared to those specimens found in nearby Ghana. Saudi Arabian venom showed an unusual pattern of substrate degradation with an apparent doublet of weak gelatin-degrading enzyme activity but little detectable no fibrinogenolytic activity; a finding also consistent with the relatively low amounts of SVMPs in this venom detected by immunoblotting. Tanzanian venom also showed unique SVMP activity with a low molecular weight area of fibrinogen degradation not observed in other venoms.

3.4.2. Variation in venom between individual *B. arietans* specimens from the same geographical origin (Nigeria):

Protein profile

The extensive venom variation observed between *B. arietans* specimens from distinct geographical origins may have been due to compositional differences in venoms of

individual specimens. To address this, we examined the individual venom protein profiles of several Nigerian *B. arietans* specimens. No apparent differences were observed in non-reduced SDS-PAGE profiles (Figure 3.3Ai). We observed a remarkable variation in SDS-PAGE protein profile under reducing conditions between venom samples of individual snakes from the same origin (Figure 3.3Aii). There were subtle and more prominent variable components; the generalised profile shows significant qualitative differences confined to a molecular mass below 25kDa with the majority of high molecular weight proteins being more intra-specifically conserved. To ensure reproducibility of these observations, venom samples extracted on two different occasions were analysed by identical SDS-PAGE experiments, yielding identical results (Figure 3.4). On first observation, the group could be equally divided into two clades based on the presence or absence of a 23kDa molecular weight protein (Figure 3.3Aii[1]), the presence of which was not gender-specific as it could be observed in both male and female specimens. However, a more detailed examination of the low molecular weight components indicates that variation between individuals may be much more complex than was initially apparent. Thus, specimen BaN61 was noted to have a particularly unique protein profile due to the high expression of a protein of approximately 8kDa (Figure 3.3A[4]), which was either absent, or expressed a very low levels in other individuals. It is noteworthy that, whilst the pooled venom and individual venoms show broadly similar protein profiles on reduced SDS-PAGE gels (with prominent components around 50, 20 and 12-15kDa), they may differ in the presence of specific venom components. Since pooled venoms contain a more heterogeneous population of proteins (in terms of molecular mass and charge variations of isoforms) extracted from a larger pool of individuals, resolution of venom components from pooled

venoms is not always comparable with that of individual specimens.

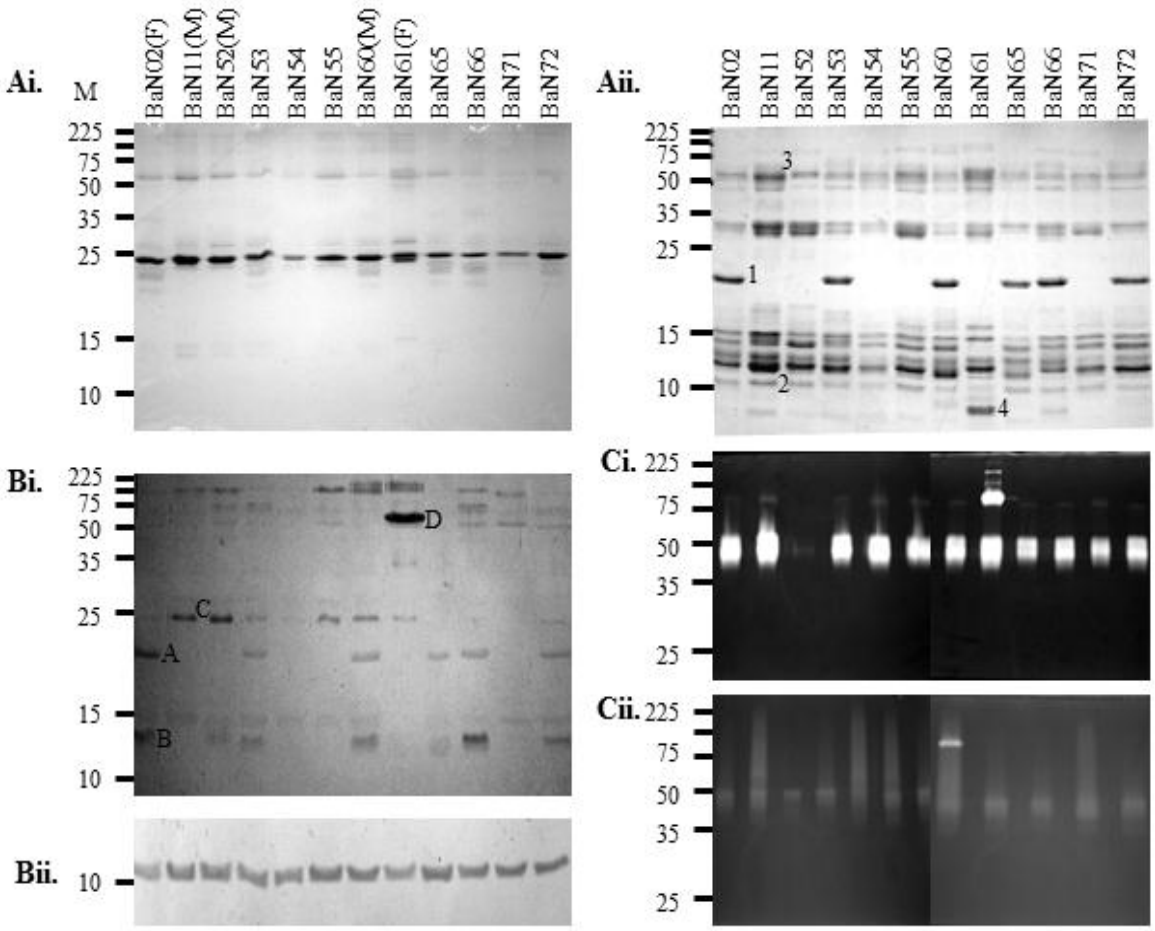

Figure 3.3 Analysis of individual Nigerian *B. arietans* venom samples: Ai) non-reduced SDS-PAGE and ii) reduced SDS-PAGE, B) reduced immunoblotting against i) E. o α-SVMP epitope string and ii) E. o α-VEGF and C) substrate zymography using i) gelatin and ii) fibrinogen substrates. Number in (Aii) illustrates proteins 1-4 which were excised and trypsin-digested for LC-MS/MS identification. Molecular weight markers (kDa) are shown on the left of each image. Note that migration on zymograms does not necessarily correspond with migration on SDS-PAGE or immunoblots due to differences in samples preparation conditions and presence of substrate in the gels. (F = Female, M = Male specimen)

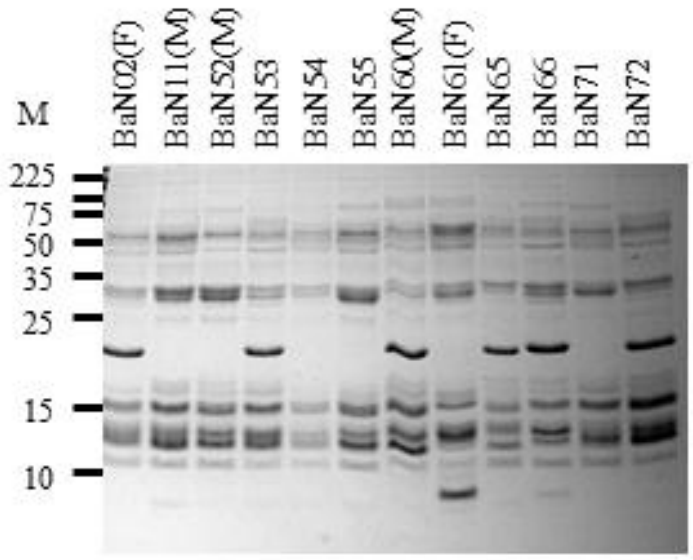

Figure 3.4 Reproducibility of venom protein profile of Nigerian *Bitis arietans* specimens: Venom samples extracted from Nigerian specimens on a different occasion to venom samples analysed in Figure 3.3Ai were analysed by identical SDS-PAGE experiments, yielding identical results. Molecular weight markers (kDa) are shown on the left of the image.

Antibody cross-reactivity

Immunoblotting with the Eo-SVMP string antibody revealed a high degree of variation in SVMP venom immunoreactivity (Figure 3.3Bi). We interpret these observations as reflecting variation in the expression, and/or differential processing, of SVMPs or disintegrins. Firstly, an immunoreactive protein of 23kDa (Figure 3.3Bi[A]) in venoms from six individuals (BaN02, 53, 60, 65, 66 and 72) was observed and appeared to correlate with the presence or absence of the variable protein of the same molecular mass clearly apparent on reduced SDS-PAGE (Figure 3.3A[1]). These individuals also share a common immunoreactive band of approximately 12kDa (Figure 3.3Bi[B]), interpreted as indicating the likely presence of an additional disintegrin. A variable 25kDa immunoreactive protein (Figure 3.3Bi[C]) was expressed in six individuals but the expression of this protein did not

co-vary with either the 12kDa or the 23kDa protein above. Of the high molecular weight proteins, an intensely immunopositive protein of approximately 70kDa was uniquely expressed in a single individual; BaN61 (Figure 3.3Bi[D]). In comparison, there was no variation between individuals in immunoreactivity when probed with the Eo-VEGF antibody (Figure 3.3Bii), indicating that the expression of this venom protein was more constitutive than that of the SVMPs.

Identification of individual venom components

We identified, by LC-MS/MS of excised protein, bands which were either significantly variable between individual *B. arietans* venoms (Figure 3.3A[1,4]) and venom proteins whose expression appeared to be highly conserved between individual specimens (Figure 3.3A[2-3]) (Table 3.1). The functional identity of venom proteins showing distinct expression profiles were determined by LC-MS/MS. The venom component exhibiting the most marked quantitative differences, a 23kDa protein (Figure 3.3A[1]), was confidently identified as an SVMP isoform (contig BAR00042 in our assembled *B. arietans* venom gland EST database) (Table 3.1). The predicted full-length protein sequence of BAR00042 (Figure 3.5) strongly suggests that it belongs with the PII class of SVMPs, containing a C-terminal RGD-containing disintegrin domain. The predicted molecular weight of the intact enzyme was 53kDa which did not correspond to the observed molecular weight of the protein band. However, the molecular weight (23kDa) and MS peptide data being exclusively recovered from within the catalytic metalloproteinase domain of the SVMP (Figure 3.5) indicated that the 23kDa protein was the processed metalloproteinase domain of a PII SVMP that lacks the disintegrin domain and not

the intact form of the enzyme. We identified further proteins (peptide sequences, ion scores, XCorr and probability values summarized in Table 3.1) which appeared to be more conservatively expressed throughout Nigerian *B. arietans* venoms. Firstly, an 11kDa protein (Figure 3.3A[2]), was identified as VEGF-encoding transcript BAR00040. A 50kDa protein (Figure 3.3A[3]) was identified as an LAO, BAR00017 (see Figure 3.5 for predicted protein sequences). Following several attempts to identify the second variable protein of interest; a unique low molecular weight protein clearly detected in the venom of only 1 of 12 *B. arietans* specimens, (Figure 3.3A[4]), we were unable to produce a confident match against either Uniprot, Serpentes or in-house generated *B. arietans* venom gland EST databases. Thus, this component most likely represents a novel, previously un-described snake venom protein whose identification remains the focus of further research in our laboratory.

										Mascot		Sequest	
Band number	**Molecular weight on gel (kDa)**	**MS-derived molecular weight (kDa)**	**Snake ID**	**Cluster**	**Protein family**	**Accession no.**	**m/z (Da)**	**z**	**MS/MS derived sequence**	**Ion score**	**Exp value**	**Probability**	**X Corr**
1	**23**	**55**	**BaN02**	BAR00042	PII-SVMP	CAJ01682	797.29	+2	SAAVVMNYQPEIDR	47	2.50E-05		
							864.30	+2	GLEMWSNGDLCTVTK	43	5.00E-05		
							805.24	+2	SAAVVMNYQPEIDR	42	6.20E-05		
							864.22	+2	GLEMWSNGDLCTVTK	35	2.90E-04		
							597.86	+2	SASDTLHSFAEWRER	18	1.70E-02		
							797.29	+2	SAAVVMNYQPEIDR			42.48	3.56
			BaN53	BAR00042	PII-SVMP	CAJ01682	856.21	+2	GLEMWSNGDLCTVTK	59	1.40E-06		
							797.24	+2	SAAVVMNYQPEIDR	40	1.10E-04		
							856.25	+2	GLEMWSNGDLCTVTK	36	2.40E-04		
							598.18	+2	SASDTLHSFAEWRER	28	1.80E-03		
							797.24	+2	SAAVVMNYQPEIDR			48.42	3.42
							598.18	+3	SASDTLHSFAEWRER			67.53	2.58
				BAR00220	No sig. hits		664.29	+1	ESDGEK	24	5.90E-03		
				BAR00133	No sig. hits		500.20	+1	LPGGR	20	9.20E-03		
			BaN60	BAR00042	PII-SVMP	CAJ01682	864.19	+2	GLEMWSNGDLCTVTK	43	4.80E-05		
							797.24	+2	SAAVVMNYQPEIDR	43	6.60E-05		
							805.17	+2	SAAVVMNYQPEIDR	34	4.00E-04		
							856.32	+2	GLEMWSNGDLCTVTK	22	6.90E-03		
							797.24	+2	SAAVVMNYQPEIDR			62.17	3.68
			BaN65	BAR00042	PII-SVMP	CAJ01682	804.82	+2	SAAVVMNYQPEIDR	40	1.10E-04		
							805.16	+2	SAAVVMNYQPEIDR	28	1.70E-03		
							797.28	+2	SAAVVMNYQPEIDR	24	4.30E-03		
							797.28	+2	SAAVVMNYQPEIDR			50.96	3.07

			BaN66	BAR00042	PII-SVMP	CAJ01682	796.77	+2	SAAVVMNYQPEIDR	52	6.00E-06		
							855.74	+2	GLEMWSNGDLCTVTK	52	6.20E-06		
							805.18	+2	SAAVVMNYQPEIDR	39	1.30E-04		
							754.16	+2	SASDTLHSFAEWR	39	1.40E-04		
							598.14	+3	SASDTLHSFAEWRER	20	9.40E-03		
							796.77	+2	SAAVVMNYQPEIDR			64.16	4.06
							754.16	+2	SASDTLHSFAEWR			51.51	2.83
				BAR00220	No sig. hits		664.28	+1	ESDGEK	25	5.70E-03		
			BaN72	BAR00042	PII-SVMP	CAJ01682	856.16	+2	GLEMWSNGDLCTVTK	51	8.40E-06		
							805.21	+2	SAAVVMNYQPEIDR	48	1.50E-05		
							864.27	+2	GLEMWSNGDLCTVTK	43	4.80E-05		
							598.20	+3	SASDTLHSFAEWRER	25	2.90E-03		
2	**11**	**16**	**BaN11**	BAR00040	VEGF	ACN22038	695.21	+2	TVELQVMQVTPK	90	1.10E-09		
							686.80	+2	TVELQVMQVTPK	44	3.70E-05		
							622.16	+3	ETLVSILEEYPDKISK	38	1.40E-04		
							695.21	+2	TVELQVMQVTPK			84.43	4.16
							686.80	+2	TVELQVMQVTPK			32.21	3.63
3	**50**	**31**	**BaN53**	BAR00017	LAO	CAQ72894	611.72	+2	SAGQLYQASLGK	68	1.40E-07		
							611.74	+2	SAGQLYQASLGK	40	9.10E-05		
							611.72	+2	SAGQLYQASLGK			72.49	3.87
							611.74	+2	SAGQLYQASLGK			41.74	3.29
				BAR00490	No sig. hits		848.00	+4	FQEFDDAANLLAANP DAVTISIDEPTEKPKK	20	9.40E-03		
				BAR00220	No sig. hits		664.33	+1	ESDGEK	25	5.50E-03		
			BaN55	BAR00017	LAO	CAQ72894	611.66	+2	SAGQLYQASLGK	49	1.40E-05		
							612.05	+2	SAGQLYQASLGK	32	6.40E-04		
							611.66	+2	SAGQLYQASLGK			68.97	3.44
							612.05	+2	SAGQLYQASLGK			23.84	2.48
				BAR00083	Ecto-5'-	BAG82602	595.70	+2	MGKVFPAVEGR	34	5.20E-04		

					nucleoti-dase							
						595.70	+2	MGKVFPAVEGR			70.09	2.6
				BAR00535	No sig. hits	586.61	+4	KSPLETFLPETGSSLQGATSHR	20	9.90E-03		
4	**<10**	**N/A**	**BaN61**	No confident hits								

Table 3.1 LC-MS/MS identification of venom proteins: Variable and conserved venom proteins were excised and trypsin-digested from individual Nigerian *B. arietans* venom samples (Figure 2). The table includes a list of peptide sequences derived by mass spectrometry for each protein of interest, the protein family assigned to each protein and the accession number of the protein which corresponds to the closest protein match identified by BLAST search. Ion score and E values indicate protein identification by Mascot algorithm and Probability and XCorr correspond to protein identification by Sequest algorithm.

>BAR00042_1 Full-length cDNA encoding PII SVMP encoding RGD disintegrin

MIQVLLVIICLAVFPYQGSSIILESGNINDYEVVHPQKVTALPKGAAKQPEQK
YEDTMQYEFKVNGEPVVLHLEKNKGLFSKDYSETHYSPDGREITTKPPVEDH
CYYHGRIQNDADSTASISACNGLKGHFTLQGETYFIEPLKITDSEAHAVFKYE
NIEKEDEAPKMCGVTQTNWESDVPIKKASQLVATSEQHRSSDPIKYINVIVV
ADQRLVTYYKGELNKITTKVHQYFNTLNEMYRYFYIRPILRGLEMWSNGDL
CTVTKSASDTLHSFAEWRERDLLSRKKHDNAQLFTGAEFDGGIIGIAYVGTM
CDLKRSAAVVMNYQPEIDRAVAAIMAHEMGHNLGIRHDGNQCYCGADACI
MAPHISNPPPMYFSDCSWNDYNRFISTHNPQCIHNQPSRTVIVSPPVCGNKILE
QGEDCDCGSPANCQDRCCNAATCKLTPGSQCNYGECCDQCRFKKAGTVCRI
ARGDWNDDYCTGKSSDCPWNH

>BAR00040_1 Full-length cDNA encoding VEGF precursor

MAAYLLAVAILFCIQGWPSGTVQGEVRPFMEVYQRSVCQPRETLVSILEEYP
DKISKIFRPSCVAVLRCGGCCSDESLTCTSVGERTVELQVMQVTPKTLSSKIK
VMKFREHTACECRPRSGSRVNIGKHKRSPEEGEREPSSPLTPGSL

>BAR00017_1 Full-length cDNA encoding L-amino oxidase

MNVFFMFSLLFLATLGSCADDKNPLEECFREADYEEFLEIARNGLKKTSNPQ
HVVIVGAGMSGLSAAYVLAGAGHKVTVLEASERVGGRVRTHRNDKEGWY
ANLGPMRLPEKHRIVREYIRKFGLKLNEFVQETENGWYFIKNIRKRVWEVKK
DPGLLKYPVKPSEAGKSAGQLYQASLGKAVEELKRTNCSYMLNKYDTYSTK
EYLIKEGNLSPGAVDMIGDLLNEDSGYYVSFIESPEHDDIFAYEKRFDEIVGG
MDQLPTSMYRAIEKSVHFKA

Figure 3.5 Full and partial-length peptide sequences identified by LC-MS/MS from adult *Bitis arietans* specimens: Peptide searches against contigs assembled from our *B. arietans* venom gland EST database were performed to identify protein bands of interest (Figure 3.3Aii). Signal peptides predicted using Signal P (Bendtsen et al., 2004) are underlined. Peptides identified by LC-MS/MS are indicated by grey shaded areas. The RGD-containing disintegrin domain of BAR00042 (identified by BLAST search as Bitistatin) is highlighted in red and the metalloproteinase domain in blue. The RGD disintegrin tripeptide is boxed.

Sequence analysis of the intact PII SVMP isoform BAR00042, identified the disintegrin domain as bitistatin isoform D1 (Figure 3.5). Bitistatin D1 has been recognised as a major component of *B. arietans* venom (Juárez et al., 2006) and is classed as a long, RGD-containing disintegrin at around 80 residues in length.

Venom enzyme activity

Variation in the gelatinolytic and fibrinogenolytic activity of venoms between individual *B. arietans* from Nigeria was observed (Figure 3.3Ci and ii). Gelatin zymography demonstrated that venoms from most specimens shared a common region of substrate degradation. Two individuals showed unique activities. Firstly, BaN52 appeared to have significantly lower enzymatic activity compared with venoms from other specimens showing relatively little degradation of either gelatin or fibrinogen substrates. This could not be attributed to any obvious variable feature of the protein profile since other individuals, for example BaN11, BaN55 and BaN71, who shared similar SDS-PAGE venom protein profiles with BaN52 (Figure 3.3Aii), demonstrated higher degradative activities. Secondly, BaN61 showed a greater molecular mass range of activity with a clear area of degradation above the conserved area of activity in the other individuals. BaN61 also has a more distinctive SVMP profile in terms of SDS-PAGE composition and immunoreactivity (Figures 3.3A and 3.3Bi); it is possible that the unique high molecular weight SVMP solely present in the venom of BaN61 (Figure 3.3Bi) may contribute to this unusual activity. Notably, a similar region of degradation was observed in both gelatin and fibrinogen zymograms raising the possibility that the same, or similar venom components, may be responsible for both these activities. Overall, the variation

observed in substrate degrading activity profiles did not correlate well with observed changes in the venom protein expression profile on SDS-PAGE. This suggests a multiplicity of variation in proteins from subunit structure to catalytic activity/substrate specificity, and that perhaps some minor components may be responsible for highly specific activity. Thus, changes in enzymes expressed at relatively low levels, but with a high catalytic activity may not be immediately apparent or easily detected when analysing venom using the proteome or transcriptome alone.

3.4.3. Comparison with variation in venom of Ghanaian *B. arietans*

We compared the venom profiles of Nigerian *B. arietans* individuals with those of a smaller group of individuals of the same species from Ghana and detected very little intra-specimen variation in Ghanaian venom samples, whether examined by SDS-PAGE, immunoblots or substrate zymogram assays (Figure 3.6). Interestingly, the only observed evidence of variation between individual Ghanaian venoms was in the intensity of immunological reactivity to the VEGF-specific antibody (Figure 3.6B), which contrastingly appears to be conserved among Nigerian specimens (Figure 3.3Bii). Also, as a group, venoms from the Ghanaian specimens differed from the Nigerians in protein profile, with venom components present in Nigerian venom at a molecular weight of 33kDa (Figure 3.3Aii) that were absent of expressed at a much lower level in Ghanaian venom (Figure 3.6A). Here, it is important to note that the smaller group size of Ghanaian individuals used in the study (6 specimens in comparison to 12 Nigerian specimens) may be limiting the levels of variation observed between individuals and further variation in venom composition may be

observed by increasing the number of specimens in the study.

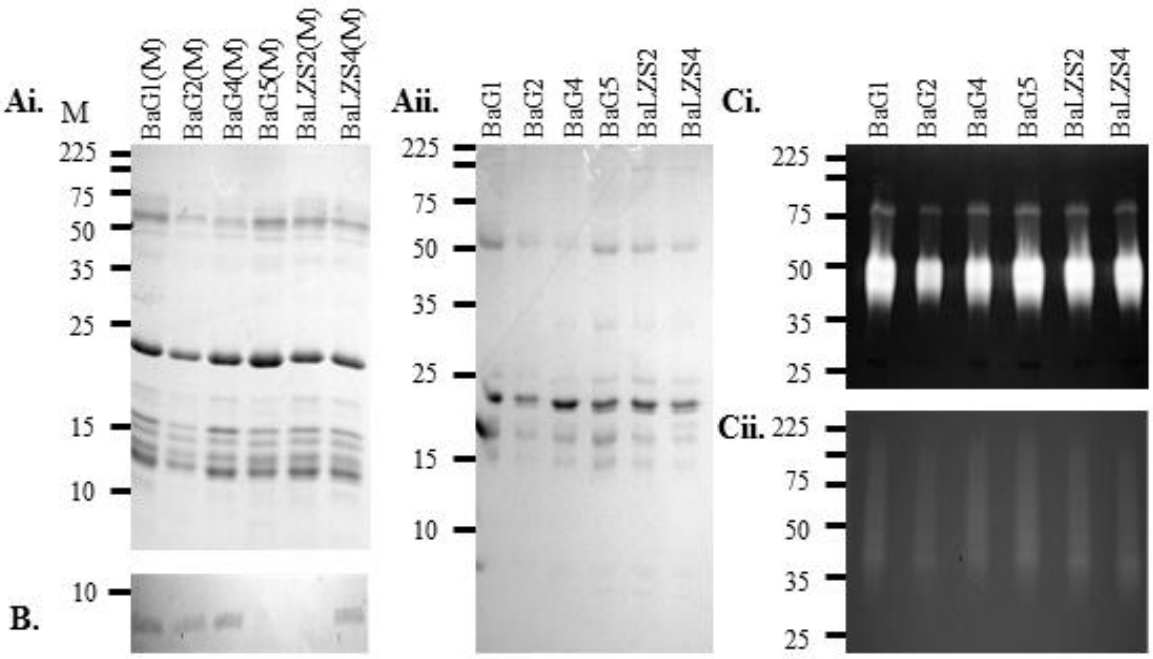

Figure 3.6 Analysis of individual Ghanaian *Bitis arietans* venom samples: Ai) reduced SDS-PAGE and ii) non-reduced SDS-PAGE, B) reduced immunoblotting against E. o α-VEGF and C) substrate zymography using i) gelatin and ii) fibrinogen substrates. Molecular weight markers (kDa) are shown on the left of each image. Note that migration on zymograms does not necessarily correspond with migration on SDS-PAGE or immunoblots due to differences in sample preparation conditions.

3.4.4. Comparison with variation in venom of *B. arietans* with other species, *Echis ocellatus* and *Cerastes cerastes*

To assess the extent to which intra-specimen variation in Nigerian *B. arietans* may also be reflected in venoms of other African vipers, we examined individual venom profiles of two other African viper species of medical importance; *Echis ocellatus* and *Cerastes cerastes*, using SDS-PAGE and zymography (Figure 3.7). This analysis revealed very little intra-specimen variation in the venom protein profile and enzyme

activity of individual *E. ocellatus* specimens (Figure 3.7Ai and Aii) and minor intra-specimen variation in the venom protein profile and enzyme activity of individual *C. cerastes* specimens (Figure 3.7Bi and Bii). Thus, the extensive variation reported here for Nigerian *B. arietans* venom is not necessarily reproduced to the same extent in the other African viper species examined. Interestingly, all *C. cerastes* venom samples showed a uniquely high molecular weight region of substrate degredation that was not apparent in *B. arietans* or *E. ocellatus* venoms, which was not reflected in the venom protein profile. These findings indicate that some low abundant venom components may be responsible for highly specific enzyme activity.

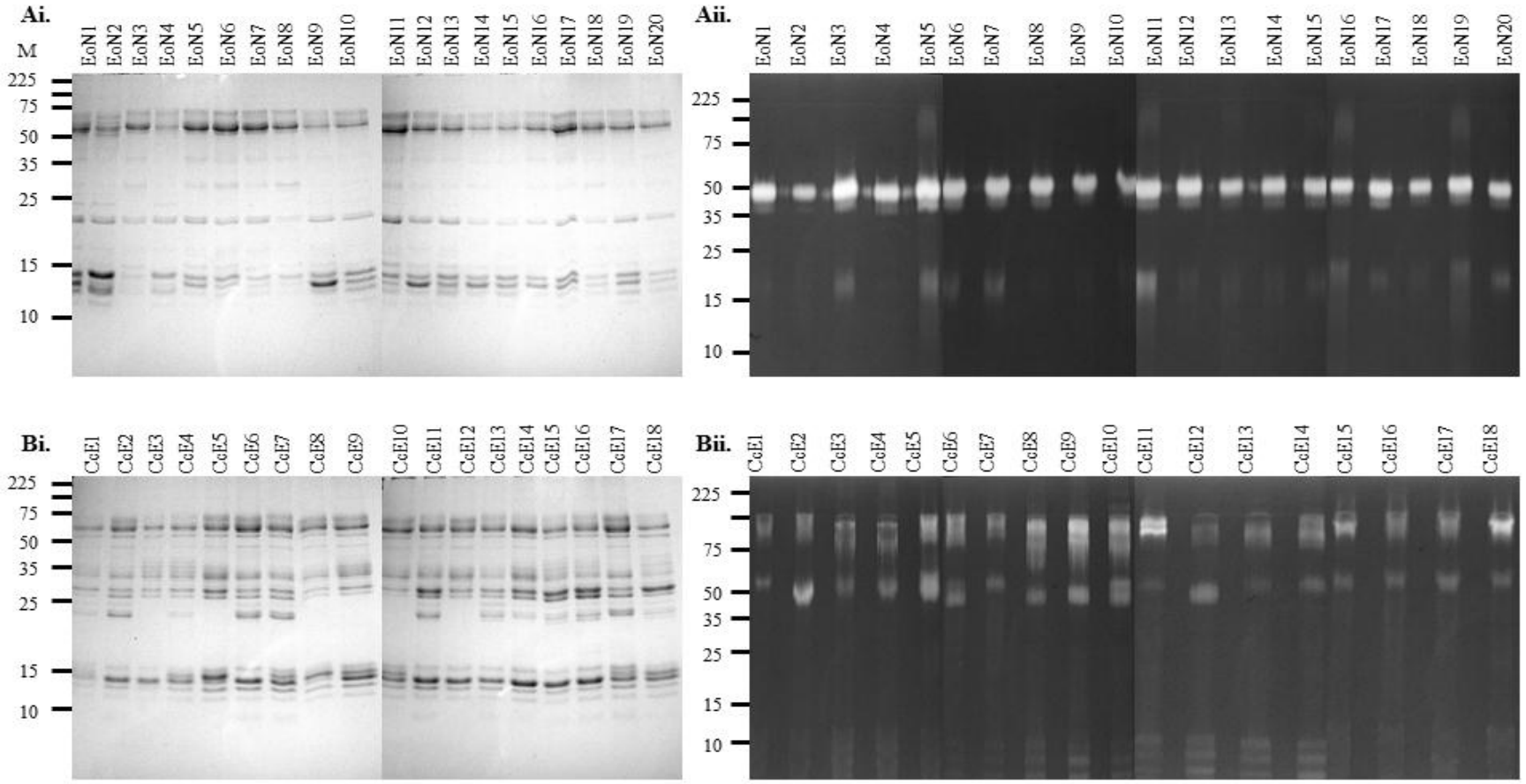

Figure 3.7 Analysis of other African viper venoms, Nigerian *E. ocellatus* (A) and Egyptian *C. cerastes* (B): by reduced SDS-PAGE (Ai, Bi) and gelatin zymography (Aii, Bii) illustrate the protein composition and enzyme activity of venoms respectively. Molecular weight markers (kDa) are shown on the left of each image. Note that migration on zymograms does not necessarily correspond with migration on SDS-PAGE due to differences in samples preparation conditions.

3.4.5. Variation in immunoreactivity of *B. arietans* venom towards Pan African polyspecific antivenom

Given the intra-specimen variation in *B. arietans* venom reported here, we examined the immunoreactivity of a polyspecific antivenom (EchiTAb-Plus_ICP, Costa Rica), which is currently used to treat *B. arietans* envenoming, to *B. arietans* venom pools from different geographical origins (Figure 3.8A) and between venoms extracted from several individuals from the same origin in Nigeria (Figure 3.8B) or Ghana (Figure 3.8C).

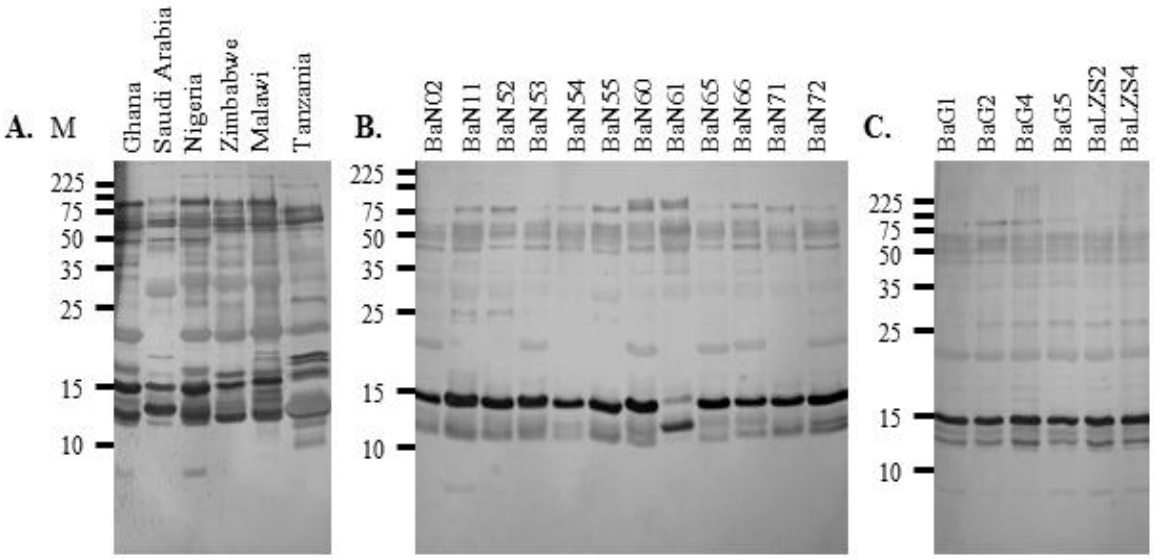

Figure 3.8 Immunoreactivity of *Bitis arietans* venoms to polyspecific antivenom: Reduced venom immunoblots probed with commercial pan-African polyspecific antivenom developed in Costa Rica (EchiTAb-Plus-ICP) against *B. arietans* venom samples from A) six different geographical origins, B) 12 individual Nigerian specimens and C) 6 individual Ghanaian specimens. Molecular weight markers (kDa) are shown on the left of each image.

Whilst the antivenom tested here seems to satisfy the requirements of broad protein specificity (assessed by immunoblotting), and has been proven successful in the

treatment of *B. arietans* envenoming (Nasidi, Warrell and Theakston, personal communication), antibodies to some rare/unusual transcripts, such as the unidentified venom component in Figure 3.3A[4], may be missing from antivenoms.

3.5. Discussion

Diversity in toxins, and shifts in venom composition and function, are considered a consequence of gene duplication and accelerated molecular evolution to recruit new proteins into the venom proteome and increase their diversity (Kordiš et al., 2002). The evolutionary driving force underpinning this isoform diversity is thought to include factors such as habitat, diet, gender or ontogeny. With such sharply contrasting expression profiles observed between individual venoms, we consider the variation identified here, which is apparently independent of influencing factors including environment, age, gender and diet, to be more biologically 'deliberate' than the gradual shifts expected as a result of random genetic drift. We have observed a high degree of qualitative and quantitative variation in several characteristics of venom including protein composition, immunoreactivity to toxin-specific antibodies and polyvalent antivenom and enzyme substrate-degradative capacity, leading us to conclude that *B. arietans* venom varies significantly between individuals in terms of its composition, immunogenicity and predicted function of perhaps the most pathologically important enzyme group in viper venom; the SVMPs. We have observed individual variation in the gelatinolytic and fibrinogenolytic activity of venom enzymes which may translate in differential symptomologies of envenoming. The most prominent variable component in venom composition was in the presence or absence of the BAR00042 isoform, the

proteolytically processed metalloproteinase domain of a PII RGD-containing SVMP, which was either present in significant quantities, or absent in 50% of individual specimens. We suggest several possible scenarios to explain this observed absence of this protein in some individual venoms; (i) the PII SVMP is not processed in some individuals and is present in the proteome at a higher molecular weight, (ii) the PII SVMP is present and processed in all individuals but the metalloproteinase domain in some individuals is unstable and cannot be detected, (iii) the PII SVMP is completely absent from the venom gland transcriptome in some specimens or iv) the PII SVMP is absent from the genome in some specimens. PII class SVMPs comprise of a metalloproteinase domain and an additional disintegrin domain which can be proteolytically processed from the metalloproteinase domain. Disintegrins, following release from the PII metalloproteinase through proteolytic cleavage, are potent inhibitors of platelet aggregation and function (Shebuski et al., 1989). RGD-containing disintegrins such as bitistatin have been shown to act through selectively blocking the binding of fibrinogen to the integrin $\alpha_{IIb}\beta_3$ receptor (Huang et al., 1987). Thus, differences in the proteolytic processing of disintegrins would be predicted to lead to an altered mechanism of action of venom. A protein band consistent with the predicted mass of bitistatin (8.6kDa) (Shebuski et al., 1989) although not evident on 15% SDS-PAGE gels, could be observed in all individual venoms separated on silver-stained 4-12% gradient gels (Figure 3.9). Overall, our data emphasizes the need for further work to characterize the precise bitistatin isoform products in venom due to the potential impact such components may have on the clinical effects of envenoming.

The full scale of intra-species variation in *B. arietans* venom is still not completely understood. From our SDS-PAGE, it appears that the presence of novel toxins in the

B. arietans venom proteome, particularly in the low molecular weight region, may be very likely and are yet to be identified. Further work is required to fully characterise the venom of this species to reveal novel and potentially important toxins which may play vital roles in envenoming or endogenous biological processes.

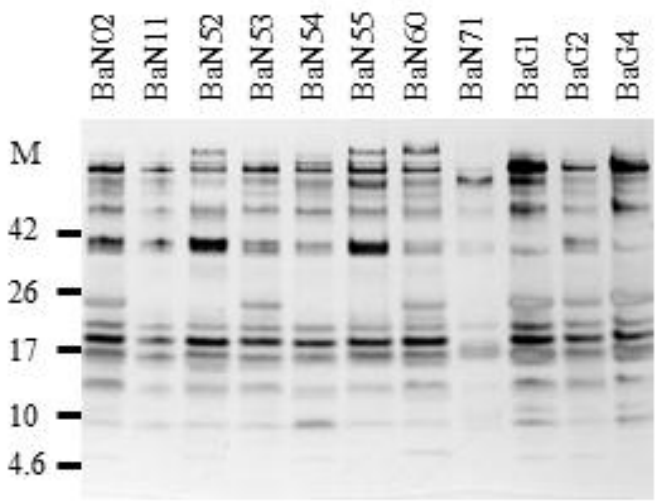

Figure 3.9 Analysis of low molecular weight protein components of *Bitis arietans* venom: A selection of venoms from individual *B. arietans* specimens originating from Nigeria and Ghana were separated by SDS-PAGE using 4-12% Bis-Tris gradient gels which were silver stained following protein separation. Low molecular weight range markers are shown to the left of the image.

In summary, *B. arietans* appears to be highly adaptive in terms of venom composition and activity and this can be reflected in their adept ability to inhabit a range of habitats over a wide geographical distribution throughout sub-Saharan Africa. It may be that this species has developed variable venom phenotypes, not only between specimens from different geographical regions but within groups occupying similar habitats. Our findings illustrate that there appears to be very little association between geographic location and similarity or differences in protein

expression or activity profiles of venom from *B. arietans* from different, and also the same geographic origin. This suggests that variation observed here may not be a simple consequence of pan-African random genetic drift and raises the possibility that African *B. arietans* could be regarded (at least in terms of venom phenotype) as a collection of subpopulations that have arisen as a result of differential evolutionary pressures such as prey type and availability or habitat (Barlow *et al* 2012, in preparation). Furthermore, such intra-species variation in venom may give rise to variability in the clinical manifestation of snakebite and ultimately affect the success of antivenom treatment. Although the current antivenom used to treat *B. arietans* envenoming appears to satisfy requirements, our findings emphasise that great care should be taken when selecting *B. arietans* specimens for antivenom production to ensure that the complete diversity of venom is considered.

The high degree of intra-species variation in venom between *B. arietans* specimens is also an important factor to take into consideration when conducting further studies including gene expression and transcriptome analyses of *B. arietans* venom. With such significant levels of individual variation in the *B. arietans* venom proteome, immunoreactivity and enzymatic function, we may also expect to observe levels of variation in the venom gland transcriptome and gene expression of venom proteins between individual specimens. Our observations in this chapter, therefore, highlight the requirement to accommodate for potentially high levels of variation in subsequent chapters in which aim to characterise the dynamics of gene expression of venom proteins.

4. OPTIMSATION OF QUANTITATIVE POLYMERASE CHAIN REACTION (PCR) PROTOCOLS; EXPLOITING VENOM AS A SOURCE OF MESSENGER RNA FOR GENE EXPRESSION ANALYSES.

4.1. Abstract

Messenger RNA (mRNA) has been demonstrated as a stable component of snake venoms. The ability to isolate mRNA encoding venom proteins from venoms therefore may provide an alternative source of genetic material for research, including real-time gene expression analyses of venom proteins. The objectives of this chapter were to optimise protocols for (i) isolating mRNA from *Bitis arietans* venom, (ii) amplifying specific venom protein-encoding transcripts from venom mRNA and (iii) detecting mRNA expression levels using a fluorescence-based quantitative PCR (qPCR) approach. The resultant optimised protocols would be applied to quantitatively track changes in gene expression during venom synthesis.

Quantitative PCR is an accurate and highly sensitive technique which can be used to simultaneously amplify and quantify DNA and has experienced a rapid rise in popularity and accessibility in recent years. Experiments require optimisation protocols for each new set of primer/DNA target combinations, thus we referred to the *M*inimum *I*nformation for publication of *Q*uantitative Real-time PCR *E*xperiments (MIQE) guidelines published 2009 which aim to ensure the generation of reliable, accurate, easily interpreted and reproducible qPCR experiments. Our results demonstrate the ability to detect and quantify gene expression levels of venom protein-encoding genes from mRNA extracted from venom in combination with fully optimised qPCR protocols.

4.2. Introduction

The overall aim of this work was to elucidate the time scale for the replenishment of venom proteins during venom synthesis and to investigate how venom synthesis is controlled and coordinated. The dynamics of venom protein gene expression and synthesis are currently little understood. This is primarily due to the limitations of current conventional methods used to interrogate venom gland transcriptional activity which requires sacrificing specimens for dissection of venom glandular tissue. Such studies prove difficult or unachievable and require an ethically unattractive sacrifice of a large number of snakes. The aim of the following work was to develop alternative protocols for investigating gene expression levels of venom proteins during venom synthesis. To enable real-time analysis of venom replenishment, we decided to exploit observations of previous studies which demonstrated an unusual presence and apparent stability of messenger RNA (mRNA) in venom and the use of venom as an alternative source of the transcriptionally active mRNA.

Messenger RNA was first shown as a stable component of snake venoms by Chen *et al* who demonstrated that intact mRNA can be recovered, and toxins can be PCR-amplified and cloned from lyophilised venoms (Chen et al., 2002). This key study demonstrated that, using magnetic oligo dT-coated beads, poly(A) mRNA could be isolated from the lyophilised venom of the Chinese Copperhead (*Deinagkistrodon acutus*), the black mamba (*Dendroaspis polylepsis*) and the venomous lizard species, Gila monster (*Heloderma suspectum*) (Chen et al., 2002). Successful PCR amplification and cloning of major toxin groups including an SVMP, PLA_2 and neurotoxin from mRNAs isolated from the venoms demonstrated that the mRNA present in venom appears to be intact and encodes for venom proteins (Chen et al.,

2002). Subsequent studies by this group demonstrated that mRNA could also be isolated from the toxic secretions of the Chinese toad (*Bombina maxima*) (Chen et al., 2003a), the fire-bellied toad (*Bombina orientalis*) (Chen and Shaw, 2003, Chen et al., 2005), and venom from the North African scorpion (*Androctonus amoreuxi*) (Chen et al., 2003b). Currently, very little is known about the properties of mRNA in venoms such as its purity, stability or function and whether mRNAs are constitutively observed in venoms from snakes of a variety of different taxonomic classification. However, the ability to obtain protein-encoding mRNA from venom appears to offer a non-evasive alternative approach to explore the transcriptional activity and gene expression of venom glands. This alternative technique circumvents the requirement to sacrifice specimens for venom gland dissection and may therefore have the potential to expand opportunities in venom transcriptomics, overcoming limitations of conventional techniques (Kwok et al., 2008).

To quantitatively track relative changes in venom protein expression, we elected to use quantitative PCR (qPCR) which has, in recent years, revolutionised DNA detection and analysis due to its high sensitivity, precision, resolution, ease of automation, increased dynamic range and minimal post-PCR processing in comparison to conventional PCR. Recent years have experienced a significant rise in the use of qPCR in many areas of research including gene expression quantitation, gene expression profiling, pathogen detection, drug efficacy testing and diagnostic applications (Bustin, 2000, Mackay et al., 2002, Bernard and Wittwer, 2002, Mackay, 2004, Kubista et al., 2006). The technology uses chemistries based on the addition of fluorescent DNA-binding dyes into the reaction, such as SYBR green I, which binds all double stranded DNA, and, once bound, emits green light. The specialised thermocycler-detector system in qPCR instruments both detects and

measures the levels of fluorescence following each successive cycle of PCR amplification, which is directly proportional to an exponential increase in the concentration of DNA. Whereas conventional (qualitative) PCR produces an endpoint DNA amplicon as a result of the total PCR amplification which can be visualised on an agarose-EtBr gel, qPCR generates an amplification growth curve which illustrates the amplification of DNA in real-time. qPCR can be applied in two approaches; absolute or relative DNA quantification. Absolute (or standard curve quantification) measures the DNA copy number of an unknown sample based on a standard curve which is prepared from a dilution series of a standard DNA template of known concentration. This approach is most applicable for use in diagnostics, for example, in quantifying pathogen load in an unknown infected sample. Relative quantification, which is the most widely used approach, enables the direct comparison of expression levels of two or more genes of interest, normalised against the expression of reference (housekeeping) genes, and therefore can be used to detect up- or down-regulation of the genes of interest, for example, in measuring gene response to drug treatment. The *M*inimum *I*nformation for *P*ublication of *Q*uantitative Real-time PCR *E*xperiments (MIQE) guidelines (Bustin et al., 2009)) were used as a guide throughout our qPCR experiment. The guidelines include information on experimental design, RNA sample quality and treatment, nucleic acid extraction, reverse transcription, qPCR primer design, thermocycling parameters, validation experiments and statistical analysis of data with the aim of producing accurate and reproducible qPCR data. By exploiting a combination of venom mRNA and highly sensitive qPCR protocols, we aim to develop and optimise non-invasive approaches through which we can track, in real-time, expression of venom proteins during venom synthesis.

4.3. Materials and Methods:

4.3.1. Venom sample preparation

In all PCR optimisation experiments, lyophilised West African *Bitis arietans* venoms extracted and pooled in 2009 and stored in a sealed container at 4°C was used as the source of mRNA.

4.3.2. Extraction of Poly(A) mRNA from venom using Dynabeads®

For PCR optimisation experiments, mRNA was extracted from 10mg lyophilised pooled West African *B. arietans* venom. Poly(A) mRNA was purified from lyophilised venom using Dynabeads® mRNA DIRECT™ Kit (Dynal, Invitrogen) as described in Section 2.6 of Chapter 2. To optimise mRNA extraction and determine the minimum quantity of mRNA required to yield mRNA amounts sufficient for cDNA synthesis and downstream PCR applications (e.g. ~ 10-20µg poly(A) mRNA in a volume of 20µl), mRNA was extracted from different quantities of pooled *B. arietans* venom ranging from 2, 10, 20, 50 and 100mg. The presence of DNA contamination of mRNA samples was evaluated by reverse transcriptase-negative controls and DNase treated mRNA. Alongside reverse transcriptase cDNA synthesis reactions, identical reactions were performed in the absence of the reverse transcriptase enzyme (referred to as no reverse transcriptase controls). For DNase treatment, DNase was added to duplicate mRNA samples and DNase treatment was performed prior to reverse transcription. PCR amplification from reverse transcriptase-negative and DNase treated controls was performed and products were analysed on a 1% agarose-EtBr gel.

4.3.3. Reverse transcription cDNA synthesis

cDNA synthesis was performed using the Superscript® III first strand synthesis system (Invitrogen) as described in Section 2.10 of Chapter 2.

4.3.4. Design of PCR primer pairs for conventional PCR and quantitative PCR reactions

PCR primers were designed to amplify a range of venom protein-encoding gene targets with varied representation in the *Bitis arietans* venom gland EST database (indicated by number of sequences in Table 4.1 and 4.2). These included class II snake venom metalloproteinases (SVMP) [BAR00042 and BAR00015], serine protease (SP) [BAR00034], phospholipase A_2 (PLA_2) [BAR00406], C-type lectins (CTL) [BAR00002 and BAR00012], L-amino acid oxidase (LAO) [BAR00017], vascular endothelial growth factor (VEGF) [BAR00040], Kunitz inhibitor (KTI) [BAR00023], disintegrin (DIS) [BAR00155], protein disulphide isomerase (PDI) [BAR00008] and QKW inhibitory peptides (QKW) [BAR00003]. Primers pairs were designed using Primer Select software (DNASTAR) complimentary to sequences within the coding regions of specific genes. Primers were designed to avoid primer dimers, secondary structures and hairpin loops, have a GC content of 40-60% and have similar melting and annealing temperatures (T_m) (Singh and Kumar, 2001). A different set of PCR primers were designed specifically for use in qPCR to amplify selected transcripts from the *B. arietans* venom gland EST database including a class II SVMP [BAR00042], SP [BAR00034], PLA_2 [BAR00406], CTL [BAR00012], LAO [BAR00017], VEGF [BAR00040], KTI [BAR00023], PDI [BAR00008] and QKW [BAR00003]. In addition, three housekeeping genes were selected as reference

transcripts including β-actin (ACTIN), glyceraldehyde 3-phosphate dehydrogenase (GAPDH) and heat shock protein (HEAT SHOCK), which are frequently used in the literature (Bustin et al., 2005, Vandesompele et al., 2002). The expression of reference genes was used as a baseline to which the expression of target genes was normalized. Three references were included to improve accuracy of normalization (Vandesompele et al., 2002). Reference gene primer pairs were designed on consensus sequences obtained from other snake species including *Oxyuranus scutellus, Laticauda semifasciata* and *Echis ocellatus* DNA sequences. Primer pairs for qPCR were designed to have approximately the same melting temperature to enable simultaneous amplification of gene targets, and an amplicon length of less than 200 base pairs. Primers were synthesised (Sigma, UK), reconstituted in MilliQ Ultrapure water (Merck Millipore, UK) to a concentration of 100μM stock solutions according to the manufacturer's instructions and diluted to 10μM working concentration for PCR.

Cluster ID	No. sequences	Toxin group	Forward primer (5'-3')	Reverse primer (5'-3')	Melting temp. °C
BAR00042	31	PII SVMP	ATGAGGCCCCCAAAATGTGT	AGCGCCTGTGAATAACTGAGC	F 55.4 R 53.7
BAR00015	90	PII SVMP	TCGGCCAGAAATAGATAGTGC	TCTCCCCTGTTGTTTAGTGATTC	F 51.4 R 51.8
BAR00406	2	PLA_2	TGCTGTTACGGGATAACGGCAGAA	CCGTTTTGGGGCCGCACTTA	F 61.4 R 61.4
BAR00034	19	SP	CTGCATGCGGTGGGACTTT	CTTTGTGCCGGTAATCGTTCATA	F 55.7 R 55.8
BAR00002	4	CTL	GGATCCATGGGGCGATTCATCTTC	CTCGAGTCAGGGAGCCTTGATCTC	F 63.2 R 59.4
BAR00012	6	CTL	GGATCCATGGGGCGATTCATCTTC	CTCGAGCTATACCCGGTACTTGCA	F 63.2 R 58.6
BAR00040	14	VEGF	GGATCCATGGCTGCGTACCTGCTG	CTCGAGTCAAAGGGATCCTGGAGT	F 65.3 R 58.7
BAR00017	14	LAO	CTCCCAAGAATTCCCATCCACA	GCGCTTTTGCCTGCTTCTGA	F 57.4 R 57.9
BAR00155	2	DIS	CCGCATAGCAAGGGGTGAT	GCCGATAATTCTGAAAAACTGCTA	F 54.8 R 53.9
BAR00023	4	KTI	TGCAGGCAGAACCGTCCAGA	TGCAGAACAGAAGGGGTGAAGC	F 58.8 R 58.0
BAR00008	32	PDI	TTTTTGTTGCTCGGTCTCTTT	CTTCTCTGCCAGCTGTGTATTC	F 51.1 R 51.0
BAR00003	122	QKW	GCAAACGCGGCTCGGCTCTGT	GGGGGCGCAAAACTCAATCCAACC	F 65.2 R 66.7

Table 4.1 Conventional PCR primer sequences: Sequences of primer pairs used to amplify venom protein targets by conventional PCR.

Cluster ID	No. sequences	Toxin group	Forward primer (5'-3')	Reverse primer (5'-3')	Melting temp. °C
BAR00042	31	PII SVMP	ATACTGCGTGGTCTAGAAATGTGG	AGCGCCTGTGAATAACTGAGC	F 54.2 R 53.7
BAR00034	19	SP	AGGAGGCGAGGAGAAGAGACG	TTCCGCCCCATCCCATAATAC	F 56.5 R 57.2
BAR00406	2	PLA_2	CGGATAAGTGCGGCCCCAAAAC	ATGGGTTTTCGTCTCCGCAGATGA	F 63.1 R 62.5
BAR00012	6	CTL	GCTCCGGCTTGCTGGTCGTGTTC	GCCCGTCCTTCCCCTGCTTCTTG	F 65.6 R 65.5
BAR00040	14	VEGF	GAAGGGGAGCGAGAGCCAAGTT	ACCCCCAGCATCAGAAAGAGGAG	F 59.7 R 59.5
BAR00017	14	LAO	GGGCCCATGCGTTTACCTG	GCGCTTTTGCCTGCTTCTGA	F 57.4 R 57.9
BAR00023	4	KTI	GGGCCTATATCCGTTCCTTCTT	ATTCCCATAGCATCCACCATAAAA	F 54.5 R 55.6
BAR00008	132	PDI	CCCGAATATTCTGGTGGAGT	AAATTGTTGGGCGAGTTCTG	F 50.5 R 51.8
BAR00003	122	QKW	TGCGCCCCCAAATCCTCCTA	TGGCATACGCAGCTGGTTTACTCA	F 61.0 R 60.5
Oxyuranus scutellus*		ACTIN	CTCAGAGTCGCCCCGGAAGAACAT	AGAGGCGTACAGGGAGAGCACAGC	F 63.3 R 61.8
Laticauda semifasciata*		GAPDH	GAATATCATCCCAGCATCCACAGG	CATCATACTTCGCCGGTTTCTCTA	F 58.3 R 56.4
Echis ocellatus*		HEAT SHOCK	AGCCCCCAAGGATGAAGAGAAGC	ATCGGGGTTGCGGGTCCAG	F 60.7 R 61.4

Table 4.2 Quantitative PCR primer sequences: Sequences of primer pairs used in quantitative PCR amplification.* denotes primer sequences which were designed based on sequences from other snake species as sequences were unavailable in the *B. arietans* venom gland EST database.

4.3.5. Amplification of venom transcripts by conventional PCR

The ability of primer pairs to amplify their specific target genes of interest was tested by PCR amplification from venom gland cDNA library as a positive control and cDNA synthesised from venom mRNA. Conventional PCR was performed as previously described in Section 2.9.2 of Chapter 2 alongside negative water controls. The presence of amplified products was confirmed and visualised on a 1% agarose-EtBr gel.

Optimisation of quantitative PCR (qPCR) protocols

All qPCR experiments were performed using the BioRad CFX 384 real-time PCR system. Optimisation and standardisation of qPCR was performed in accordance with the MIQE guidelines (Bustin et al., 2009) (Appendix II).

4.3.6. Experimental optimisation of annealing temperature for qPCR amplification

qPCR experiments were performed in order to experimentally determine the optimal annealing temperature for efficient qPCR amplification of venom components was determined, based on the theoretical primer annealing temperatures which were calculated by Primer Select software (DNASTAR) during primer design. KAPA SYBR® FAST qPCR Kit (KAPA Biosystems, AnaChem) was used as previously described in Section 2.9.4 of Chapter 2. The experimental qPCR plate set up and reaction parameters are shown in Figure 4.1 with a temperature gradient ranging

from 50 to 65°C. Amplification was followed by melt curve analysis to ensure specific PCR products were amplified.

A. Plate set-up

Temperature gradient

		1	2	3	4	5	6	7	8	9	10	11	12
A	65.0	SVMP	SP	CTL	PLA2	LAO	VEGF	KTI	PDI	QKW	GAP	ACT	HSP
B	64.7	SVMP	SP	CTL	PLA2	LAO	VEGF	KTI	PDI	QKW	GAP	ACT	HSP
C	64.2	SVMP	SP	CTL	PLA2	LAO	VEGF	KTI	PDI	QKW	GAP	ACT	HSP
D	63.6	SVMP	SP	CTL	PLA2	LAO	VEGF	KTI	PDI	QKW	GAP	ACT	HSP
E	62.5	SVMP	SP	CTL	PLA2	LAO	VEGF	KTI	PDI	QKW	GAP	ACT	HSP
F	61.5	SVMP	SP	CTL	PLA2	LAO	VEGF	KTI	PDI	QKW	GAP	ACT	HSP
G	60.0	SVMP	SP	CTL	PLA2	LAO	VEGF	KTI	PDI	QKW	GAP	ACT	HSP
H	58.5	SVMP	SP	CTL	PLA2	LAO	VEGF	KTI	PDI	QKW	GAP	ACT	HSP
I	56.6	SVMP	SP	CTL	PLA2	LAO	VEGF	KTI	PDI	QKW	GAP	ACT	HSP
J	55.1	SVMP	SP	CTL	PLA2	LAO	VEGF	KTI	PDI	QKW	GAP	ACT	HSP
K	53.8	SVMP	SP	CTL	PLA2	LAO	VEGF	KTI	PDI	QKW	GAP	ACT	HSP
L	52.6	SVMP	SP	CTL	PLA2	LAO	VEGF	KTI	PDI	QKW	GAP	ACT	HSP
M	51.6	SVMP	SP	CTL	PLA2	LAO	VEGF	KTI	PDI	QKW	GAP	ACT	HSP
N	50.8	SVMP	SP	CTL	PLA2	LAO	VEGF	KTI	PDI	QKW	GAP	ACT	HSP
O	50.3	SVMP	SP	CTL	PLA2	LAO	VEGF	KTI	PDI	QKW	GAP	ACT	HSP
P	50.0	SVMP	SP	CTL	PLA2	LAO	VEGF	KTI	PDI	QKW	GAP	ACT	HSP

B. 2-step protocol

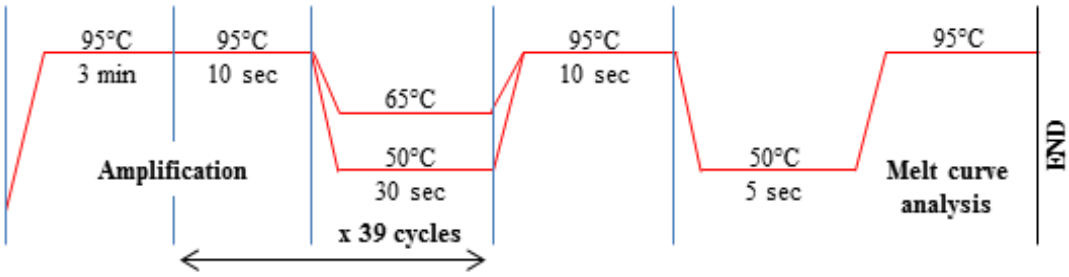

Figure 4.1 qPCR plate and thermocycling for optimisation of annealing temperature: A) Layout of qPCR plate set up using BioRad CFX 384 real-time PCR system with a temperature gradient from 65 to 50°C and B) thermocycling parameters using a temperature gradient in order to optimise PCR amplification.

4.3.7. Optimising cDNA concentration for qPCR

To optimise the concentration of cDNA per qPCR reaction, cDNA was firstly synthesised from mRNA was extracted from 10mg venom. The concentration of total cDNA synthesised was 1270ng/µl which was subsequently diluted to 50, 20, 10 and 5ng/µl aliquots and each sample was performed in duplicate. qPCR amplification protocol was performed accordingly; 3 minute enzyme activation at 95°C, 30 seconds DNA annealing at 55°C for 40 cycles.

4.3.8. Standard curve analysis to determine the amplification reaction efficiency in qPCR

Standard curve construction is essential for the absolute quantification of DNA in an unknown sample with reference to a standard sample of known concentration. However, it was also necessary to conduct standard curves during relative quantification and gene expression analyses. Here, standard curve analysis was used to (i) assess that the optimal starting concentration of cDNA in the venom samples was used in order to produce a linear standard curve within the dynamic range for each gene target and (ii) to obtain the PCR reaction efficiencies for each gene of interest. Standard curves were constructed by plotting the log of the concentration of a standard cDNA sample against the Ct value (the cycle number at which exponential amplification occurs). To do this, the standard cDNA sample was diluted across a range of serial dilutions (between 5-10 different concentrations) and amplified by qPCR to generate a standard curve. The amplification efficiency of the PCR reaction (E) was calculated from the gradient of the standard curve by the formula $E = 10^{(-1/slope)}$ and subsequently converted into a percentage; % PCR reaction efficiency = (E-

1) x 100%. For standard curves, two different templates were used. Firstly, for a model standard sample, PCR products amplified by conventional PCR from venom cDNA of each gene of interest were excised and purified. Here, we aimed to determine the efficiency of qPCR reactions under ideal conditions. Secondly, cDNA synthesised from mature *B. arietans* venom pooled from several individual specimens was used as a standard sample. Here, we aimed to determine the PCR reaction efficiency values of amplification under more representative conditions which would be more relevant in practice and take into consideration the differences in abundance/expression level of specific targets. For each standard sample, ten doubling dilutions of pooled venom cDNA were carried out to produce a range of cDNA concentrations; 1000, 500, 250, 125, 62.50, 31.25, 15.63, 7.81, 3.91 and 1.95ng/µl. For some genes of interest, the pooled venom cDNA sample concentration was subsequently increased in quarter-dilutions in order to enter the linear dynamic range as follows; 2000, 1500, 1125, 843.75, 632.81, 474.61, 355.96 and 266.97ng/µl. cDNA was added to qPCR KAPA SYBR green reaction master mix as previously described. Duplicate samples were amplified by qPCR amplification protocol alongside negative controls as previously described.

4.3.9. Melt curve analysis to determine the specificity of primer pairs in qPCR

Melt curve analysis following qPCR amplification was necessary to assess the sensitivity and specificity of PCR primers, and was subsequently performed for each gene of interest. Melt curves were constructed by gradually heating the final PCR amplicon to 95°C in small increments which melted the double stranded DNA. At

the specific melting point of the product, the fluorescently-bound DNA begins to dissociate and the levels of fluorescence decrease due to the breakdown of DNA. The point at which the loss in fluorescence is maximal is said to be the melting temperature of the DNA characterised by a sharp peak on the melt curve. The negative of the first derivative of the dissociation curve is plotted which produces a peak on the chart which enables a more accurate estimation of the melt temperature. The presence of a single peak on the melt curve indicates the presence of a single, specific amplicon. Melt curve analysis was performed following qPCR amplification as follows; 10 seconds at 95°C, ramping from 50°C to 95°C in 0.5°C increments for 5 seconds. The plate layout and thermocycling parameters for standard curve and melt curve analysis are shown in Figure 4.2.

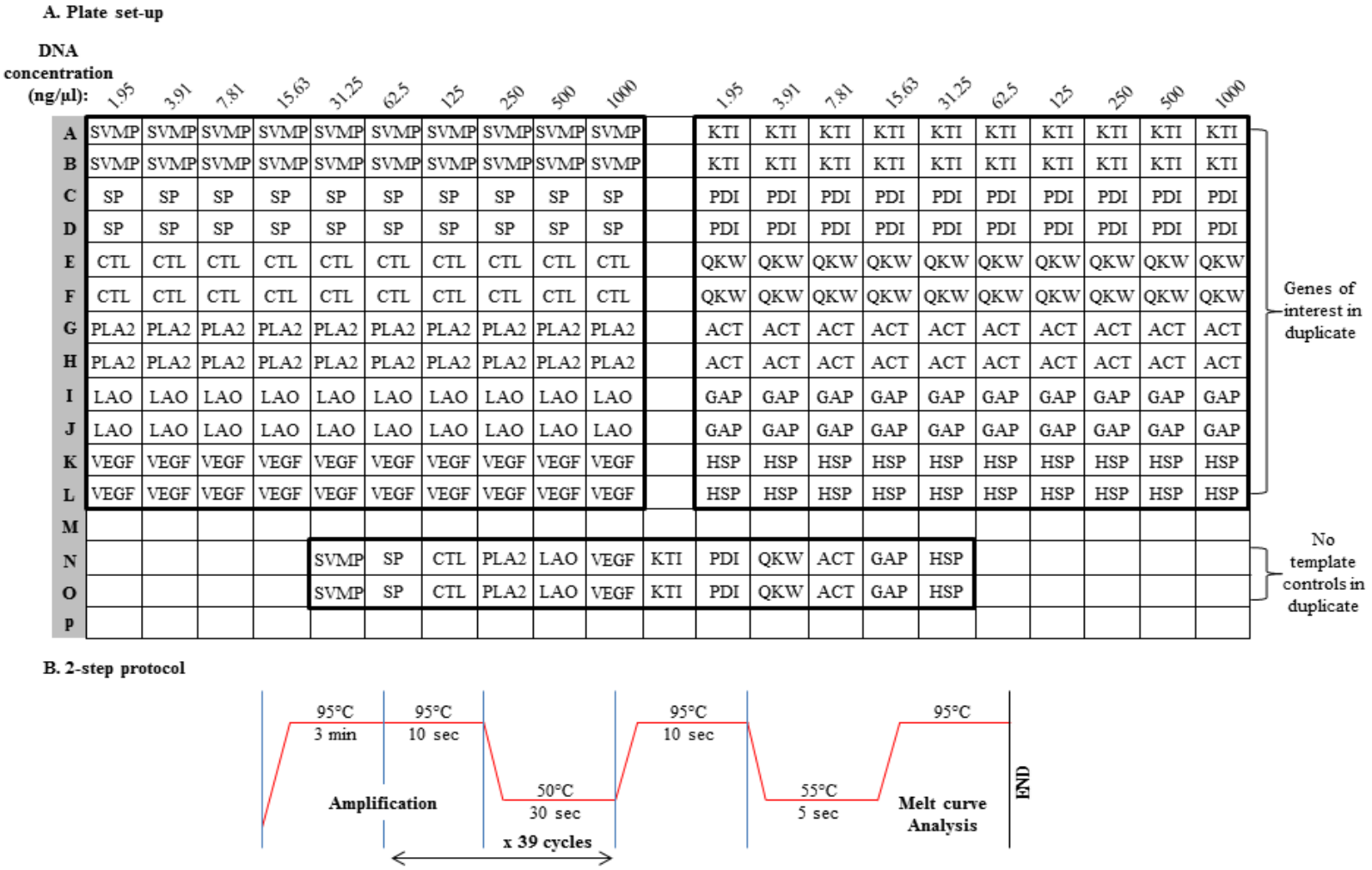

Figure 4.2 qPCR plate and thermocycling for standard and melt curve validation: Layout of qPCR plate set up using BioRad CFX 384 real-time PCR system for standard curve and melt curve analysis (A) and thermocycling parameters using a temperature gradient (B).

4.4. Results:

4.4.1. Quantity of mRNA recovered from venom

To determine the effect of the quantity of venom on the yield of mRNA and cDNA from venom, mRNA was extracted from different quantities of lyophilised *B. arietans* venom ranging from 2 to 100mg. The concentration of mRNA eluted from venom was measured using the ND-1000 spectrophotometer. Figure 4.3 shows that the amount of mRNA eluted from venom increases as the quantity of venom increases (Figure 4.3A), thus the concentration of first strand cDNA synthesised from mRNA also increased as venom quantity increased (Figure 4.3B). The ND-1000 spectrophotometer was also used to assess RNA purity. The optical density (OD) was measured at 260 and 280nm wavelengths. The ratio of absorbance at 260 and 280nm ($A_{260/280}$) gives an indication of the purity of the DNA/RNA sample. The $A_{260/280}$ of pure RNA should be greater than 1.8 (Fleige and Pfaffl, 2006, Becker et al., 2010) which is considered suitable for gene expression studies. The average 260/280 absorbance ratios of the venom mRNA samples was 2.43 ±0.57 indicating the absence of proteins, phenol or other contaminating compounds. These results demonstrate that potentially large quantities of mRNA can be reproducibly recovered from *B. arietans* venom. A mass of 2mg lyophilised *B. arietans* venom was determined as the minimum mass yielding a quantity of mRNA sufficient for downstream applications.

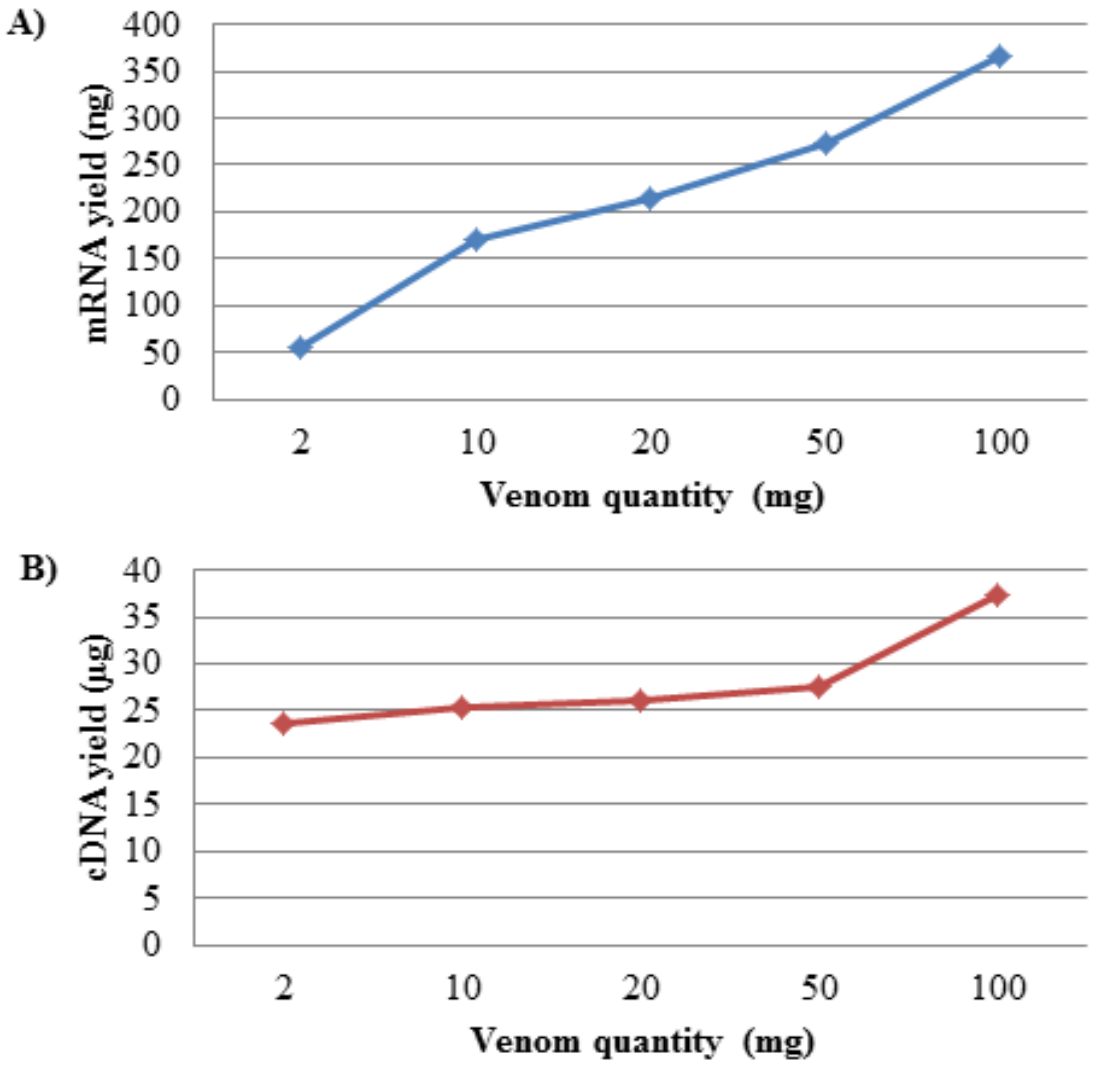

Figure 4.3 Identifying the optimal venom quantity for mRNA and cDNA yield: Effect of initial weight of lyophilised *B. arietans* venom (mg) on A) quantity of eluted mRNA from venom (ng) and B) quantity of 1st strand cDNA synthesised (µg). Results showed that the mRNA yield increased from 50 to over 350ng with increasing venom quantity but cDNA yield was less affected.

4.4.2. Testing the ability of primer pairs to specifically amplify a range of venom protein targets from venom gland and venom cDNA

Electrophoresis of PCR products amplified from the *B. arietans* venom gland cDNA library (positive control) showed that a range of venom components of varied

representation in the venom gland transcriptome, indicating that primer pairs were sensitive and specific to amplify target transcripts (Figure 4.4Ai). However, the PLA_2 gene (BAR00406) could not be efficiently amplified from the venom gland library. This may be due to the fact that PLA_2s are very poorly represented in the *B. arietans* venom gland cDNA library (represented only by three clusters in the *B. arietans* venom gland EST database; BAR00406, BAR00424 and BAR00538).

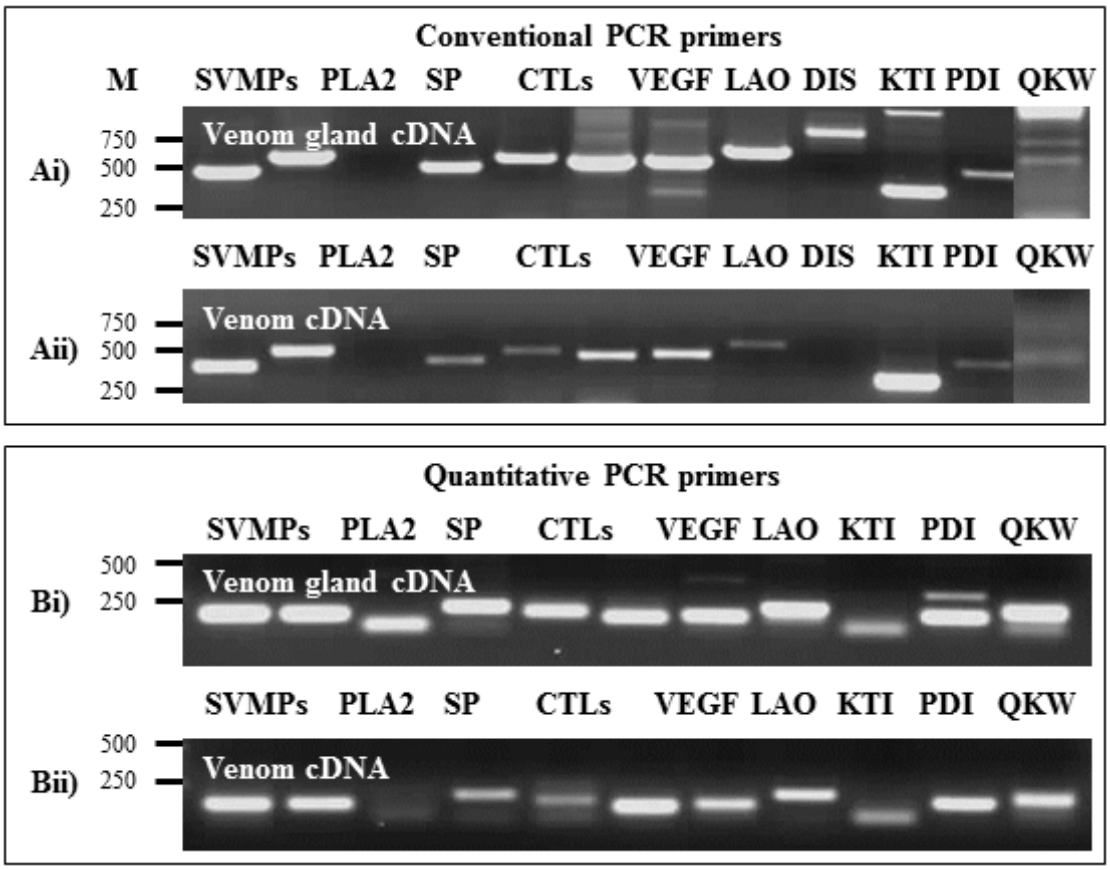

Figure 4.4 Amplification of venom targets from venom vs. venom gland cDNA: PCR amplification of a range of venom protein targets from *Bitis arietans* venom gland cDNA library (Ai and Bi) and cDNA synthesised from mRNA extracted from venom (Aii and Bii) using full length conventional PCR primers (A) and primer pairs designed specifically for quantitative PCR. Molecular weight markers are shown to the left of the gel.

However, using qPCR primers in conventional PCR reactions, the venom gland cDNA positive controls showed that amplicons were produced by each protein-specific primer pair, including the PLA_2 (Figure 4.4Bi). The difference in amplification of the PLA_2 target when using two different primer pairs suggested that primer design may have influenced amplification success could be explained by the different regions of DNA targeted by the two different primer pairs. The qPCR primers may be more efficient in amplifying truncated cDNA due to the fact that they are specifically designed to amplify shorter DNA sequences. PCR amplification of venom targets from cDNA synthesised from mRNA extracted from venom suggested that, of the targets surveyed in this study including those of high (SVMPs) and lower representation (PLA_2s), a similar spectrum of mRNA can be amplified from venom and venom gland cDNA (Figure 4.4Aii and Bii).

PCR amplification of targets from mRNA extracted from different quantities of venom showed that overall, as the amount of venom from which mRNA was extracted increased, the apparent amount of amplicon produced by PCR using conventional primer pairs and visualised on an agarose-EtBr gel also qualitatively increased (Figure 4.5). PCR amplicons were visible following amplification from mRNA isolated from 2 mg venom, but products from some targets (PLA_2, SP, LAO and DIS) were faint due to the reduced sensitivity. Following amplification from 10 mg venom, the visual appearance of some amplicons became more intense (SP and LAO). Subsequently, by increasing venom quantity from 10 to 100mg, PCR products became progressively more intense but there did not appear to be an overall significant difference in the amount of PCR amplicon produced.

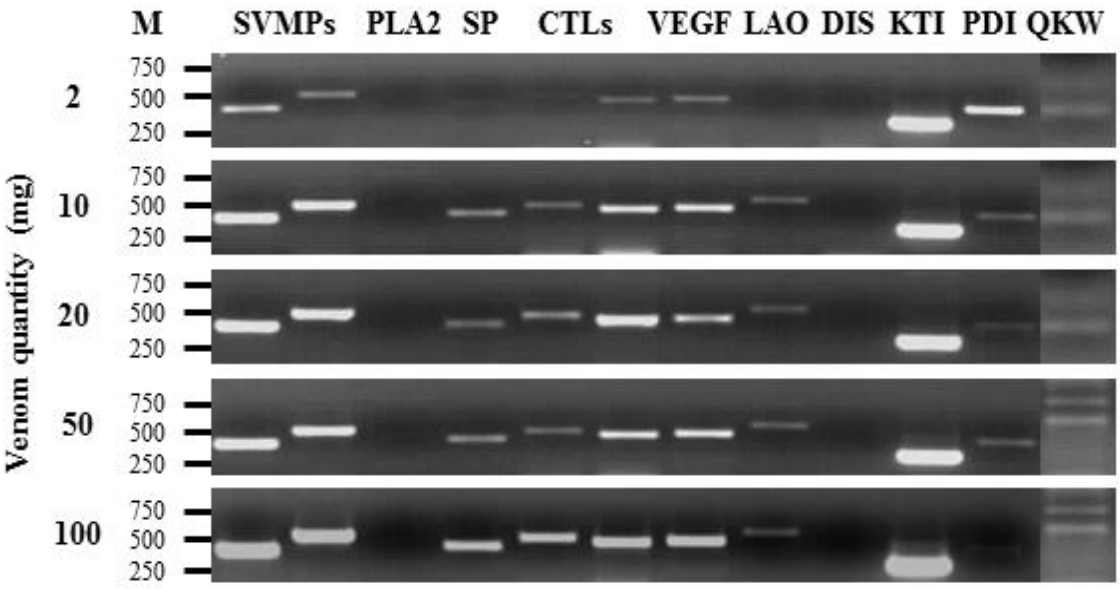

Figure 4.5 Amplification of venom targets from different quantities of venom: PCR amplification of venom targets from different initial starting weights of lyophilised *B. arietans* venom PCR amplification of venom targets showed very little effect on the qualitative amount of PCR amplicon. Molecular weight markers are shown to the left of the gel.

4.4.3. Assessing DNA contamination of mRNA samples

To assess for the presence of DNA contaminating mRNA samples, two approaches were used. Firstly, during reverse transcription of mRNA, duplicate reactions were performed whereby the reverse transcriptase enzyme was omitted from the reaction. In addition, for qPCR primers, a DNase treatment of mRNA prior to reverse transcription was performed. Using conventional PCR primers in the 'no reverse transcriptase' control we showed that there was no DNA contamination of venom sample mRNA (Figure 4.6) to interfere and distort PCR results. For qPCR primer pairs, in addition to the 'no reverse transcriptase' controls where again no amplicons were visible following gel electrophoresis, a DNase treatment of mRNA was included. There was no difference in the PCR products amplified between DNase

treated controls and non-treated mRNA indicating that there was no interference from DNA contamination (Figure 4.7).

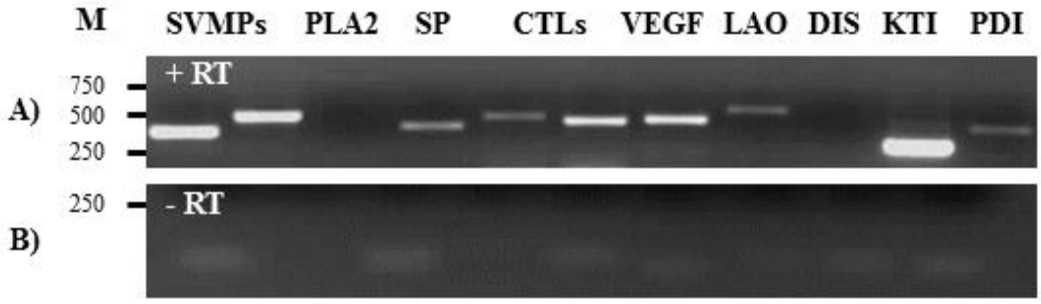

Figure 4.6 Assessing DNA contamination of mRNA samples using reverse transcriptase negative controls (conventional PCR primers): A) shows amplification of venom protein targets using conventional PCR primer pairs. B) shows PCR amplification following omission of reverse transcriptase from cDNA synthesis. Absence of products in B indicates that samples were free from DNA contamination. Molecular weight markers are shown to the left of the gel.

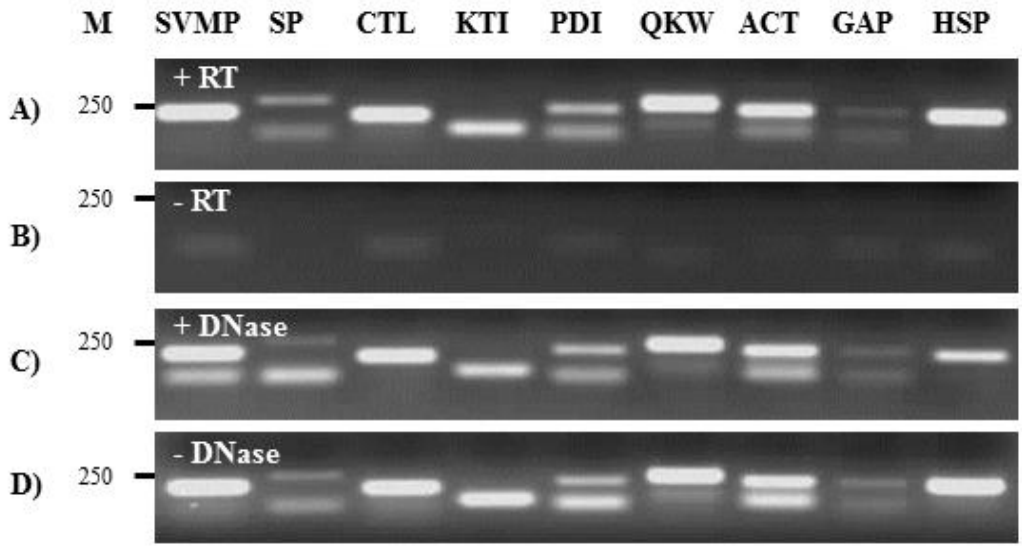

Figure 4.7 Assessing DNA contamination of mRNA samples using reverse transcriptase negative controls and DNase treatment (qPCR primers): A) and B) shows amplification of venom protein targets using qPCR primer pairs including and omitting reverse transcriptase respectively. C) and D) show that there was no difference in PCR amplification following DNase treatment of mRNA (C) or no DNase treatment (D). Molecular weight markers are shown to the left of the gel.

4.4.4. Experimental optimisation of annealing temperature for qPCR amplification

The cycle time (Ct) values (i.e. the cycle time at which the fluorescence level exceeded the given threshold) of qPCR amplifications for each gene of interest performed across a temperature gradient were analysed (Figure 4.8) (raw qPCR data is shown in Appendix III). Overall, we could not identify a specific optimal temperature for all primer pairs, alternative to the predicted optimal annealing temperature generated by primer design software, which improved the amplification of targets. The average difference in cycle time between the maximum and minimum Ct value across all genes of interest including reference genes across the temperature gradient was only 2.91 cycles (individually the greatest difference in Ct across the temperature gradient was observed in amplification of the heat shock protein reference gene at a difference of 8.6 cycles). The standard deviation across all target genes ranged from between ±0.36 to ±3.09 cycles demonstrating very little effect of the temperature gradient on primer annealing. With the exceptions of the SP, PLA_2, PDI and β-actin primers, which could potentially be more efficient at a lower temperature between 50-53.8°C, Ct values following amplification of targets using most primers appeared to fluctuate showing no clear trend in efficiency due to temperature. These results could not identify a significant difference in the amplification growth curves for each gene from 50-65°C and so we were unable to experimentally determine a specific optimal annealing temperature for all primers. Subsequently, the computational optimal annealing temperatures determined by primer design (Primer Select, DNASTAR) were averaged for all primers (55°C) was used in PCR to enable ease of amplifying all genes of interest on a single plate.

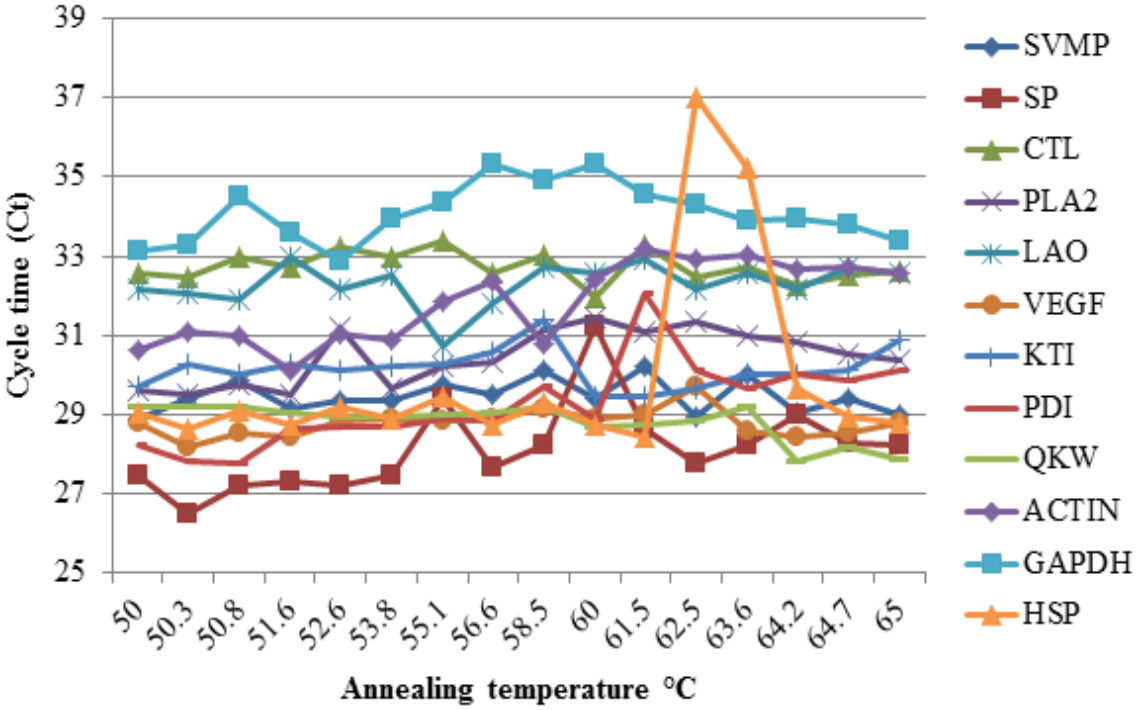

Figure 4.8 Optimisation of annealing temperature for amplification by quantitative PCR: Ct value of amplification for each gene of interest across an annealing temperature gradient from 50 to 65°C demonstrating very little effect of the temperature gradient on primer annealing.

4.4.5. Optimising cDNA concentration for qPCR amplification

To optimise the initial starting quantity of venom cDNA per reaction, qPCR amplification of all genes of interest was performed on a range of cDNA concentrations; 5, 10, 20 and 50ng per reaction. We observed very little difference in the cycle time (Ct) in relation to the initial starting quantity of cDNA per PCR reaction (standard deviation for all targets ranged from ±0.11 to ±0.75 cycles) (Figure 4.9) (Raw qPCR data is shown in Appendix IV).

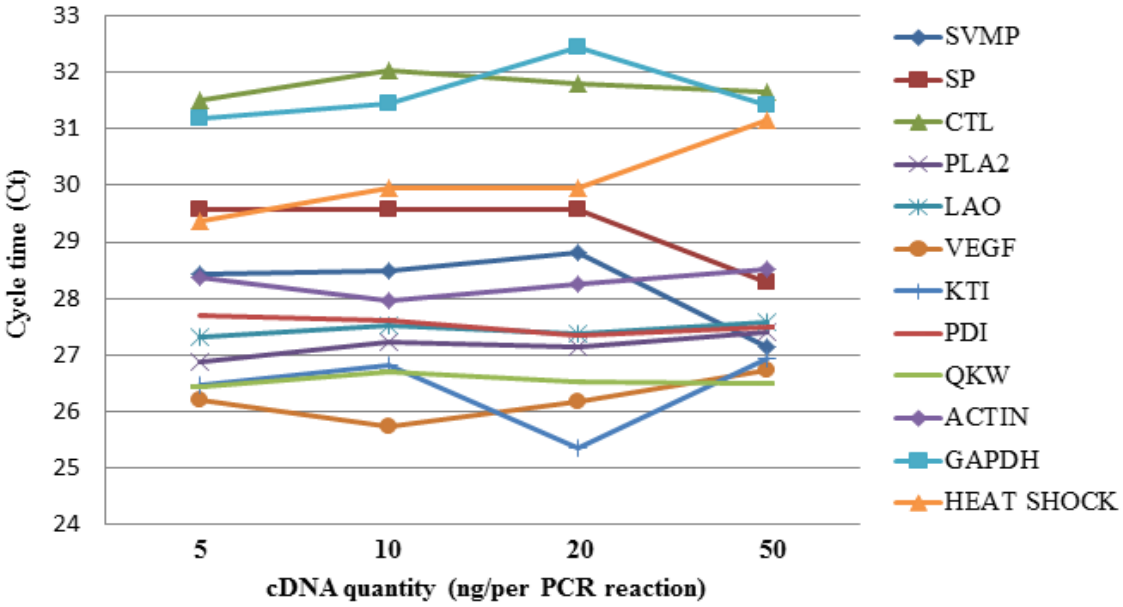

Figure 4.9 Optimisation of initial cDNA concentration for amplification by quantitative PCR: Relationship between initial cDNA quantity per qPCR reaction and cycle time (Ct) score showed that there appeared to be no direct correlation between Ct score and starting cDNA quantity following amplification for all genes of interest.

4.4.6. Standard curve analysis to determine amplification reaction efficiency in qPCR

Standard curves for all genes of interest are shown in Figures 4.10 and 4.11. Raw qPCR data from standard and melt curve analysis (Ct values, melt temperature and melt peak height) are shown in Appendix V. Firstly to consider standard curves generated using purified PCR products as the standard DNA sample; for all targets, linear standard curves were produced with PCR reaction efficiencies between 69.8 and 91.6% were observed. Notably, the Ct values were consistently between 5-15 cycles with the exception of CTL and GAPDH which took between 20-30 cycles for the fluorescence level to reach the threshold.

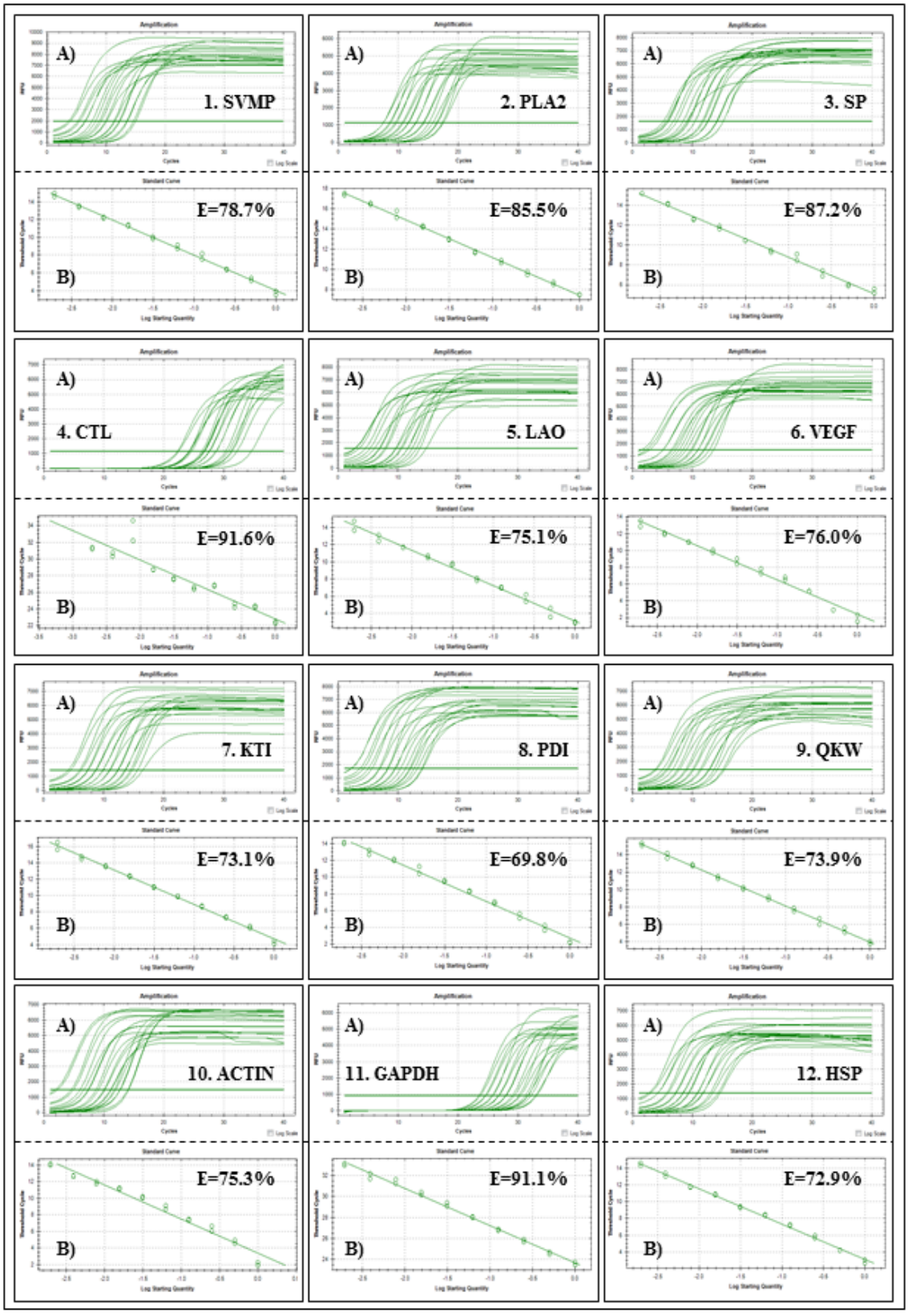

Figure 4.10 Standard curves generated by qPCR using purified PCR products as a standard cDNA sample: Panel A) shows amplification growth curve and panel B) shows the standard curve. E = % PCR reaction efficiency, *x* axis = relative fluorescence levels (RFU) in panel A or threshold cycle in panel B, *y* axis = Log starting cDNA concentration.

To consider standard curves generated using pooled, mature venom cDNA as a more representative standard sample; for most targets, linear standard curves were produced with PCR reaction efficiencies between 63.3 and 100.7%. However, it is important to note that the Ct values were around 20-30 cycles; higher that previously observed following amplification of purified product standard samples. This may be expected as the mature venom cDNA was synthesised from whole venom, thus containing numerous cDNA sequences corresponding to up to hundreds of venom proteins. For some genes (PLA_2, LAO and VEGF), we were unable to generate a linear standard curve. There may be several explanations for this; firstly the concentration of cDNA used was outside the linear dynamic range for some specific genes. Secondly, the low abundance of certain toxins in *B. arietans* venom (e.g. PLA_2) may also affect the ability to detect and quantify toxin expression using qPCR. Some standard curves which produced poor % reaction efficiencies using a cDNA concentration range from 1.95 to 1000ng/µl were significantly improved when the cDNA concentration range was increased to 266.97 to 2000ng/µl (e.g. SVMP, ACTIN and GAPDH).

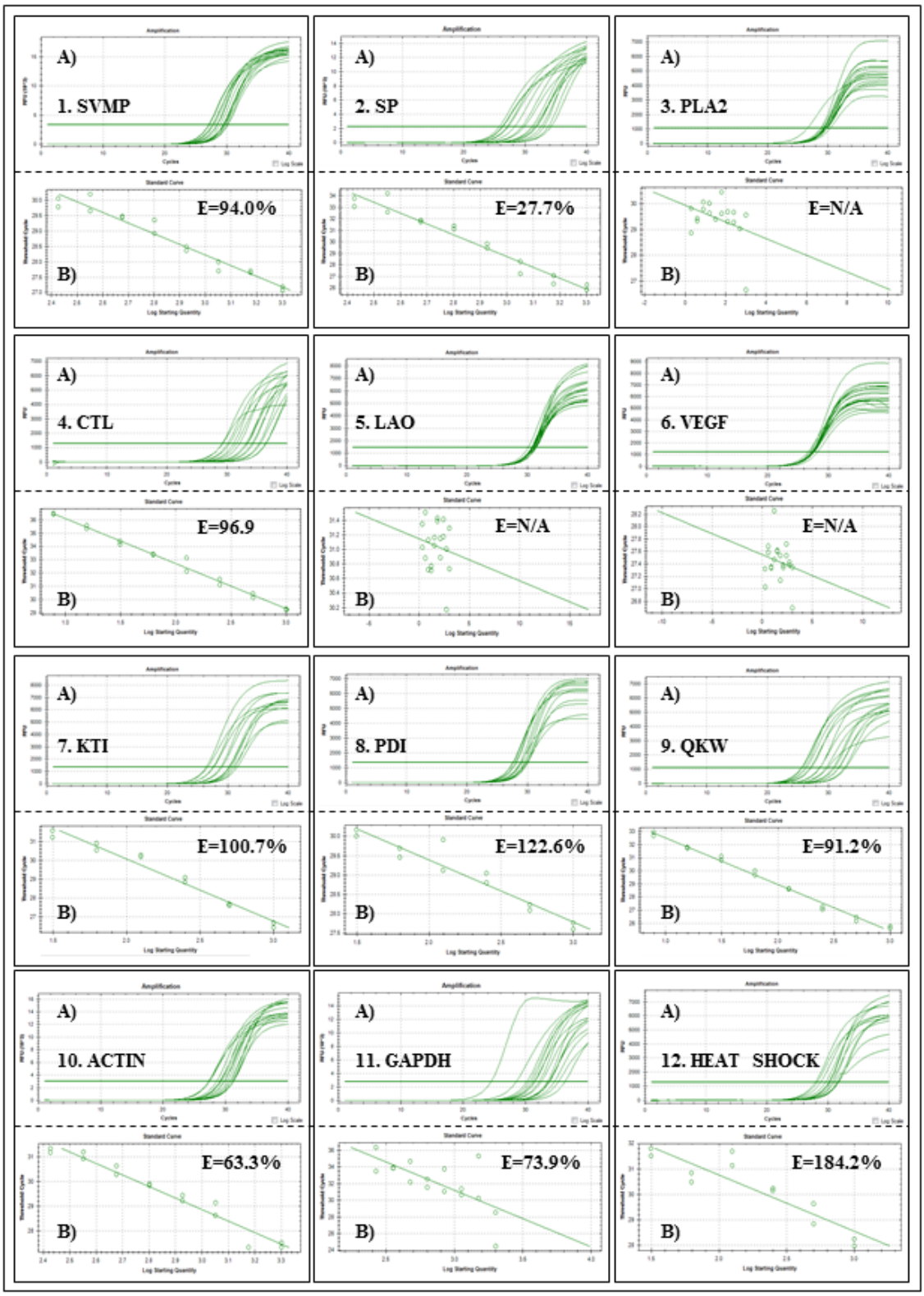

Figure 4.11 Standard curves generated by qPCR using pooled mature venom cDNA as a standard cDNA sample: Panel A) shows amplification growth curve and panel B) shows the standard curve. E = % PCR reaction efficiency, *x* axis = relative fluorescence levels (RFU) in panel A or threshold cycle in panel B, *y* axis = Log starting cDNA concentration.

The qPCR reaction efficiency values following amplification of targets from both standard cDNA samples are summarized in Table 4.3. We acknowledge the observation that the amplification efficiencies vary and that the amplification of some targets is sub-standard, however, we do not consider variation in amplification efficiency to be a significant issue. This is because in subsequent chapters we will apply standardised techniques to determine changes in the relative gene expression levels of targets genes between different samples, following which we will be able to correct for differences in PCR reaction efficiencies, therefore accommodating for these observations.

Gene target	PCR reaction efficiency %:	
	Purified PCR product	Venom cDNA standard
SVMP	78.7	94.0
SP	87.2	27.7
PLA_2	85.5	N/A
CTL	91.6	96.9
LAO	75.1	N/A
VEGF	76.0	N/A
KTI	73.1	100.7
PDI	69.8	122.6
QKW	73.9	91.2
ACTIN	75.3	63.3
GAPDH	91.1	32.1
HSP	72.9	184.2

Table 4.3 Quantitative PCR reaction efficiencies: PCR reaction efficiency values for each gene of interest generated by standard curve analysis.

4.4.7. Melt curve analysis to determine qPCR primer specificity

Melt curve analysis was used to determine the ability of primer pairs to specifically anneal to and initiate amplification of specific DNA targets. Melt curves following qPCR amplification shown in Figure 4.12 and 4.13 indicated the presence of single peaks for most genes of interest. The curves, which plot relative fluorescence against temperature, showed that as temperature increases, the level of fluorescence decreases as double stranded DNA dissociates. The negative first derivative of DNA dissociation generates a melt curve containing a single peak indicating the amplification of a single target, and therefore high specificity of PCR primer pairs.

Melt curves following amplification of targets from purified PCR product standard samples showed single peaks for all genes of interest indicating the presence of a specific amplicon, as may have been expected here (Figure 4.12). In the case of the mature venom cDNA sample, melt curves also showed the amplification of a single specific target for most targets of interest (Figure 4.13). The exception was PDI as there appeared to be a minor second peak with a melting temperature of approximately 6 °C lower than the major peak. This suggests that there may be two different amplicons produced as result of non-specific binding by PCR primers.

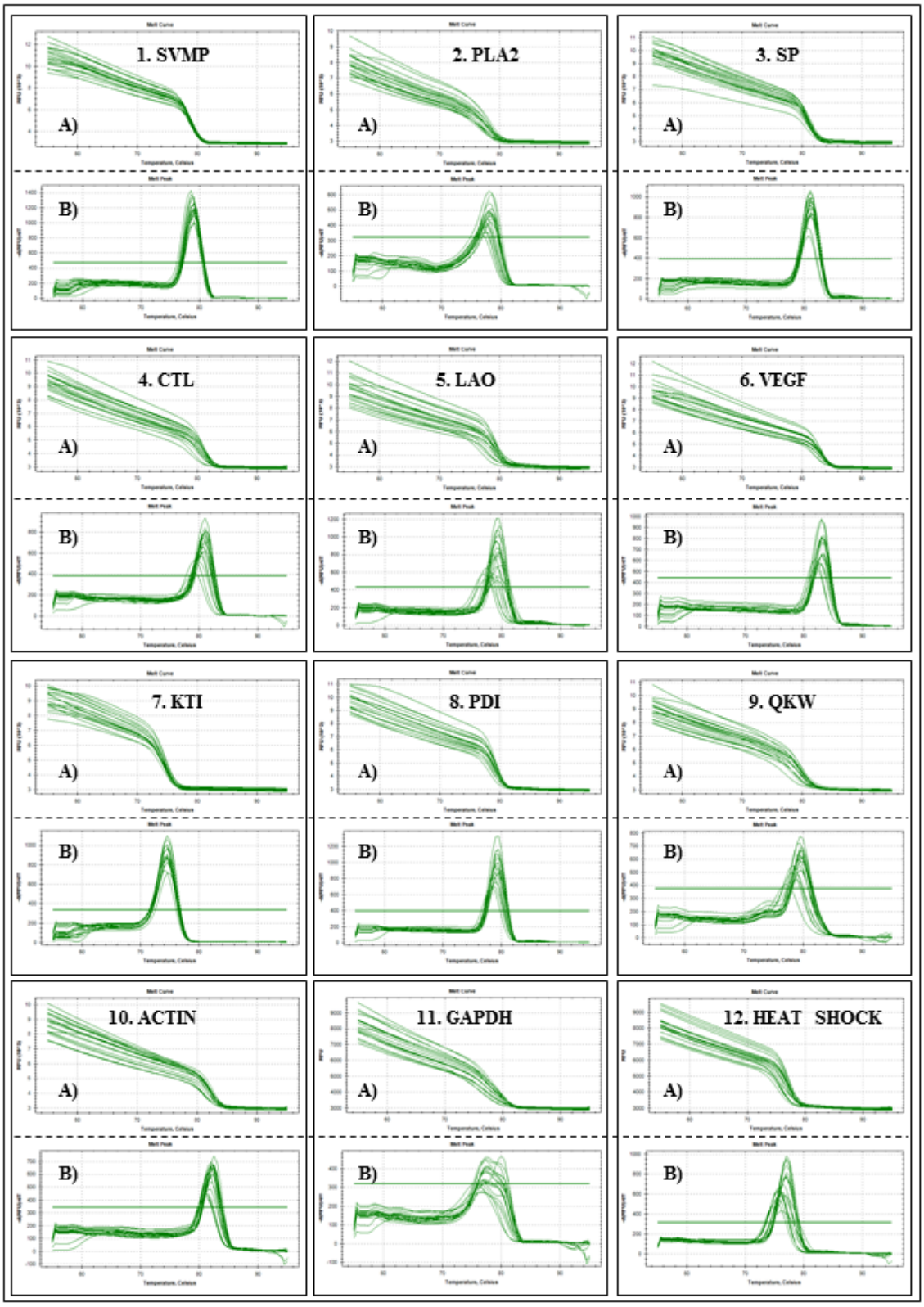

Figure 4.12 Melt curves generated by qPCR following amplification using purified PCR products as a standard cDNA sample: Panel A shows the decrease in relative fluorescence levels (RFU) during DNA dissociation. Panel B shows the melt curve generated from the negative first derivative of RFU. *x* axis = RFU in panel A or the negative first derivative of RFU in panel B, *y* axis = Temperature °C.

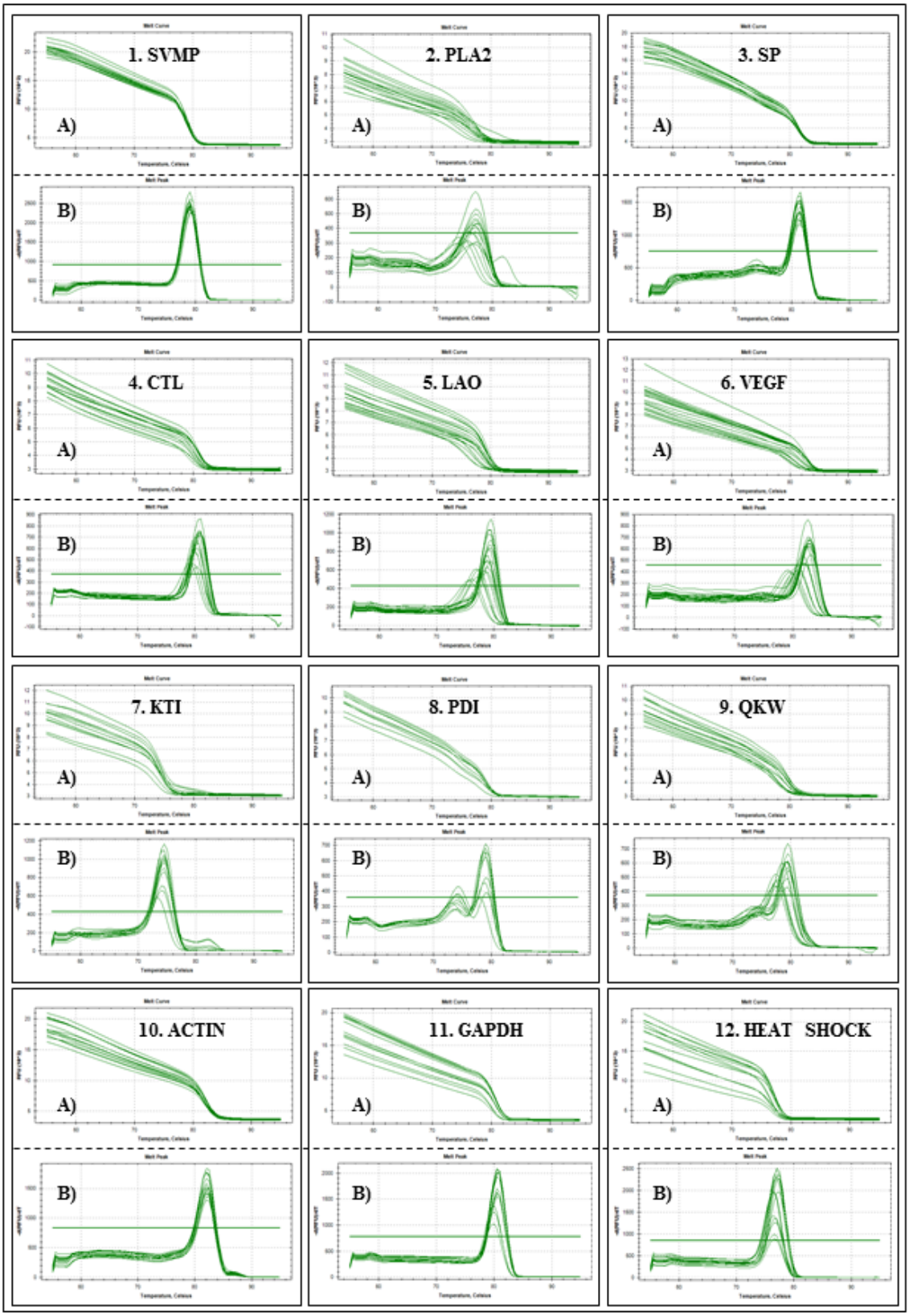

Figure 4.13 Melt curves generated by qPCR following amplification using mature venom cDNA as a standard cDNA sample: Panel A shows the decrease in relative fluorescence levels (RFU) during DNA dissociation. Panel B shows the melt curve generated from the negative first derivative of RFU. *x* axis = RFU in panel A or the negative first derivative of RFU in panel B, *y* axis = Temperature °C.

4.6. Discussion

The results of this chapter illustrate the potential value of our real-time approach, utilising venom stocks as a source of mRNA and advanced quantitative PCR technologies, as a tool for analysing the transcriptional activity of the venom gland, and to monitor expression levels of venom protein-encoding genes.

The most commonly employed technique used to extract RNA from biological samples involves precipitation of total RNA using organic solvent-based extraction which results in the co-precipitation of mRNA subpopulations with other RNAs, which are more predominant than mRNA (Cheng et al., 1999, de Azevedo et al., 2001, Guo et al., 2001). Conventional techniques require obtaining venom gland tissue from sacrificed snakes as the source of transcriptionally active mRNA, which is often a difficult, undesirable and unsustainable approach.

Organic solvent-based RNA extraction fails to capture reverse transcriptase PCR-compatible mRNA from lyophilised venoms. As an alternative approach, the capture of mRNA using magnetic beads (Dynabeads^{TM}) was first described by Chen *et al* to isolate mRNA from the lyophilised venoms from several snakes, lizards, scorpions and amphibians (Chen et al., 2002, Chen et al., 2003a, Chen et al., 2003b, Chen and Shaw, 2003, Chen et al., 2005, Chen et al., 2006). The use of oligo dT-coated magnetic Dynabeads enables the capture of PCR-compatible mRNA from lyophilised venoms.

To optimise mRNA isolation using this technique, we included a longer incubation time of the lysed venom sample with oligo dT magnetic beads (increased to 10 min) and we also repeated the isolation procedure for each venom sample to increase the yield of mRNA. Our results demonstrate that substantial quantities of venom protein-

encoding mRNAs can be extracted from the venom of *Bitis arietans* (over 350ng from 100mg lyophilised venom). We identified that relatively small quantities of lyophilised venom (2mg), which were much lower than those used in previous studies (10mg) (Chen et al., 2002) were required to yield substantial quantities of mRNA (around 50ng). Total mRNA extracted from 2mg venom samples was synthesised into cDNA (around 20µg) which was easily sufficient for downstream PCR and qPCR applications. Although the amount of mRNA extracted from venom increased as the amount of lyophilised venom increased, the quantity of cDNA synthesised from mRNA did not appear to significantly increase. This suggests that there may be some limitations in the reverse transcription protocol. Although modifications were performed in order to improve the capture of mRNA from venom, further work could aim to enhance the cDNA synthesis reaction and subsequently improve cDNA yields accordingly.

We demonstrated that a wide range of venom protein targets could be efficiently PCR amplified from venom mRNA, in comparison to previous literature demonstrating amplification of single targets of high abundance in venom e.g. SVMPs from viper venom and neurotoxin from elapid venom (Chen et al., 2002). Here we demonstrated amplification of a range of venom protein targets, including pathologically important enzymes such as SVMPs and SPs, and venom components thought to play a less toxic role in snakebite envenoming such as inhibitory peptides and structural proteins (PDI, QKW peptides). Importantly, PCR results demonstrated that a similar spectrum of mRNA could be efficiently amplified from venom as venom gland cDNA. This provided encouraging results indicating that the venom transcriptome may be an accurate representative of the venom gland transcriptome. Although the full diversity, stability and function of mRNAs in lyophilised venom

remain uncertain, these observations emphasise that this approach, and specifically the utilisation of venom mRNA, could provide a significantly valuable tool in snake venom research as an alternative to conventional methods, thus expanding the possibilities for gene expression studies and the study of rare/CITES listed venomous species.

This work describes the optimisation of relative qPCR protocols to monitor changes in gene expression of venom protein-encoding genes. Standardisation experiments included the optimisation of initial cDNA starting quantity and annealing temperature required for effective qPCR amplification of targets, and evaluating PCR reaction efficiency and specificity of primer binding. These experiments resulted in the generation of stringently optimised qPCR protocols which were used in subsequent studies aiming to quantitatively compare gene expression levels of venom protein targets during the course of venom protein synthesis.

5. INVESTIGATION OF VENOM PRODUCTION IN JUVENILE *BITIS ARIETANS* SPECIMENS; ANALYSIS OF GENE EXPRESSION, PROTEIN COMPOSITION AND ENZYME ACTIVITY OF VENOM FROM BIRTH TO MATURITY.

5.1. Abstract

Variation in venom composition can be influenced by several factors including diet, gender, age and habitat. In this study, we aimed to monitor the maturation of venom production by exploring changes in the protein composition, toxin expression and enzyme activity of venom from juvenile *Bitis arietans* siblings from birth.

Using relative quantitative PCR gene expression analyses, SDS-PAGE, mass spectrometry and substrate zymography we showed that gene expression activity, protein composition and functional activity of juvenile *B. arietans* venom did not appear to significantly change over time from birth to four years and venom from juvenile specimens appeared to be relatively similar to the maternal venom. A key difference in the venom protein composition between the captive-bred juvenile specimens and maternal adult specimen was notably in the presence of an additional PII SVMP, BAR00015, in the maternal venom, although the proteolytic activity of juvenile and maternal venoms, indicated by gelatin zymography, was similar.

In conclusion, we demonstrate that venom of *B. arietans* appears highly developed and enzymatically active immediately from birth. In the light of these results, we discuss the potential role of factors, both internal and external, influencing the composition and function of venom in this viper species.

5.2. Introduction

Variation in snake venom composition has been documented on several taxonomic levels and can be attributed to several factors including diet and age, and less influentially by gender. We previously demonstrated high levels of intra-species variation in protein composition and biological activity of venoms from groups of unrelated, wild caught *Bitis arietans* specimens (Chapter 3) (Currier et al., 2010). This variation appeared to be irrespective of environmental conditions, but could have been a result of inter-species individual differences. The aims of this chapter were to determine (i) venom production system and (ii) venom composition and enzyme activity in a group of sibling, captive-bred juvenile specimens.

As previously mentioned, differences in diet have been closely associated with variation in venom composition and function. This correlation was firstly demonstrated by Daltry *et al* who showed that variation in venom composition and activity in the Malayan pitviper, *Calloselasma rhodostoma* was related to diet, suggesting that venom composition may be subject to strong natural selection pressures (Daltry et al., 1996b). Variation in the venom protein composition between closely related subspecies of *Sistrurus* rattlesnakes (Sanz et al., 2006) and *Echis* species (Barlow et al., 2009, Casewell et al., 2009) have been correlated with the recruitment of different toxins into the proteome of species with predominantly mammalian or varied diets.

Changes in the diet (and size) of venomous snakes may also be related to changes in the composition and function of venom from juvenile snakes as they mature, known as ontogenetic shifts. The first observations of ontogenetic variation in venom were demonstrated by Reid and Theakston who identified changes in the coagulant

activity of *Crotalus atrox* venom as snakes age (Reid and Theakston, 1978). This study concluded that the venom of juvenile snakes was more lethal (indicated by LD_{50}) and showed greater ability to induce platelet aggregation (indicated by *in vitro* platelet aggregation assays) than venom from adults. This study emphasises the importance of understanding ontogenetic variation in venom from a clinical perspective as different venom activities could explain conflicting reports of snakebite envenoming symptoms (Reid and Theakston, 1978). A study by Furtado *et al* demonstrated variation in venom from *Bothrops* species and sub-species by analysing venom protein content and composition by SDS-PAGE, toxicity by LD_{50}, clotting activity by minimum coagulant dose (MCD) and proteolytic activity by substrate assays (Furtado et al., 1991). This study showed that venoms from the offspring of some species (*B. cotiara*) had differing coagulant activity to the maternal venom and, overall, venoms from offspring were shown to possess higher levels of procoagulant activities (Furtado et al., 1991). Another study identified (by SDS-PAGE, immunoblotting, chromatography, lethality, haemorrhagic, coagulant and haemolytic activity assays), a shift in the composition of venom from *Bothrops asper* and *B. atrox* from predominantly high molecular weight proteins (in specimens <1 year of age) to low weight proteins as snakes aged (Saldarriaga et al., 2003). This study also demonstrated higher lethal, haemorrhagic and coagulant activities in juvenile venoms, whereas venoms from older specimens (3 years of age) showed higher indirect haemolytic (PLA_2) activity, which was more significant in *B. asper*. Further studies on venom from the Brazilian pitviper, *Bothrops insularis*, indicated that venom from juveniles snakes showed higher coagulant activities than adult venom, particularly acting on factors X and II (Zelanis et al., 2007). A more recent study showed differences in the activity between venoms from juvenile and adult

Bothrops jararaca; one of the most medically important vipers in Brazil. Here, juvenile venoms showed higher L-amino acid oxidase, hyaluronidase, platelet aggregating and procoagulant activities, although adult venoms were showed to be more lethal than juvenile venoms (Antunes et al., 2010). Studies have also demonstrated that ontogenetic variations in venom may be closely related to diet. A study showed that juvenile *B. jararaca* venom was more toxic to amphibian prey in comparison to endothermic prey (mice) than adult venom (indicated by LD_{50}), and adult venom was more toxic to endothermic prey than juvenile venom (Andrade and Abe, 1999). These observations are reflected in the natural shifts in feeding patterns from ectothermic (frogs) to endothermic (mice) prey as snakes mature from juveniles to maturity. A recent proteomic study demonstrated fine scale ontogenetic shifts in the relative abundance of SVMPs (class I and II) and PLA_2 in the venom of *Sistrurus miliarius barbouri* which was distinctly related to changes in diet (Gibbs et al., 2011). This study identified no substantial changes in the overall composition of venom toxin groups, but a decrease in some PIII SVMPs isoforms was observed, most evident in mouse-fed juveniles. There was also variation in the abundance of a specific PLA_2 with a higher percentage in venom from in juveniles with an ectothermic diet and lower proportion in the venom from juveniles with endothermic diets (Gibbs et al., 2011).

The consensus conclusions for the majority of studies investigating ontogenetic variation in viper venoms indicate that juvenile venoms, overall, exert a distinct pathology to adult venoms, particularly in the coagulant activity of venom, and are at least equal to, and in some cases more toxic than there adult counterparts. This could lead to variations in the clinical manifestation of snakebite and the effectiveness of antivenom treatment if the immunising venom used in the manufacture of

antivenoms does not incorporate venoms from snakes of different levels of maturity. Thus, it is important to characterise levels of ontogenetic venom variation. In this chapter, we aimed to monitor variation in venom composition in *B. arietans* by investigating the development of venom in juvenile *B. arietans* siblings from birth across the course of the study (four years) and identify changes in toxin expression, venom protein composition and enzyme activity of juvenile specimens as snakes mature.

5.3. Materials and Methods:

5.3.1. Venom sample collection and preparation

A gravid wild-caught female specimen was imported to herpetarium in the Alistair Reid Venom Unit from Nigeria, and three months later gave birth to 22 *B. arietans* specimens in captivity in July 2008. New born specimens were fed the same murine diet and were exposed to the same environmental conditions throughout the course of this study. Larger photographs of individual new born *B. arietans* specimens are shown in Appendix VI which show some variation in the coloration and scale patterns between related siblings. Venom samples were extracted from individuals on the day of their birth and subsequently extracted at regular intervals (approx. monthly) until January 2012 (Figure 5.1). At each venom extraction, the following were recorded; (i) specimen health, (ii) specimen bodyweight and (iii) wet venom weight. Venoms samples were frozen at -20°C for 24 hours and lyophilised for 3-4 hours. Due to natural attrition, only three specimens remained throughout the course of the study. This resulted in a variable number (1-20) of venom samples obtained for each individual specimen for analysis at the end of the study.

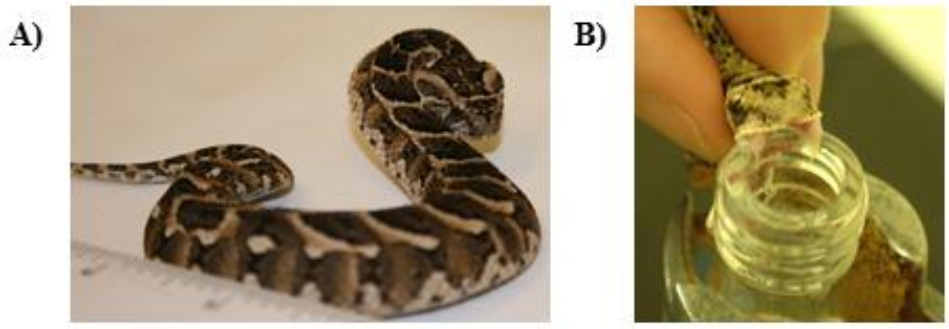

Figure 5.1 *Bitis arietans* juvenile specimen: Individual juvenile *B. arietans* specimen coloration (A) and venom extraction (B).

5.3.2. Extraction of Poly(A) mRNA from venom using Dynabeads®

Messenger RNA was extracted from 2mg selected venom samples from three specimens using the Dynabeads® mRNA extraction protocol (Section 2.6 of Chapter 2). We selected one venom sample from each specimen per year across 4 years. For individuals BaN58-1, BaN58-3 and BaN58-9, we selected venom samples from October 2008 (Year 1), June 2009 (Year 2), November 2010 (Year 3) and November 2011 (Year 4). To increase *n* number BaN58-12 and BaN58-19 were also included in the study, however, these specimens survived only for 3 years and so venom from year 4 was unavailable for these specimens.

5.3.3. Monitoring gene expression levels using relative quantitative PCR (qPCR):

For relative qPCR experiments, 10µl KAPA SYBR® FAST qPCR master mix (containing 0.22µl forward primer (10µM), 0.22µl reverse primer (10µM), 5.5µl KAPA SYBR green dye and 4.06µl ultrapure water) (KAPA Biosystems, AnaChem)

was added to 1µg cDNA. Samples were prepared in triplicate alongside no template controls. PCR amplification of a range of venom protein-encoding gene targets (including a class PII SVMP [BAR00042], group II PLA_2 [BAR00406], SP [BAR00034], CTL [BAR00012], VEGF [BAR00040], LAO [BAR00017], KTI [BAR00023], PDI [BAR00008] and QKWs [BAR00003] (Wagstaff et al., 2008)), normalised against three reference transcripts (β-actin, GAPDH and heat shock protein) was performed using the BioRad CFX 384 real-time PCR system and analysed using the BioRad CFX manager software (version 1.5) in gene expression mode with an initial denaturation step of 95°C for 3 min followed by 40 cycles of 95°C for 10 seconds, 55°C for 30 seconds. Fold expression change for each gene of interest was calculated using the ΔΔCt comparative method (Pfaffl, 2001, Vandesompele et al., 2002) normalised against three reference genes: β-actin, GAPDH and heat shock protein. The data were transformed onto a log scale and analysed by univariate analysis of variance using PASW statistics version 18 (SPSS Inc.) (IBM, 2009) fitting individual snake, time point and venom protein as fixed effects. Differences in venom production attributable to time points were investigated allowing a Bonferroni correction for multiple comparisons. Following statistical analysis, raw data for each individual specimen was standardised by converting fold expression to a percentage of the maximum expression value for each specimen. At each time point, the expression of each toxin target was averaged for all specimens in the study.

5.3.4. Venom protein composition profiling 1D SDS-PAGE:

The protein composition of all venom samples available for each individual was analysed. Venom samples for each individual specimen were reconstituted at 10mg/ml in PBS and diluted to 1mg/ml in reducing SDS-PAGE sample buffer. Samples were separated on 1mm 15% SDS-PAGE gels and stained with Coomassie Blue R-250 as described in Section 2.2.2 of Chapter 2.

5.3.5. Identification of venom proteins by LC-MS/MS

Proteins of interest from SDS-PAGE profiles of individual juvenile and adult *B. arietans* specimens were excised, trypsin-digested and identified by LC-MS/MS as described in Section 2.5 of Chapter 2.

5.3.6. Venom enzyme activity profiling by substrate zymography:

Zymography was carried out using gelatin substrate to visualise the degradative activity of the enzymes present in all individual venom samples as described in Section 2.4 of Chapter 2.

5.4. Results:

5.4.1. Juvenile *Bitis arietans* survival, growth and venom yield rate

Within the initial group of juvenile specimens (22 individuals), we experienced a rapid rate of attrition within the first 12 months of the study and a survival rate of

13.6% at completion of the study in year 4. However, the % of specimens yielding venom per venom extraction was consistently high throughout the course of the study with most specimens producing venom at each extraction, even during the first year of the study. Figure 5.2 shows specimen weight and wet venom weight data collated for all individuals.

We observed correlation between the specimen weight and wet venom weight. Figure 5.2 A indicates that, on average for all specimens, the juvenile snake bodyweight and wet venom yield showed a gradual increase across time from birth throughout the course of the study. The increase in specimen weight (Figure 5.2 B) and wet venom weight (Figure 5.2 C) is also shown on an individual level. Snake bodyweight increased from 19.7g ±2.7 at birth to 393.3g ±25.2 in year 4. The wet venom yield increased from 28.0mg ±13.7 at birth to 185.1mg ±134.4 in year 4 per specimen, demonstrating a positive correlation between snake bodyweight and venom yield across time from birth to year 4.

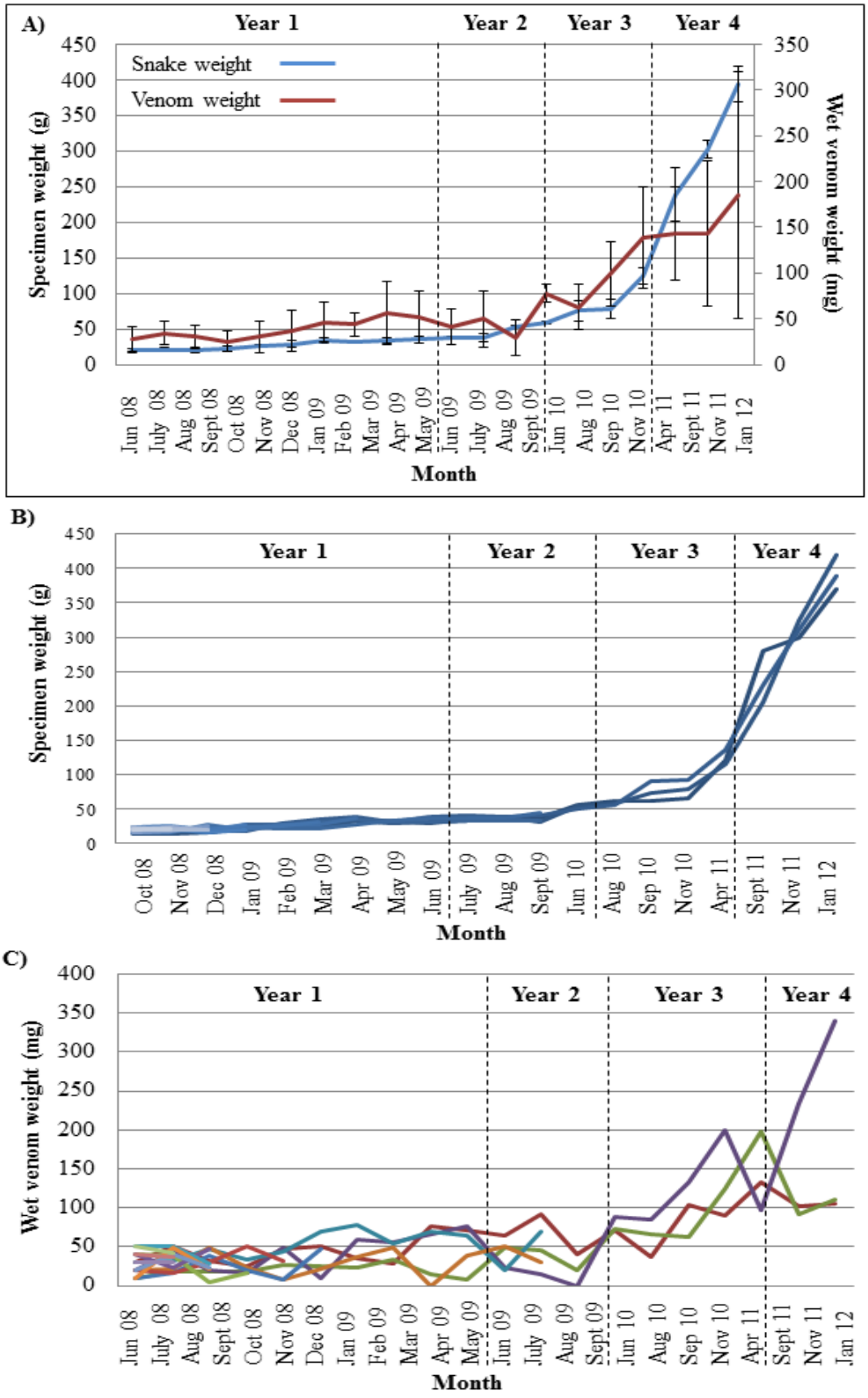

Figure 5.2 Juvenile *Bitis arietans* growth rate and venom production: Relationship between snake weight (g) and weight of extracted venom (mg) in juvenile *B. arietans* specimens on average (panel A) and on an individual level; individual growth rate (panel B) and individual wet venom weight (panel C). Data shows a positive correlation between snake weight and quantity of venom produced.

5.4.2. Quantitative PCR (qPCR) toxin expression profiles of juvenile *B. arietans* siblings from birth

Toxin expression profiles were generated by relative qPCR for five juvenile snakes (BaN58-1, 3, 9, 12 and 19) to monitor changes in expression of mRNA from birth until years 3-4. The data showed variation in fold changes in expression levels between individual specimens (Table 5.1 and Figure 5.4 A). Specimens BaN58-1, BaN58-3, BaN58-12 and BaN58-19 showed broadly similar expression profiles whereas BaN58-9 showed a different expression profile with unusually high levels of expression of SVMP, SP and PDI genes in year one compared to other specimens.

On average, analysis of juvenile toxin expression profiles showed a peak in expression of all transcripts analysed in this study observed in year 2 (Figure 5.3 B). This peak in expression in venom extracted in year two was shown to be statistically significant, confirmed by ANOVA and Bonferroni post-hoc testing. Statistically significant p-values (<0.005) were generated showing differences in expression between year 2 and years 1, 3 and 4 (Table 5.2).

Toxin	Time point	Snake ID BaN58-1	BaN58-3	BaN58-9	BaN58-12	BaN58-19
SVMP	Year 1	1.00	1.00	5.78	0.50	0.83
	Year 2	2.22	1.79	0.70	0.64	1.07
	Year 3	2.14	1.77	0.83	1.29	1.24
	Year 4	0.98	1.83	0.75	-	-
SP	Year 1	1.00	0.96	5.00	1.11	1.16
	Year 2	3.79	2.34	1.00	1.35	0.28
	Year 3	4.32	2.12	1.70	1.11	1.02
	Year 4	2.01	1.59	1.47	-	-
CTL	Year 1	1.00	0.30	0.13	0.86	1.02
	Year 2	6.14	2.34	1.00	1.25	1.49
	Year 3	0.71	0.19	0.11	1.29	0.27
	Year 4	0.36	0.10	0.05	-	-
KTI	Year 1	0.76	0.38	0.27	1.11	1.16
	Year 2	7.19	2.34	1.00	1.73	1.15
	Year 3	0.75	0.27	0.30	1.28	0.84
	Year 4	0.40	0.12	0.13	-	-
PDI	Year 1	1.00	1.00	2.68	0.47	0.69
	Year 2	0.76	1.65	1.00	1.61	1.34
	Year 3	0.58	1.11	0.30	0.88	0.58
	Year 4	0.75	1.99	1.61	-	-
QKW	Year 1	0.44	0.18	0.13	0.69	0.64
	Year 2	7.19	2.34	1.00	2.01	1.49
	Year 3	0.27	0.09	0.10	1.02	1.01
	Year 4	0.50	0.20	0.14	-	-

Table 5.1 Relative qPCR gene expression levels during venom production in juvenile *Bitis arietans* specimens: Raw qPCR data generated from relative expression analysis to show fold changes in expression of venom genes of interest, including snake venom metalloproteinase (SVMP), serine protease (SP), C-type lectin (CTL), Kunitz inhibitors (KTI), protein disulphide isomerase (PDI) and QKW inhibitory peptides (QKW) in juvenile *B. arietans* venom from birth until year 3-4. Dashes indicate samples in year 4 which were not available in individuals BaN58-12 and 19. Blue shaded areas indicate peak values in expression levels for each specimen and each gene of interest.

Time point (I)	Time point (J)	Mean difference (I-J)	P-value
Year 1	Year 2	-0.3203	0.003*
	Year 3	0.0571	1.000
	Year 4	0.1034	0.342
Year 2	Year 3	0.3774	0.003*
	Year 4	0.5193	0.000*
Year 3	Year 4	0.1418	1.000

Table 5.2 Statistical analysis of gene expression data from juvenile *Bitis arietans* venom samples: Fold changes in relative expression levels of venom genes of interest in juvenile *B. arietans* specimens analysed by ANOVA and Bonferroni post-hoc testing showed a statistically significant difference in gene expression levels in year 2. * indicated significant p-value.

Figure 5.3 B indicates that the expression of SVMPs and SPs, major enzymatic and highly pathogenic components of *B. arietans* venom, appeared to be maintained at a more consistent level with a less-pronounced peak in expression in year 3. In contrast, the non-enzymatic venom components which were surveyed in this study (CTL, KTI, PDI and QKW) appeared to show more highly variable levels of gene expression which appeared to peak in venom extracted in year 2.

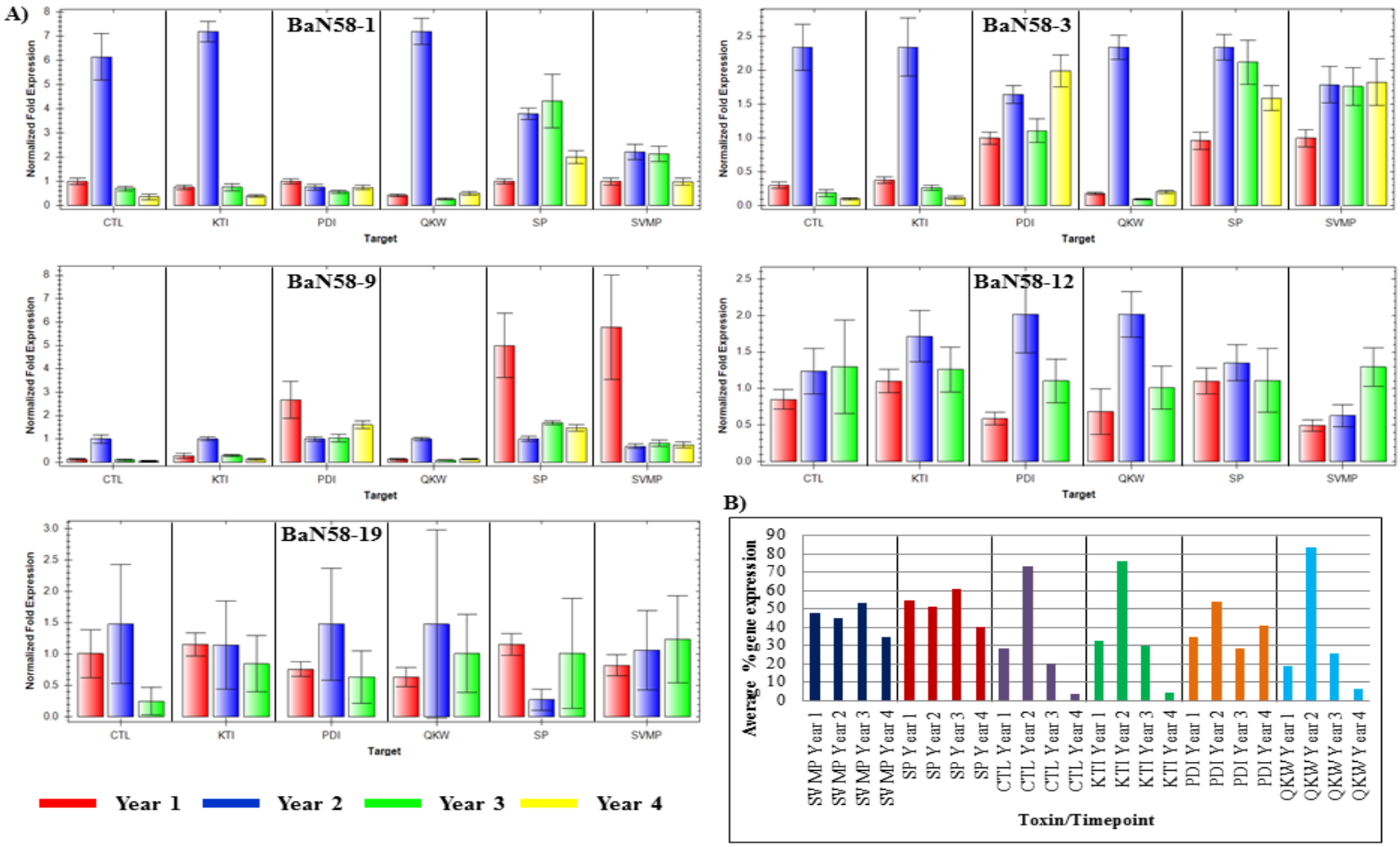

Figure 5.3 Juvenile *Bitis arietans* toxin gene expression profiles during venom production: qPCR profiles for five individual *B. arietans* specimens showing fold changes in expression levels of a range of venom genes of interest relative to three references genes for 5 individual juvenile *B. arietans* specimens (A) and % expression levels averaged for three specimens (BaN58-1, 3 and 9) indicating a peak in the expression of some genes in year 2 (B).

5.4.3. Venom protein profiles of juvenile *B. arietans* siblings from birth

The venom protein profile was analysed by SDS-PAGE for every available venom sample for each individual juvenile *B. arietans* specimen. Venom protein profiles are shown in Figure 5.4 indicating that, qualitatively, there were no pronounced changes in the overall protein composition of venom from birth to 4 years. The juvenile *B. arietans* venom protein profile consisted of numerous low molecular weight proteins, few mid-molecular weight proteins and several proteins present in the high molecular weight region and showed very little variation between individual siblings. In comparison to the maternal venom (BaN58), juvenile venom samples shared the majority of proteins present in adult venom, although all juvenile venoms appeared lack a distinct protein present in the maternal venom of around 33kDa in weight (Figure 5.4 BaN58, band circled in red).

Although for many specimens, few venom samples were available for protein analysis due to poor survival rate, we found that interestingly, there was little change in venom protein composition during the 4 year maturation of specimens which survived the course of the study. Also, the protein composition of venom did not change in snakes which did not survive the course of the study, indicating that death of snakes was not reflected in venom composition.

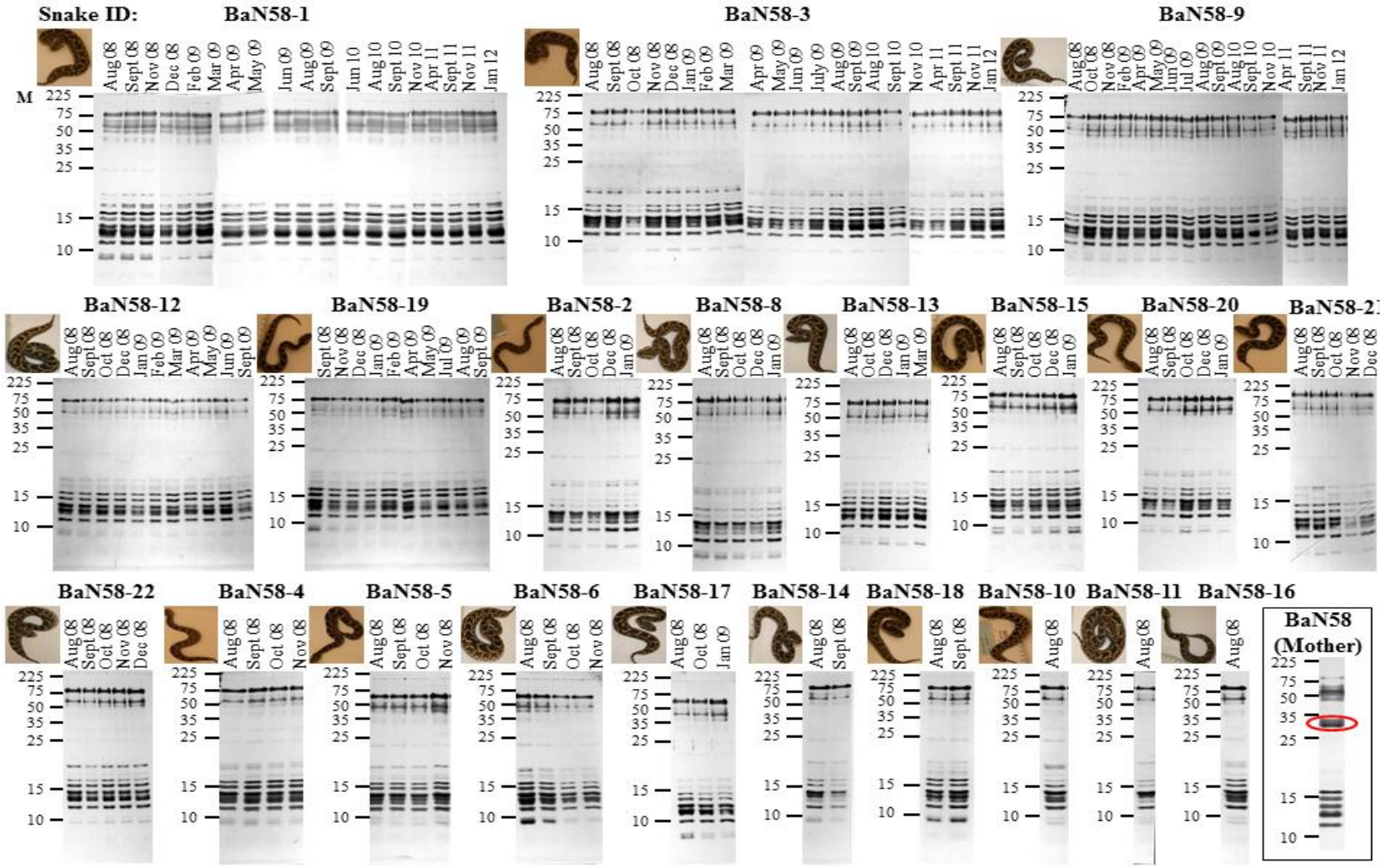

Figure 5.4 Juvenile *Bitis arietans* venom protein profile: SDS-PAGE profiles for individual juvenile *B. arietans* specimens of venom (10mg/ml) extracted at regular intervals from birth until 4 years. Molecular weight markers (kDa) are shown on the left of each image. Band (circled) on BaN58 (mother) profile indicates protein present in maternal venom which was apparently absent in juvenile venoms.

5.4.4. Mass spectrometry identification of proteins of interest from juvenile *B. arietans* samples

For the three surviving specimens (BaN58-1, 3 and 9), several proteins from low, mid and high molecular weight regions were excised from SDS-PAGE protein profiles and trypsin-digested for identification by mass spectrometry. Proteins of interest were also excised and identified from the maternal venom (BaN58). These proteins from *B. arietans* venom were confidently identified by mass spectrometry (Figure 5.5). Figure 5.6 shows full and partial length peptide sequences assigned to protein bands by LC-MS/MS.

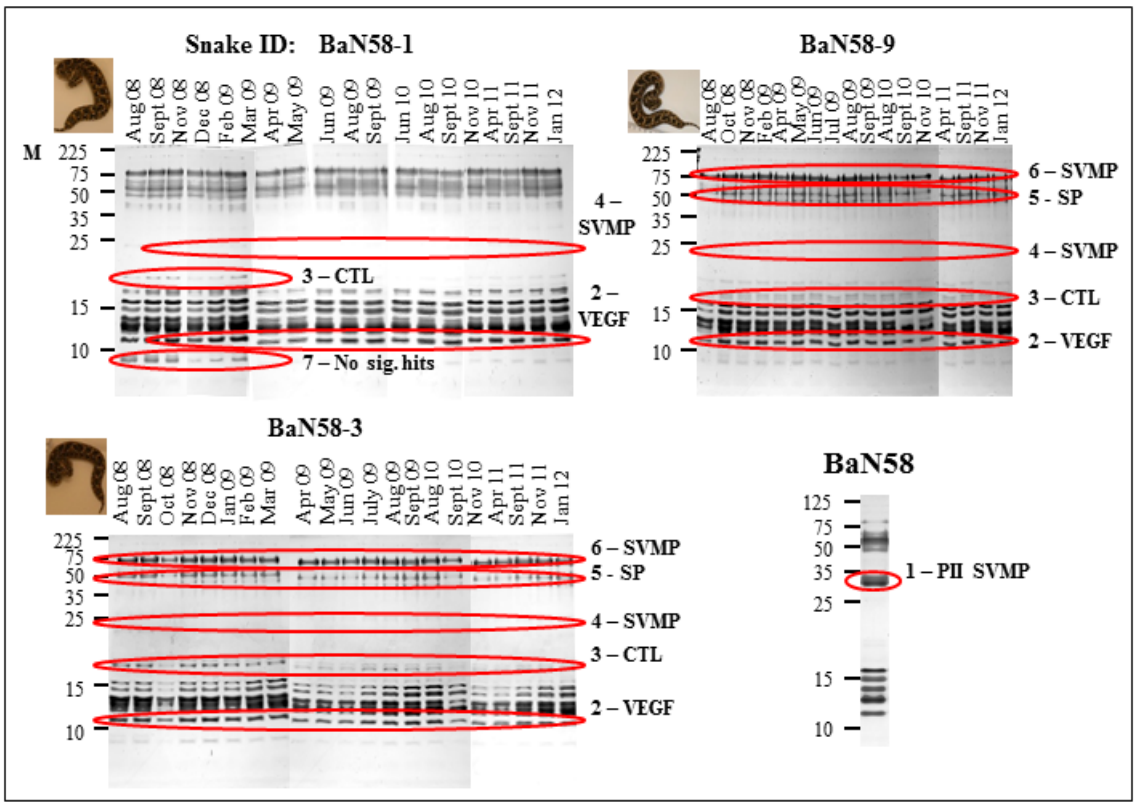

Figure 5.5 Mass spectrometry identification of protein bands from juvenile *Bitis arietans* venom: Protein bands of interest were excised from SDS-PAGE protein profiles of three individual juvenile and adult *B. arietans* specimens, including a protein band present in adult maternal venom which appeared to be absent in juvenile venoms (band 1).

1. PII SVMP 33kDa

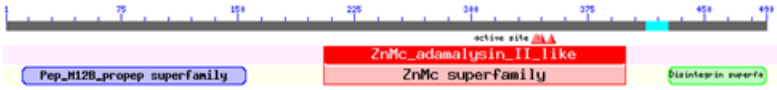

BAR00015:MIQVLLVIICLAVFPYQGSSIILESGNINDYEVVHPQKVTALPKGAAKQPEQKYEDTM
QYEFKVNGEPVVLHLEKNKGLFFKDYSETHYSPDGREITTKPPVEDHCYYHGRIQNDADSTASIS
ACNGLKGHFTLQGEMYLIEPLKITDSEAHAVFKYENIEKEDEAPKMCGVTQTNWESDVPIKKAS
QLVATSEQHRSCDLNRDLKIMVVADHRLVNYYKGBBBBBBBBBIFQVFNMLKEIFRYLYIRPILDG
IEIWSNGDLCTVTNSAYDTLRSFAEWRDRDLRQRKKHDNAQLFTGTKFNGGIIGKAYIGTICDLK
LSSGVVMNYRPEIDSAAAAIMAHEIGHNLGINHDGNQCYCYGYSCIMAAQISDPPPKYFSNCSWN
EYNKFINTDKAQCLCNETSRTVIVSPPVCGNELLEEGEECDCGSPANCQDRCCNAATCKLTPGSQ
CNHGECCDQCKFKKARTVCRIARGDWNDDYCTGKSSDCPWNH

2. VEGF 12kDa

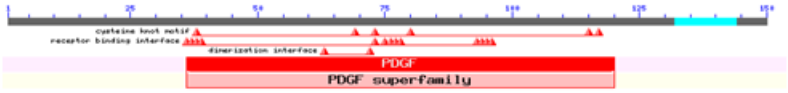

BAR00040:MAAYLLAVAILFCIQGWPSGTVQGEVRPFMEVYQRSVCQPRETLVSILEEYPDKISKIF
RPSCVAVLRCGGCCSDESLTCTSVGERTVELQVMQVTPKTLSSKIKVMKFREHTACECRPRSGSR
VNIGKHKRSPEEGEREPSSPLTPGSL

3. C-type lectin 18kDa

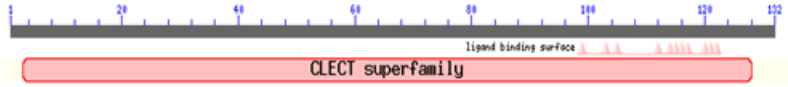

BAR00473:FECPTEWCPYDQHCYRAFDEPKRSVDAEKFCVEQAGHLASIESKEEADFVAQLVSEN
VKSSPDYVWIGLWNQRKEQYCNKKWTDGSSVIYQNMVERFRKNCFGLEKESGYRTWLNLRCG
DDYPFVCKFPPRC

4. SVMP 24kDa

BAR00027:CKNECCEAATCKLKPGAKCADGGCCERCQFRTAGAECRVSKDDCDLPEHCTGQSAE
CPMNRFQKNGHPCQNNLGYCFRGTCPTLTNQCIALFGPDAKVAPDTCFLKNQKGDTNGHCTNEE
DINIPCKEKDVKCGRLYCTDGSGDKKSCNFHISKEISEYGMVDPGTKCGEGMVCNXGGLQRNVK
MNAAKLQLVN

5. SP 50kDa

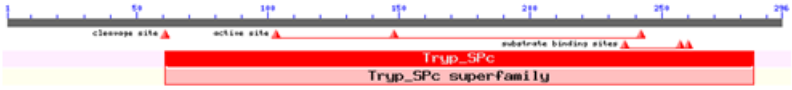

BAR00031:MVLIRVLANLLLLQLSYAQKSSELVIGGDECDINEHPSLALIYNSTSMRFHCSGTLLNQ
EWVVTAAHCDMENMQIYLGVHNKIKPNPDQQKRLPKETFFCLSNKSYTMWDKDIMLIRLNSPVS
YSTHITSFSLPSSPPTVGSVCRIMGWGAIKSPNETYPDVPHCANIKLYDYSVCRDAYGDLPEKSRTL
CAGVLEGGKDTCIADSGGPLICNGEFHGIVAWGRHPCAQPHLPAFYTKVFDYGDWIKNIIAGNTA
ATCPP

BAR00263:SRSLCLGYLIRLIQYFSFKFGTGILQANSLPHRIEAMVLIRVLANLLVLQLSYAQKSSEL
VIGGDECDINEHPFLVALHTLKSKRFHCAGTLLNQEWVLTAARCNRKNIRINFGVHSKNVQNEDE
EIRVPKEKHFCLSSKIYTKWDKDIMLIRLKRPVNNTTHIAPLSLPSNPPSVGSVCRIMGWGSITTTK
EIYPDVPHCANIKLFDYSVCRAAHQKLPEKSRTLCAGILEGGIDSCKVDNGGPLICNGQIHGIVSW
GGHPCAQPLKPALYTNVLDYTDWIEGIIAGNTAATCPP

Figure 5.6 continued on following page:

Figure 5.6 continued:

Figure 5.6 Full and partial-length peptide sequences identified by LC-MS/MS from juvenile *Bitis arietans* specimens: Peptide searches against contigs assembled from our *B. arietans* venom gland EST database were performed to identify protein bands 1-7 (Figure 5.5A). Signal peptides predicted using Signal P (Bendtsen et al., 2004) are underlined. Peptides identified by LC-MS/MS are indicated in red. For SVMP sequence BAR00015, the RGD disintegrin tripeptide is boxed. 'B' amino acids = asparagine or aspartic acid.

Firstly, we identified a 33kDa protein band – PII SVMP isoform, BAR00015 - which was present in the maternal venom (Figure 5.5, band 1) but was not detected in any of the juvenile venoms. This was the most notable difference in protein composition between adult and juvenile venoms. We also identified several proteins which appeared to be conserved between individual juvenile specimens and which also did

not appear to significantly change in abundance across time from birth. These included CTL [BAR00473] (band 3), SP [BAR00031/BAR00263] (band 5) and class PI and PII SVMPs [BAR00027] (band 4) and [BAR00076/BAR00462/BAR00346] (bands 6), all of which are components of *B. arietans* venom known to significantly contribute to the pathological effects of envenoming, and VEGF [BAR00040] (band 2) which is thought to play a less toxic role in venom. One protein band (band 7) could not be confidently identified following searches against our *B. arietans* database which could potentially indicate the presence of novel, uncharacterised protein groups. Table 5.3 shows a list of peptide sequences identified by mass spectrometry and Proteome Discoverer 1.1.0 (ThermoScientific) software for each protein of interest. For most proteins, a single cluster was confidently identified following searches of Uniprot databases and a *B. arietans* venom gland EST database using Proteome Discoverer.

Band	Snake	Molecular weight on gel (kDa)	MS-derived molecular weight (kDa)	Cluster identified	Protein family	Accession no.	Peptide ion m/z (Da)	z	MS/MS derived sequence	Mascot		Sequest	
										Ion score	Exp value	Probability	XCorr
1	Adult	33	53	BAR00015	PII-SVMP	ADW54354	403.535	+2	FNGGIIGK	47	2.27E-05		
							616.130	+2	HDNAQLFTGTK	47	7.64E-06		
							470.580	+2	IMVVADHR	39	1.69E-04		
							577.475	+2	AYIGTICDLK	34	2.27E-04		
							577.500	+2	AYIGTICDLK	18	9.42E-03		
							616.130	+2	HDNAQLFTGTK			76.57	3.72
							577.475	+2	AYIGTICDLK			70.75	2.71
							470.580	+2	IMVVADHR			63.49	2.41
							577.500	+2	AYIGTICDLK			19.99	2.15
							1153.400	+1	AYIGTICDLK			33.23	2.10
							403.535	+2	FNGGIIGK			30.96	2.06
							795.205	+1	SFAEWR			9.41	1.33
							796.200	+1	SFAEWR			21.12	1.24
							795.215	+1	SFAEWR			2.43	1.23
2	Juvenile	12	14	BAR00040	VEGF	C0K3N1.1	687.075	+2	TVELQVMQVTPK	84	2.93E-09		
							686.590	+2	TVELQVMQVTPK	69	9.71E-08		
							695.105	+2	TVELQVMQVTPK	66	2.46E-07		
							686.610	+2	TVELQVMQVTPK	64	3.92E-07		
							695.070	+2	TVELQVMQVTPK	62	5.17E-07		
							686.640	+2	TVELQVMQVTPK	57	1.91E-06		

							687.055	+2	TVELQVMQVTPK	52	5.04E-06			
							687.045	+2	TVELQVMQVTPK	38	1.24E-04			
							695.095	+2	TVELQVMQVTPK	34	3.27E-04			
							686.910	+2	TVELQVMQVTPK	28	1.41E-03			
							660.265	+2	IFRPSCVAVLR	28	1.60E-03			
							439.935	+3	IFRPSCVAVLR	26	2.85E-03			
							1372.545	+1	TVELQVMQVTPK	25	2.88E-03			
							659.245	+2	IFRPSCVAVLR	21	8.59E-03			
							1373.570	+1	TVELQVMQVTPK	20	1.02E-02			
							687.075	+2	TVELQVMQVTPK			70.72	4.61	
							695.070	+2	TVELQVMQVTPK			59.24	4.26	
							1017.775	+2	CGGCCSDESLTCTSVGER			86.76	4.24	
							695.105	+2	TVELQVMQVTPK			75.68	4.02	
							686.640	+2	TVELQVMQVTPK			63.89	3.93	
							695.095	+2	TVELQVMQVTPK			40.25	3.67	
							686.610	+2	TVELQVMQVTPK			42.51	3.56	
							686.910	+2	TVELQVMQVTPK			57.90	3.51	
							687.055	+2	TVELQVMQVTPK			49.31	3.49	
							686.590	+2	TVELQVMQVTPK			60.39	3.46	
							1018.630	+2	CGGCCSDESLTCTSVGER			58.59	3.46	
							439.935	+3	IFRPSCVAVLR			40.77	3.42	
							687.045	+2	TVELQVMQVTPK			46.63	3.13	
							1372.545	+1	TVELQVMQVTPK			3.80	2.57	
							1373.570	+1	TVELQVMQVTPK			20.34	2.49	
							659.245	+2	IFRPSCVAVLR			18.47	2.39	
3	Juvenile	18	16	BAR00473	CTL	Q6T7B6	731.145	+2	NCFGLEKESGYR	51	3.89E-06			
							730.185	+2	NCFGLEKESGYR	41	5.86E-05			

							802.315	+1	TWLNLR	23	4.41E-03		
							434.470	+2	NCFGLEK	22	5.27E-03		
							401.970	+2	TWLNLR	22	8.35E-03		
							401.500	+2	TWLNLR	19	9.87E-03		
							631.010	+2	CGDDYPFVCK	19	8.91E-03		
							631.010	+2	CGDDYPFVCK			37.03	3.54
							630.985	+2	CGDDYPFVCK			41.82	3.25
							730.185	+2	NCFGLEKESGYR			73.75	2.99
							867.225	+1	NCFGLEK			6.48	1.90
							802.315	+1	TWLNLR			30.49	1.48
							803.275	+1	TWLNLR			10.65	1.30
				BAR00015	PII SVMP	ADW54354	577.065	+2	AYIGTICDLK	26	2.08E-03		
							577.065	+2	AYIGTICDLK			49.75	2.79
				BAR00076	SVMP	ADI47583.1	679.550	+2	ACQLAATSEFMK	34	3.74E-04		
							679.550	+2	ACQLAATSEFMK			40.49	3.88
4	Juvenile	24	21	BAR00027	SVMP	ABN72547.1	713.545	+2	EISEYGMVDPGTK	53	5.70E-06		
							1033.685	+2	GTCPTLTNQCIALFGPDAK	50	6.15E-06		
							721.525	+2	EISEYGMVDPGTK	49	8.24E-06		
							908.495	+2	VSKDDCDLPEHCTGQSAECPMNR			107.58	4.82
							1032.325	+2	GTCPTLTNQCIALFGPDAK			68.37	3.89
							713.545	+2	EISEYGMVDPGTK			79.22	3.45
							721.525	+2	EISEYGMVDPGTK			51.53	3.25
							1032.715	+2	GTCPTLTNQCIALFGPDAK			103.55	3.24
							907.560	+3	VSKDDCDLPEHCTGQSAECPMNR			22.29	2.60
							1050.305	+1	VAPDTCFLK			26.99	1.75
5	Juvenile	50	29	BAR00031	SP	E0Y418.1	626.090	+2	DAYGDLPEKSR	26	1.87E-03		

							538.005	+2	LYDYSVCR	23	6.31E-03			
							538.005	+2	LYDYSVCR			28.57	2.98	
							626.090	+2	DAYGDLPEKSR			45.70	2.35	
				BAR00263	SP	Q6T6S7.1	785.685	+2	NVQNEDEEIRVPK	51	7.77E-06			
							530.475	+2	LFDYSVCR	51	1.37E-03			
							785.685	+2	NVQNEDEEIRVPK			42.83	3.74	
							530.475	+2	LFDYSVCR			48.07	3.04	
6	Juvenile	75	39	BAR00076	SVMP	ADI47583.1	823.170	+2	ENDVKIPCAQEDVK	34	1.74E-04			
							548.990	+3	ENDVKIPCAQEDVK	27	9.16E-04			
							530.055	+2	IPCAQEDVK	25	5.78E-03			
							717.080	+2	IPCAQEDVKCGR	19	8.23E-03			
							823.670	+2	ENDVKIPCAQEDVK	18	1.10E-02			
							823.170	+2	ENDVKIPCAQEDVK			51.71	3.45	
							717.080	+2	IPCAQEDVKCGR			66.76	2.78	
							548.990	+3	ENDVKIPCAQEDVK			28.10	2.67	
							530.055	+2	IPCAQEDVK			31.60	2.59	
				BAR00462	SVMP	ADI47619.1	595.560	+2	VVNNVNVIYR	54	4.64E-06			
							596.050	+2	VVNNVNVIYR	39	1.67E-04			
							594.935	+2	VVNNVNVIYR	28	1.70E-03			
							712.190	+1	YFNIR	21	6.79E-03			
							595.560	+2	VVNNVNVIYR			65.52	3.61	
							596.050	+2	VVNNVNVIYR			46.86	2.50	
							594.925	+2	VVNNVNVIYR			32.80	2.34	
							713.200	+1	YFNIR			14.11	1.18	
							712.190	+1	YFNIR			10.62	1.18	
				BAR00346	SVMP	Q98UF9.3	633.440	+3	FINIHNPQCISNKPSK	39	8.95E-05			
							900.125	+2	TDIVSPPVCGNELLER	38	1.04E-04			

					633.440	+3	FINIHNPQCISNKPSK	68.08	3.77
					882.155	+3	GECDVSDLCTGQSAECPLDVFKR	57.09	3.53
					900.125	+2	TDIVSPPVCGNELLER	77.06	2.98
7	Juvenile	9	N/A	No confident hits					

Table 5.3 LC-MS/MS identification of venom proteins from juvenile *Bitis arietans* venom samples: Identification of protein components excised and trypsin-digested from individual juvenile and adult *B. arietans* venom samples in Figure 5.8. The table includes a list of peptide sequences derived by mass spectrometry for each protein of interest, the protein family assigned to each protein and the accession number of the protein which corresponds to the closest protein match identified by BLAST search. Ion score and E values indicate protein identification by Mascot algorithm and Probability and XCorr correspond to protein identification by Sequest algorithm.

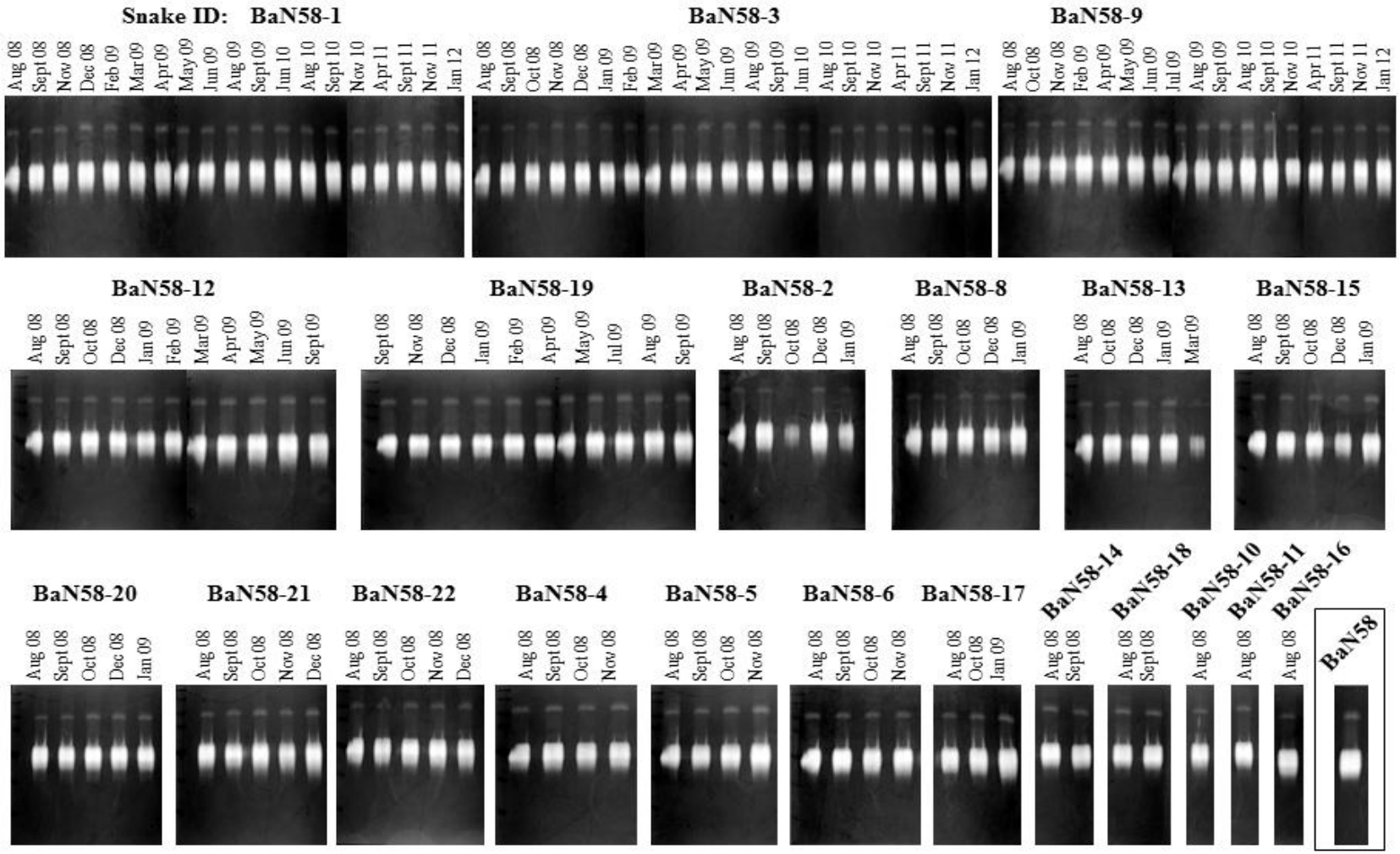

Figure 5.7 Juvenile *B. arietans* venom enzyme activity profiles: Gelatin zymography to visualise enzyme activity of venom samples from juvenile and adult *B. arietans* specimens from birth until present/death shows that venom is highly enzymatically active immediately from birth and that juvenile venom activity appears to be comparable to that of adult (maternal – BaN58) venom.

5.4.5. Enzyme activity of venom samples from juvenile *B. arietans* specimens

Figure 5.7 illustrates the proteolytic activity of enzymes, such as SVMPs, present in venom samples extracted from juvenile specimens from birth until present/death using gelatin zymography. All juvenile venoms showed very similar regions of substrate degradation with a major mid-molecular weight region and a less intense, distinct region of degradation at a high molecular weight. Importantly, venom was highly enzymatically active immediately from birth and appeared to be maintained at a constant level throughout the course of the study. Again, it is interesting to note that enzyme activity of venom did not change or was not compromised in specimens which did not survive for the course of the study. The region/intensity of substrate degradation by juvenile venoms seemed to be comparable to that of the maternal venom (BaN58) (Figure 5.7).

5.5. Discussion

Several studies have demonstrated that venom composition and function are, to some extent, plastic and can be influenced by environmental conditions such as diet. It has been suggested that changes in diet, i.e. shifts from smaller (ectothermic) to larger (endothermic) prey, which are often observed as snakes mature from juveniles to adults, may be responsible for resulting in changes in the protein composition and toxicity of venoms (Andrade and Abe, 1999, Gibbs et al., 2011). Currently, limited information is available to understand the mechanisms underlying variation in venom composition and toxicity. Our previous findings in Chapter 3 indicated significant levels of intra-species variation in protein composition and enzyme activity of venom from a group of unrelated, wild-caught adult *B. arietans* specimens originating from

the same and different geographical origins (Currier et al., 2010), demonstrating that the adaptability of this species to occupy a wide range of habitats may be reflected in the composition of its venom. In contrast, here we have investigated the levels of variation in venom between a group of sibling, captive-bred *B. arietans* specimens and demonstrated that very little variability in venom composition and activity exists between familiarly related specimens. We also showed that the protein composition and activity of venom did not appear to significantly change from birth until 4 years, within the resolutions of SDS-PAGE and substrate zymography techniques used in the study. We observed that both the composition and enzymatic activity of juvenile venoms was highly developed and appeared to be comparable to that of the maternal adult venom immediately after birth. This indicated that the ability of specimens to produce biologically functional venom may be genetically 'hard wired', which most likely reflects the vital role of venom in both defensive and predatory mechanisms. This was also emphasised following observations that the high rate of attrition of specimens in the study did not appear to affect the production of venom.

Our results generated by qPCR indicated a change in the gene expression profiles of venom proteins during maturation of snakes. We observed a peak in gene expression levels of all transcripts surveyed in this study in year 2. This was not reflected in our analyses of the venom protein composition and enzyme activity which remained relatively constant across time, although it was difficult to directly compare changes in gene expression with protein composition due to the high sensitivity of qPCR technology compared with gel electrophoresis. The peak in toxin expression in year 2 did not appear to relate to any defined environmental or biological factors as the diet and environmental conditions were maintained constant throughout the study. However, due to circumstances beyond our control (herpetarium refurbishment),

specimens were moved to a temporary accommodation for a three month period from November 2009 to February 2010 during which a change in temperature and humidity may have occurred. During the three month period of temporary accommodation, venom was not extracted from specimens for safety reasons. This resulted in an interruption in the frequency of venom extractions which may have affected venom production in juvenile snakes as it has been documented that the total volume of venom present in venom glands of snakes may dictate venom synthesis, i.e. venom depletion of venom stores initiates re-synthesis of proteins (Mackessy, 1991). For qPCR gene expression profiling, we selected a single venom sample for each year of the study which was available for all three specimens surviving the course of the study (BaN58-1, 3 and 9), in sufficient amounts required for qPCR (2mg). The venom samples we selected for qPCR profiling were extracted three months prior to and several months after the change in environmental conditions during temporary accommodation. Therefore, we cannot conclude whether the peak in gene expression observed in year two was related to the 3-month interruption in venom extractions. To conclude whether an interruption in the frequency of venom extraction resulted in a change in gene expression levels, we aim to increase the number of venom samples in qPCR profiling experiments to include venom samples extracted immediately prior to and after the change in environment.

Although the results of this study demonstrated that venom from juvenile *B. arietans* specimens appeared to be similar to adult venom in terms of enzyme activity, we observed a difference in the protein composition of venom in the presence/absence of a class PII SVMP isoform BAR00015. We could not detect BAR00015 in the proteome of juvenile venom, potentially due to a complete absence of this transcript from the venom gland transcriptome or due to proteolytic processing of the protein.

This PII isoform is thought to be an important component of *B. arietans* venom as it contains an RGD-containing disintegrin domain, corresponding to bitistatin, a long-chain disintegrin isolated from the venom of *B. arietans* (Juárez et al., 2006). Bitistatin, following release from the PII metalloproteinase domain through proteolysis, has been shown to act as a potent inhibitor of platelet aggregation and function through selectively blocking the binding of fibrinogen to the integrin $\alpha_{IIb}\beta_3$ receptor (Shebuski et al., 1989, Huang et al., 1987). As SVMPs are highly pathogenic and important for *B. arietans* envenoming, we could suggest that the composition of these enzymes in venom could have implications on the overall toxicity and clinical effect of venom. Although our findings here showed that the overall proteolytic activity of juvenile and adult venoms were comparable, our tests were not sensitive enough to reveal differences in specific toxin activity.

Further experiments including *in vivo* assays, are currently on going to explore differences in the clinical effects of envenoming. Differences in the toxic effects induced by juvenile and adult *B. arietans* venom may affect the manifestation of clinical symptoms in snakebite victims. This could have implications on the treatment of envenoming, if differences in activity of juvenile venoms are not accommodated for in the manufacture of antivenom. Previous *in vivo* studies have shown some differences in the clinical effects of *B. arietans* envenoming between adult and juvenile specimens (Theakston and Reid, 1983). The LD_{50} of juvenile *B. arietans* venom following injection into mice was slightly lower than adult venom at 20.3µg/mouse compared to 25.0µg/mouse of adult venom indicating that juvenile venom may be more toxic. Differences in other venom-induced pathology were observed including haemorrhage, defibrinogenation and necrosis. The MHD (minimum haemorrhagic dose) indicated that juvenile venom (from Saudi Arabia)

was twice as haemorrhagic as adult venom (from Nigeria), although here it is important to note that snakes originated from different geographical locations. The MDD (minimum defibrinogenating dose) also indicated that the juvenile venom had a higher defibrinogenating activity than adults, although adult venom was more necrotizing than juvenile venom (Theakston and Reid, 1983). We are currently conducting MHD experiments to compare levels of venom-induced haemorrhage following injection of mice with either juvenile or adult *B. arietans* venom and also to assess whether the toxicity of venom changes as juvenile specimens mature.

6. UNUSUAL STABILITY OF MESSENGER RNA IN SNAKE VENOM REVEALS GENE EXPRESSION DYNAMICS OF VENOM REPLENISHMENT.

The results of most of the work performed in this chapter have been published in Public Library of Science One (Currier et al., 2012).

6.1. Abstract

Venom is a critical evolutionary innovation enabling venomous snakes to become successful limbless predators; it is therefore vital that venomous snakes possess a highly efficient venom production and delivery system to maintain their predatory arsenal.

Here, we exploit the unusual stability of messenger RNA in venom to conduct, for the first time, quantitative PCR to characterise the dynamics of gene expression of newly synthesised venom proteins following venom depletion. Quantitative PCR directly from venom enables real-time dynamic studies of gene expression in the same animals because it circumvents the conventional requirement to sacrifice snakes to extract mRNA from dissected venom glands. Using qPCR and proteomic analysis, we show that gene expression and protein re-synthesis triggered by venom expulsion peaks between days 3-7 of the cycle of venom replenishment, with different protein families expressed in parallel. We demonstrate that venom re-synthesis occurs very rapidly following depletion of venom stores, presumably to

ensure venomous snakes retain their ability to efficiently predate and remain defended from predators.

The stability of mRNA in venom is biologically fascinating, and could significantly empower venom research by expanding opportunities to produce transcriptomes from historical venom stocks and rare or endangered venomous species, for new therapeutic, diagnostic and evolutionary studies.

6.2. Introduction

Snake venom is an evolutionary innovation contributing to the success of venomous snakes as proficient limbless predators. Venom consists of a complex mixture of proteins and peptides that have evolved from normal physiological proteins (Fry, 2005) into multi-isoform, multi-domain protein families with distinct biochemical targets. The collective spectrum of pharmacological specificities and biological potency of venom ensures rapid and efficient immobilisation, killing and digestion of a diverse range of prey species, irrespective of physiological differences (Kordiš et al., 2002). The pathological consequences of snakebite may also constitute an effective defence against predators and aggressors. Thus, an efficient venom production system is vital for venomous snakes to overcome their vulnerability following depletion of venom glands after a predatory or defensive snakebite.

Venom glands are modified parotid glands comprising a densely folded secretory epithelium consisting of several distinct cell types, including glandular secretory, mitochondria-rich, horizontal and ‘dark’ cells (Oron and Bdolah, 1978, Mackessy, 1991, Mackessy and Baxter, 2006). This abundance of secretory cells is required for

rapid re-synthesis of venom proteins and other components to replenish venom stores after a bite. The systems for storage of venom following exocrine secretion depends upon the snake species, and include in (i) the central venom gland lumen, (ii) smaller tubular ductules, (iii) intracellular granules (Oron and Bdolah, 1978) and (iv) microvesicles within the lumen (Carneiro et al., 2007). The dynamics of venom accumulation and expression of individual venom components during synthesis is of great interest but little understood. Early studies observed temporal changes in the transcriptional activity of total venom gland RNA and total protein levels which peaked at day 3 and days 4 to 8 days post venom expulsion respectively (Paine et al., 1992). However, as messenger RNA (mRNA) only constitutes 1-2% of total RNA, here it was not possible to elucidate variations in the expression profile of venom-coding mRNA. Although it is thought that each secretory cell within the glandular epithelium produces all venom components (Taylor et al., 1986), early immunohistochemical studies suggested that the regeneration of depleted venom following expulsion may be asynchronous and that unique protein groups may be independently expressed, possibly relating to their toxic or physiological role in venom (Oron and Bdolah, 1973, Sobol Brown et al., 1975, Oron and Bdolah, 1978). Due to a lack of tools and the unpalatable need to sacrifice specimens (often rare, difficult to capture and CITES listed) for dissection of venom glandular tissue in conventional methods, the real-time study of gene expression of snake venom glands has been historically problematic and dynamic studies to track the expression of individual venom protein-encoding genes during venom synthesis have not been possible to date.

Exploiting the unusual observations of Chen *et al* (Chen et al., 2002), which demonstrated that intact mRNA can be recovered, and toxins can be PCR-amplified

and cloned from snake venoms and other venomous animals, we aimed to characterise the expression profiles of venom genes during the course of venom protein replenishment following depletion of venom and correlate the resultant gene expression profiles with venom protein composition and enzyme activity, using the African Puff Adder (*Bitis arietans*) as a model viper species. We previously demonstrated in Chapter 5 that the venom delivery system of juvenile *Bitis arietans* snakes appears to be functional and capable of producing biologically active venom immediately from birth emphasising venom as an important predatory tool. Subsequently, in this chapter we aimed to monitor the expression of venom protein-encoding genes during the course of venom replenishment following depletion and investigate how venom synthesis is coordinated. Here, we also demonstrate that mRNA is a remarkably stable component of venom during long-term storage of lyophilised venom samples and discuss how this unusual phenomenon has potential to significantly empower venom research.

6.3. Methods

6.3.1. Venom samples and standards:

Eight adult *B. arietans* specimens originating from Ghana (BaG) or Nigeria (BaN) were maintained in the herpetarium at the Liverpool School of Tropical Medicine under identical dietary and environmental conditions. Snakes were identified as BaG2, BaG4, BaG-LZS2, BaN11, BaN60, BaN68, BaN80 and BaN81. No venom was extracted from the animals for at least 25 days prior to the start of the study. The first venom extraction was referred to as mature venom. Thereafter, venom was extracted from the same individuals at four time points, referred to as day 0-1, day 0-

3 and day 0-7, and immediately frozen at -20°C, lyophilised and stored at 4°C. Wet and dry masses of venom samples were recorded. Lyophilised venom samples were reconstituted in phosphate buffered saline (PBS) at their natural concentrations by re-suspension in volumes of PBS identical to that lost during lyophilisation.

6.3.2. Extraction of Poly(A) mRNA from venom using Dynabeads®:

Poly(A) mRNA was purified from 2mg of each individual lyophilised venom samples from all specimens using the Dynabeads® mRNA extraction protocol (Section 2.6 of Chapter 2). Concentration and purity of mRNA (measured by the ND-1000 Spectrophotometer) were recorded.

6.3.3. cDNA synthesis:

cDNA was synthesised from 8µl of eluted mRNA per reaction using Superscript® III first strand synthesis system (Invitrogen) (described in further detail in Section 2.7 of Chapter 2) and stored at -20°C until required.

6.3.4. Quantitative PCR (qPCR):

QPCR experiments were performed in accordance with the MIQE guidelines (Appendix VII) as described by Bustin *et al* (Bustin et al., 2009). Relative qPCR experiments to amplify a range of venom protein-encoding genes including a class PII SVMP [BAR00042], SP [BAR00034], CTL [BAR00012], KTI [BAR00023], PDI [BAR00008] and QKWs [BAR00003] (Wagstaff et al., 2008) were performed

using optimised protocols as described in Section 5.2.3 of Chapter 5 using the BioRad CFX 384 real-time PCR system and analysed using the BioRad CFX manager software (version 1.5) Fold expression changes for each gene of interest normalised against three reference genes were transformed onto a log scale and analysed by univariate analysis of variance using PASW statistics version 18 (SPSS Inc.) (IBM, 2009) fitting individual snake, time point and venom protein as fixed effects. Differences in venom production attributable to time points were investigated allowing a Bonferroni correction for multiple comparisons. Following statistical analysis, raw data for each individual specimen was standardised by converting fold expression to a percentage of the maximum expression value for each specimen. At each time point, the expression of each toxin target was averaged for all 8 specimens in the study.

6.3.5. One-dimensional SDS-PAGE and gelatin zymography:

Venom samples reconstituted to their natural concentrations were prepared in reducing SDS-PAGE sample buffer, separated on 1mm 15% SDS-PAGE gels according to the manufacturer's recommendations (BioRad) and silver stained using a rapid staining protocol (Nesterenko et al., 1994) as described in Section 2.2 of Chapter 2. For zymography, venoms prepared in non-reducing SDS-PAGE buffer were separated on 0.75mm polyacrylamide gels co-polymerised with molten gelatin as described in Section 2.4 of Chapter 2.

6.3.6. HPLC separation of venom and mass spectrometry protein identification

Venom samples were fractionated and proteins identified as described in Currier *et al* (Currier et al., 2012).

6.4. Results:

6.4.1. Quantity and quality of mRNA recovered from venom:

An average yield of 46.2ng (±13ng std. dev) mRNA was purified from the 2mg venom samples (approximately 7% of the typical venom yield). These venom mRNA recovery figures varied little from days 0-1 to mature venom. The average 260/280 absorbance ratios of the venom mRNA samples was 2.43 ±0.57. These results demonstrate that potentially large quantities of mRNA, of high quality and purity, can be reproducibly recovered from *B. arietans* venom. More than adequate amounts of mRNA were recovered from each venom sample for downstream qPCR analysis: a representative cDNA synthesis reaction yielded 22.74µg (±3.03 µg std. dev) of cDNA (20µl) per reaction from 18.5ng of mRNA (8 µl) - amounts easily sufficient for 20 qPCR reactions.

6.4.2. Venom protein expression profiles during venom re-synthesis:

We collected venom samples from eight puff adders (of varying size/age, sex and geographic origin) at intervals after venom the initial extraction of mature venom (day 0-1, 0-3 and 0-7) to investigate the time scale of venom re-synthesis. Relative

expression profiles of six venom transcripts (SVMP, SP, CTL, KTI, PDI and QKW) across the time course of venom re-synthesis were determined by relative quantitative PCR (qPCR). Table 6.1 and figure 6.1 show raw data generated by qPCR for all individual specimens. Figure 6.1 shows that there was variability in the levels of venom protein expression between individual specimens. Figure 6.2 confirms reproducibility of venom gene expression profiles for three individuals using venom samples collected on a separate occasion. On average for all specimens, we identified a peak between day 0-3 and 0-7 in the mRNA expression of all transcripts surveyed in this study (Figure 6.3).

Toxin	Time point	Snake ID/Relative expression value							
		BaG2	**BaG4**	**BaGLZS2**	**BaN11**	**BaN60**	**BaN68**	**BaN80**	**BaN81**
SVMP	Day 0-1	33.60	0.01	4.36	5.36	0.24	0.38	1.00	0.93
	Day 0-3	6.30	0.21	6.04	8.15	1.04	1.00	3.71	0.30
	Day 0-7	69.92	1.02	3.42	1.00	0.10	0.95	10.25	6.62
	Mature	0.15	0.00	1.00	2.65	1.66	0.89	6.63	2.45
SP	Day 0-1	10.49	0.62	10.68	9.12	0.35	11.84	1.00	4.01
	Day 0-3	1.89	0.83	10.69	17.74	2.08	1.00	6.58	0.75
	Day 0-7	8.28	1.02	7.57	1.00	0.46	1.44	30.01	6.62
	Mature	2.48	0.34	0.93	7.58	1.04	5.37	11.00	10.38
CTL	Day 0-1	58.40	0.00	6.02	0.74	0.40	0.04	1.00	0.24
	Day 0-3	4.40	0.07	8.17	0.49	0.80	1.00	7.14	0.06
	Day 0-7	69.91	1.02	8.03	1.00	0.24	1.07	13.94	6.62
	Mature	0.06	0.00	0.59	0.45	0.45	1.54	3.49	0.32
KTI	Day 0-1	15.24	0.040	4.22	3.18	0.13	0.22	1.00	1.01
	Day 0-3	0.43	0.22	7.74	2.71	0.34	1.00	8.02	0.15
	Day 0-7	4.30	1.02	8.03	1.00	0.47	0.87	26.43	6.62
	Mature	2.48	0.01	0.28	1.61	0.60	2.57	6.18	0.79
PDI	Day 0-1	0.04	0.29	0.79	10.10	0.07	0.19	1.00	1.21
	Day 0-3	0.19	0.32	1.15	15.04	0.17	1.00	0.15	1.00
	Day 0-7	0.03	1.02	0.54	1.00	0.35	0.95	0.23	1.44
	Mature	2.48	0.13	1.00	3.52	0.22	0.17	0.34	3.97
QKW	Day 0-1	7.94	0.01	3.77	14.55	0.14	0.02	1.00	1.13
	Day 0-3	0.78	0.14	9.36	4.67	0.98	1.00	1.43	0.10
	Day 0-7	6.01	1.02	8.03	1.00	0.09	1.30	3.22	6.62
	Mature	2.48	0.00	0.26	12.00	0.50	2.49	1.66	0.88

Table 6.1 Relative qPCR gene expression levels during venom replenishment for individual adult *Bitis arietans* specimens: Fold changes in relative expression levels of six venom transcripts including SVMP, SP, CTL, KTI, PDI and QKWs across the time course of venom re-synthesis were determined by relative quantitative PCR (qPCR) for each individual specimen. Shaded areas indicate peak levels of gene expression for each specimen.

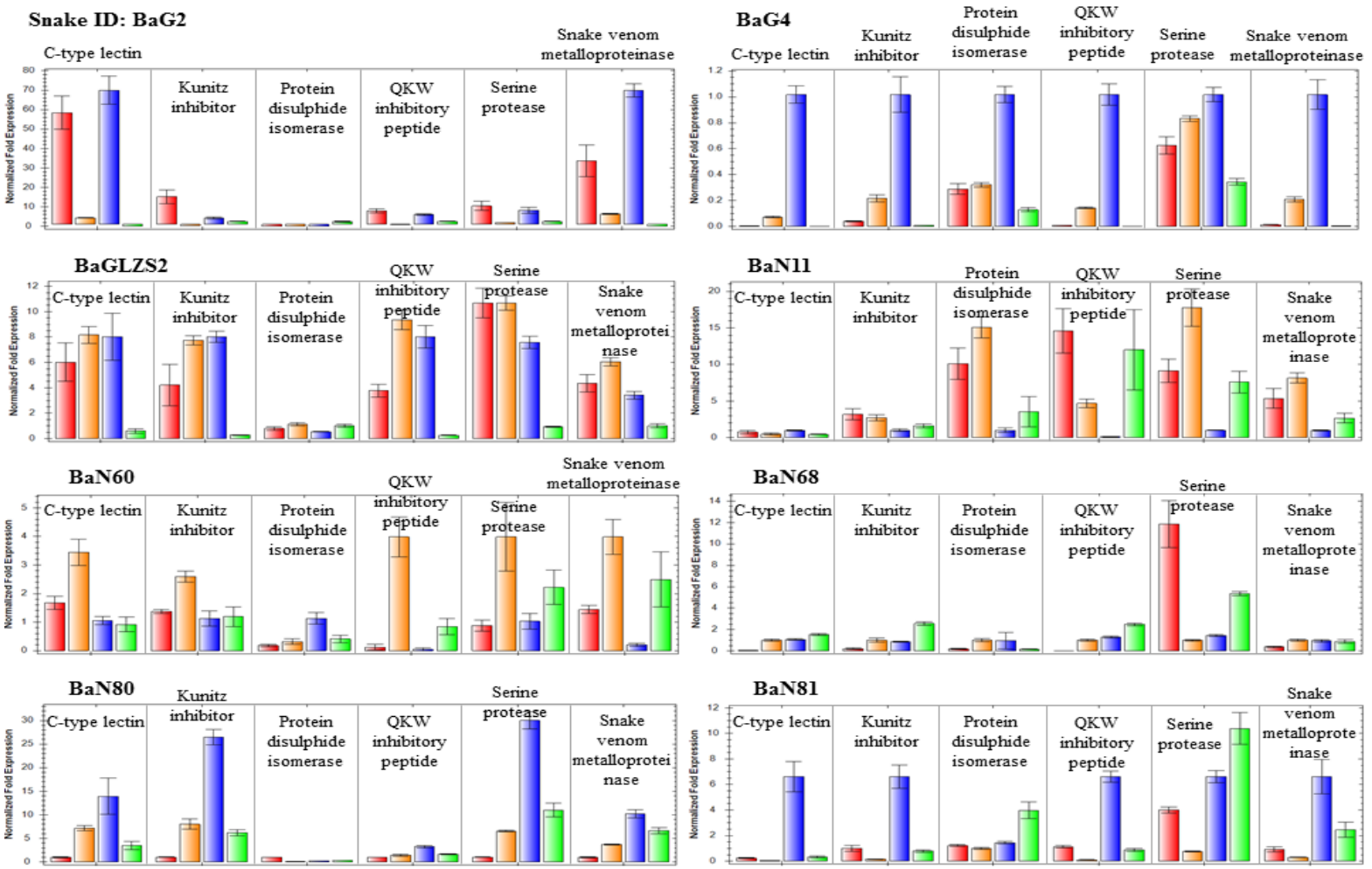

Figure 6.1 Venom gene expression profiles during venom replenishment: Relative expression profiles of six venom transcripts (SVMP, SP, CTL, KTI, PDI and QKWs) across the time course of venom re-synthesis were determined by relative quantitative PCR (qPCR). (Red = day 0-1, orange = day 0-3, blue = day 0-7, green = mature venom).

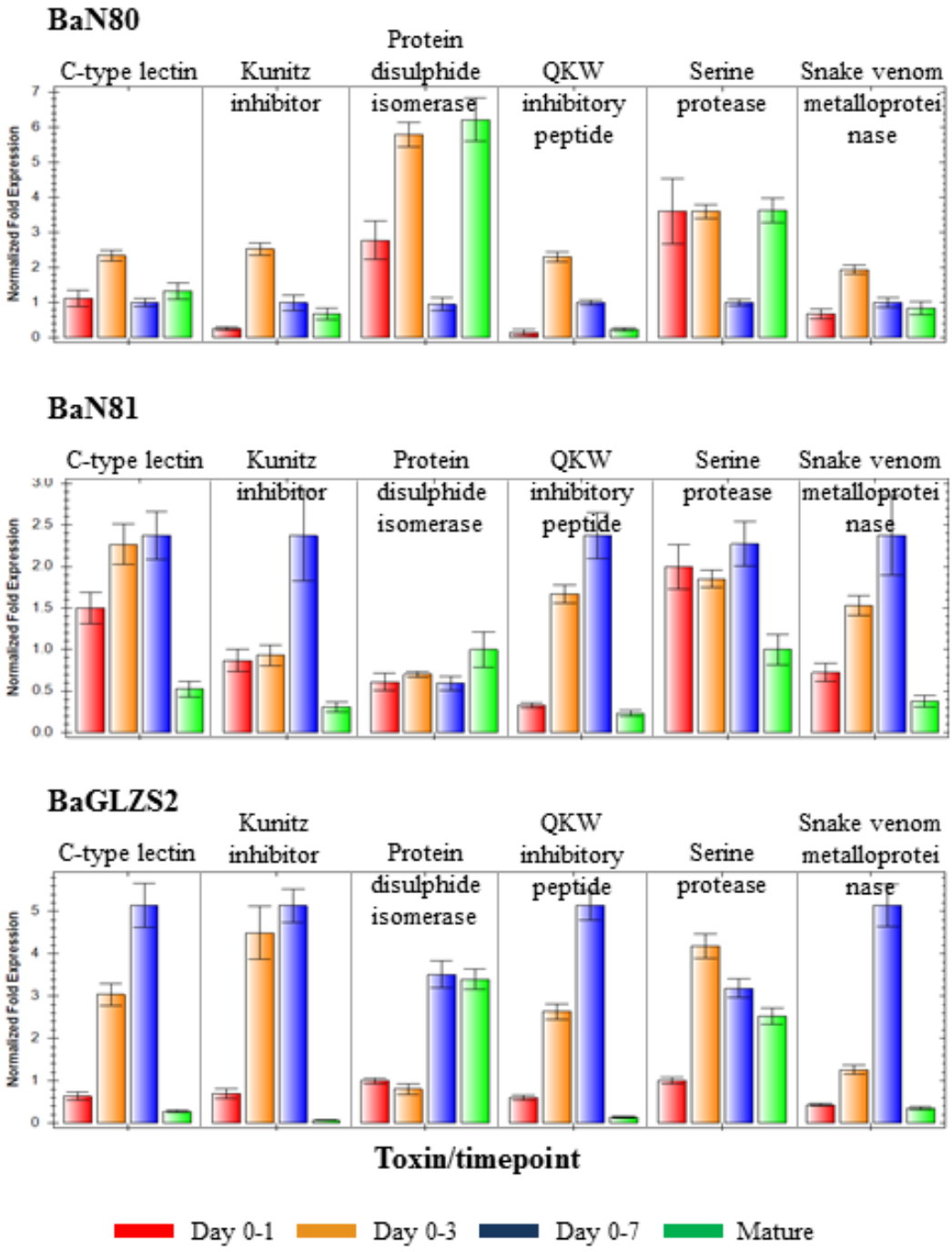

Figure 6.2 Repeated venom gene expression profiles: The venom extraction time course was repeated for three available specimens to ensure reproducibility of results. Relative expression profiles of six venom transcripts (SVMP, SP, CTL, KTI, PDI and QKW) across the time course of venom re-synthesis determined by relative qPCR showed similar gene expression profiles in repeated venom extractions with a peak in expression levels in venom extracted on day 0-3 to 0-7. (Red = day 0-1, orange = day 0-3, blue = day 0-7, green = mature venom).

On average for all specimens, we identified a peak between day 0-3 and 0-7 in the mRNA expression of all transcripts surveyed in this study (Figure 6.3). Statistical analysis of relative gene expression data revealed highly significant differences in expression between individual snakes (p=0.001). These observations are in agreement with our previous studies in Chapter 3 which illustrated that venom from *B. arietans* showed considerable levels of intra-species variation in venom protein composition, enzyme activity and immunoreactivity between specimens of the same and different geographical origins, possibly in response to environmental pressures (Currier et al., 2010). Our findings here suggest that venoms from individual specimens also vary in terms of (i) toxin expression levels and (ii) expression of toxins at different time points after venom expulsion (p=0.006). Individual changes in toxin expression profiles over time are shown in Table 6.2 with p values Bonferroni-corrected for multiple comparisons, demonstrating that the relatively lower mRNA expression levels observed in day 0-1 and mature venom samples were statistically significant. The standard error in statistical analysis was 0.131 for all samples.

Time point (I)	Time point (J)	Mean difference (I-J)	P-value
Day 0-1	Day 0-3	-0.149	1.000
	Day 0-7	-0.375	0.028*
	Mature	0.054	1.000
Day 0-3	Day 0-7	-0.226	0.515
	Mature	0.202	0.747
Day 0-7	Mature	0.429	0.008*

Table 6.2 Statistical significance of relative changes in gene expression during venom replenishment: Analysis by ANOVA and Bonferroni post-hoc testing shows a statistically significant difference in gene expression between day 0-1 and 0-7, and day 0-7 and mature venom. *indicates significant p-value (<0.05) (shaded areas).

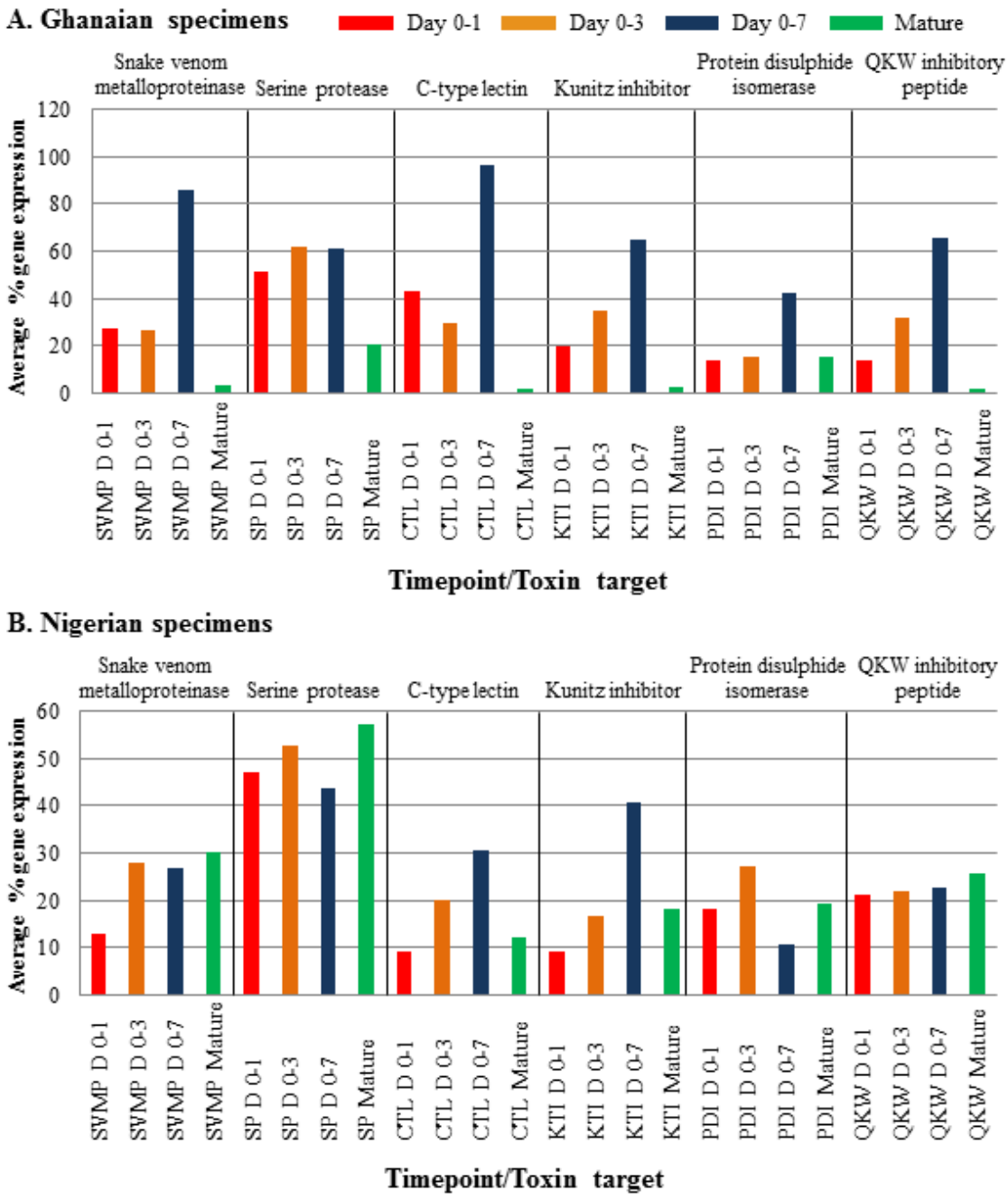

Figure 6.3 Average gene expression profiles of all *Bitis arietans* specimens: Relative expression profiles of six venom transcripts (SVMP, SP, CTL, KTI, PDI and QKW) across the time course of venom re-synthesis were determined by relative quantitative PCR (qPCR). The average fold changes in % venom protein gene expression for A) 3 Ghanaian *B. arietans* specimens and B) 5 Nigerian *B. arietans* specimens was normalised against three references genes (β actin, glyceraldehyde-3-phosphate dehydrogenase and heat shock protein) and indicate that the expression of venom protein genes peaks on day 0-3 to 0-7 (Red = day 0-1, orange = day 0-3, blue = day 0-7, green = mature venom).

6.4.3. Protein profiles and venom activity during venom re-synthesis:

The same *B. arietans* venoms samples used in relative gene expression analyses were fractionated by HPLC to examine the protein composition of venom during the course of venom re-synthesis (Figure. 6.4). HPLC protein profiles of pooled venoms extracted at different time points from Ghanaian specimens (Figure 6.4 A-D) and Nigerian specimens (Figure 6.4 E-H) revealed very little quantitative differences in venom composition and relative proportions of venom proteins within the time-course of venom replenishment examined (day 0-1 to maturity). We further observed very little quantitative changes in venom protein composition between individuals (Figure 6.5). Proteomic data suggested that the majority of venom proteins appear to be synthesised rapidly following extraction.

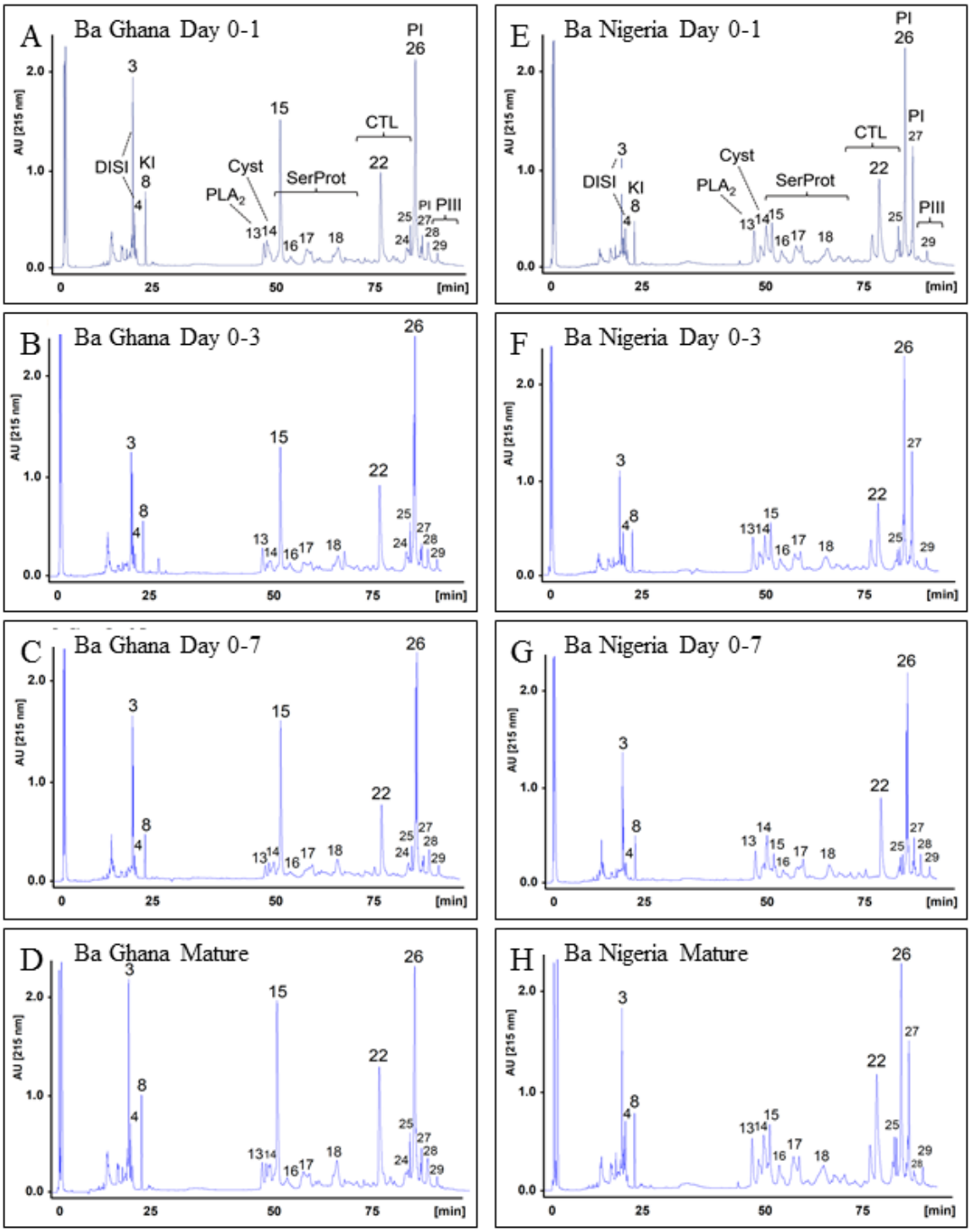

Figure 6.4 HPLC-MS/MS protein profiling of Ghanaian and Nigerian *Bitis arietans* venoms: Identification of proteins from pooled venom samples from Ghana and Nigeria showed very little quantitative changes in the protein composition of venom during protein re-synthesis. A range of proteins were identified by mass spectrometry including disintegrins (DISI, peaks 3, 4), Kunitz inhibitors (KI, peak 8), PLA_2 (peak 13), cysteine-rich secretory proteins (Cyst, peak 14), serine proteases (SerProt, peaks 15-18), CTLs (peaks 22, 25) and PI (peak 26, 27) and PIII SVMPs (peak 29) which were present in all venom samples from day 0-1 to mature venom.

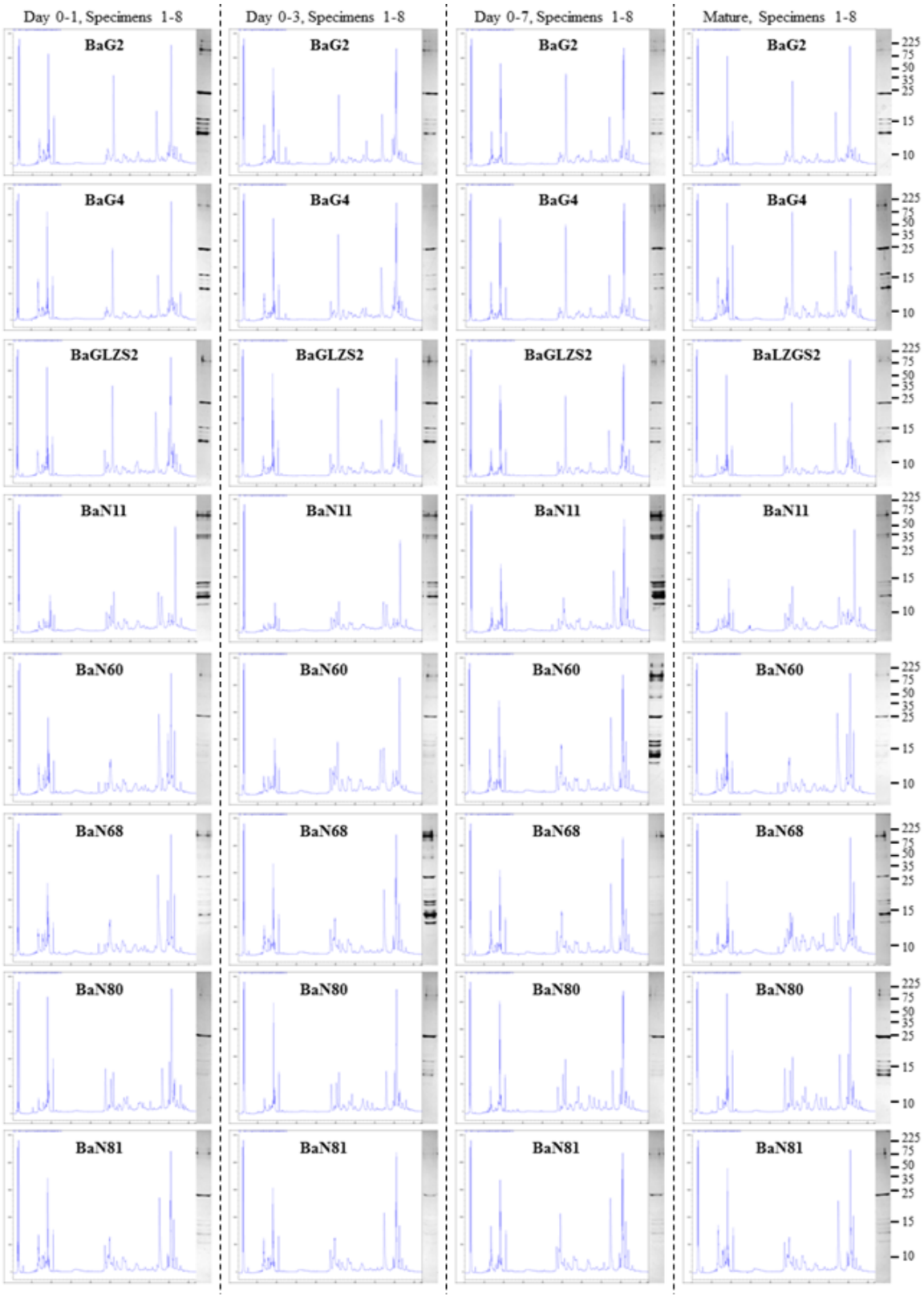

Figure 6.5 Protein profiling of individual venom samples by HPLC and 1D SDS-PAGE: Analysis of venom samples extracted on day 0-1, day 0-3, day 0-7 and mature venom for each individual specimen across the time course of venom re-synthesis by HPLC showed very little quantitative differences in protein profile. 1D-SDS-PAGE panels are shown to the right of HPLC profiles which confirm observations by HPLC. Molecular weight markers (M) are shown to the far right.

This result also correlates with gelatin zymography assays, used to assess venom proteolytic activity during the time course of venom re-synthesis. Our results showed that the enzyme activity of venom did not appear to change over the time course of venom re-synthesis and, most notably, venom extracted on day 0-1 was equally efficient at degrading gelatin substrate as mature venom (Figure. 6.6 A). There was also little variation in the substrate-degrading ability of venoms from different specimens, irrespective of geographical origin (Ghana or Nigeria) (Figure 6.6 A). We also demonstrate that this assay was not saturated by the levels of enzyme degradation by venom used in these experiments (Figure 6.6 B).

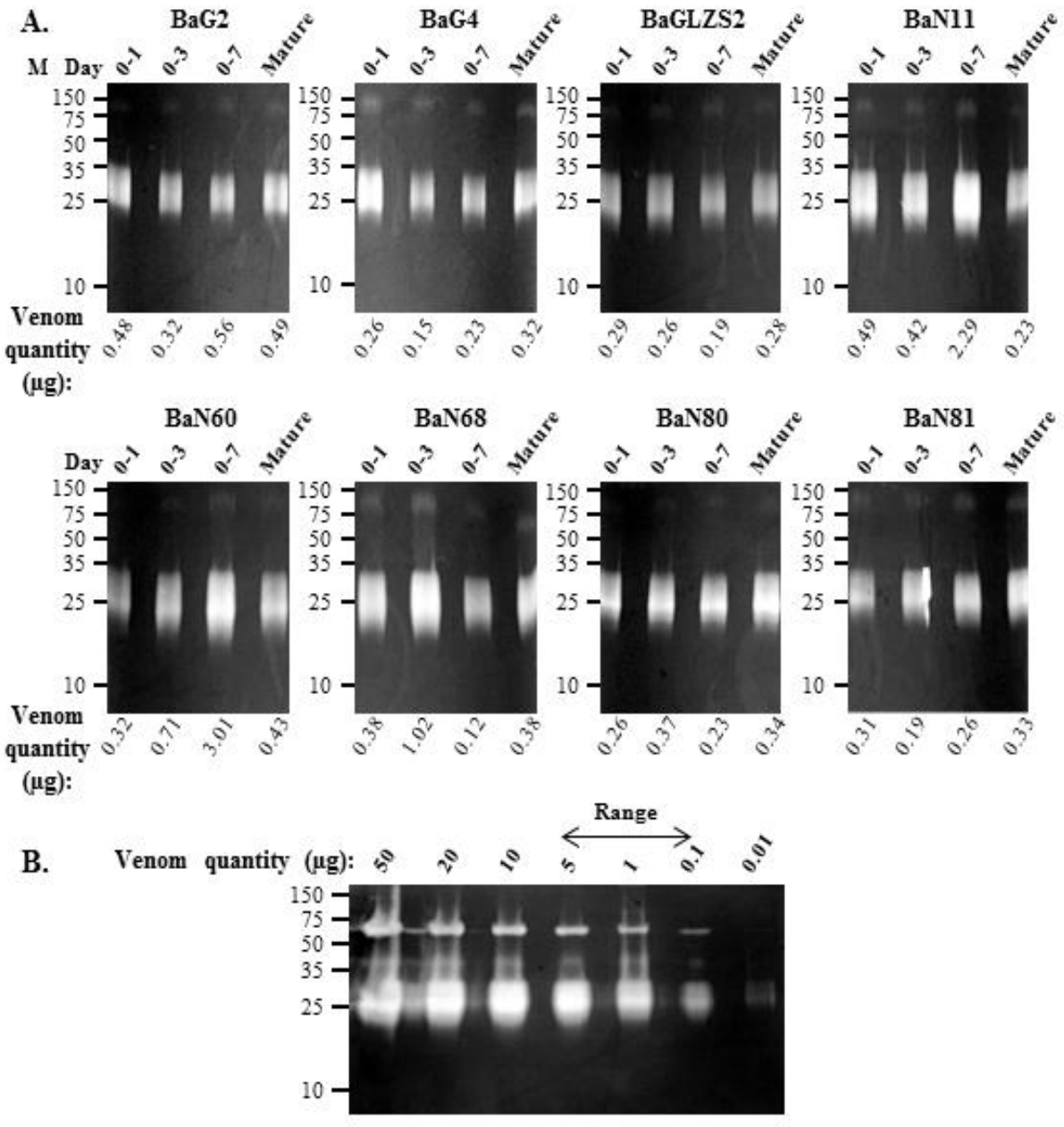

Figure 6.6 Venom enzyme activity profiles during venom replenishment: Gelatin zymography of venom samples extracted at day 0-1, 0-3, 0-7 and mature venom and reconstituted at natural protein concentration was used to assess enzyme activity of venom (A). The enzymatic degradation of substrate by venom extracted on day 0-1 was equal to mature venom. Panel B shows a range-finding zymogram which shows that the dynamic range of this assay (arrow above indicate the range of venom quantity used in panel A). Molecular weight markers (M) are shown to the left.

6.5. Discussion

Here we describe a novel technique which utilises mRNA in venom to monitor gene expression and transcriptional activity of venom glands throughout the course of venom synthesis in a dynamic real-time study. This would be unachievable using conventional methods which require sacrificing specimens for dissection of venom glandular tissue. Results following PCR amplification of proteins from venom indicate that a similar spectrum of intact mRNA is present in venom as venom gland, suggesting that the venom transcriptome may be an accurate representative of the venom gland transcriptome, demonstrating the potential viability of utilising venom as an alternative source of mRNA. Our study shows that the ability to extract toxin-encoding mRNA from venom, thus obviating the need to sacrifice animals, has the potential to substantially improve the volume and diversity of venom research, including therapeutic, diagnosis and toxin evolutionary studies and in the study of rare or endangered venomous snakes.

As proof of concept, we have utilised this technique to monitor transcription of venom protein genes in response to their requirement for venom re-synthesis, for the first time, and demonstrate using qPCR and proteomics, that venom proteins appear to be rapidly replenished following depletion of venom stores by manual extraction. We observed that a range of venom proteins including proteases, C-type lectins, Kunitz inhibitors, protein disulphide isomerases and QKW inhibitory peptides, we synthesised within 7 days following initial depletion of venom.

The prolonged presence/stability of mRNA in snake venom is very unusual and interesting from both a biological and research standpoint. In most organisms, mRNAs are characteristically highly labile with rapid turnover rates (Sachs, 1993,

Meyer et al., 2004). In *E. coli*, the half-life of typical mRNAs is 1-2 min, and 15 min for the most stable mRNAs (Coburn and Mackie, 1999). In yeasts, half-lives range from 2-3 min to over 90 min in stable mRNAs (Herrick et al., 1990, Wang et al., 2002) and in mammals, from 15 min to 24 hours for the most stable mRNA, β globin (Shyu et al., 1989). This instability of mRNA in biological systems is important as it permits the cell to adapt and respond to changing environmental or developmental cues requiring rapid up or down-regulation of gene expression (Ross, 1995). Our demonstration that mRNA can be detected in venom at each time point during the complete time course of venom synthesis is remarkable because we would expect snake venom glands to present a highly unfavourable environment for mRNA preservation due to the diverse array of destructive nucleases and phosphodiesterases (Dhananjaya and D'Souza, 2010), and naturally acidic conditions (Mackessy and Baxter, 2006). In an extreme extension of this investigation, we also demonstrated that mRNAs encoding SVMP, SP, CTL, KTI, PDI and QKWs could be PCR amplified from *B. arietans* venom which was extracted and lyophilised in 1984 (Figure. 6.7 Ai and Bi), emphasising the potential of this approach to exploit historical venom stocks for gene expression and transcriptomic investigations. Here we also show that a similar quantity and purity of mRNA (indicated by the absorbance 280/260 ratio measured by the ND-1000 spectrophotometer) could be yielded from venom stocks extracted from specimens nearly 30 years ago in comparison to venom extracted more recently (2009), indicating that mRNA may not be susceptible to degradation in venom (Figure 6.7 Bi and Bii).

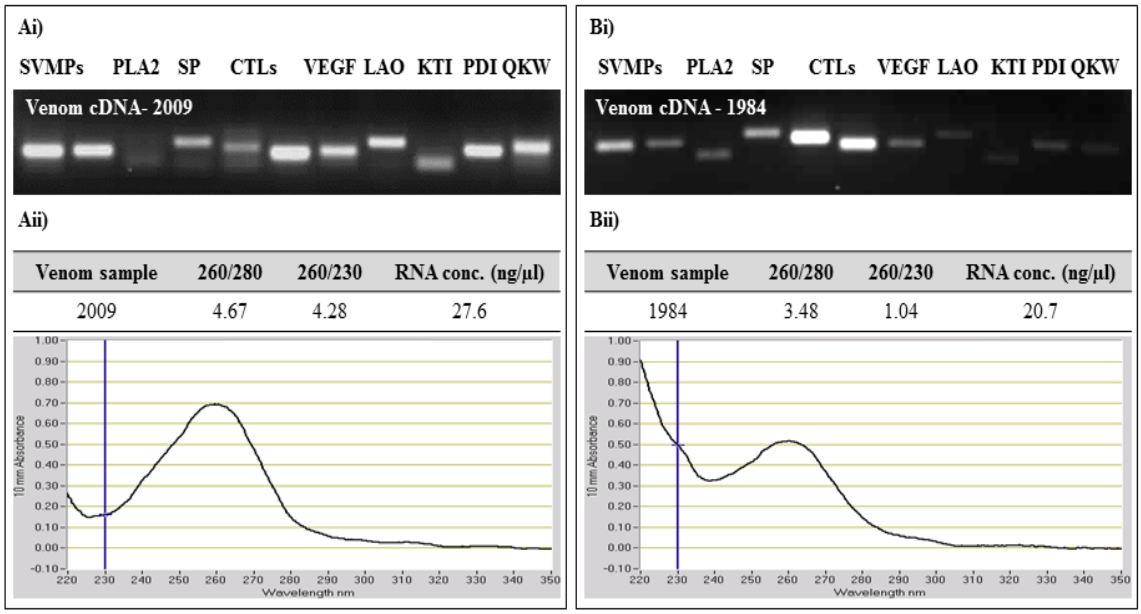

Figure 6.7 Stability of venom mRNA during long-term storage of lyophilised venom: PCR amplification of a range of venom protein transcripts including SVMP, PLA_2, SP, CTLs, VEGF, LAO, KTI, PDI and QKW (Ai) and ND-1000 Spectrophotometer absorbance profile of mRNA (Aii) isolated from venom extracted from *Bitis arietans* specimens in 2009 and PCR amplification (Bi) and Bii) ND-1000 Spectrometer absorbance profile of mRNA isolated from venom extracted from *B. arietans* specimens in 1984 showed amplification of similar range of PCR products.

Understanding the stability and potential role of mRNA in venoms is the focus of future work. We expect that multiple factors are involved in maintaining mRNA stability. Firstly, lyophilisation and preservation of venom may initially prevent degradation of venom components, although mRNAs found specifically in venom could have unique properties leading to an unusual long-term stability. Physiochemical properties of venom, including the presence of high concentrations of citrate (Francis et al., 1992, Frietas et al., 1992, Odell et al., 1998) and a weakly acidic pH (Mackessy and Baxter, 2006, Sousa et al., 2001, Viljoen and Botes, 1979), may provide universal stability to many venom components. Finally, there is

evidence for toxin-specific inhibitors in venom such as the QKW tri-peptide inhibitors of SVMPs (Wagstaff et al., 2008), and such specific or non-specific inhibitors may play a role in stabilising other components of venom, including mRNAs. Overall, the venom gland microenvironment appears to impart unusual stability upon mRNA. Our studies demonstrate that venom as a source of mRNA can be exploited to significantly expand opportunities to research venoms and venom biology, particularly in the study of CITES listed venomous species and in conducting real-time investigations of the venom gland transcriptional activity.

In the first study of its kind, we applied this technique to investigate the time scale of venom synthesis and established that expression of several venom transcripts peaks between days 3 to 7 of the cycle of protein replenishment. Analysis of venom transcript and protein expression profiles suggests that there is a close temporal correlation between transcription and incorporation of proteins into venom during venom synthesis. Our results also demonstrate that biologically active venom proteins, such as the tissue-destructive SVMPs, are present in venom within one day of venom depletion. The speed at which venom was replenished reflects the critical requirement for snakes, as limbless predators, to rapidly re-synthesise functional venom for both predatory and defensive purposes.

The qPCR transcription profiling indicates that re-synthesis of all of the venom transcripts examined in this study occurs in parallel rather than by a coordinated serial expression of different venom protein families. This appears to be contrary to early immunohistochemical reporting the asynchronous regeneration of distinct venom protein families (Oron and Bdolah, 1973, Sobol Brown et al., 1975, Oron et al., 1978), that utilised very different methods from those used here. Since the venom proteins we surveyed exhibit a wide range of pharmacological/physiological

functions, our observations suggest that the dynamics of venom replenishment may not be dependent on the biological roles of venom proteins. Using these new tools, further work will aim to characterise the complete transcription profile of all venom components during the entire venom production cycle, thus confirming our observations of a parallel expression of venom transcripts.

Although the evolution of venom protein-coding sequences has been extensively studied, we currently have very little understanding of the machinery involved in coordinating venom expression and gene regulation. This is important for our understanding of both the biology of venomous animals and the evolution of toxicity. Snake venom has evolved into a highly complex mixture of proteins and peptides by mechanisms of gene duplication and selection from 'normal' ancestral non-toxin homologues, and is continually subjected to adaptive evolutionary pressures involving gene recruitment and domain loss events (Casewell et al., 2011b, Casewell et al., 2011a). Understanding how newly recruited toxin prototypes are placed under the control of the venom production apparatus is the focus of future work aimed at characterising and comparing the specific regulatory machinery responsible for robust, yet selective expression of different toxins in venom.

3.1. Author contributions

All experimental work in this chapter was conducted by myself apart from the HPLC separation and mass spectrometry identification of protein components of *B. arietans* venom samples which was conducted by Professor Juan Calvete from the Laboratorio de Proteinomica Estructual at the Instituto de Biomedicina de Valencia in Spain.

7. INVESTIGATION OF THE GENETIC ORGANISATION AND MECHANISMS RESPONSIBLE FOR REGULATING THE EXPRESSION OF VENOM PROTEIN-ENCODING GENES

7.1. Abstract

Snake venom is a highly complex mixture of multi-isoform, multi-domain protein families as a result of repeated gene recruitments, duplication and selection processes from proteins with normal physiological functions expressed in non-salivary tissues. The mechanisms responsible for controlling and regulating the recruitment and expression of proteins by the venom production apparatus are currently little understood. Previously in chapter 6, we observed a peak in gene expression levels of several different venom protein-encoding genes during the cycle of venom replenishment. As it appeared that different venom proteins may share similar expression levels, the overarching aims of this work were to investigate whether venom genes also show similarities in their genomic location, organisation and structure, and regulatory elements responsible for controlling expression levels.

Here, we have taken the first steps to begin to investigate the genomic structure and organisation of genes encoding key venom protein families. Sequence analysis of genes encoding venom protein families expressed in *Bitis arietans* venom including serine protease and vascular endothelial growth factors, suggested that the genomic structure and organisation of genes may be highly complex.

7.2. Introduction

Snake venom has evolved into a highly complex and diverse mixture of proteins and peptides with distinct pharmacological effects (Kordiš et al., 2002, Kordiš and Gubenšek, 2000). Venom toxins have been recruited into the venom arsenal by accelerated evolutionary mechanisms including gene duplication and selection from 'normal' ancestral non-toxin homologues (Fry, 2005). Selective expression of proteins in the venom gland and subsequent structural and functional divergence of proteins has resulted in the formation of multi-isoform, multi-domain protein families in snake venom (Fry, 2005). Venom protein families are continually subjected to adaptive evolutionary pressures involving frequent gene duplication and alterations in the protein domain structure, and as a result show complex evolutionary histories (Casewell et al., 2011b, Casewell et al., 2011a). Following recruitment of venom proteins from ancestral homologues, we assume that newly recruited proteins, or 'toxin prototypes', require testing before selection into the venom arsenal. However, we currently have little understanding of how newly recruited 'toxin prototypes' are placed under the control of the venom production apparatus and the mechanisms involved in controlling venom gene expression.

The genomic structure and organization of snake venom protein-encoding genes has not been fully investigated. The majority of studies have focussed on elucidating the structure of neurotoxins and three finger toxins (3FTXs) genes. Studies observed a high level of homology in the structure of neurotoxin genes of elapids, including cardiotoxins from *Naja naja atra* (Taiwan cobra) and *Naja naja sputatrix* (spitting cobra) (Chang et al., 1997, Lachumanan et al., 1998), α neurotoxins from *N. n. sputatrix* (Afifiyan et al., 1999), γ-bungarotoxin from *Bungarus multicinctus* (Taiwan banded krait) (Chang et al., 2002), short/long chain neurotoxins from *Laticauda*

semifasciata (black-banded sea krait) (Fujimi et al., 2003) and demonstrated that the genomic structure of genes encoding neurotoxins in elapids comprise of three exon regions interrupted by two introns. The organisation of toxin genes from vipers and colubrids is less well studied. Doley *et al* characterised the genomic structure of 3FTXs from the viperid species, *Sistrurus catenatus edwardsii* (Doley et al., 2008), demonstrating a structural similarly to those from elapid and hydrophiid 3FTX genes comprising 3 exons and 2 introns (Doley et al., 2008), whereas a low similarity of colubrid 3FTXs with the elapid 3FTXs has been observed (Pawlak and Kini, 2008). Regarding the gene structure of other toxin families, a recent study by Sanz *et al* provided the first report of the genomic structure of a PIII SVMP transcript from *Echis ocellatus* (Sanz et al., 2012). This study employed an iterative strategy to PCR-amplify each domain of the enzyme (including the signal peptide, pro-domain, N-terminal of the metalloproteinase domain and disintegrin domain) to produce overlapping sequences. Sequences were assembled to produce a 15 kb sequence containing 12 exons interrupted by 11 introns (Sanz et al., 2012).

In chapter 6, we showed that several different venom components, including enzymatic and non-enzymatic proteins, appeared to be co-expressed at the same time point during venom replenishment (between days 3-7 following the initial depletion of venom). This suggests that the expression of different venom protein-encoding genes may be controlled by conserved regulatory mechanisms. The underlying mechanisms controlling gene expression in eukaryotes are complex and multifaceted. Each stage in the process of gene expression can be subject to dynamic regulation, from structural changes in chromatin, transcription of DNA into RNA, splicing/editing of RNA, translation of mRNA into protein and finally post-translational modifications of the protein (Maniatis and Reed, 2002). Initiation of

transcription occurs as a result of interplay between multiple factors including those in the vicinity of the transcription start site (promoters), enhancers lying upstream of transcription start sites and other DNA-binding regulatory proteins (transcription factors and non-coding RNAs) (Heintzman and Ren, 2007, Venters and Pugh, 2009). The core promoter element in eukaryotic protein-encoding genes, containing the transcription start site, RNA polymerase binding site and TATA box, is sufficient to initiate basal transcription (Lee and Young, 2000). However, many other upstream transcription factors and regulatory sequences acting in several different combinations are involved in regulating transcription initiation (Pedersen et al., 1999). This diversity and complexity of eukaryotic promoters leads to difficulties in promoter prediction and characterisation. Although the regulatory regions of venom protein-encoding genes have not been well defined, it is thought that snake venom gene promoters contain common promoter elements, such as TATA motifs and multiple transcription initiation factors (Afifiyan et al., 1999, Lachumanan et al., 1998) and studies have shown similarities between the putative promoter regions of human, murine and snake venom genes (Ohbayashi et al., 1996, Reza et al., 2007). It is also thought that the genomic organisation and regulation of venom protein-encoding genes may be further complicated by the role of accelerated segment switch in exons to alter targeting (ASSET) which involves radical changes in sequences within exons of venom genes (Doley et al., 2009, Doley et al., 2008) and intragenic transposable elements (Sanz et al., 2012).

The overarching aims of this work were to investigate the genomic organisation of viper venom protein-encoding genes and to identify and characterise the mechanisms responsible for regulating gene expression. As many eukaryotic gene promoters have several conserved elements, we decided to look for promoter regions upstream of the

transcription start site as an initial step to identify regulators controlling venom gene expression through the use of a genome walking approach.

7.3. Materials and methods

7.3.1. Isolation, quality control and PCR amplification of venom transcripts from *Bitis arietans* genomic DNA

Extraction of genomic DNA from *B. arietans* liver tissue is described in greater detail in Section 2.10.1 in Chapter 2. Genomic DNA at a concentration of approximately 0.1µg/µl was eluted and stored at -20°C until further use. To assess whether the genomic DNA was clean and of high quality/molecular weight, *DraI* digestion of *B. arietans* genomic DNA and control human genomic DNA was performed (Section 2.10.2 in Chapter 2) and long range PCR was performed using primer pairs designed to amplify full length sequences of venom toxin groups including SVMP, SP, PLA_2, CTL and VEGF from genomic DNA using the Advantage 2 PCR kit (ClonTech).

'GENOME WALKING'

'Genome walking' is a PCR-based method which enables regions of DNA outside of known boundaries to be characterised. By designing specific primers complimentary to the extremities of a known sequence (e.g. the signal peptide of a cDNA sequence), we can amplify flanking regions of unknown DNA which may contain upstream regulatory elements. Figure 7.1 shows the overall experimental strategy of genome walking. Figure 7.2 illustrates the primer-directed approach to amplify the region of

DNA upstream of the signal peptide in greater detail. Methods are described in further detail in Section 2.10.4 of Chapter 2.

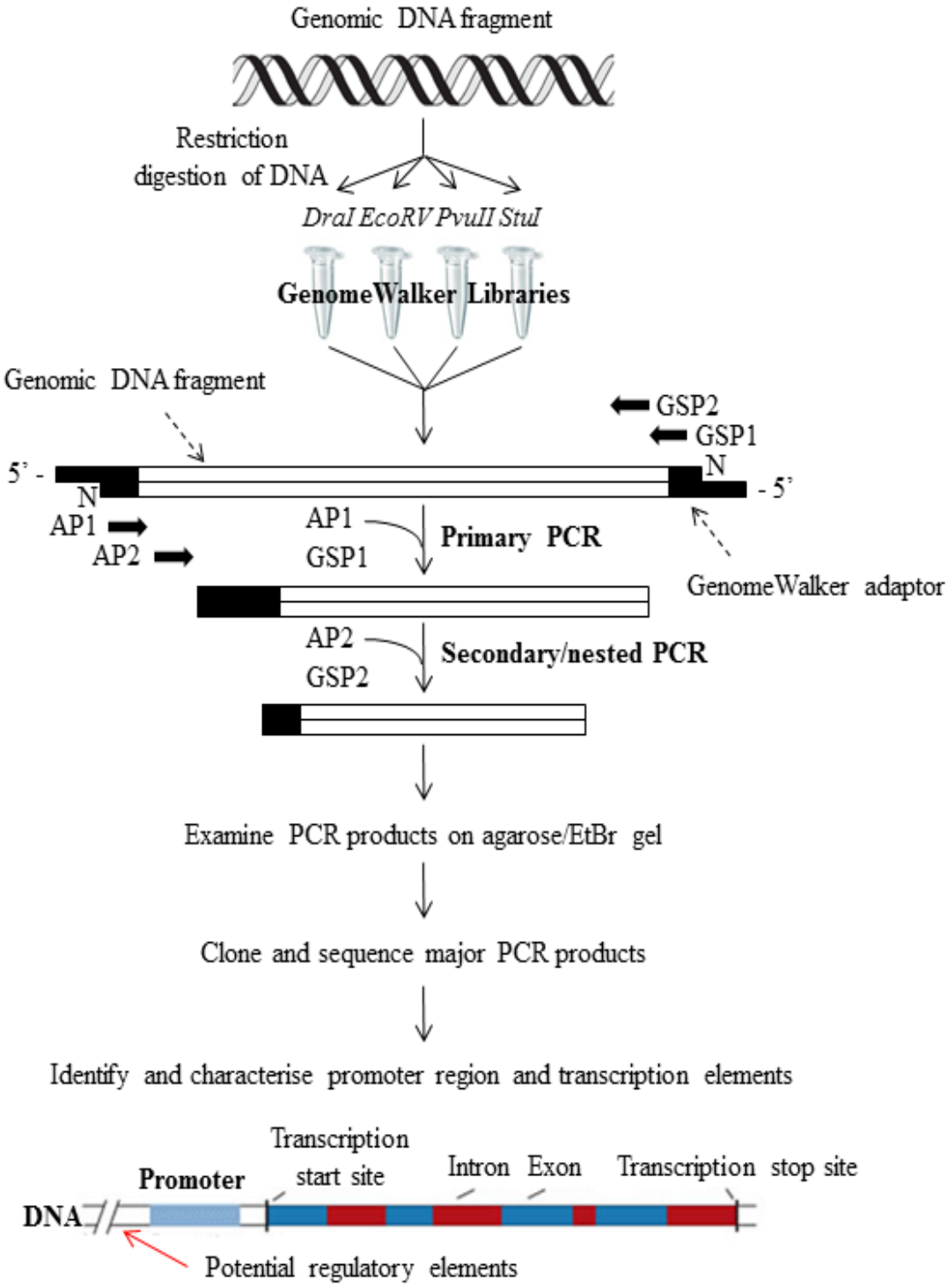

Figure 7.1 Genome walking protocol: Flowchart of the GenomeWalker™ (ClonTech) Protocol (N = amine group at 3' end of DNA, AP = adaptor primer, GSP = gene specific primer).

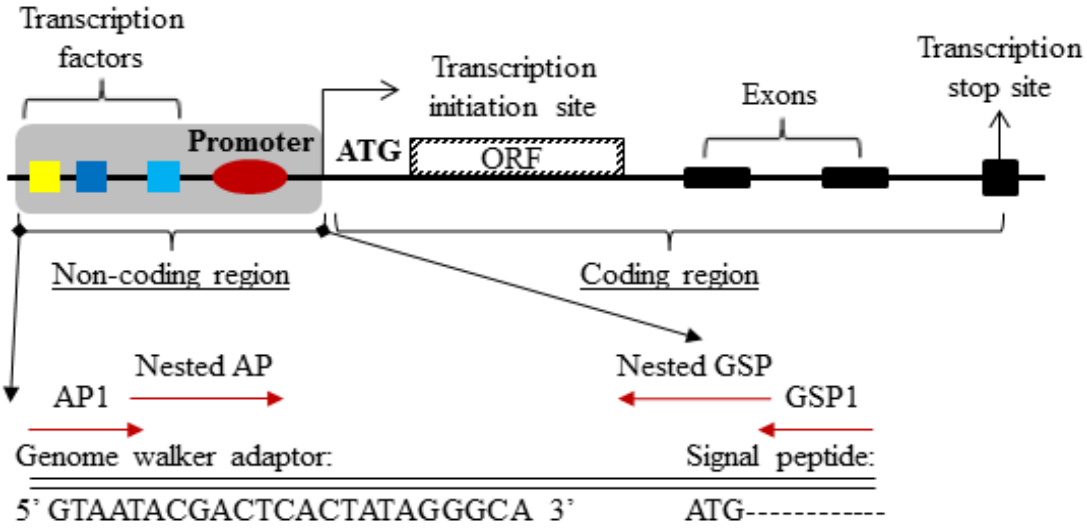

Figure 7.2 Identification of DNA upstream of transcription start site by genome walking: Region of non-coding DNA amplified by Genome Walking protocol (ORF = open reading frame, AP = adaptor primer, GSP = gene specific primer).

7.3.2. Construction of 'Genome Walker libraries'

Pools of uncloned, adaptor-ligated genomic DNA fragments (referred to as genome walker libraries) were constructed using the Genome Walker Universal Kit (ClonTech, UK) as shown in Figure 7.1 using four different restriction enzymes (*DraI*, *EcoRV*, *PvuII* and *StuI*).

7.3.3. Genome walking by long-range PCR

Long range PCR amplification of targets from genome walker libraries was carried out using the Advantage 2 PCR kit (ClonTech) as described in Section 2.10.5 of Chapter 2. PCR amplicons were excised and purified as described in Section 2.10.5 of Chapter 2.

7.3.4. Primer design

PCR primers were designed complementary to the conserved signal peptide sequences of 8 venom protein families; SVMPs, SPs, CTLs, VEGF, LAOs, KTIs, QKWs and PDIs. Primers were 28 nucleotides in length, had a GC% content of approximately 40-60% and similar melt temperatures of 65-70°C. The primary gene-specific primer (GSP1) was designed to bind close to the 5' end of the known sequence. The secondary gene-specific primer (GSP2) was designed to avoid overlapping the GSP1. Primer sequences of gene-specific and adaptor primers are shown in Table 7.1.

Toxin group	Primer length (bp)	Melt temperature °C	GC%	Primer sequence
SVMP GSP1	28	70.5	64.3	CTCAGGCTGCTTAGCTGCTCCCTTGGGC
SVMP GSP2	28	53.5	32.1	TGGACTACTTCATAATCATTAATGTTCC
SP GSP1	28	54.2	32.1	GATGTTCATTTATGTTACATTCATCACC
SP GSP2	28	62.8	46.4	CAATGACCAGTTCAGAAGACGTTTGTGC
CTL GSP1	28	71.0	60.7	GGACATGAGATCCCCACCGTTCACCAGC
CTL GSP2	28	69.7	53.6	TCCTTGCAGAATTTCTCTGCATCGGCCC
LAO GSP1	28	64.7	53.6	CCCTGCAAGAACATAGGCTGCACTAAGC
LAO GSP2	28	63.4	50.0	CTGCTCCTACAATCACAACGTGTTGTGG
VEGF GSP1	28	74.2	64.3	GCATCGCAACACAGCCACACAGGACGGC
VEGF GSP2	28	58.4	46.4	CTGCTCCTACAATCACAACGTGTTGTGG
KTI GSP1	28	66.7	50.0	GCATATTTTCCATGTCGCAGTGTGCAGC
KTI GSP2	28	71.3	60.7	AGCGGTGACCACCCATTCCTGGTTGAGC
QKW GSP1	28	79.0	71.4	AAGCTCGTGCGGCTCCATCGGCGACGGC
QKW GSP2	28	64.4	53.6	GAGCTTTACAGTGACCACACCATGGTGC
PDI GSP1	28	68.1	50.0	TTGCAGCTGCTTTCGCATATTCAGGTGC
PDI GSP2	28	77.4	71.4	GGGTTGCAGCGGCTTCCGCCAGTCCTGC
AP1	22	59.0	45.5	GTAATACGACTCACTATAGGGC
AP2	19	71.0	57.9	ACTATAGGGCACGCGTGGT

Table 7.1 PCR primer sequences for genome walking protocol: Genome walking gene-specific primer (GSP) sequences for venom toxin families including SVMP, SP, CTL, LAO, VEGF, KTI, QKWs and PDIs. GSP1 indicates primary primer and GSP2 secondary (nested) primer. AP1 and AP2 indicate primary and secondary adaptor primer sequences.

7.3.5. Sub-cloning and sequencing

Sub-cloning of PCR amplicons from genomic DNA using full length toxin-specific primers (Section 7.3.1) and amplicons generated from 'genome walking' (Section 7.3.2) was performed using the TOPO® XL PCR cloning kit (Invitrogen, UK), designed to efficiently clone long (3-10kb) PCR products, as described in Section 2.10.6 of Chapter 2. Purified PCR amplicons were sub-cloned into the linearized plasmid vector, pCR-XL-TOPO®. The construct was transformed into chemically competent *E. coli* cells and cultured on IPTG/Xgal/Kanamycin impregnated agar plate. Recombinant plasmids were identified by restriction digestion purified using the mini-spin kit (Qiagen) and submitted to Beckman Coulter Genomics UK for DNA sequencing with M13 forward and reverse primers.

7.3.6. Bioinformatics interrogation of sequences for promoter and transcription factors

The bioinformatics pipeline used to analyse genomic sequence data is described in Section 2.10.10 of Chapter 2. Briefly, the ORF for each contig was identified using the ORF finder tool from NCBI (NCBI, 2012b) and a protein family was assigned to each sequence by performing a BLAST similarity search (NCBI, 2012a). To map intron-exon boundaries in gene sequences, Wise2 algorithm (NCBI, 2012c) was used to compare translated protein sequences and genomic DNA sequences, allowing for frameshifting errors. Gene structure schematics were constructed using Gene Structure Display Server (GSDS) (Guo et al., 2007).

7.4. Results:

7.4.1. Isolation and quality control of genomic DNA from *B. arietans* liver tissue

Following isolation of genomic DNA from *B. arietans* liver tissue using the DNeasy Kit (Qiagen® UK), DNA was run on an agarose-EtBr gel alongside DNA ladder and control human genomic DNA (Figure 7.3). In comparison to the control human genomic DNA, which had a high molecular weight of >10kb, (Figure 7.3A, lane 2), the *B. arietans* genomic DNA (Figure 7.3A, lanes 1 and 3) appeared to be smeared across the gel and a lower molecular weight than the human genomic control DNA. The human control DNA was efficiently digested by *DraI* (Figure 7.3B, lane 3) indicated by smearing and a reduction in molecular weight of DNA following restriction digestion. This was also the case for the *B. arietans* genomic DNA although more difficult to observe due to some initial smearing of DNA prior to digestion (Figure 7.3B, lanes 1 and 2). Due to the smearing of *B. arietans* genomic DNA observed, it was possible that the DNA was sheared/damaged during the DNA isolation procedure. However, due to time constraints and insufficient sample material, isolation of genomic DNA from liver tissue could not be repeated as obtaining fresh liver tissue would require sacrificing snakes. To assess whether the quality of genomic DNA was sufficient for downstream applications (e.g. PCR), we decided to PCR-amplify gene targets from genomic DNA. The amplification of amplicons with the expected molecular weight would suggest that genomic DNA had not been degraded.

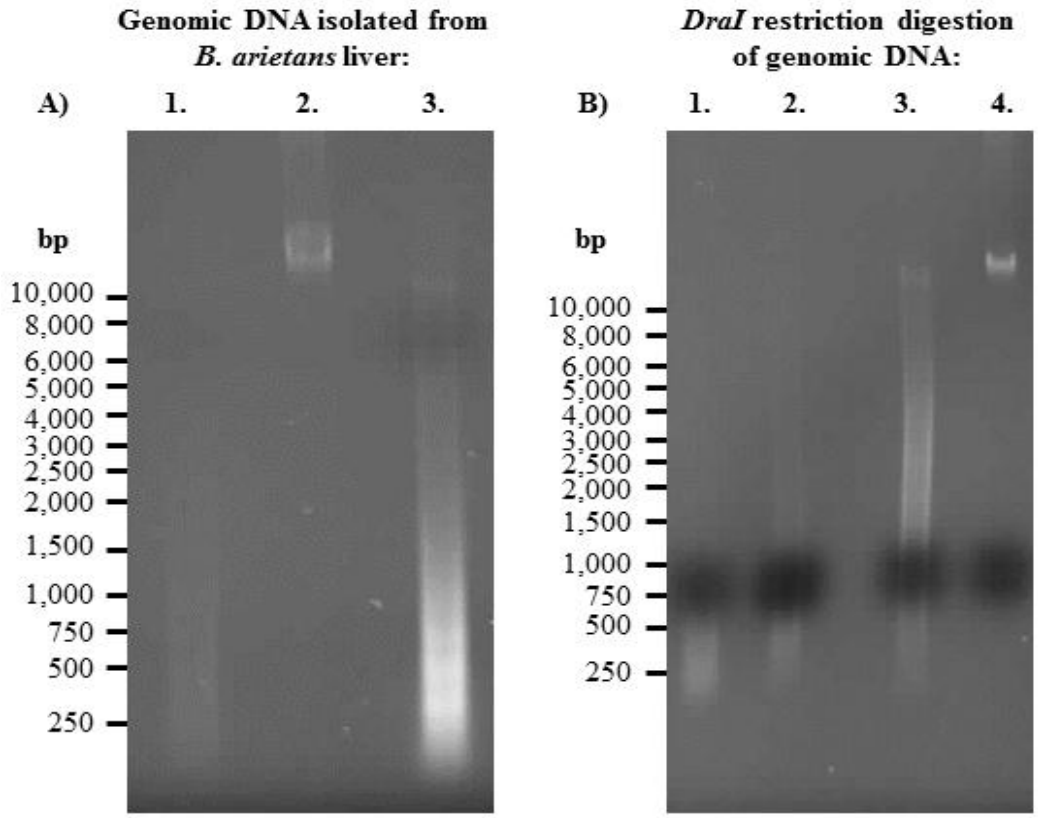

Figure 7.3 Analysis of genomic DNA extracted from *Bitis arietans* liver tissue: Agarose gel electrophoresis of genomic DNA isolated from *B. arietans* liver tissue. Gel A) shows *B. arietans* genomic DNA separation on a 0.6% agarose gel (lane 1: 1µg *B. arietans* genomic DNA, lane 2: 1µg human genomic DNA and lane 3: 100µg *B. arietans* genomic DNA). Gel B) shows electrophoresis of genomic DNA following *DraI* digestion (lane 1: 1 µg *B. arietans* DNA + *DraI*, lane 2: 1µg *B. arietans* DNA – *DraI*, lane 3: 1µg *B. arietans* DNA – *DraI* and lane 4: 1µg human genomic DNA – *DraI*. DNA ladder is shown to the left of each gel.

7.4.2. Amplification of venom protein targets from *B. arietans* genomic DNA using long-range PCR

Long-range PCR amplification of a range of venom targets including SVMP, SP, PLA_2, CTL and VEGF from genomic DNA was performed to assess the quality of

DNA isolated from *B. arietans* liver tissue and to obtain genomic sequences encoding venom proteins. Firstly, targets were amplified from *B. arietans* venom gland cDNA as a positive control. Figure 7.4A shows that all targets could be amplified from venom gland cDNA with the exception of SVMP, possibly due to problems with primer efficiency. Analysis of PCR amplicons from genomic DNA showed that only SP and VEGF targets could be efficiently amplified (Figure 7.4B). SP and VEGF amplicons amplified from genomic DNA were of a higher molecular weight (approx. 6 and 3kb respectively) (Figure 7.4B) than the same targets amplified from *B. arietans* venom gland cDNA (approx. 600bp-1.75kb and 600bp respectively) (Figure 7.4A). It was possible that other components (e.g. PLA_2 and CTL) were not efficiently amplified from genomic DNA due to their large size.

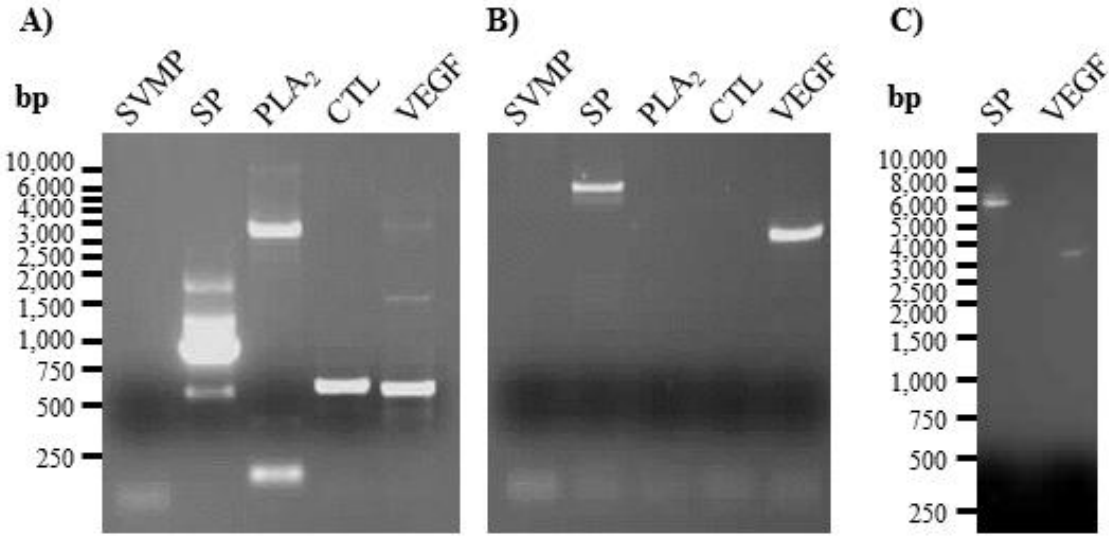

Figure 7.4 PCR amplification of venom targets from *Bitis arietans* genomic DNA: Agarose gel electrophoresis of PCR products amplified from A) *B. arietans* venom gland cDNA library and B) genomic DNA isolated from *B. arietans* liver tissue. PCR products include SVMP, SP, PLA_2, CTL and VEGF. Panel C indicates purified PCR products (SP and VEGF) from *B. arietans* genomic DNA. DNA ladder is shown to the left of the gels.

7.4.3. Sub-cloning and sequencing of PCR products amplified from *B. arietans* genomic DNA

Purified SP and VEGF PCR amplicons from Figure 7.4C were excised and sub-cloned into the plasmid vector (pCR-XL-TOPO®). A sample of each clone was restriction-digested with *EcoRI* and analysed on an agarose-EtBr gel to check that (i) the insert was present and (ii) the insert was of the correct size (Figure 7.5A).

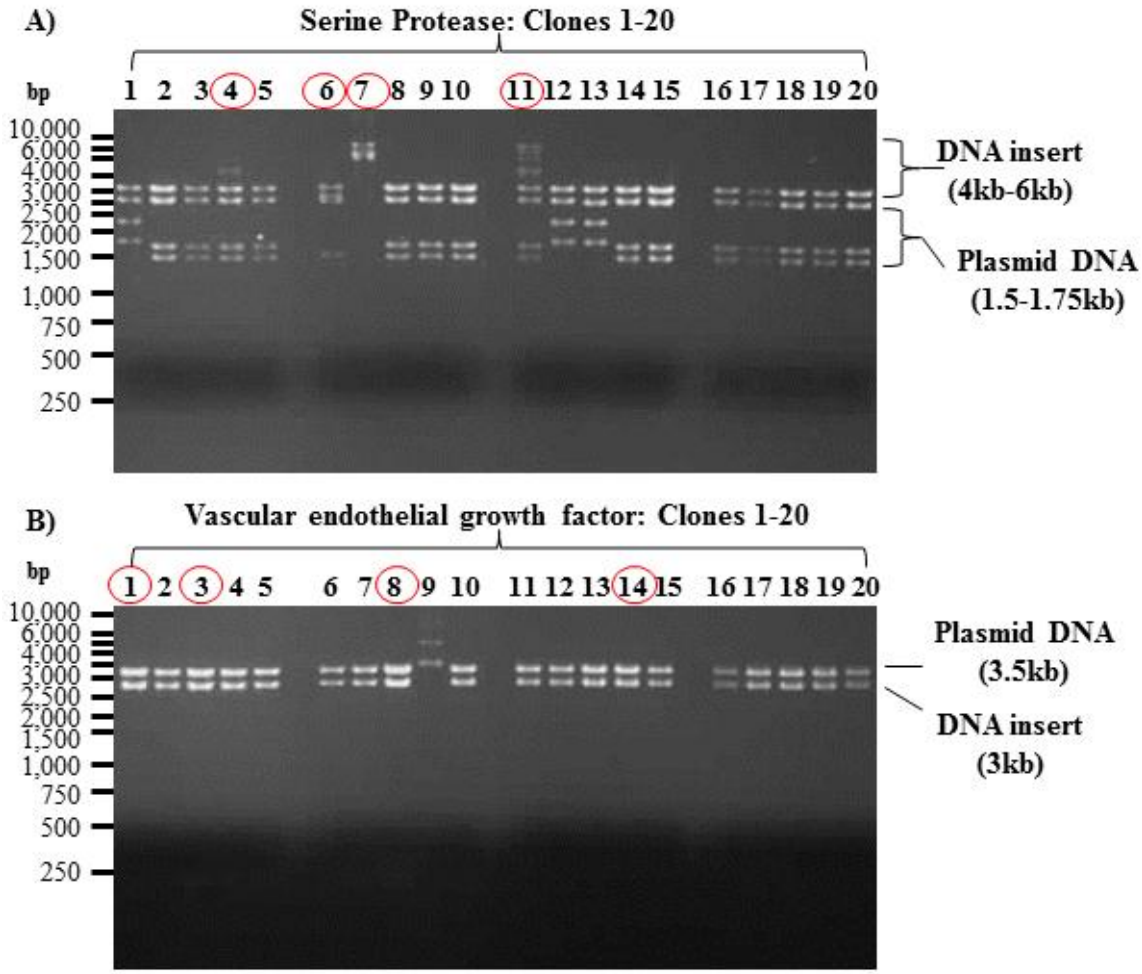

Figure 7.5 Analysis of venom target inserts following sub-cloning: Agarose gel electrophoresis of *EcoRI*-digested clones containing A) serine protease (SP) PCR construct and B) vascular endothelial growth factor (VEGF) PCR construct excised from Figure 7.2. Numbers circled in red indicate constructs which were submitted for sequencing. DNA ladder is shown to the left of each gel.

For each venom protein family, two clones were submitted for sequencing (circled in red, figure 7.5). Two sequences (forward and reverse) were obtained for each clone and assembled using SeqMan (DNASTAR) and for each protein family, sequences clustered into two contigs named SP contig 1 and 2 and VEGF contig 1 and 2. Full sequences are shown in Figure 7.6.

7.4.4. Sequence analysis of PCR products amplified from *B. arietans* genomic DNA

Each genomic contig was firstly assigned a protein family by performing a BLAST search against the NCBI nucleotide sequence database. SP contig 1 and contig 2 sequences showed highest sequence homology to *Bothrops atrox* batroxobin, a thrombin-like SP (BLAST accession number X12747.1). Both VEGF contig 1 and contig 2 sequences showed highest sequence homology to *Trimeresurus flavoviridis* VEGF precursor sequence (BLAST accession number FJ554640.1). To investigate the structure and organisation of genomic sequences, intron-exon boundaries were predicted using Wise2 algorithm (NCBI, 2012c). In SP contig 1 sequence, one intron was predicted from base pairs 662-1003 and no intron regions were predicted in the sequence of contig 2. For VEGF contig 2, three intron regions were predicted from 316-447, 525-997 and 1036-1206 and no intron regions were predicted in the sequence of contig 1. The genomic structure schematic of SP and VEGF genomic sequences were generated using Gene Structure Display Server (GSDS) and are shown in Figure 7.7.

>SP contig 1

TTCCTCCCCCAAGGGATCTTTTAGCCAAGATTCCTGCCTTTTTGTTTTGGGCCCCA
ATCCAAAATTTATGGGTTTTTCTTCATTTTTCAGATATGGAAGTTTCAATACACTG
GCTTGAGGAATTTTGGGAGTGGAAGTTCAAAAGTCTTGAAGTTGCCAAGTTTGG
AGACCCCCATTCTTAGGTCACCTCCAGGGGATGCGAGATCAGTTCTATGACTTTT
GAACTAGCAAAAGCCCCACTTTTCCAACAAGGCAATCTTTGCGTAGAGTGCCAC
GAGAAATTTGAGAAGCCTTCAAATGCCCATCAGCTGATTTAATACTTATTAATAT
CTTGACAAAAAAACATTTAACTAAGTCCATTTTTCCCAGGAGTCCCTTTGAACAG
CTTTGAAAGACAATACTTTCTATTCCCAGGCAATGAGATCAGCTCCATTGGTTGG
AGACTATGGAAATTATAGCTCTAGGCATCTAGGTGATAAATTATGAAAGGTAAA
ATTTTGCCTATTTTTTATTTTTtCCAGAGTTTTATCCTGATGTCCCTCATTGTGCTA
ACATTAAGTTATTTGATTATTCGGTGTGTCGAGCAGCTCACCAAAAGTTGCCAGA
GAAAAGTAGAACATTGTGTGCAGGTATCCTGGAAGGAGGCATAGATTCATGTAA
GGTAAGAGGATCCATTTTAAGACAGATTCCTAAAGAAATGATGCCAATTTTCAA
AGCTATGACAGAGATCTAGCCTTAAAGGCATCTTGTAGAAACATACAAAGTTAT
GGCTTTTTCTAACTCAAGTAGTTACTAGGTATCTAGATTTCCAGACTTCCCAATA
CTGGTGATTCTGGTGGGGGAAACTCAAGAATTTAAATTCTTCTACAAGGATCCTG
AATTGGGGAACACTGAAGTGAAACATTTGGGGCTGTATGTGAATGGACGATGGG
AGGGAATTGTTTGCTTCACTTCCCATTTATAGATACGGTAGTAATGTTTCATGTTT
GATTTTTCTCAAAAGGTTGACAATGGGGGACCCCTCATCTGTAATGGACAAATC
CATGGCATTGTATCTTGGGGGGGGCATCCTTGTGCCCAACCGCTTAAGCCTGCCC
TATACACCAATGTCTTTGATTATACTGACTGGATCGAGGGCATTATTGCAGGAAA
TACAGCTGCGACTTGCCCCCGGTGACTCGAGAAGGGCGAATTCTGCAGATATCC
ATCACACTGGCGGCCGTTACTAGCATGGATCCGAGCTCGGTACCAAGCTTGATG
CATAGCTGATATC

>SP contig 2

TAGATACTCAAGCTATGCATCAAGCTTGGTACCGAGCTCGGATCCATGCTAGTA
ACGGCCGCCAGTGTGATGGATATCTGCAGAATTCGCCCTTGGATCCATGGTGCT
GATCAGAGTGCTAGCAAACCTTCTGGTACTACAGCTTTCTTACGGTAAGAGCCTG
GACAATGGAGCAAAGGATGGACGGAGCTTTAGGGGTCTTTTTTGGTTTAAACCT
CAAGTTACAGGAATAAACTTGGACGTAACTATTAGCTCTAGATGTACAAGCGAG
TCACGAGTAGAGAGTGGGTGAAGAAGTCCCAGTTGGTGCAATGGGGAAGACCA
TTGCTGTGTTTCTAATGATAGTATGAATTGATACATTTATTCATATCAGAAAAAC
TAGTCAGTTAAAAATATATAGTCCAATTATGGTCAGCTTCCTTTCGTGTTTCTATT
TATTTGGCAACTGACTTCAATAGAAGACGATAATTTATTAATTAATATAAGATGC
ATTGAGAAAAAAGTTGGGGAGTGGTTTGCAGTGTTAAGGTTGCCTTTATAAAAT
GCCACTGATTTTTATTCAAACTGGTAAAATAAATGTGTTGGATTTTAGCTAGCTG
CCACTCTGTTAGATTTGCTGCATTATATAGCGTGCAATATCTGGGTCATTGCTTCT
GAAACAAATATGAAAACCGGTATGTAGGGATTTTACTACCATCAATGTTGGCTC
AAACTGCTTTTAGTTAACTAAATCCTAATGGTATCAACTTCCCATCCAAACTCAT
AGATTAAATTCCATTTTCTTTGATCTCTTCCCAATTTCACTTCTTCTGCCCCCTATT
CTCCCCATCACAAGAGCATACTGTATATTTTGCTTTGCAATGCGGTACAGCAAGA
TCACACTCTGGGCCAAATGCTTCTAAATGTCCATCCTTTTTAGAAGCTCATCTGA
GCCGTTCTTCTTACTTCAACTGATTAGCGTAAACTGGCTGGCCGTGATACATTAA
GTTACTGGG

>VEGF contig 1

TCATAGGCGATTGGCCCTCTAGATGCATGCTCGAGCGGCCGCCAGTGTGATGGA
TATCTGCAGAATTCGCCCTTGGATCCATGGCTGCGTACCTGCTGGCAGTTGCCAT
CCTCTTCTGCATCCAGGTGAGAAACTGTGGGGATCTGGCCTGGAATCCTCACAG
GCAATTTTCAGCCAAACAAGGGGGGAAAACAGATTAAATCTGTTATTTAGCCAG
GGTAACCAATAAAAGTAACTTCTAAGGTTGGAGAATTCATGTCCCTCTGTTGCA
GTTTAGAATTAAATTACCTCTGTAGGATCCTGCAGTTTTATGCATCTCTGGGAGA
CAAAGGAGTGGGTTGGGGATGGGGATGGGAGAAGCTGTGGCAGGAGGCAGAAA
TTACTTCTGTCCTTCACAGCTGGGTCAAGCATGGTGCTCTGAGTTGCTTTGCTTCA
TGGAAGGACAGGGGGCTGTGCTGGATTCAAGCAGGAGCTTTCTTCCAAAGTCAC
CTTGGGTTCTGCGCCAGCTTTCCAGAGGCCAGAGCAGGGTTGGGGGGGGGGGGT
GTCTGCTGTACATGTAGATGATGGCAGATTTAATTTGGGGGGGCTGAAAGTGGG
GGAGCTCAATGTGCTGCTGCTGCTGCCTGTGAAGGGAGAGGCAGAGAATCG
GGCCCTTCCCTCAAGACCAGGCGGGGCCCCCTGGTGCTGGAAACAGAAGATGGT
CCAGGAGAACAGGGGCACCACAGCAGGGCATAATAACCAAGCGCTCCTGGCAT
AGGTCAATCTGCCACGGGCACGGAAAAGGCTCGGGTGCCTGGGAGATATTGCTC
AGGTGTCTTGCCCTGCAGGGTGCAAAGCGACAGCAGTCCTGACTTTGGAGCTGG
GGTCTTCTGAGGGCTGACCCACAGCCAGTGGAGCTTTCCCCAAGGAATGGATGC
CCGGGTCCATTAAAGGGTCCAGGACCCCCGAAGCTCCTCCTTCCGGATGAACGT
GGGTGCCCTTGCGAAACGTCCAAGGTTTTGCTTGGGGGAAAGAAACAaGGTTGG
GCAGGTGGTTGGCAAGCCCTCCTCCAACTAACAATGGCATTGGGCACCCTGGGC
TTTGATTTCCCCATGACAATCCACAGAGCAGCTTGGATGCTTCTAGGGAGAAAA
AACCGACCTGGTTCTCTCTTGCCCCCTGGAAGGAAACCCAGAACAGGTGCCCCG
GCTGGCATCTCCCTTCTGGGGGTCATCCAAGGGGCCTAAAAAGCTTCTTGGATTT
CAAAAGTTAAGCCATTGGACTGGCCAAGGAACCCCTGAAGGACAAGGCAACTG
GGGCAAGGGGTTAAAACTTTCCATGGCCAGCTTTTGAGATTGTGGGGAATTCCA
CTCC

>VEGF contig 2

TCATAGGCGATTGGCCCTCTAGATGCATGCTCGAGCGGCCGCCAGTGTGATGGA
TATCTGCAGAATTCGCCCTTGGATCCATGGCTGCGTACCTGCTGGCAGTCCCCTT
CTTCAGGGAGGCCCTTTATGGAAAGTTCCCAGGGCAGGGTTTTGCCAAGCCCAG
GGAGCCAATCGTGTCCCATACTTGAAGAGTACCCTGATAAAATTTTTAAGATCTT
CAGGCCGTCCTGTGTGGCTGTGTTGCGATGCGGTGGCTGCTGCTCTGACGAAAG
CTTGACGTGCACCTCTGTGGGAGAGCGCACTGTCGAACTGCAGGTCAGGGGCGG
TTTGTGCTGAGGCGACTGGAGTGTGTCTCAGGACAGCTCTTGGGAGCCGGGAAG
AGCAGCACCCAGCCTTGGACTGCTGCTGGGGTGCAGCTGAACGGTGCCTTTCTCT
CCCCTCGGGTAGGTCATGCAGGTGACTCCCAAAACACTGTCTTCCAAAATCAAG
GTGATGAAATTCAGGGAGCACACAGCCTGTGAATGCAGGTGAGGAAGGGGGCC
GAAGAGTGGCCGTCCTGGGCGGCTGGTCAGAGGGGTGGGGAAAACGGGGAGAA
TTGCTGGAGGTGGAAGATGACAAGTAGTTCTTAGTTCACACAACCCTTCCCCTCC
CTCCATTTTTCTTGCTTGCTTGCTTTCTCCCACCTTTATTATTTTTACAAATAACTC
AAGGTGGCAAAGATACCCTCCTCCTATTTTCCCTGCCACAACAGCCCTGTGAGGC
AGGTTTGGCTGAGAGAGATGGAACAGGCCAAAGTCACCCGGCTCATTTTCTACA
CTGGGGCTCTGCAGGGGTCTCTGAGCAGGAGGAGAGAAGTGGGGGCTCCAGAC
CTGTGCAGGCGCCTCCTCAGAGGCCATGCTTCTTTGCCTCTTTCCTCTTCCTGGAG
CCCCCAGCTGTGGGTCAAGCCCTGCGCCCACTGGTTATGCAGACTGTATCTGGGT

TATTTCCTCTTTCCAGGCCTCGATCAGGAAGCAGGGTGAACATCGGGAAGCACA
AGAGGTACGTGGGGTGGGGCTGGGGGTTAACAGAATAAGAAAGTTGTAAGGGA
CCTTGGAGGTCTTCTAGCCCAACCCCTGGCTCAGGTTGGCTGGGGGCAGGCTGG
GAGGGTGGGGCAGGAGGGCAAGATGGCCCACTTGAGCCGAACTCTTTTTTTTCC
CCCTTTGCAGAAGCCCAGAGGAAGGGGAGCGAGAGCCAAGTTCCCCTTTGACTC
CAGGATCCCTTTGACTCGAGAAGGGCGAATTCCAGCACACTGGCGGCCGTTACT
AGTGGATCCGAGCTCGGTACCAAGCTTGATGCATAGCTGATATCTACG

Figure 7.6 Genomic DNA sequences encoding *Bitis arietans* venom proteins: Sequences of SP and VEGF contigs amplified from *B. arietans* genomic DNA. Open reading frames (ORF) were predicted using ORF finder (NCBI, 2012b) and are highlighted in red. Intron regions were predicted using est2genome (Mott, 1997) and are highlighted in grey.

Alignment of *B. arietans* genomic sequence SP contig 1 and 2 with the closest homologue identified by BLAST, batroxobin (*B. atrox*) demonstrated that SP contig 1 showed homology only to the 3' region of the batroxobin sequence whereas the SP contig 2 showed homology only to the 5' region of the batroxobin sequence. This indicated that the contigs were not overlapping and therefore did not form the complete genomic sequence encoding the *B. arietans* SP. The structure of the gene encoding batroxobin has been defined. The gene spans 8kb and contains 5 exons (the mature batroxobin enzyme encoded for by exons 2-5) and shows exon/intron organization very similar to those of the trypsin and kallikrein genes (Itoh et al., 1988). Alignment of *B. arietans* VEGF contig 1 and 2 with the closest homologue identified by BLAST search, VEGF precursor from *T. flavoviridis* venom again demonstrated that VEGF contig 1 showed homology to the 3' region of the *T. flavoviridis* VEGF sequence whereas the VEGF contig 2 showed homology to the 5' region of the *T. flavoviridis* VEGF sequence. Alignments of genomic DNA sequences with batroxobin and *T. flavoviridis* VEGF gene sequences are shown in Appendix VIII.

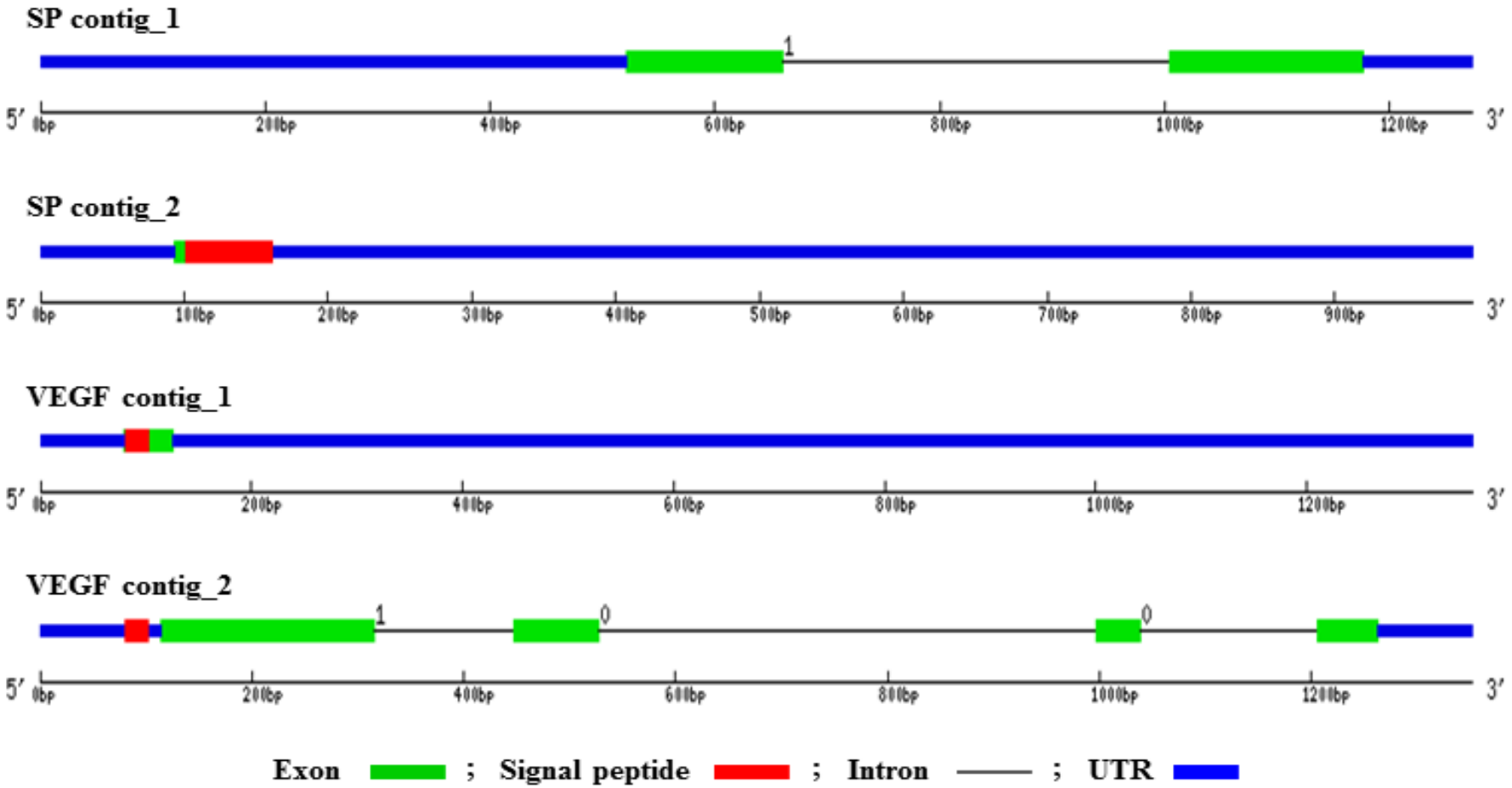

Figure 7.7 Gene structures of venom protein-encoding genes: Schematic diagram to illustrate gene structure of venom genes encoding serine protease and vascular endothelial growth factor generated using GSDS (Gene structure display server) (Guo et al., 2007). Green box indicates exon, red box indicates signal peptide, blue box indicates untranslated region (UTR) and black line indicates intron.

7.4.5. Amplification of gene targets from 'Genome walker' libraries

Genome walking protocols were used with the aim of amplifying regions of DNA upstream of the transcription start site. DNA was amplified from genome walker libraries by PCR using gene specific primers and primers specific to bind the adaptors ligated onto DNA fragments. Following primary PCR cycles, products were amplified with low specificity, observed by smearing of PCR products (Figure 7.8). This could be because PCR primers were designed to amplify a region of DNA in the signal peptide, which is conserved across many different isoforms within a large, multi-gene protein family. It appeared that all targets were amplified from each genome walker library, except in the case of QKWs which were not efficiently amplified.

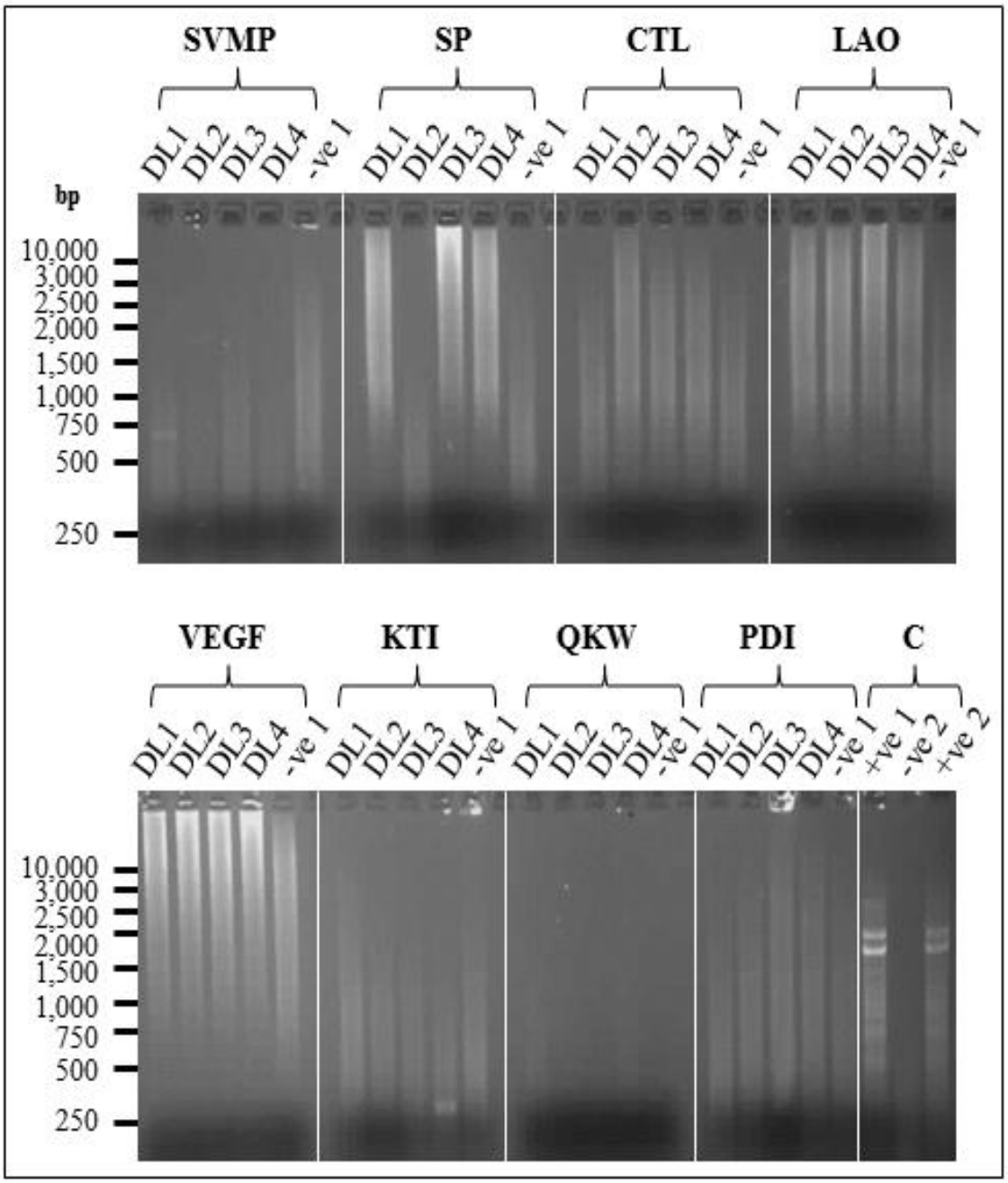

Figure 7.8 Primary PCR amplification of targets from Genome Walker libraries: Analysis of PCR products amplified from restriction digested genome walker libraries following primary PCR including SVMP, SP, CTL, LAO, VEGF, KTI, PDI and QKW. *B. arietans* genomic DNA was digested with four different restriction enzymes to generate DL (digestion library): DL1 = *DraI*, DL2 = *EcoRV*, DL3 = *PvuII* and DL4 = *Stu I*. Controls (C) : -ve 1; negative water control for each primer pair (absence of genomic library), +ve 1; amplification of tPA from human *PvuII* genomic library, -ve 2; negative water control for human genomic library and +ve 2; amplification of tPA from pre-constructed human *PvuII* genomic library provided in Genome Walker kit).

Following secondary PCR, which aimed to increase the specificity of PCR amplification, we observed several clear DNA bands and an absence of smeared DNA for most venom protein families (Figure 7.9). All target genes could be amplified following secondary PCR with the exception of CTLs. This could be due to inefficiency of the secondary PCR primers to amplify specific targets, or that the incorrect gene had been amplified following primary PCR cycles. For other venom protein families, numerous products were amplified from each genome walker library of a range of molecular weights (250bp-3kb), indicating the multiple isoforms present in venom protein families. For cloning, products amplified from each venom protein family (one product per family) were excised from an agarose gel and purified (circled in red in Figure 7.9). PCR products with the largest molecular weight were selected for sub-cloning and sequencing as we considered these more likely to contain sequences of interest upstream of the signal peptide to which the primers were designed to specifically bind.

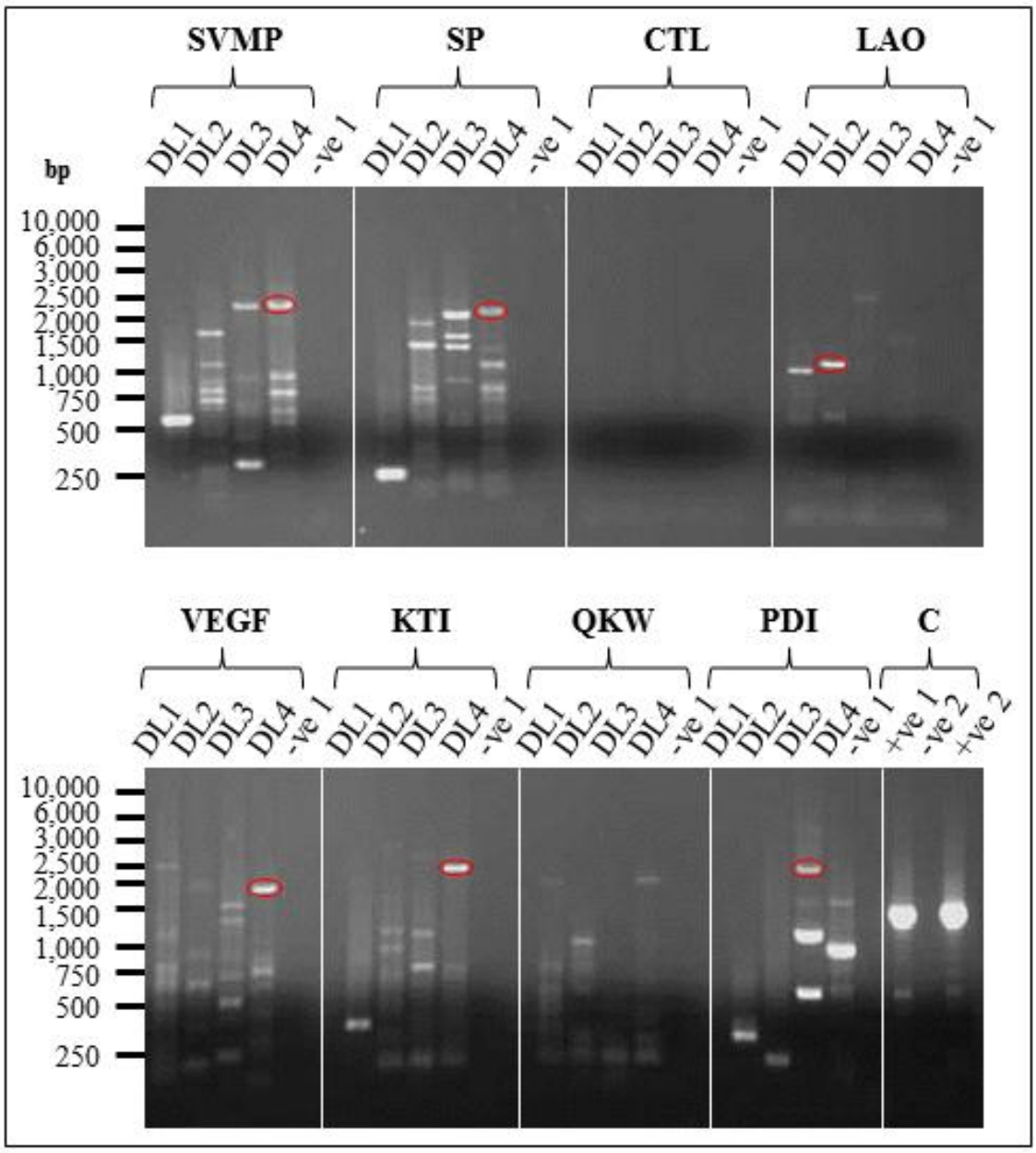

Figure 7.9 Secondary PCR amplification of targets from Genome walker libraries: Analysis of PCR products amplified from restriction digested genome walker libraries following secondary PCR including SVMP, SP, CTL, LAO, VEGF, KTI, PDI and QKW. *B. arietans* genomic DNA was digested with four different restriction enzymes to generate DL (digestion library): DL1 = *DraI*, DL2 = *EcoRV*, DL3 = *PvuII* and DL4 = *Stu I*. Controls (C) : -ve 1; negative water control for each primer pair (absence of genomic library), +ve 1; amplification of tPA from human *PvuII* genomic library, -ve 2; negative water control for human genomic library and +ve 2; amplification of tPA from pre-constructed human *PvuII* genomic library provided in Genome Walker kit). Bands circled in red in panel B were excised and sub-cloned for sequencing.

Although sequences of PCR products amplified from genome walker libraries were obtained, these were shorter in length (700bp-2kb) than expected (2-3kb) which possibly suggests that the quality of DNA was not optimal for this work. Sequences of PCR products amplified by genome walking protocols are shown in Appendix IX, annotated with the open reading frame (ORF) predicted by ORF Finder (NCBI, 2012b), regions of the sequence showing highest sequence homology to BLAST hits and exons boundaries predicted by Wise2 (NCBI, 2012c).

Sequences amplified from genome walker libraries were screened against the *B. arietans* EST library using est2genome (Mott, 1997), assigning a specific EST to each genomic sequence. Protein families were assigned to each genomic sequence amplified from genome walker libraries by BLAST searching the NCBI nucleotide database (Table 7.2). Proteins were correctly assigned to most sequences amplified from genomic DNA, however, several genomic sequences (e.g. SP, VEGF and PDI) showed homology to the PLA_2, ammodytin from *Vipera ammodytes* venom, by BLAST search although est2genome assigned the correct EST sequence to the each genomic sequence.

Protein group	PCR amplicon size (kb)	Sequence length (bp)	EST sequence	Highest scoring BLAST hit	Accession number	BLAST sequence coverage (%)	EST sequence coverage with BLAST hit (%)
SVMP contig 1	2.25	1143	BAR00015	*Crotalus adamanteus* metalloproteinase	HQ414109.1	23	98
SVMP contig 2	2.25	967	BAR00015	*Agkistrodon contortrix* microsatellite	GQ192660.1	8	11
SP contig 1	2	1094	BAR00596	*Vipera ammodytes* ammodytin PLA_2	AJ580214.1	5	18
SP contig 2	2	1078	BAR00377	*V. berus berus* ammodytin PLA_2	AJ580250.1	4	7
SP contig 3	2	1124	BAR00034	*Vipera aspis aspis* ammodytin PLA_2	AJ580156.1	5	11
LAO contig 1	1	1432	BAR00017	*E. ocellatus* LAO	FM177950.1	11	100
VEGF contig 1	2	2098	BAR00040	*A. contortrix* microsatellite	GQ184956.1	9	14
KTI contig 1	2.5	1085	BAR00596	*Bothrops atrox* batroxobin	X12747.1	64	40
KTI contig 2	2.5	700	No sig. hits	*B. atrox* batroxobin	X12747.1	39	N/A
PDI contig 1	2.5	1309	BAR00008	*V. ammodytes* ammodytin PLA_2	AJ580214.1	4	11
PDI contig 2	2.5	1077	No sig. hits	*V. aspis aspis* ammodytin PLA_2	AJ580156.1	6	N/A

Table 7.2 Identification of PCR products amplified from genome walker libraries: For each PCR product, the amplicon size (kb) and sequence length (bp) are recorded. The EST sequence was assigned to each genomic DNA sequence using est2genome (Mott, 1997). A BLAST search against the NCBI nucleotide database was used to assign a protein family to each genomic sequence. The protein family, accession number and sequence coverage of the protein with the highest sequence homology are provided in the table.

7.5. Discussion

The genomic organization of venom protein-encoding genes and the mechanisms involved in regulating gene expression are currently little understood, but thought to be complex due to the continual adaptive evolutionary pressures exerted on venoms (Fry, 2005). Here, we have begun to characterise the structure of genes encoding SP and VEGF in *B. arietans* venom and initial analyses indicated a complexity in the organisation of these genes. Analysis of sequences amplified from *B. arietans* genomic DNA illustrate different architectures in the genomic structure between the two venom protein families (SP and VEGF) in the number of introns in the genomic DNA sequences with the sequence encoding SP containing one intron and the sequence encoding VEGF containing three intron regions. Here, the genomic structure of SP and VEGF genes were not fully determined and further investigation may reveal additional complexity in genomic organisation.

Genome walking is a method regularly used to characterise unknown regions of DNA flanking the coding regions of a gene and has been employed to effectively identify and characterise regulatory regions controlling the expression of eukaryotic genes (Leoni et al., 2008, Rishi et al., 2004, Siebert et al., 1995), including snake venom genes. Previous studies suggested that multiple transcription initiation sites may be commonly present in snake venom genes (Afifiyan et al., 1999, Lachumanan et al., 1998), which has also been frequently observed in other highly regulated eukaryotic genes (Kozak, 1986). In our study, the region of genomic DNA upstream of the transcription start site which was amplified using PCR walking was unusually short (700bp-2kb). Although it is thought that some regulatory elements are relatively close to the transcription start site, including promoters of venom protein

genes (Pawlak and Kini, 2008), others may be present in locations more distant from the transcription start site or span intron-exon boundaries. Due to a lack of data, we could not find the promoters or transcription factors of venom protein-encoding genes. This could potentially be due to poor quality of genomic DNA used in these experiments, or because the distance of the promoter from the transcription start site was longer than expected. In this study, we were not able to obtain DNA of a higher quality by repeating genomic DNA extraction from *B. arietans* tissues due to time and sample constraints, as repeating genomic DNA isolation from fresh tissue would require sacrificing specimens.

As we have begun to observe, the genomic structure and organisation of venom genes are complex. In snake venom toxins, an accelerated segment switching in exons to alter targeting (known as ASSET) has been shown (Doley et al., 2009, Doley et al., 2008). ASSET, and other such alternative splicing variations has resulted in the formation of ordered, conserved exon structure within members of a gene family and could play a significant role in the genomic organisation of venom protein genes. Currently, elapid and viperid 3FTXs genes have been shown to undergo changes in genomic structure due to ASSET (Doley et al., 2009, Doley et al., 2008). The role of ASSET in other protein families such as Kunitz inhibitors, phospholipase A_2, serine proteases and metalloproteinases has also been investigated but not yet clearly defined. Although the molecular mechanisms of ASSET are currently unknown, it is thought that this phenomenon plays an important role in the functional evolution of venom proteins. A study by Sanz *et al* also identified that retrotransposable elements contained in intron regions of the gene structure may play an important role in recruitment and neofunctionalization of multi-gene protein families in venom (Sanz et al., 2012). Transposable elements can represent a large

proportion of eukaryotic genomes and are a rich source of genomic variation as they are inserted into genes or gene regulatory regions, disrupting the gene structure and potentially altering gene function (Biemont and Vieira, 2006). The importance of intragenic regions and mobile elements could be explored by investigating the distribution of transposable elements in the structure of venom genes in comparison to physiological non-toxin homologues.

Substantial work is required to fully investigate and define the genomic organisation of genes encoding other families of venom proteins in viper venom. To date, very little is known about the genomic structure of venom genes and, until very recently, only the organisation and regulation of some neurotoxins and PLA_2s genes has been elucidated. A study by Sanz *et al* provided the first report of the genomic structure of a PIII SVMP transcript from *Echis ocellatus* venom (Sanz et al., 2012) employed an exhaustive strategy to PCR-amplify and assemble sequences for each domain of the enzyme, producing overlapping sequences to form the complete gene sequence. Although genome walking has been shown to be an efficient method to obtain large amounts of sequence data for several multi-gene venom protein families in a single experiment, the approach described by Sanz *et al* may provide a more direct and comprehensive method to determine the organisation of venom protein-encoding genes.

8. GENERAL DISCUSSION

Venom is a highly complex predatory tool with the primary function of immobilising, killing and digesting prey (Kordiš et al., 2002). Therefore, the production of venom is vital to the success of venomous snakes as proficient predators. Venom is a complex mixture of multi-isoform, multi-gene protein families which evolved following accelerated adaptive evolutionary processes including repeated gene recruitment, duplication and selection events. Venom is synthesised by specialised secretory glands but the dynamics of venom production are yet to be fully understood. The overarching aims of the work described in this thesis were to investigate the protein composition of venom, the dynamics of venom protein replenishment, the production of venom in juvenile snakes, the genomic organisation of venom protein-encoding genes and the mechanisms by which venom protein synthesis is controlled and regulated. This work has provided a detailed investigation into the protein composition, gene expression and production of venom in the African Puff Adder, *Bitis arietans*.

Inter and intra-species variation in venom composition and function has been reported on several taxonomic levels, reflecting the complexity of the protein composition of snake venoms. Variation in venom composition is most evident in species with wide-ranging geographical distributions, emphasising that environmental factors (most importantly diet) play a role in influencing the composition and activity of venom (Calvete et al., 2007b, Casewell et al., 2009, Daltry et al., 1996a, Daltry et al., 1996b). Variation in venom composition has been previously documented for other members of the *Bitis* genus (e.g. *B gabonica gabonica, B. g. rhinoceros*, *B. nasicornis* and *B. caudalis*) (Calvete et al., 2007a, Calvete et al., 2007b), but had not yet been investigated in the most medically

important species of the genus, *B. arietans*. We have observed high levels of intra-species variation in the protein composition, immunoreactivity and proteolytic activity of venom between *B. arietans* variants of different and the same geographical origin. Variation was most notable in the expression and activity of the SVMP enzyme group which are responsible for the characteristic symptoms of viper envenoming such as tissue necrosis and haemorrhage (Gutiérrez and Rucavado, 2000, Gutiérrez et al., 2005b). These observations could have significant clinical implications if variations in the protein composition and activity of venom translate into variations in the clinical manifestation of *B. arietans* envenoming. From an evolutionary perspective, *B. arietans* is one of the most geographically diverse viperid species in sub-Saharan Africa and we have demonstrated that this is reflected in its venom phenotype (Currier et al., 2010). There are currently two recognised sub-species of *B. arietans*; *B. arietans arietans* and the Somali Puff Adder, *B. arietans somalica*. However, phylogenetic and phylogeographic studies using multiple independent loci are currently aiming to define the speciation of African and Arabian specimens (Barlow *et al* 2012, in preparation), suggesting that *B. arietans* may be a collection of sub-species based on geographical distribution. Our observations of intra-species variation in venom composition and activity between different *B. arietans* geographical variants across sub-Saharan Africa and Saudi Arabia could be used to support the speculation that a number of *B. arietans* sub-species exist, particularly between the African and Saudi Arabian variants, the latter of which showed a distinctive venom profile with lower SVMP expression and activity in comparison to African venoms.

Several studies have also demonstrated intra-species variation in venom composition and biological function between juvenile and adult specimens with the overall

consensus conclusions that venom from juvenile specimens may be more toxic than adult venoms (Furtado et al., 1991, Reid and Theakston, 1978, Saldarriaga et al., 2003, Zelanis et al., 2007). We investigated changes in the protein composition and proteolytic activity of venom from juvenile *B. arietans* specimens from birth until maturity. Although the proteolytic activity of juvenile venoms appeared to be qualitatively comparable to the maternal adult venom, we observed differences in the composition of SVMPs between juvenile and maternal *B. arietans* venoms. The current literature emphasises that diet is a major factor influencing the protein composition and prey-specific toxicity of venoms (Barlow et al., 2009, Casewell et al., 2009, Daltry et al., 1996a, Daltry et al., 1996b). Our findings indicate that some aspects of venom are genetically hard-wired and not plastic, as functional venom appeared to be produced by juvenile snakes immediately from birth. The protein composition and enzyme activity of juvenile venoms did not appear to change from birth to maturity, which most likely reflects the vital role of venom in both defensive and predatory mechanisms.

We have demonstrated that venom shows great complexity and diversity, even within a single viperid species. Our observations lead us to question how such a complicated, yet fundamental predatory tool is controlled, synthesised and regulated by snake venom glands? The dynamics and mechanisms underlying the regulation and synthesis of venom are thought to be equally complex and multifaceted but little understood. To investigate this we aimed to explore how our observations of the *B. arietans* venom proteome may be reflected in the transcriptome. However, current conventional methods used to analyse the transcriptional activity of the venom gland require sacrificing snakes to dissect venom gland tissue, making the real-time study of venom gene expression ethically undesirable or unachievable. To address this, we

developed and optimised novel techniques which exploited the unusual stability of messenger RNA in lyophilised snake venoms. The major outcomes of this work were to determine the amplification of venom transcripts from venom vs. venom gland cDNA and to exploit new protocols to elucidate the real-time dynamics of venom production. Messenger RNA was identified as an unusually stable component of venoms ten years ago when several key studies demonstrated that mRNAs could be isolated, amplified and sequenced from venoms of snakes (Chen et al., 2002), scorpions (Chen et al., 2003b), lizards (Chen et al., 2006) and amphibians (Chen et al., 2003a, Chen and Shaw, 2003, Chen et al., 2005), although little attempt has been made to explore the mechanisms of mRNA stability, nor to demonstrate how mRNA in venom can be exploited to empower venom research. Our studies have demonstrated, for the first time, that venom mRNA can be applied in research to address important biological questions, such as investigating the time course of venom production using quantitative PCR gene expression analyses (Currier et al., 2012). Venom, as an untapped alternative source of transcriptionally active mRNA, could have numerous applications in venom biology ranging from the generation of transcriptomes for the venoms of CITES-protected venomous species, the comparison of relative gene expression levels of specific venom proteins in venoms from different geographical variants and in the identification of species by DNA barcoding from mitochondrial DNA isolated from lyophilised snake venoms (Pook and McEwing, 2005).

The stability of mRNA in venom is a highly unusual and exciting phenomenon. The mechanisms responsible for regulating mRNA stability in eukaryotes has been reviewed, suggesting that stability of mRNA is achieved through a balance of intracellular transcriptional activity and degradative processes (Saini et al., 1990). In

eukaryotes, the importance of the poly(A) tail, the 5' and 3' untranslated regions (UTR) and regulatory sequences at the 5' end of mRNA have all been implicated in protecting mRNA from degradation (Dreyfus and Régnier, 2002, Sheiness et al., 1975), illustrating that the complexity of the mechanisms regulating mRNA stability/decay are clearly still not well defined. It is thought that components including the 5′-cap structure, 5′-UTR, the protein coding region, 3′-UTR and the 3′-poly(A) tail act synergistically to regulate mRNA stability (Gallie, 1991, Guhaniyogi and Brewer, 2001).

The stability of mRNA in venom is surprising as venom contains many destructive enzymes including nucleases and phosphodiesterases (Dhananjaya and D'Souza, 2010). In other systems, the nearest biological comparison to venom would be saliva, which has also been shown to contain full length and partially degraded mRNAs in humans (Park et al., 2006). Studies suggest that salivary mRNAs could be used as biomarkers for disease (e.g. oral cancer) (Li et al., 2004b). However, the stability of mRNA in saliva is little understood as saliva also contains an abundance of ribonucleases and digestive enzymes (Eichel et al., 1964, Morita et al., 1986). It has recently been suggested that microvesicular bodies, derived from endosomal membrane compartments after fusion with the plasma membrane, present in human saliva (Kapsogeorgou et al., 2005) may provide an environment to contain and protect mRNA from extracellular RNases, ensuring the stability of mRNA (Palanisamy et al., 2010). As microvesicles have also be identified in snake venom (Carneiro et al., 2007), we could suggest that they could also play a role in regulating mRNA stability in venom.

We exploited the stability of mRNA in venoms using our novel optimised approaches to (i) establish the real-time gene expression dynamics of venom

replenishment and (ii) investigate venom production in juvenile *B. arietans* specimens during maturation from birth. In the literature, the dynamics of venom protein production are currently unclear (i.e. whether venom proteins are synthesised in parallel or independently). We could predict that perhaps physiological/structural proteins or components involved in inhibiting and stabilising venom enzymes during storage (e.g. QKW peptides) may be synthesised prior to components with primary toxic functions (e.g. SVMPs). On the other hand, venom proteins which play a vital role in subduing or killing prey may be synthesised as a priority as in the absence of their toxic arsenal, venomous snakes may be vulnerable. Early studies using immunohistochemical techniques suggested that although all venom gland epithelial cells are capable of synthesising and secreting all venom proteins, some proteins may be synthesised at a different rate than others, possibly relating to their biological role in venom (Oron and Bdolah, 1973, Sobol Brown et al., 1975, Oron and Bdolah, 1978). By quantitatively surveying the transcription levels of venom protein-specific mRNAs during the cycle of venom replenishment, we demonstrated that the expression of genes encoding different venom proteins, which included enzymatic toxins and inhibitory components or physiological proteins, peaks between days 3-7 following venom extraction. Although we did not survey the complete range of venom proteins in this study, we targeted transcripts which we considered to be the most important and abundant in *B. arietans* venom such as SVMPs, SPs, CTLs and QKWs. The transcripts surveyed in the study also encompassed venom proteins with a range of biological activities such as proteolytic enzymes (SVMPs), enzyme inhibitors (QKWs) and structural proteins (PDI). Our data conflicts the previous literature by demonstrating that several different venom components, whether enzymatic or non-enzymatic, appear to be expressed at the same time during venom

synthesis. Replenishment of depleted venom proteins occurs relatively quickly emphasising the critical requirement for snakes, as limbless predators, to rapidly re-synthesise functional venom for both predatory and defensive purposes.

Here, we have demonstrated levels of variation in the proteome and transcriptome of *B. arietans* venom. Our findings suggest that tightly-controlled mechanisms may be in position to ensure the rapid synthesis of venom, both in terms of the production of venom in juvenile snakes at birth and in the expression of proteins during replenishment of venom stores following snakebite. However, the mechanisms responsible for operating and controlling venom synthesis and secretion remain to be fully elucidated, implicating the overall complexity of the venom production system. Our questions may be addressed by exploring the genomic structure and organisation of venom protein-encoding genes. In this work, we have taken initial steps to investigate the genomic structure of venom genes and, following initial investigations aiming to define the organisation of vascular endothelial growth factor and serine protease genes expressed in *B. arietans* venom, we suggest that the structure of venom genes is highly complex. Studies have shown that accelerated segment switching in exons to alter targeting (ASSET) observed in the structure of venom genes may play an important role in the functional evolution of venom proteins (Doley et al., 2009, Doley et al., 2008). Studies have also shown that intragenic regions containing retrotransposable elements (Sanz et al., 2012) and domain alteration/loss events (Casewell et al., 2011a, Fry et al., 2008, Wagstaff et al., 2006) are important in the recruitment and neofunctionalization of multi-gene venom protein families. These observations suggest that the structure of genes encoding these venom protein families may be complex and diverse.

Most of the current literature has focussed on defining the genomic organisation of genes encoding neurotoxins in elapid venoms (Afifiyan et al., 1999, Chang et al., 2002, Chang et al., 1997, Fujimi et al., 2003, Lachumanan et al., 1998), and to a lesser extent in viper and colubrid venoms (Doley et al., 2009, Doley et al., 2008, Pawlak and Kini, 2008) and the first genomic structure of an SVMP has only very recently been reported (Sanz et al., 2012). Thus, the lack of genomic data for snake venom genes may be concealing details on the mechanisms of gene recruitment and the molecular events which have resulted in the formation of multigene toxin families. A recent advance and drive in snake genomics has seen sequencing of the first model snake genomes from the Burmese Python (*Python molurus bivittatus*) (Castoe et al., 2011) and King Cobra (*Ophiophagus hannah*) which aim to provide insight into the diversity, structure and organisation of snake genomes.

9. FUTURE WORK

Our observations of variation in protein composition and biological activity of venom from *B. arietans* specimens from different and the same geographical origins may be of therapeutic importance if they directly translate to variations in the clinical manifestation of envenoming following snakebite, and subsequent patient response to antivenom treatment. To address this, investigations to determine further levels of variation in activity between venoms from multiple *B. arietans* geographic variants could be performed. Firstly, we could perform a range of *in vitro* spectrophotometric assays to assess and identify variation in the specific activity of venom enzymes such as LAO, PLA_2 and hyaluronidase. Following this, the lethality of venom determined by LD_{50} experiments (the dose of venom required to induce death in 50% of a group

of mice) and haemorrhagic activity of venom by determining the minimum haemorrhagic dose (MHD) could be investigated. The effect of intra-specific variation in venom composition and enzyme activity on the efficacy and effectiveness of antivenom treatment could be tested by ED_{50} experiments (the minimum dose of antivenom that is required to neutralise venom-induced pathology in 50% of a group of mice). Potential differences in the toxic effects induced by juvenile and maternal *B. arietans* venoms, which may translate to differences in the symptoms of snakebite victims, could be investigated by performing MHD experiments. Although the current antivenom used to treat *B. arietans* envenoming (EchiTAb-Plus_ICP) has been shown to be effective by preclinical testing (Segura et al., 2010), there is no data on the clinical efficacy of antivenom treatment in victims of *B. arietans* snakebite. Our observations of high levels of variation in venom composition and activity of *B. arietans* emphasise that great care should be taken when selecting *B. arietans* specimens for antivenom production to ensure that the complete diversity of venom is considered.

The unusual stability of mRNA in lyophilised snake venom provided an alternative non-invasive approach to conventional methods which enabled the interrogation of the venom gland transcriptome without sacrificing specimens. However, to validate and support the use of venom as an alternative source of mRNA to venom gland tissue, future experiments would firstly aim to determine whether preservation of toxin-encoding mRNA in venom is a universal property of all venoms including viper and elapids representing a spectrum of species, geographic origin, size and habitat of venomous snake taxa. To determine whether the *B. arietans* venom transcriptome is an accurate representation of the venom gland transcriptome we would aim to sequence and compare each transcriptome. This would be one of the

most important assessments in our future work as by confirming the venom transcriptome as a true representative of the venom gland transcriptome, we will prove that venom is a reliable and accurate source of transcriptionally active mRNA. To define the mechanisms potentially involved in preserving mRNA in venom, including inhibitors of mRNA degradation (e.g. other RNAs or protein/peptide components) and physiochemical properties of venom, the degradation rates of venom mRNAs from different species in the presence of total RNA, micro RNAs and small interfering RNAs could be examined. Other potential protective components (e.g. proteins and peptides) could be identified by chromatography and mass spectrometry.

In this work, we have begun to investigate the genomic structure and organisation of venom protein-encoding genes, demonstrating that the structure of venom genes may be highly complex. Further work would aim to characterise the gene structure of different viper venom-encoding genes and expand genome walking protocols to find elements such as promoters and transcription factors responsible for regulating gene expression of proteins by snake venom glands. By focussing primarily on the SVMP enzyme group, we could utilise our knowledge of the domain organisation of this medically important toxin family to elucidate the structure and organisation of genes encoding different classes of SVMPs in a directed approach as described by Sanz *et al* (Sanz et al., 2012) to produce the complete genomic sequences encoding one of the most important and diverse toxin groups in viper venoms.

APPENDICES

APPENDIX I: Recipes for buffers and stock solutions

1D SDS-PAGE and staining:

- 10X Phosphate-buffered saline (PBS):

  80g NaCl

  2g KCl

  14.4g Na_2HPO_4

  2g KH_2PO_4

  Up to 1L dH_2O

- Non-reduced 2X protein loading buffer (2X PLOB):

  10ml 0.5M Tris-base pH 8.5

  6ml 20% SDS

  30ml glycerol

  1.8mg bromophenol blue

  Up to 100ml dH_2O

- 1.5M Tris solution, pH 8.8:

  181.71g Tris-base

  Up to 1L dH_2O

- 0.5M Tris solution, pH 6.8:

  60.57g Tris-base

  Up to 1L dH_2O

- 5X Tris-glycine-SDS (TGS) running buffer:

  151g Tris-base

  720g glycine

  50g SDS

  Up to 10L dH_2O

- Coomassie blue stain:

2.5g Coomassie Blue R-250

500ml methanol

400ml dH_2O

100ml glacial acetic acid

- Coomassie Blue de-stain:

  4.5L methanol

  1L acetic acid

  Up to 10L dH_2O

Immunoblotting:

- Immunotransfer buffer:

  6g Tris-base

  28.8g glycine

  400ml methanol

  Up to 2L ice cold dH_2O

- 1X Tris-buffered saline-Tween (TBST):

  10ml Tween-20

  50ml 2M Tris-base (pH 8.5)

  300ml 5M NaCl

  Up to 10L dH_2O

- 1 X Ponceau S dye

  2g Ponceau S

  30g trichloroacetic acid

  30g sulphosalicylic acid

  Up to 100ml dH_2O

- Blocking buffer:

  5% skimmed milk (Marvel) in 1 x PBS.

- DAB peroxidase developing solution:
  100mg DAB
  50µl hydrogen peroxide
  200ml 1 x PBS

Substrate zymography:

- Re-naturing buffer (per gel):
  2.5ml Triton X-100
  97.5ml distilled H_2O

- Developing buffer (per gel):
  2.5ml 1M Tris pH 8
  250µl 1M $CaCl_2$
  Up to 50ml dH_2O

In-gel trypsin digestion of protein gel bands:

- Destaining solution:
  50ml 100mM Ammonium bicarbonate
  50ml 100% Acetonitrile

- DTT reducing solution:
  15.4mg dithiotheitol
  10ml 100mM Ammonium bicarbonate

- IAN alkylating buffer:
  102mg iodoacetamide
  10ml 100mM Ammonium bicarbonate

- Trypsin digestion solution:

25µg trypsin in 250µl of 50mM acetic acid, diluted 1:10 in 50mM Ammonium bicarbonate/50%Acetonitrile.

Agarose gel electrophoresis:

- 50X Tris-Acetate-EDTA (TAE) buffer:

  242g Tris-base

  100ml 0.5M Na_2EDTA pH 8

  57.1ml glacial acetic acid

  Up to 1L dH_2O

- 6 x DNA loading buffer:

  1X TAE

  20% (w/v) glycerol

  1mg/ml Bromophenol Blue

APPENDIX II: The 'Minimum information for Publication of Quantitative Real-time PCR Experiments' (MIQE) guidelines.

MIQE checklist for authors, reviewers and editors[a]			
Item to check	**Importance**	**Item to check**	**Importance**
Experimental design:		**qPCR oligonucleotides:**	
Definition of experimental and control groups	Essential	*Primer sequences*	Essential
Number within each group	Essential	*RTPrimerDB identification number*	Desirable
Assay carried out by the core or investigator's laboratory?	Desirable	*Probe sequences*	Desirable
Acknowledgement of authors' contributions	Desirable	*Location and identity of any modifications*	Essential
Sample:		*Manufacturer of oligonucleotides*	Desirable
Description	Essential	*Purification method*	Desirable
Volume/mass of sample processed	Desirable	**qPCR protocol:**	
Macrodissection or microdissection	Essential	*Complete reaction conditions*	Essential
Processing procedure	Essential	*Reaction volume and amount of cDNA/DNA*	Essential
If frozen, how and how quickly?	Essential	*Primer, (probe), Mg^{2+}, and dNTP concentrations*	Essential
If fixed, with what and how quickly?	Essential	*Polymerase identity and concentration*	Essential
Sample storage conditions and duration	Essential	*Buffer/kit identity and manufacturer*	Essential
Nucleic acid extraction:		*Exact chemical composition of the buffer*	Desirable
Procedure and/or instrumentation	Essential	*Additives (SYBR Green I, DMSO etc.)*	Essential
Name of kit and details of any modifications	Essential	*Manufacturer of plates/tubes and catalog number*	Desirable
Source of additional reagents used	Desirable	*Complete thermocycling parameters*	Essential
Details of DNase or RNase treatment	Essential	*Reaction setup (manual/robotic)*	Desirable
Contamination assessment (DNA or RNA)	Essential	Manufacturer of qPCR instrument	Essential
Nucleic acid quantification	Essential	**qPCR validation:**	
Instrument and method	Essential	*Evidence of optimization*	Desirable

		(from gradients)	
Purity (A_{260}/A_{280})	Desirable	*Specificity (gel, sequence, melt or digest)*	Essential
Yield	Desirable	*For SYBR Green I, Ct of the NTC*	Essential
RNA integrity: method/instrument	Essential	*Calibration curves with slope and y intercept*	Essential
RIN/RQI or Ct of 3' and 5' transcripts	Essential	*PCR efficiency calculated from slope*	Essential
Electrophoresis traces	Desirable	*CIs for PCR efficiency or SE*	Desirable
Inhibition testing (Ct dilutions, spike or other)	Essential	*r^2 of calibration curve*	Essential
Reverse transcription:		*Linear dynamic range*	Essential
Complete reaction conditions	Essential	*Ct variation at LOD*	Essential
Amount of RNA and reaction volume	Essential	*CIs throughput range*	Desirable
Priming oligonucleotide (if using GSP) and concentration	Essential	*Evidence for LOD*	Essential
Reverse transcriptase and concentration	Essential	*If multiplex, efficiency and OD of each assay*	Essential
Temperature and time	Essential	**Data analysis:**	
Manufacturer of reagents and catalogue numbers	Desirable	*qPCR analysis program (source, version)*	Essential
Cts with and without reverse transcription	Desirable [B]	*Method of Ct determination*	Essential
Storage conditions of cDNA	Desirable	*Outlier identification and disposition*	Essential
qPCR target information:		*Results for NTCs*	Essential
Gene symbol	Essential	*Justification of number/choice of reference gene*	Essential
Sequence accession number	Essential	*Description of normalization method*	Essential
Location of amplicon	Desirable	*Number and concordance of biological replicates*	Desirable
Amplicon length	Essential	*Number and stage of technical replicates*	Essential
In silico specificity screen (BLAST etc.)	Essential	*Repeatability (intra-assay variation)*	Essential
Pseudogenes, retropseudogenes or homologs	Desirable	*Reproducibility (inter-assay variation, CV)*	Desirable
Sequence alignment	Desirable	*Power analysis*	Desirable

Secondary structure analysis of amplicon	Desirable	*Statistical methods for results significance*	Essential
Location of each primer by exon or intron	Essential	*Software (source, version)*	Essential
What splice variants are targeted?	Essential	*Ct or raw data submission with RDML*	Desirable
[a]All essential information must be submitted with the manuscript. RIN, RNA integrity number; RQI, RNA quality indicator; GSP, gene-specific priming; dNTP, deoxynucleoside triphosphate. [B]Assessing the absence of DNA with a no-reverse transcription assay is essential when first extracting RNA. Once the sample has been validated as DNA free, inclusion of a no-reverse transcription control is desirable but not essential.			

Appendix II: The Minimum Information for Publication of Quantitative Real-time PCR experiments (MIQE) guidelines (Bustin et al., 2009).

APPENDIX III: Optimisation of annealing temperature for amplification by quantitative PCR.

Predicted optimal Temp.°C (PrimerSelect):												
	SVMP	52.3	SP	55.8	CTL	57.7	PLA_2	54.5	LAO	54.8	VEGF	58.7
Temp. °C	Ct	Tm °C	Ct	Tm °C	Ct	Tm °C	Ct	Tm °C	Ct	Tm °C	Ct	Tm °C
65.0	28.98	78.50	28.20	75.00	32.61	81.00	30.38	76.50	32.58	79.00	28.79	83.00
64.7	29.39	78.50	28.29	74.50	32.50	81.00	30.51	76.50	32.70	79.00	28.55	82.50
64.2	29.06	78.50	28.98	75.00	32.28	81.00	30.81	76.50	32.16	79.50	28.42	83.00
63.6	30.00	78.50	28.22	75.00	32.70	81.00	30.98	77.00	32.58	79.00	28.58	83.00
62.5	28.92	78.50	27.77	75.00	32.48	81.00	31.36	N/A	32.14	79.50	29.73	N/A
61.5	30.21	78.50	28.61	N/A	33.26	81.00	31.08	75.50	32.90	78.00	28.98	83.00
60.0	29.42	79.00	31.24	75.00	31.94	81.00	31.46	76.50	32.55	79.00	28.90	82.00
58.5	30.09	78.50	28.24	N/A	33.01	81.00	31.14	76.00	32.74	N/A	29.12	82.00
56.6	29.48	78.50	27.64	72.50	32.59	80.00	30.32	77.00	31.81	78.50	28.88	81.50
55.1	29.78	78.00	29.38	74.00	33.39	79.50	30.20	76.50	30.73	81.00	28.83	83.00
53.8	29.35	79.00	27.46	73.00	32.99	80.00	29.68	76.50	32.50	75.00	28.87	81.50
52.6	29.37	78.50	27.19	75.00	33.25	N/A	31.17	N/A	32.18	79.00	28.83	82.00
51.6	29.15	79.00	27.31	74.00	32.74	81.00	29.52	76.00	32.98	N/A	28.42	83.00
50.8	29.85	76.50	27.19	74.50	33.00	81.00	29.77	76.50	31.88	78.50	28.54	82.50
50.3	29.39	77.00	26.48	75.00	32.47	81.00	29.49	75.50	32.07	78.50	28.19	83.00
50.0	28.90	78.50	27.44	N/A	32.57	81.00	29.58	76.00	32.15	79.00	28.53	82.50
Mean	**29.46**	**78.34**	**28.04**	**74.42**	**32.74**	**80.77**	**30.47**	**76.32**	**32.29**	**78.75**	**28.76**	**82.50**
Std. Dev.	**0.42**	**0.68**	**1.12**	**0.84**	**0.40**	**0.50**	**0.70**	**0.46**	**0.54**	**1.28**	**0.36**	**0.57**
	KTI	58.2	PDI	51.6	QKW	53.0	ACTIN	58.6	GAPDH	54.8	HSP	56.8
Temp. °C	Ct	Tm °C	Ct	Tm °C	Ct	Tm °C	Ct	Tm °C	Ct	Tm °C	Ct	Tm °C
65.0	30.88	74.50	30.14	79.50	27.89	79.50	32.58	82.00	33.38	74.00	28.77	77.00
64.7	30.10	74.50	29.87	79.50	28.17	79.50	32.73	81.50	33.79	74.00	28.92	76.50
64.2	30.01	74.50	30.01	79.00	27.80	79.50	32.65	81.50	33.95	73.50	29.66	76.00
63.6	30.00	74.50	29.66	79.50	29.20	78.00	33.04	81.50	33.91	73.50	35.24	N/A
62.5	29.64	74.00	30.11	79.50	28.86	77.50	32.90	81.50	34.31	N/A	37.01	77.50
61.5	29.45	74.00	32.04	N/A	28.75	79.50	33.17	82.00	34.56	73.50	28.41	76.50
60.0	29.46	74.00	28.90	78.00	28.66	79.00	32.42	82.00	35.33	74.00	28.74	76.00

58.5	31.41	71.00	29.69	N/A	29.20	N/A	30.78	N/A	34.91	N/A	29.29	77.00
56.6	30.55	71.50	28.86	N/A	29.02	79.00	32.38	N/A	35.34	80.50	28.75	76.50
55.1	30.28	72.50	28.90	N/A	29.01	78.00	31.84	81.50	34.37	80.50	29.46	77.00
53.8	30.22	74.50	28.67	79.00	28.92	78.50	30.88	82.00	33.92	80.50	28.89	76.50
52.6	30.13	74.00	28.67	N/A	28.92	79.50	31.03	81.50	32.87	80.00	29.19	75.00
51.6	30.29	73.50	28.62	N/A	29.06	78.00	30.14	N/A	33.60	79.00	28.72	77.00
50.8	30.02	73.50	27.75	74.00	29.18	79.50	31.00	N/A	34.51	78.00	29.10	76.50
50.3	30.25	73.00	27.83	N/A	29.20	79.00	31.11	80.00	33.29	77.50	28.61	77.00
50.0	29.71	74.00	28.24	N/A	29.21	77.50	30.65	N/A	33.15	80.00	29.03	76.50
Mean	**30.15**	**73.59**	**29.25**	**78.50**	**28.12**	**78.77**	**31.83**	**81.55**	**34.07**	**77.04**	**29.86**	**76.57**
Std. Dev.	**0.50**	**1.08**	**1.07**	**1.89**	**0.46**	**0.78**	**1.01**	**0.57**	**0.74**	**3.09**	**2.49**	**0.59**

Appendix III: Optimisation of annealing temperature for amplification by quantitative PCR: The cycle time (Ct) value of amplification across an annealing temperature gradient from 50 to 65°C was recorded for each gene of interest. Very little variation in the cycle time across the annealing temperature gradient was observed (Standard deviation: 0.36-3.09 cycles).

APPENDIX IV: Optimisation of starting cDNA quantity for amplification by quantitative PCR.

Venom protein target/Ct: SVMP				SP			CTL			PLA_2			LAO			VEGF		
cDNA ng/reaction	**Rep 1**	**2**	**Average**	**Rep 1**	**2**	**Average**	**Rep 1**	**2**	**Average**	**Rep 1**	**2**	**Average**	**Rep 1**	**2**	**Average**	**Rep 1**	**2**	**Average**
5	28.18	28.67	28.43	30.00	29.15	29.58	31.36	31.63	31.50	26.98	26.80	26.89	27.40	27.22	27.31	26.10	26.30	26.20
10	28.70	28.29	28.50	29.76	29.40	29.58	31.95	32.10	32.03	27.14	27.29	27.22	27.70	27.32	27.51	25.62	25.86	25.74
20	28.70	28.89	28.80	29.82	29.30	29.56	31.73	31.85	31.79	27.20	27.05	27.13	27.03	27.72	27.38	26.15	26.18	26.17
50	27.10	27.15	27.13	28.20	28.36	28.28	31.57	31.70	31.64	27.30	27.48	27.39	27.42	27.71	27.57	26.70	26.73	26.72
Standard deviation:			**0.74**			**0.65**			**0.21**			**0.21**			**0.12**			**0.40**
	KTI			**PDI**			**QKW**			**ACTIN**			**GAPDH**			**HSP**		
5	26.39	26.54	26.47	27.23	28.14	27.69	26.47	26.42	26.45	28.39	28.35	28.37	31.64	30.72	31.18	29.50	29.26	29.38
10	27.01	26.60	26.81	27.40	27.79	27.60	26.59	26.79	26.69	27.98	27.94	27.96	31.32	31.56	31.44	29.89	30.02	29.96
20	25.37	25.35	25.36	27.27	27.40	27.34	26.94	26.49	26.52	28.17	28.35	28.26	31.53	33.32	32.43	29.64	30.28	29.96
50	26.85	27.01	26.93	27.56	27.44	27.50	26.29	26.69	26.49	28.61	28.42	28.52	31.28	31.55	31.42	30.76	31.55	31.16
Standard deviation:			**0.72**			**0.15**			**0.11**			**0.24**			**0.55**			**0.75**

Appendix IV: Optimisation of initial cDNA quantity per reaction for amplification by quantitative PCR: The cycle time (Ct) value of amplification by qPCR was recorded for each gene of interest using different initial quantities of cDNA per reaction ranging from 5 to 50ng. Results showed very little difference between amplification (Ct score) between reactions with less than 1 cycle difference between different initial starting quantity of cDNA.

APPENDIX V: Optimisation of quantitative PCR by standard and melt curve analysis.

Gene target	cDNA conc.	Ct		Average Ct	Melt temp. °C		Peak height		Gene target	cDNA conc.	Ct		Average Ct	Melt temp. °C		Peak height	
	ng/µl	Rep 1	2		Rep 1	2	Rep 1	2		ng/µl	Rep 1	2		Rep 1	2	Rep 1	2
SVMP	2000	27.08	27.19	**27.14**	79.00	79.00	2422.40	2436.42	**KTI**	1000	26.43	26.69	**26.56**	74.50	74.00	1095.46	709.77
	1500	27.64	27.70	**27.67**	79.00	79.00	2351.72	2529.77		500	27.61	27.69	**27.65**	74.50	74.50	1047.71	863.84
	1125	27.71	28.00	**27.86**	79.00	79.00	2393.54	2376.25		250	28.85	29.10	**28.98**	74.50	74.50	1166.09	961.26
	843.75	28.49	28.37	**28.43**	79.00	79.00	2794.84	2492.94		125	30.21	30.29	**30.25**	74.50	74.50	986.05	903.48
	632.81	29.36	28.92	**29.14**	79.00	79.00	2460.80	2565.13		62.50	30.55	30.92	**30.74**	74.50	73.50	1026.16	579.97
	474.61	29.45	29.48	**29.47**	79.00	79.00	2446.97	2399.96		31.25	31.24	31.59	**31.42**	74.50	74.00	1004.70	661.98
	355.96	29.66	30.21	**29.94**	79.50	79.00	2247.97	2349.04		15.63	N/A	N/A	N/A	N/A	N/A	N/A	N/A
	266.97	29.79	30.07	**29.93**	79.00	79.00	2622.35	2275.28		7.81	N/A	N/A	N/A	N/A	N/A	N/A	N/A
SP	2000	25.83	26.28	**26.06**	81.50	81.00	1346.70	1228.55		3.91	N/A	N/A	N/A	N/A	N/A	N/A	N/A
	1500	27.09	26.36	**26.73**	81.00	81.50	1504.01	1175.27		1.95	N/A	N/A	N/A	N/A	N/A	N/A	N/A
	1125	28.30	27.25	**27.78**	81.50	81.50	1478.69	1434.77	**PDI**	1000	27.77	27.61	**27.69**	78.50	79.00	656.06	655.42
	843.75	29.47	29.86	**29.52**	81.50	81.50	1596.04	1353.44		500	28.24	28.09	**28.17**	79.00	79.00	681.51	709.49
	632.81	31.13	31.40	**31.27**	81.50	81.50	1522.45	1231.22		250	28.81	29.05	**28.93**	79.00	76.50	624.74	370.16
	474.61	31.76	31.90	**31.83**	81.50	81.50	1542.89	1367.49		125	29.12	29.91	**29.52**	79.00	75.00	489.20	333.80
	355.96	34.23	32.61	**33.42**	81.50	81.50	1268.86	1321.62		62.50	29.46	29.69	**29.58**	79.00	78.00	491.34	356.76
	266.97	33.09	33.80	**33.45**	81.50	81.50	1654.04	1335.10		31.25	30.01	30.17	**30.09**	79.00	79.00	455.34	389.82
CTL	1000	29.23	29.30	**29.27**	80.00	81.00	705.14	741.31		15.63	N/A	N/A	N/A	N/A	N/A	N/A	N/A
	500	30.44	30.14	**30.29**	81.00	80.50	719.04	724.26		7.81	N/A	N/A	N/A	N/A	N/A	N/A	N/A
	250	31.12	31.54	**31.33**	81.00	80.50	865.19	649.73		3.91	N/A	N/A	N/A	N/A	N/A	N/A	N/A
	125	32.12	33.15	**32.64**	80.50	80.00	739.54	567.06		1.95	N/A	N/A	N/A	N/A	N/A	N/A	N/A
	62.50	33.38	33.42	**33.40**	81.00	80.00	750.16	588.38	**QKW**	1000	25.76	25.62	**25.69**	79.50	79.00	666.09	605.49

	31.25	34.39	34.17	**34.28**	81.00	80.50	757.75	600.74		500	26.45	26.17	**26.31**	79.50	79.50	607.17	737.15
	15.63	35.59	35.34	**35.47**	79.00	81.00	469.65	744.29		250	27.25	27.07	**27.16**	79.50	77.50	616.40	522.39
	7.81	36.44	36.50	**36.47**	79.50	80.50	464.06	435.52		125	28.65	28.62	**28.64**	78.50	78.00	602.49	482.76
	3.91	N/A	N/A	N/A	N/A	N/A	N/A	N/A		62.50	29.69	30.00	**29.85**	77.50	79.50	469.44	355.43
	1.95	N/A	N/A	N/A	N/A	N/A	N/A	N/A		31.25	31.11	30.82	**30.97**	79.50	79.50	546.23	568.19
PLA_2	1000	26.66	29.56	**28.11**	76.50	75.50	294.91	313.98		15.63	31.74	31.80	**31.77**	77.00	77.50	436.88	435.86
	500	29.03	N/A	**29.03**	77.00	N/A	451.08	N/A		7.81	32.95	32.69	**32.82**	79.50	79.50	430.40	490.35
	250	29.28	29.67	**29.48**	77.00	77.00	529.33	407.98		3.91	N/A	N/A	N/A	N/A	N/A	N/A	N/A
	125	29.30	29.68	**29.49**	77.00	77.50	496.49	434.08		1.95	N/A	N/A	N/A	N/A	N/A	N/A	N/A
	62.50	29.62	30.45	**30.04**	76.00	77.00	378.54	307.69	**ACTIN**	2000	27.46	27.28	**27.37**	82.00	82.00	1401.66	1352.96
	31.25	29.40	N/A	**29.40**	77.00	N/A	466.12	N/A		1500	27.27	27.73	**27.50**	82.50	82.00	1502.60	N/A
	15.63	30.02	29.64	**29.83**	74.50	77.00	341.71	430.93		1125	28.57	29.10	**28.84**	82.00	82.00	1762.19	1545.41
	7.81	29.79	30.07	**29.93**	77.50	77.00	450.24	376.65		843.75	29.18	29.39	**29.29**	82.00	82.00	1776.96	1427.34
	3.91	29.43	29.33	**29.38**	76.50	76.50	426.20	366.14		632.81	29.79	29.85	**29.82**	82.00	82.00	1586.77	1503.81
	1.95	28.87	29.82	**29.35**	77.00	74.00	648.70	296.03		474.61	30.25	30.59	**30.42**	82.00	82.00	1768.03	1456.04
LAO	1000	31.29	30.74	**31.02**	75.50	79.00	486.33	750.30		355.96	30.88	31.16	**31.02**	82.00	82.00	1666.15	1301.34
	500	30.17	31.01	**30.59**	79.00	76.00	983.96	500.63		266.97	31.15	31.31	**31.23**	82.00	82.00	1832.43	1499.32
	250	31.42	31.18	**31.30**	77.50	78.50	602.13	587.33	**GAPDH**	2000	28.54	24.49	**26.52**	81.00	81.00	2093.75	1214.42
	125	31.15	30.89	**31.02**	79.50	79.00	839.26	698.82		1500	30.25	35.31	**32.78**	80.50	78.50	2090.13	957.54
	62.50	31.39	31.43	**31.41**	79.00	78.50	631.02	579.32		1125	30.66	31.38	**31.02**	80.50	80.50	1932.03	1700.08
	31.25	31.06	31.17	**31.12**	79.50	79.50	924.76	699.99		843.75	31.08	33.76	**32.42**	80.50	80.00	2070.54	1374.73
	15.63	30.77	30.71	**30.74**	77.00	79.50	611.16	873.48		632.81	31.55	32.54	**32.05**	80.50	80.50	1997.44	1616.25
	7.81	30.72	31.13	**30.93**	79.50	77.00	1030.99	525.10		474.61	32.21	34.66	**33.44**	80.50	80.00	2010.73	1257.04
	3.91	30.88	31.51	**31.20**	79.50	79.00	1029.12	700.95		355.96	33.87	33.91	**33.89**	80.50	80.50	1632.25	1554.41
	1.95	31.03	31.35	**31.19**	79.50	79.00	1149.00	833.82		266.97	33.51	36.35	**34.93**	80.50	80.00	1996.45	1030.75
VEGF	1000	27.35	26.69	**27.02**	79.50	83.00	395.77	549.78	**HSP**	1000	27.99	28.24	**28.12**	76.50	76.50	975.42	873.97
	500	27.38	27.43	**27.41**	81.50	80.50	533.81	445.63		500	28.85	29.64	**29.25**	77.00	76.50	951.01	906.75

	250	27.53	27.72	**27.63**	83.00	81.00	620.55	403.92		250	30.24	30.15	**30.20**	77.00	77.00	1208.82	1165.18
	125	27.35	27.38	**27.57**	82.50	83.00	673.92	670.00		125	31.69	31.14	**31.42**	77.00	77.00	760.41	752.93
	62.50	27.14	27.54	**27.34**	83.00	82.00	640.71	473.06		62.50	30.84	30.48	**30.66**	76.50	74.00	1012.19	640.77
	31.25	27.61	27.60	**27.61**	79.00	81.00	412.33	421.69		31.25	31.51	31.81	**31.66**	77.00	76.50	937.25	944.70
	15.63	27.47	28.25	**27.86**	83.00	80.00	639.78	383.03		15.63	N/A	N/A	N/A	N/A	N/A	N/A	N/A
	7.81	27.33	27.35	**27.34**	82.00	82.50	622.45	623.42		7.81	N/A	N/A	N/A	N/A	N/A	N/A	N/A
	3.91	27.58	27.69	**27.64**	83.00	82.00	684.44	474.66		3.91	N/A	N/A	N/A	N/A	N/A	N/A	N/A
	1.95	27.03	27.32	**27.18**	82.50	82.50	854.63	703.63		1.95	N/A	N/A	N/A	N/A	N/A	N/A	N/A

Appendix V: Optimisation of quantitative PCR by standard and melt curve analysis: The cycle time (Ct) value of amplification, melt temperature and height of melt peak following standard curve and melt curve were recorded for each gene of interest across a series of diluted cDNA concentrations.

APPENDIX VI: Juvenile *Bitis arietans* specimens


BaN58-6


BaN58-7


BaN58-8


BaN58-9


SUPPLIER
BATCH NO. BH (N) 58-10
BaN58-10


BaN58-11


BaN58-12


BaN58-14


BaN58-13


BaN58-15


BaN58-16


BaN58-17


BaN58-18


BaN58-20


BaN58-19

Appendix VI: Juvenile Bitis arietans specimens: Variation in the coloration and scale patterns of related juvenile *B. arietans* siblings.

APPENDIX VII: Optimisation of relative real-time gene expression analysis with reference to the MIQE guidelines.

Experimental design:	
Number within each group	8 individual *Bitis arietans* specimens (originating from Ghana or Nigeria) were used in the study.
Location where assay carried out	Laboratories of the Alistair Reid Venom Unit of the Molecular and Biochemical Parasitology Research Group, Liverpool School of Tropical Medicine.
Acknowledgement of authors' contributions	All experiments were carried out by RB Currier.
Sample:	
Description	Lyophilised venom extracted from 8 individual adult *Bitis arietans* specimens originating from Ghana or Nigeria (historical snake ID numbers: BaG2, BaG4, BaLZS1, BaN11, BaN60, BaN68, BaN80 and BaN81).
Volume/mass sample of processed	2-10mg lyophilised venom.
Processing procedure	Once extracted, venom was frozen at -20°C before being lyophilised for 3-4 hours.
If frozen, how and how quickly?	Fresh venom samples were frozen immediately after extraction.
Sample storage conditions and duration	Freeze-dried venom samples were stored at 4°C.
Nucleic acid extraction:	
Procedure and/or instrumentation	mRNA extraction
Name of kit	Dynabeads® mRNA DIRECT™ kit (Dynal, Invitrogen, UK).
Details of DNase or RNase treatment	DNase treatment was performed on a standard sample (pooled mature venom). Conventional PCR was carried out and products were run on a 1% agarose gel. There were no differences in PCR products between DNase and non DNase treated mRNA samples.
Contamination assessment	Reverse transcriptase negative controls for all toxin, non-toxin and reference genes were carried out using a standard mRNA sample (isolated from pooled mature venom). Amplicons from conventional PCR were run on a 1% agarose gel. No products were visible indicating that there was no contamination.
Nucleic acid quantification	The concentration of mRNA extracted from venom was measured using the Nanodrop spectrophotometer.
Instrument and method	Nanodrop spectrophotometer, Thermo Scientific.
Purity(A_{260}/A_{280})	$OD_{260/280}$ of a control sample (pooled mature venom mRNA) measured using a Nanodrop. The $OD_{260/280}$ reading of mRNA extracted from 10mg lyophilised *B. arietans* venom was 4.67.
Inhibition testing	Standard curves of cDNA dilutions (including cDNA concentrations of up to 2µg/µl) were sufficient to detect the presence of PCR inhibitors introduced in nucleic acid preparation.

Reverse transcription:				
Complete reaction conditions	1µl Primer (50µM oligo dT) and 1µl 10mM dNTP mix were added to each mRNA sample. The cDNA synthesis master mix contained (per reaction): 2µl 10x RT buffer, 4µl 25mM $MgCl_2$, 2µl 0.1M DTT, 1µl RNaseOUT (40U/µl), 1µl Superscript III RT (200U/µl). 1µl RNase H was added to each reaction following termination of cDNA synthesis to degrade any RNA template.			
Amount of RNA and reaction volume	8µl 2-5ng/µl mRNA was added to each 20µl reaction volume.			
Reverse transcriptase and concentration	Superscript® III reverse transcriptase (Invitrogen) at a concentration of 200U/µl.			
Temperature and time	First, samples were incubated for 5 minutes at 65°C and placed on ice for 1 minute. Following addition of the mastermix, samples were incubated for 50 minutes at 50°C. The reactions were terminated following incubation at 85°C for 5 minutes. Following addition of RNaseH, samples were incubated at 37°C for 20 minutes.			
Manufacturer of reagents and cat. numbers	Superscript® III first strand synthesis system manufactured by Invitrogen (cat. number 18080-051).			
Storage conditions of cDNA	cDNA was stored at -20°C.			
qPCR target information:				
Amplicon length	Amplicon lengths for toxin, non-toxin and reference gene primers: Snake venom metalloproteinase – 150 Serine protease – 195 C-type lectin – 131 Kunitz inhibitor – 80 Protein disulphide isomerase – 160 QKW inhibitors – 181 β-actin – 156 GAPDH – 158 Heat shock protein - 148			
Secondary structure analysis	Secondary structures were avoided during primer design.			
qPCR oligonucleotides:				
Primer sequences	**Cluster number**	**Protein group**	**Forward primer sequence**	**Reverse primer sequence**
	BAR00042	SVMP	ATACTGCGTGGTCTAGAAATGTGG	AGCGCCTGTGAATAACTGAGC
	BAR00034	SP	AGGAGGCGAGGAGAAGAGACG	TTCCGCCCCATCCCATAATAC
	BAR00012	CTL	GCTCCGGCTTGCTGGTCGTGTTC	TCGATCGGCCCAGGTCTTCTCTAC
	BAR00023	KTI	GGGCCTATATCCGTTCCTTCTT	ATTCCCATAGCATCCACCATAAAA

	BAR00008	PDI	CCCGAATATTCTGGTGGAGT	AAATTGTTGGGCGAG TTCTG
	BAR00003	QKW	TGCGCCCCCAAATCCTCCTA	TGGCATACGCAGCTG GTTTACTCA
	-	β-actin	CTCAGAGTCGCCCCGGAAGA ACAT	AGAGGCGTACAGGGA GAGCACAGC
	-	GAPDH	GAATATCATCCCAGCATCCAC AGG	CATCATACTTCGCCG GTTTCTCTA
	-	Heat shock protein	CTGCCAGAAGATGAAGATGA AAAG	CAATACAACACGGGG AAGAGACTA
Manufacturer of oligonucleotides	Sigma, UK.			
Purification method	Desalting			
qPCR protocol:				
Complete reaction conditions	1µl cDNA sample per reaction was added to 4µl ultrapure water. 6µl KAPA SYBR® FAST qPCR master mix was added to the diluted cDNA sample.			
Reaction volume and amount of cDNA	11µl reaction volume containing 1µl cDNA.			
Primer, Mg^{2+} and dNTP concentrations	Primers were added to the master mix from 10µM solutions to produce a final concentration of 200nM in the master mix. There was no deviation in Mg^{2+} and dNTP to those provided within the manufacturer's mastermix.			
Polymerase identity and concentration	There was no deviation in the concentration of KAPA SYBR® DNA polymerase to that provided within the manufacturer's mastermix.			
Buffer/kit identity and manufacturer	KAPA SYBR® FAST qPCR kit, KAPA Biosystems, AnaChem.			
Additives (SYBR green I, DMSO etc.)	SYBR green I was contained within the manufacturer's mastermix.			
Manufacturer of plates and cat. number	BioRad, UK (Cat. HSP-3805)			
Complete thermocycling parameters	The following thermocycling protocol was used: enzyme activation 95°C, 3 minutes, [denaturation 95°C, 10 seconds, anneal/extend 55°C, 30 seconds] x 40 cycles. Melt curve were performed following amplification: 10 sec (95°C), ramping from 55°C to 95°C at 0.5°C increments.			
Reaction setup	Manual.			
Manufacturer of qPCR instrument	BioRad CFX 384 real time PCR detection system manufactured by BioRad.			
qPCR validation:				
Evidence of optimisation	PCR with a temperature gradient from 50-65 ºC using all primer pairs was performed in order to determine optimal annealing temperature. An average optimal temperature for all primer pairs was calculated to be 55ºC.			
Specificity (gel, sequence, melt or digest)	Melt curves for example primer pairs are provided in supplementary figure 1.			
For SYBR green I, Ct of the NTC	All Cts for NTCs were negative indicating no DNA contamination.			

Calibration curves with slope and y intercept	Standard curves example primer pairs are provided in supplementary figure 1.
PCR efficiency calculated from slope	Amplification efficiency (%) - Snake venom metalloproteinase: 94.0 Serine protease: 28.0 C-type lectin: 96.9 Kunitz inhibitor: 100.7 Protein disulphide isomerase: 122.6 QKW inhibitory peptide: 91.2 β-actin: 62.2 GAPDH: 51.7 Heat shock protein:89.5
Data analysis:	
qPCR analysis program (source, version)	BioRad CFX manager version 1.5.
Method of Ct determination	Single threshold.
Number/choice of reference genes	3; β-actin, GAPDH and heat shock protein were used as reference genes.
Description of normalised method	The ΔΔC(t)) method for normalized relative gene expression was used.
Number of biological replicates	8 individual West African *B. arietans* specimens were used in this study.
Repeatability (intra-assay variation)	To assess intra-assay repeatability, samples used for standard curve analysis were run in duplicate. All unknown samples were run in triplicate.
Reproducibility (inter-assay variation, CV)	The venom extraction time course was repeated for all available specimens used in the study. mRNA extraction, cDNA synthesis and qPCR were performed under identical conditions as in the first time course. Relative expression analysis from both runs was in agreement.
Statistical methods for results significance	Multiple regression analysis and Bonferroni post-hoc testing.
Software (source, version)	PASW Statistics, SPSS Inc. Version18.

Appendix VII: Optimisation of relative real-time gene expression analysis with reference to the MIQE guidelines: Reference to the 'Minimum information for Publication of Quantitative Real-time PCR Experiments' (MIQE) guidelines in conducting real-time PCR experiments to monitor relative changes in gene expression levels of venom transcripts during venom replenishment.

APPENDIX VIII: Sequence alignments of *Bitis arietans* serine protease and vascular endothelial growth factor gene sequences with homologous genes.

A)

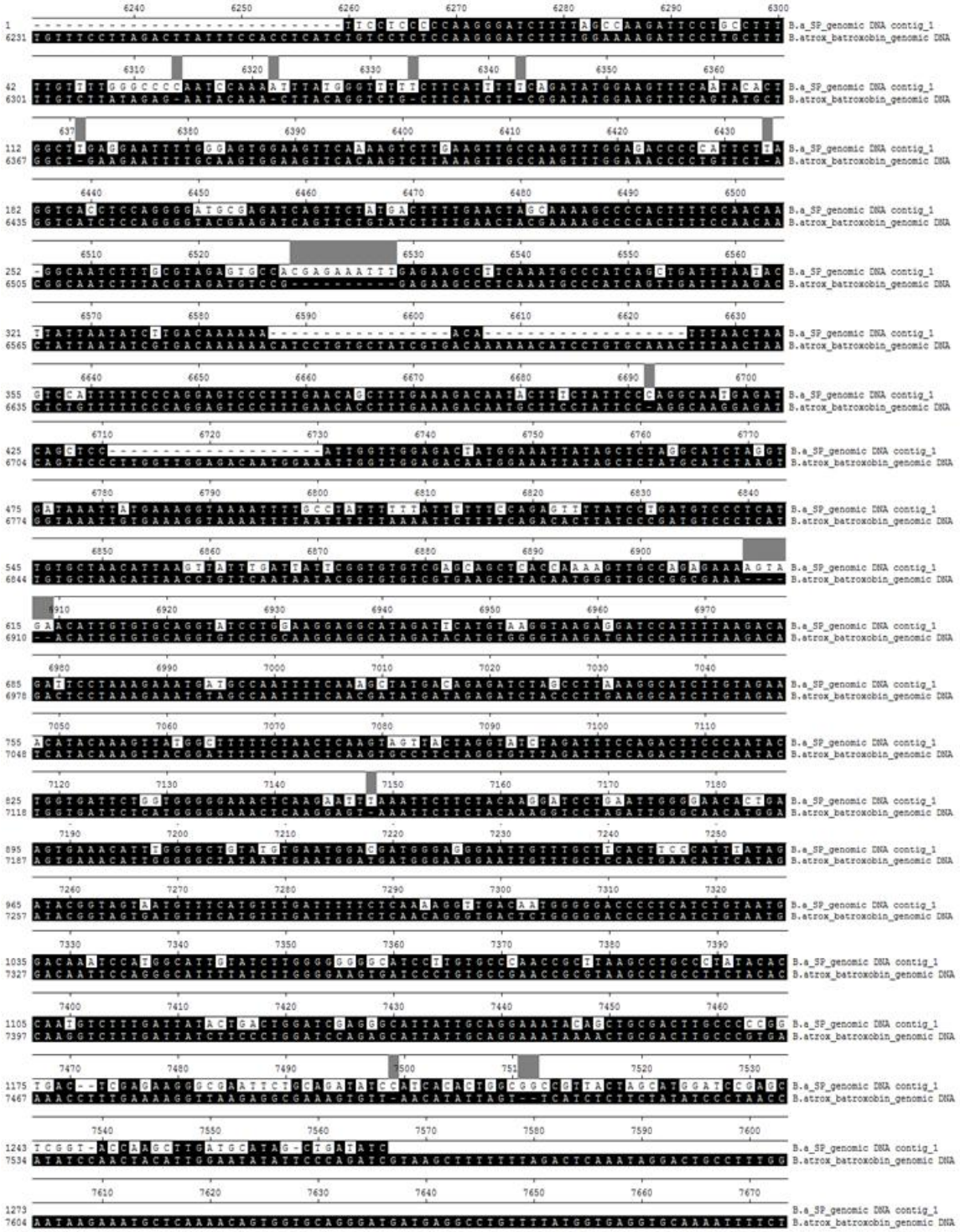

Appendix VIIIA continued on following page:

Appendix VIIIA continued:

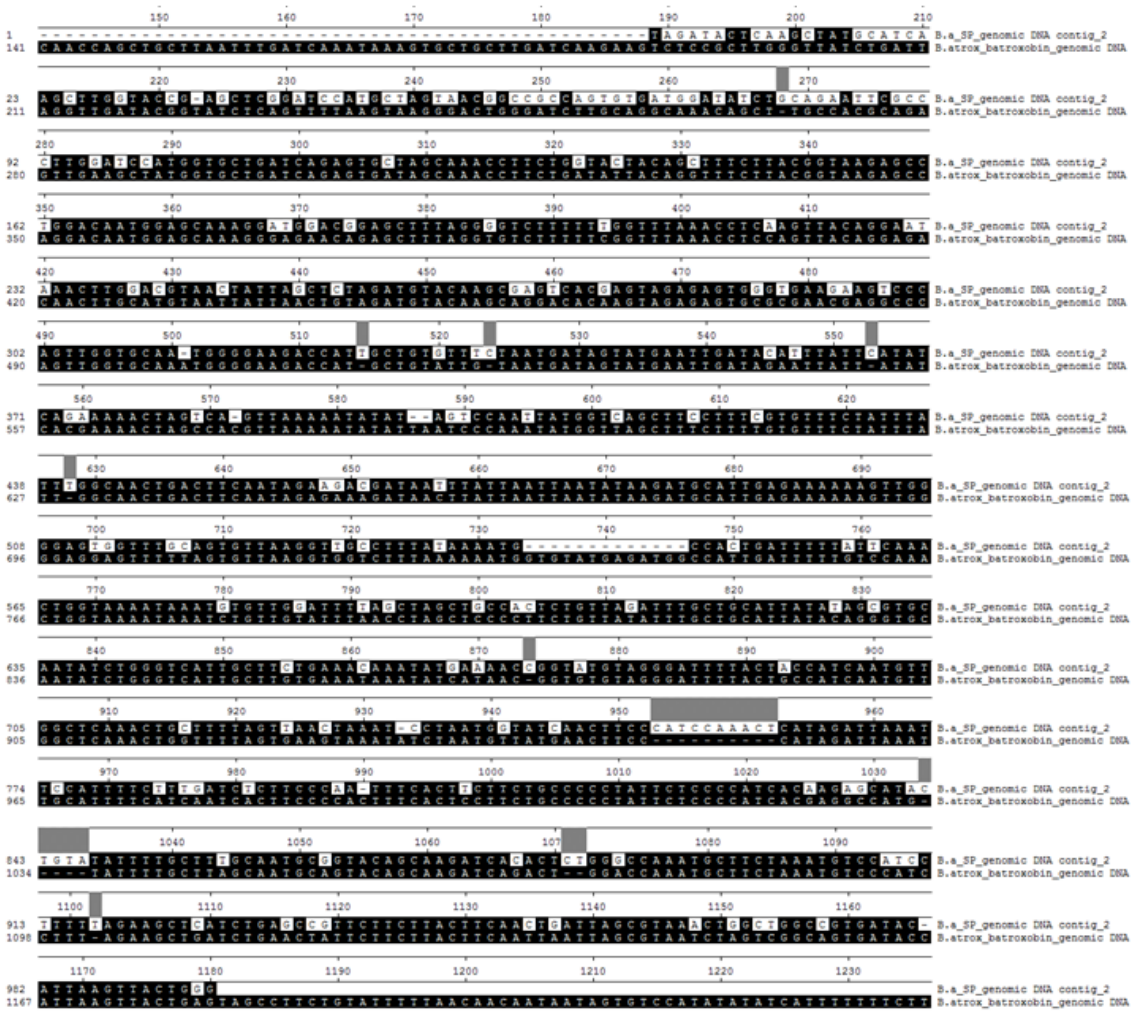

B)

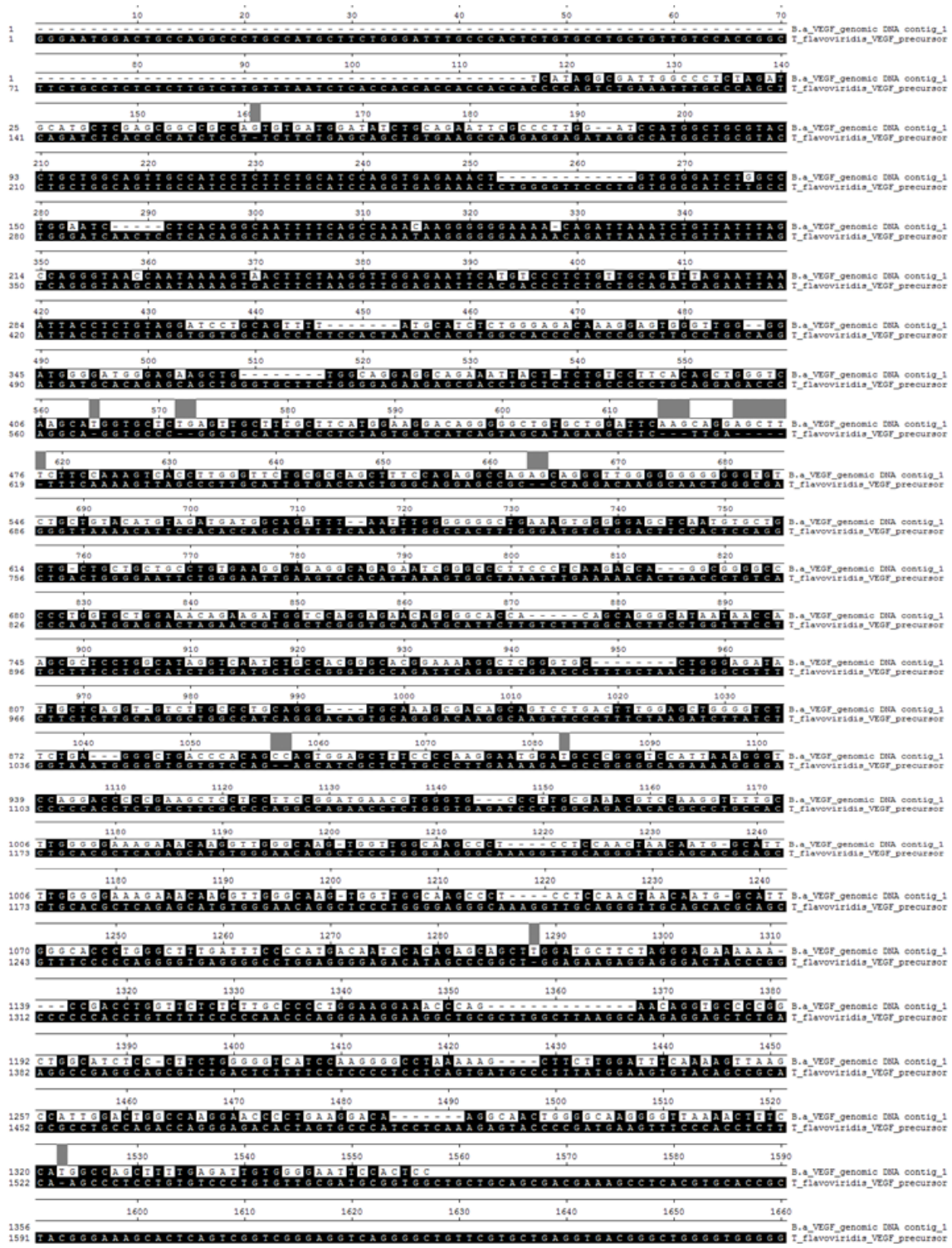

Appendix VIIIB continued on following page:

Appendix VIIIB continued:

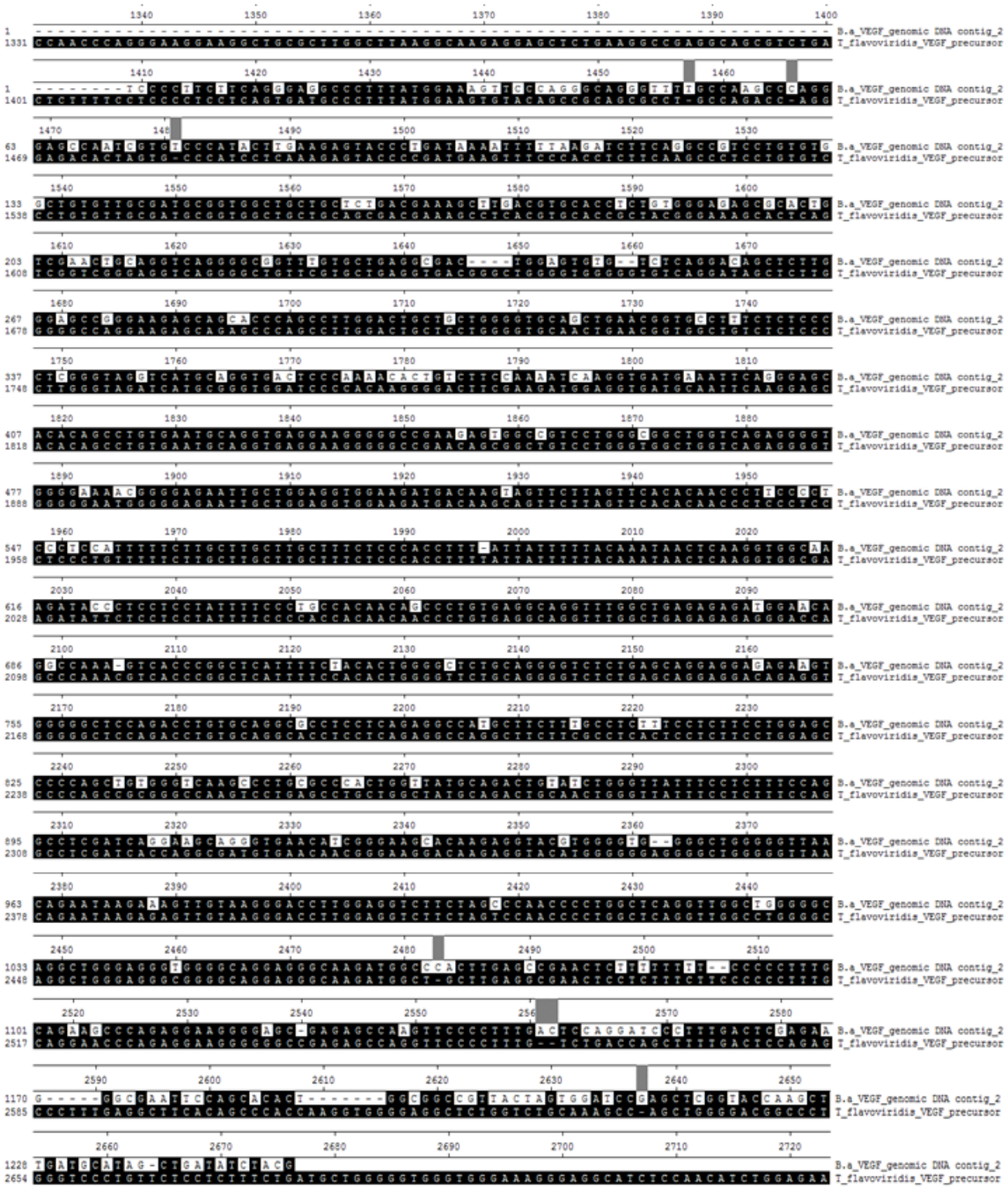

Appendix VIII: Sequence alignments of *Bitis arietans* serine protease and vascular endothelial growth factor gene sequences with homologous genes: A) *B. arietans* genomic SP contigs 1 and 2 aligned with *Bothrops atrox* batroxobin gene sequence and B) *B. arietans* genomic VEGF contigs 1 and 2 with *Trimeresurus flavoviridis* VEGF precursor gene sequence. Alignments show that the *B. arietans* genomic sequences showed sequence homology to each of the 5' and 3' ends of the *B. atrox* batroxobin and *T. flavoviridis* VEGF gene sequences but regions did not overlap, thus do not form the complete sequence of *B. arietans* SP and VEGF-encoding genes.

APPENDIX IX: Sequences and BLAST analysis of PCR products amplified and cloned from genome walker libraries.

SVMP_contig 1 BLAST ID: *Crotalus adamanteus* metalloproteinase (Accession number HQ414109.1)

ATCAGCTATGCATCAAGCTTGGTACCGAGCTCGAGATCCATGCTAGTAACGGCCGCCAGT
GTGATGGATATCTGCAGAATTCGCCCTTACTATAGGGCACGCGTGGTCGACGGCCCGGGC
TGGTCTGTCATTTTTGGAGTGACATGCGCTAAGCCACCTGGAAAACTGCCCTCCAGTAGT
ATTGTTACAACTCAGAATTTGTGCAAATCCTTCTCATATAAAGTCATGA**ATGAAGCTGAA**
GGAGTCATTCCTTGCTTCTCATAGTCAAAGGGAGAAGAGCTCAGGTTGGCTTGAAA
GCAGAAAGAGGTTGCCTCTCTTCAAGCCAAATCCAGCCTCCAAAATGATCCAAGTTC
TCTTGGTAATTATATGCTTAGCGGTTTTTCCATATCAAGGTAAGATGTTCTCTTTGG
TTCCCTTGTTCAGAATCTTACTGCTAAAAGACTATTGTCCCCAACAGATTACTATGT
TGTTGGGTTTTGTTTTGGCTTTTATTTTTGACAATTAACCAAAATTTGTTCCACATTTG
TTCTAAAGTTACATTAATGGTTACTTGGTATTTGTTTAACTTTTGTCAAGCCACAAGCAGA
TCCTTATGAGAAAAGCATGTTCTAGTTGGAGAGAAAGTTTTCCAATGATGTGAGTTTTAA
AAAAAGGATTAGAAGACTGAAGAGGACAGAGAGACAGAGTTTGACAAGAAAATGTCAG
AAAGCAATATTTTAAAGAAAAATAAAGTGTTTTCAGTTTCAATTTTCTTTCAGTGGGTCA
GTTAGACATCTTATAATTAAGCTTGCATAATATTTAGCCAAATAATAGCCAGTTCTTTCAT
TGTTACAGAGAATCTTCAACCTGTACTCATGATAATATGACACTAACTTTTCTCCATGCAA
GATTTTGAATTATTTTAAATTATTTCTTCCCTCTTTTCCTTTTACTCTGCAGAGAACCAGGG
AGGTTCTCTTCTGAAATTCCTCCCAAGTTATCCTTCCTTCTGTGGGCTGAAATACTTTTTA
GATGTCAGTTAACCAGTCTATGGCTCTTCTCCCTATGTACCTAAGTCATTCCCACATATCA
TTACAAACGATGATACTGAATTGATACAGAAGTTGCCAAAATCTATTAACAGTCAGAGG
CTCACTGGAATAA

SVMP_contig 2 BLAST ID: *Agkistrodon contortrix* microsatellite (Accession number GQ192660.1)

AATACTCAAGCTATGCATCAAGCTTGGTACCGAGCTCGAGATGCATGCTCGTAGCGGCCG
CCAGTGTGATGGATATCTGCAGAATTCGCCCTTTGGACTACTTCATAATCATTAATGTTCC
CAGATTCCAGGATTATAGAGCTCCCTTTGTAAGGAAACAGAAAAGAAGGTTTTGTTTACT
TTGGGATATTATTTTACCATTTTCACATCCACAACACGATTTGTTATTCAGTTATCAGTGA
AGAAAGGAATCTTTTTCCAGTGGGACACAGCACAGAAGTTCAGATTTTCTCTGGAAATGC
AATTTGCTGAATGACGTTTGGGAGATGGAAGTCTAGGTGGAGACATTGCTTTGGCAGGTG
CAAAGGAAATATTTTGCAGCTTGAATAATCAGAAAAATATATAAACAAATCTGAACCAA
TGTGCAAGTTTGTGCACTGAGAGATAAGGCTAAGATGAGAAATCACAATAATCTGTTTCA
CATAGTTTAGTAAACCTACTGTATTATGGTTAGCATATCCATTAATCAAAAAGCTAGGCA
AACTTAGATTTTTATGCAAATGCAACTTATTAAGAATTCCCTTCAGTTGAACTGCTATTTC

ACTGCCATCCTAATAGTTTGCTGACTTTCCTTTCTTTCATTTTTAAAAGAATCTATGGACA
GCCCACAGAATCTTAATTATCAAAGGGGCATCTAACAACATGTAAATAACTCAGTGGTTT
CAGAATTAGACTAATAGCAGAAAAAAATAGAGTTGGTCCCCATATGGATATTGTATGTTC
ACCTGGTATTTGCTCCTTGACTTATTTTGTAAATGTGGCAGTCTGACACCTGCAAGATCCT
TTTGGATGCACAATTACAACTGAGACCAAGATATGTTAGCAGATTAAAGGAAAGAAGGA
AAGAAGGAAAGAAGGAAGGAAGGAAGGAAGGAAGGAAGGAAGGAAGGAAGGAAGGA
AGGAAGGG

SP_contig 1 BLAST ID: *Vipera ammodytes* ammodytin (Accession number AJ580214.1)

TATCAAAAATTATATTTGTTTAATGCTGAAGGAGGAGAATACTATTGGGAGAAGGGAAG
CTCAAGGAAATATATTATCTATTGGTGTACTAATTATGGAAATTTTAAAAATAATTATTAT
TGACTGTTAATTAACTATTATTGATTGTATATCTTTTTTTTAAAAAAAATCATGAACCCAG
ACAACACGCTGCACACCAGGCACTAAGGTTGTTATTTAAAAAAAAAATTCAATAAAATT
CTTACCCCTCCTCCCCAAAAATAAAYAAATTTTGAGCTCAGTTGTGGTTGTAAAGTAGAG
GACTACCTGTAGATGGCTAAATCTGACTTTGCAAGTCTGCACAGCTATACTTTCCAGTGC
TTTTTTGCAYACSAGTTAGGGTCCTTGTACTGGAGCCAAAAACTGGGATCATYTTGGTCA
AATCACGACAAATGGCAAACATAAAGAGTAATTCCTGGTTTCAGGTTTAACATCCAAGA
AAATTAATTAGAAACAAAAAGGAATATTTGATTTTCCAGCTTCAGATCTAAAAATTAATA
TTCTTCACATCTCCAGTAATGCTGCAAATAGGTTAAAGAGCATGATTCTGAATAGCTTCA
GCCATTCCAATGGCTGAGATCTAAGGCATCTGGTCTTATGAGAAGCTTTGGCATATTTTG
CTTCACTTCTCCACTGCTCAGTAACTTAATGCCAGCCAGATTACACTAAGTAAGAAGTAA
GAAGAATAGCTCAGATGAGCTTCTAAAAAGGATGGACATTTAGAAGCACTTGGTCCAGA
GTGTCATCTTGCTATACTGCATTGCTAAGCAAAATCTATGGCCTCGTGATGGGGAGAATA
GGAGGCAGAAGGATTGAAAGTAGGAAAGAGATTGATGAAAATGGAATTTAATCTATGGG
AAGTTGATACCATTAGTATTTAGTTTGGATGGGAAGTTGATATTGTTATGTTGTGGGCTCT
GATGAGCAGGAATGAAGACACACAGACCAGCCCGGGCCGTCGACCACGCGTGCCCTATA
GTAAGGGCGAATTCCAGCACACTGGCGGCCGTTACTAGTGGATCCGAGCTCGGTACCAA
GCTTGATGCATAGCTGAG

SP_contig 2 BLAST ID: *Vipera berus berus* ammodytin (Accession number AJ580250.1)

ATGCTGCTCGAGCGGCCGCCAGTGTGATGGATATCTGCAGAATTCGCCCTTACTATAGGG
CACGCGTGGTCGACGGCCCCGGCTTCTTTACCGTCGCCTCGCGTAAACAGGGCGATGGGG
TGTGGGGACGCCGCCTGAGCGGATTCTTTACCGCTGCCGCCTGTATAAAGGGCGAAGGG
GCGTGGGGCGGTCACCGGAGCGGCTTCTTTCCCGCTGCCGCCCGTAAATAGGCCGAAGG
GGCGTCGGGCAATCGCCTGAGCAGCTCGTTTACCGCTGCTGCCCGTAAACAGGGCAAAG
TGGCGTGGGGCTGGAGCGGCTTCTTTACCGCTGCCGCCCGTAAATAGGGCGACGTGGCGT
GGGGAGGCCGCCGGAGCGGCTTCCTTACCGCTGCCGCCCGTAAACAGGGCGACGGGGCG

TGGGGCCGGAGCGGCTTCTTTACCGCTGCTGCCCGTATAAAGGTCGAAGTGACGGGGGG
CGGCCGCCGGAGCGGCTTCTTTACCGTCGCGGCCCTATAGTGAGTCGTATTACTATGATA
TTCATTTATGTTACATTCATCACCTA**TGTTCATTTATATTACATTCATTACTGATGTTCA**
TTTATGTTACATTCATCACCCTATAGGGCCCTATAGTGAGTCGTATTACACTGATGTTCAT
TTATGTTACATTCATCACCGATGTTCATTTATGTTACATTCATCACTGATGTTCATTTATGT
TACATTCATCACTCTATAGGGCCCTATAGTGAGTCGTATTACACTGATGTTCATTTATGTT
ACATTCATCACCGATGTTCATTTATGTTACATTCATCACTGATGTTCATTTATGTTACATTC
ATCACCCTATAGTGAGTCGTATTACAGTGATGTTCATTTATGTTACATTCATCACCTTATA
GGGCCCTATAGTGAGTCGTATTACATGATGTTCATTTATGTTACATTCATCACCCTATAGT
GAGTTGATGTTCATTTATGTTACATTCATCACTGATGTTCATTTATGTTACATTCATCACC
CTATAGTGAGGGATGTTCATTTATGTTACATTCATCACCCGATAAGGTCATTTA

SP_contig 3 BLAST ID: *Vipera aspis aspis* ammodytin (Accession number AJ580156.1)

GGCCCTCTAGATGCATGCTCGAGCGGCCGCCAGTGTGATGGATATCTGCAGAATTCGCCC
TTCAATGACCAGTTCAGAAGACGTTTGTGCTGCAAAGAAATAAAAAAAGCTCAGTGTTTG
GCTGTGGAGTAGAACAGAATATCTTTTATTGGTAATGTTTCTATCAGTACACTAATATTG
AAGGGTAACAGATGACTGAGGGACACACAGCATCAAACCAGTTGAATAAAATGGAGATC
ACCAAAACTAAAAATGTATTTAAAATTTAGCTTTCCTCAGCGTCTGCTGAGATCGTCAGA
GTTTAAGCCAGGATTGAGGGCAGGAGCTCAATAGACCCGATGTTATGTACATAAGGGGT
GATCCTTGCAGCATGAGCCACTGACACCACCAGGTGGCATTGTACTATGTCTGGATTGGC
TGGGTGGCCACACAGTGGGAAATCYAGATAAGGGGATTGGTCCCAGGTATGCCTGGCCA
GGTATATATGAGGGACCAGTAGCCCCTTTGTTCCAGTTCAGTGCTAACATCAATAAAGAG
CTGTTATGCTGCACTCTGCTGTCCAGCGTTTGCCATGCAGTCCTTGCGGTCCAGAACTCAC
TACACAATTCCCGTAACATGCTCATTAGGTAAACTTTTGGCTTTGCAGAGACTATAAGAA
TGTGTCCCTTAATCCTGGCTTAAACTCTGACAATGTCAGCAGATGCTGACAAAAGCTAAG
TTTTAAATAAATTTTTAGTCTTGGTGATCTGCGTTTTTTGATGTTTTATAAGATTTCCAAAA
CAGGAGAGTTGATTTATTCAACAGGGAAGTGAAACAGACACTTTTATCACGCCCTGAATT
CACACTCCAGGATCGTAGTTATTTAAAGCAGGGTCTTTAGAGCACTTTATAAATTACAAT
ACCAATGAGCTGATTGTACTTTCAACCCATTAAACCAGTGTTTCTCAAGCTTGGCAACTT
AGAGATGTATGGATTTCAATTCCCAAAAGTCCCTGGCCAGCATGGCGAATTCTGGGAACT
GAGCTCCATATGCCTTCAAACTGCAAGAGAAAGGCCATAACCTGAAAGCTTGGACTGCA
AAGCTGGAGACAGATGTGTAGTACTTTCCACTCAGTCTCCCTGGC

LAO_contig_1 BLAST ID: *Echis ocellatus* LAO (Accession number FM177950.1)

GCTATGCATCAAGCTTGGTACCGAGCTCGGATGCATGCTCGAGCGGCCGCCAGTGTGATG
GATATCTGCAGAATTCGCCCTTACTATAGGGCACGCGTGGTCGACGGCCCGGGCTGGTAT
CAAATAAATGTACTATGTGTATTATGGATCATAGAAACCAACTGTTAATTATTTTTCTTTA

CAAATGTAAACCCAGCAAACACACTGTTTACCAACTATTGAGTGATTTATGTTTTTAAAA
AAATCAATAAAATATATGGGGGGAAAATGTGTACAAAATCAATTAATGTCTGTGCATGG
GAAGTTTGAATGACAGTTTTGGAAGAGCGTCAGACTAACCAAATATCCACTTGGTGAGA
AATATTTGAGTAGAAGGATACTTTGAATGTTGTAATATTTGCAGAAATCTGGAAATCAGA
ATTGTCCCACCAACCAACATTCAAGTATTATACACTGGATGGCACAACACCCTGAGACCT
AGCCAATCAGAAAATCTCCAGATATAACAGAATAATAGAGTTGGAAGGGATCTTAAAGG
TCTTCTAATCCAATCCCCAGTTCAAGCAGGAAACGCTATAACAATTCTACACAAATGATG
TGTTGGGAGCACACACAACTTTTGGAAGCAAATTGTTCTGGAGGCAAGTTGTTAATTGTT
CTGTCAGGAAATTTCTCCTTAGTTCTAGGTTGGTTCTGTGAAGCACTTGAGTATAATTTTC
AGGCCAGATTAATTTCATTATAGGTATTATTACAGCTACTTGGGAGGATAATCTCAAAAA
ACTAAGCAAGTAAGAATTTGAATAAGAGTCCGCCAAGAAAATACTTGAGATTGGGAAGC
AAAACCCCTTCCAAGTAGCAACCCCTTTCATGCTGCTGCCAAGAAAAGAAGATGGACGTT
GAAATCGAAAAGAGTTAAGCTTGGGTTGAAGAGGACTTATTTGTGATGAGGTCCTTTGTG
TGACCAGAGAAGCAGAAGGAATGATTCTGTGTCCATTTTTCCTCATTTTATAGCAGTTTA
GATGTAGCGTAGGAGACCTCAGAAACTCTAGTTAGAAGGTGGTTCAATGACACATATAA
AAGAATGAAACAAATGAACAGAACCAGAGGCAAAAAATCCAGAATAAGAAAAAACAGG
AAAATGCCATCCTTGTACAT**ATTCCATTTTTGTATGTGTTTTATCCA**GTT**ATGTTCTCA**
CTGCTGTTCTTGGCTACCTTGGGAAGCTGTGCAGATGACAAAAACCCCCTAGAGGA
ATGCTTCCGAGAAGCTGACTATGAAGAATTTCTAGAGATCGCCAGAAATGGTCTGA
AAAAGACATCAAACCCACAACACGTTGTGATTGTAGGAGCAGAAGGGCGAATTCTG
CAGATATCCATCACACTGGCGGCCGTTACTAGCATGGATCTCGAGCTCGGTACCAA
GCTTGATGCATAGC

VEGF_contig_1 BLAST ID: *Agkistrodon contortrix* microsatellite (Accession number GQ184956.1)

GGCCCTCTAGATGCATGCTCGAGCGGCCGCCAGTGTGATGGATATCTGCAGAATTCGCCC
TTACTATAGGGCACGCGTGGTCGACGGCCCGGGCTGGTCCTGGAGGACCGTTGTCCGTAG
GGTCACAATGGGTCGGACACGACTGCGCAGCTAACAACAACAACATCATGCACTAAAGC
TCTTTCCACTTACCCTCCCTCTCCCCAAATAGTTGTTTAATGTTGCCCTTTAATTATTCAAA
ATAGCAAGAATAAGAGTTTACTTTTTAGGAGAAGACACCCTTCTGCCATTTTAATGGCAG
ATTGAGCTCTGCCATGGGGCCAGGCCCCCCTCACTTGAGATGCTTCCCACCCTGGCCTCG
GCCCTGGTAGGAAGCTGCCTCTGCCAGGCTGGGTTCCTTGGGGACCCTTGCTGGGGCAGC
CCTGGGCTGACAAAGGGGCCTGGACACGGGTATGGGGAGAACCTAGGGGAGCAGGCTG
AGCCCCAGGCATGCCCAGCCCTCTTTACCAGGAGCTGGGCAGGCTGCAAGGCACAGGGG
GCGGGGCATGTGGCTCTCTGATGCAATGCACTGGGGAGATGCCCCTCCTTCCAAGAGCAG
ACCCCCATGGGGACTCCTCCTTCCCCTTTTCCTCCTCCTCCTCCTCCTCCTTTCCTGGTTGC
AGAGCAACTGCTGCCCACCAGGAGCCCCCTGCACCAGAAGCCAAAGAACTGAGGAAGCT
TCTTTAATGAGAAGCAAAACATTTTCAAGGAAAAAATCCCAAGAAAGTCCAGTTGCCTTT
TGGAAAAAAGCACCTTTGGGACAACCACGATCTGGATGATGGAGAATCTCCAGAGACAT
CTAGAATAAATTGGCACCCGGTCCAGAAAGGAGGCAGCGCTGCCGATGGGCAATGGGGA

GGGAGAAACGTAGAATCCCCTGGAGATCCGAGTGGGATCAACCCCCCCACCCCCCCAGT
GCAGAAGGAGGCGGAGGGGGCTCCACAGAGTCTTCCTTTGCAAGCAACAGAGGCTCCAA
GGAACCGGAAGGCAACTGTGCCCGCAGCATCGCCCGACTCGCCAGTTCAGACTCTTCCG
GGAGCCAGGAAGAGACGGAGAAAGACCCCTCAGTCAACCAGTGGACTGCAGAAGAGAT
AATTATTCCTATTTAAGAGTACGTTCTCCATTAAGCGAAGAGGCGGGATTGGCTTTGAGC
CAAACTTGTATGGCTGCTGCAAAGCCAGAATATGAAAGCCTGAGGCAGAAGACTTTTGC
CACCAGGCAAGAAAGAGATCTCAAGCAAGCAAGTCGGAGAAAAGGAGGAAAACTAGAT
AACCTTTGGGTCACCCTTTCAGAGATAGTGCCTTACCTACACAGATCCACAGGGTGGCCA
CAGGCAGTGGAAGCAGGAAGGACTTCTGACTTCCTGCTGGCTTCCCCATTGAGTTTCCTT
GTGGGAAGTTGGCAGAGAGAAAGTCAACGGGGAAACTGGCAGGGGAGGCCACAAGTTG
CTCTGGTAAGTTTCCCCCATCTGTGCACATTCCCTAGCCCATTCCTGAGTACTCTCAATCA
ATCAATCAATCAATCAATCAGAATAGAGCTGGAAAGGACCTTGGAGTCTTCTAGTCCAAC
GCCCCTGGCTCAAGGAGGACACCCTATACCATTTCTGACAAGCAACTGTCCAGTCTCTTC
TTGAAAGCCTCCAGTGTTGAAGCACCCATAATTTCTAGAGGCAGATTGTTCCACTGGTTA
ATTGTCCTCAATTATTCTTCTTAATTTCAGACTGCTTCTCCCCGCGATTAGTTTCCAACCGT
CGGCACTAACATAGGCACTAACATAGTCGAAGCCAAAAACTGAGTTCCCCTGCCTTGAG
CACCGAGTATCAAAGCACAATTTCTTCCCCCAGCTAACAGTCACAAATTACAATCCCCAC
TTAGTTTGAAATGCGAGCTTCCCCCCAGCTCTCCAGCCTGCCAATTCTTTATCATCTCTTA
TTTCAATTACCTTGGTTCTC**ACACTCGTGTCCATACTTGAAGAGTACCCTGATAAG**GGC
GAATTCCAGCACACTGGCGGCCGTTACTAGTGGATCCGAGCTCGGTACCAAGCTTGATGC
ATAGCTTGA

KTI_contig_1 BLAST ID: *Bothrops atrox* batroxobin serine protease (Accession number X12747.1)

GGCGAATTGGGCCCTCTAGATGCATGGCTCGAGCGGCCGCCAGTGGTGATGGATATCTGC
AGAATTCGCCCTTACTATAGGGCACGCGTGGTCGACGGCCCGGGCTGGTCCTGGTTGGTG
CAAATGGGGAAGACCATTGCTGTATTTGTAATGATAGTATGAATTGATATATTTATTTATT
AGACCAAAGCTAGCCAATTAAAAATATATAATCTCAAATATGGTCAGCTTCCTTACGTGT
TTCTATTTATTTGGCATCTGACTTCAATAGAAGAAGATAACTTATTAATTAATATAAGATG
CATTGAGAAAAAAGTTGGGGAGTGGTTTGGAATGTTAAGGTTGTCTTGATAAAATGCCAT
TGATTTTTGTCCACACTGGTAAAATAATCTGTTGGATTTAAGCTAGCTCCCATTCTGTTAG
TTTTGCTGCATTATACAGCATGCAATATCTGGGCCAGTGCTTCAGAAACAAATATCAAAC
CTGGTATGTAGGGATTTCACTGCCATCAGTGTTGGCTCAAACTCTTTTTAGTGAATATTTA
TTTTTAGTGAACTAAATGTTATCAACTTCCCAGAGATTAAATTGCATTTTCATCAATCTCT
TCCCCATTTTCACTGCTTCTGTCCCTTATTCTCCCCATCACGAGGCCATATATTTTGCTTAG
CAATGCAGAACAGCAAGATCACAATCTGGGCCAAGTGCTTCTAAATGTCCATCCTTTTTA
GAAGCTCATCTGAACTATTCTTCTTACTTCAACTGTTTAGCGTAATCTGGCTGGCAGTGAT
ACCATTAAGTTACTGAGCAGCAGAGAAGTGAAGCAGAATATGCCAGTGTTTCTCATAAG
ACCAGATACCTTAGATCTTAGCCATCAGAATGGCTGATGCTATTCAGA**ATCATGCTGTTT**
AACCTATTTGTACCATTACTGGAGATRTGAAGAATGATAATTTTTAGATCTGAAACTTG

AAAATCAAATATTTCTTTTTGCTTCTACTTAATTTCTCTTGGGTTGTTTGCCATATGTCCTG
ATTTGATTAAGATGATCCCAGTTTTTGGCTCCAGTACAAGCACCCTAACTGGTGTGC

KTI_contig_2 BLAST ID: *Bothrops atrox* batroxobin serine protease (Accession number X12747.1)

ACATATACACACACAAACACACAATACACATACACACACAGAGAGAGAGAGACACACA
CACACAGACACATTTTTTATACATTAAAAAACGGAGATCACCAAGACTAAAAAAATTATT
TAAAATTTAGCTTTCTTCAGTGTTTAGCCAGGATTGAGGGACACATTCTTATATTCTCTGC
AAAGCCAATAGTTTAGCTAATGAGTGTGTTACGGGTTTCTTCGTCTCCTGCCCTCAATACT
GGCTTAAACTCTTACAATGTCAGCACACGGTGATGAAAGCTAAGTTTTAAATAATTTTTT
ACTCTTGGTGATCTCTGTTTTATTCAACTGGTTTGATACTATGTGTCCCACATTTAACTCTT
ACCCTCCAAAATTAGTGTACTGACAGAAACTCTACCAATGAAAGCGATTCGGTTCTACTC
TACAGCCAAACACTGAACTGTTTTGATTTCTTTGCAGCACAAAAGTCTTCTGAACTGGTC
ATTGGAGGTGATGAATGTGACATAAATGAACATCCTTTCCTTGCACTCATCTATAACTCT
ACATCTATGAGGTTTCACTGTTCTGGGACTTTGCTCAACCAGGAATGGGTGGTCACCGCT
AAGGGCGAATTCCAGCACACTGGCGGCCGTTACTAGTGGATCCGAGCTCGGTACCAAGC
TTGATGCATAGCTTGAGTATTCTAACGCGTCCCTAAAGC

PDI_contig 1 BLAST ID: *Vipera ammodytes* ammodytin (Accession number AJ580214.1)

TGTGATGGATATCTGCAGAATTCGCCCTTACTATAGGGCACGCGTGGTCGACGGCCCGGG
CTGGTCTGCAACAGGATTTGCGCTGATTCTGGCTTGTCACTGGCCCAGGCGCCGGCGGAG
TGTTTAGCCTGCAAATATCCCGGCAACCTTGGCTGTGGGCGACTAACGAAAGCTGTGCAG
GAAAGCGAGCATAAAACGATAAATGTTGCTTTCCGGACCCGAATAGCAAGCAGTAAGGC
CTGCGCGAAATATGAAGAAATTGCATCGCATCGCGAAAAAGAGGGGTGTGCGGCTTAAG
TGAAGGCGTTGGATAAAGTGTCAGGTGTGCAGGGGTAGTTGTGTGTTCCCCGCAGATCCT
CTATGCTATTCACGGATAGACATTTTTTTAAAAAAAAAATAATAGAGCGAAATATTGTAC
AACGGGGGAGTTGAGTACCTTTTATCAAGAGACTTGTAAATTCTGGCTTAAAGTAATCTA
GAAAGGTACCATACTTTTTCTAAAATACTGCCTTGGTTGTAAGAAAACTGCGCCCCCCCT
TTTTTTTTTTTGCTGCTCTACGTACACGTCTTAATTTTGTGAGACGTGACTCCCCACATGTG
GAAGGCATGAGGGATGGTGTAATTCCTACTATGTTCCTGCTAATTTCCTTAATAAAACAG
TTGCACTTTCTGCTGCTCAGCTTTGAAAGGAAAGTTAAAGTAGTCTACTTTTTTTCTCAGC
ATTAACTTTTAAATAGTGTTAAAAGCCTAGTAGTTTATCAAATGTTTATCACAGTCAAGG
ATTTCTGGAGTAATTTTGGCACACAATGCTTTGCACTAATGCGGCAATTGCTTATAAGGT
GAGAGCTATACCAAGCATTTTTTAAATTAAGGGTCTATTGTGGCATTCTAAAGCTGAATG
ATATACCTCAAACATTTTTAGGCACTTTTTAAAGTGAAATTTTCCTGTAGGAGAATAATG
CACTTTTACTGTGAAAATTCATGGGGCTAGATAAGTTTATAGACAGTATTATAAATTAAA
GTTGAAATGTTTTGAATAAAATTTTGGATATCATTCTATTGGAGGATAATTCTTGAGAAA
TTTTTGCA**ATGCTACTGGCATTTTTACGAATGGAAGGTATCCGTAGAAAATACACAAT**

TCATTTGATGCTGTGTTTTCTAGATGTTCATTTTTTTTTTTCCACAGATGCACCATGG
TGTGGTCACTGTAAAGCTCAAGGGCGAATTCCAGCACACTGGCGGCCGTTACTAGT
GGATCCGAGCTCGGTACCAAGCTTGATGCATAGCTTGAGTATTCTAACGCGTCACT

PDI_contig 2 BLAST ID: *Vipera aspis aspis* ammodytin (Accession number AJ580156.1)

GGCGAATTGGGCCCTCTAGATGCATGCTCGAGCGGCCGCCAGTGTGATGGATATCTGCAG
AATTCGCCCTTACTATAGGGCACGCGTGGTCGACTGCCCGGGCTGGTCTGGAAAAGCTGG
CACCCAAAGCATCATGCAATGGGGCGAGTTTCTGTCCTCACCCCAGCTCCTGACAATCTA
TCAGTAAAATCCAGACTCCTTTTACCTTTTTCTTATATTATTCACATTTGTTAACATGTGCC
ACAAATGTAGCACCCCACTCTCATATATTTATTTTTATGCAAGATAGAAAAGGATTGTAC
TGATATGAAAAGTGCTCCAATTTTCATAAAAACAAGCCAAATGATACTGTTTCTTCTTAC
TTCTTTTATTATTTTTGTAATCATTTGGTTCTGTAGTTTTGTTGTGTGTGTGTTTTAAAAAT
ATATAAACGCATGAATAAACGGTTTGGAGAATATTTATTCTTTTTAAGCCACCCAGTAAT
GGTTAAACTGGAAGGCAAGACTTTTATCTCAGAAGCAGCGAAAGACCACTTCAGCCTAC
ATTCCTTGTCCCAGGCAAGTGCGTTACTAAGTATCCTCGACCCTCCCACAAGTAATTTTGC
AATCAGCCCAGTTCCCACTCATACATCATCTCACCCATTCTTTATAGGCAGTTTGACGTAC
TACACAGATTCATCCACACATTTCATATTTCCCACCACTCAGTCAATTATTTTCCTCTCTTC
TCCCCAACCAACGACATCTCAAACAGAAAACGCCTACATATGTTTGATTTCTTCTAACCG
GAAATACTTGTTGCTTATTATTCCGGGTATCTTATAAAACGCGGTCCAGTCAGAATCAAA
CACGAACGAGACCTCTCCAATACGCATGCGCATTACGAAACGGGCAGGCTTCCTAGATG
CCACGTTCCAAAGGCGAGAGGTGAAATGTAATGGAGGAAGAGATAGACTCCGTTTAAGC
TTTCACCGAGCAACCAATCAAAGCCGGTTGAACCAGTGAACGAGAACGGCGCTGTTGTC
CAATCGCAGCCAACAAAGAAGTCTGACAAACCAATCCTAGTTGACGGAACGTA

Appendix IX: Sequences and BLAST analysis of PCR products amplified and cloned from genome walker libraries: Protein families with highest sequences homology were assigned to genomic sequences amplified from genome walker libraries for snake venom metalloproteinase (SVMP), serine protease (SP), L-amino acid oxidase (LAO), vascular endothelial growth factor (VEGF), Kunitz inhibitors (KTI) and protein disulphide isomerase (PDI). Underlined in black (bold) indicates the open reading frame (ORF) predicted by ORF Finder (NCBI, 2012b), grey shaded area indicates sequences matching BLAST hits and underlined in red (bold) indicates exons predicted by Wise2 (NCBI, 2012c).

REFERENCES

ABBRACCHIO, M. P., CERUTI, S., BARBIERI, D., FRANCESCHI, C., MALORNI, W., BIONDO, L., BURNSTOCK, G. & CATTABENI, F. 1995. A Novel Action for Adenosine: Apoptosis of Astroglial Cells in Rat-Brain Primary Cultures. *Biochemical and Biophysical Research Communications,* 213**,** 908-915.

ABE, Y., SHIMOYAMA, Y., MUNAKATA, H., ITO, J., NAGATA, N. & OHTSUKI, K. 1998. Characterization of an apoptosis-inducing factor in Habu snake venom as a glycyrrhizin (GL)-binding protein potently inhibited by GL in vitro. *Biol Pharm Bull,* 9**,** 924-927.

AFIFIYAN, F., ARMUGAM, A., TAN, C. H., GOPALAKRISHNAKONE, P. & JEYASEELAN, K. 1999. Postsynaptic α-Neurotoxin Gene of the Spitting Cobra, *Naja naja sputatrix*: Structure, Organization, and Phylogenetic Analysis. *Genome Research,* 9**,** 259-266.

AHN, M. Y., LEE, B. M. & KIM, Y. S. 1997. Characterization and cytotoxicity of l-amino acid oxidase from the venom of king cobra (*Ophiophagus hannah*). *The International Journal of Biochemistry & Cell Biology,* 29**,** 911-919.

AIRD, S. D. 2002. Ophidian envenomation strategies and the role of purines. *Toxicon,* 40**,** 335-393.

AIRD, S. D. 2005. Taxonomic distribution and quantitative analysis of free purine and pyrimidine nucleosides in snake venoms. *Comparative Biochemistry and Physiology Part B: Biochemistry and Molecular Biology,* 140**,** 109-126.

ALAPE-GIRON, A., SANZ, L., ESCOLANO, J., FLORES-DIAZ, M., MADRIGAL, M., SASA, M. & CALVETE, J. J. 2008. Snake venomics of the

lancehead pitviper *Bothrops asper* geographic, individual, and ontogenetic variations. *Journal of Proteome Research,* 7**,** 3556–3571.

ALI, S. A., STOEVA, S., ABBASI, A., ALAM, J. M., KAYED, R., FAIGLE, M., NEUMEISTER, B. & VOELTER, W. 2000. Isolation, Structural, and Functional Characterization of an Apoptosis-Inducing l-Amino Acid Oxidase from Leaf-Nosed Viper (*Eristocophis macmahoni*) Snake Venom. *Archives of Biochemistry and Biophysics,* 384**,** 216-226.

ANDRADE, D. V. & ABE, A. S. 1999. Relationship of Venom Ontogeny and Diet in *Bothrops*. *Herpetologica,* 55**,** 200-204.

ANDREWS, R. K., KROLL, M. H., WARD, C. M., ROSE, J. W., SCARBOROUGH, R. M., SMITH, A. I., LÓPEZ, J. A. & BERNDT, M. C. 1996. Binding of a Novel 50-kilodalton Alboaggregin from *Trimeresurus albolabris* and Related Viper Venom Proteins to the Platelet Membrane Glycoprotein Ib-IX-V Complex. Effect on Platelet Aggregation and Glycoprotein Ib-Mediated Platelet Activation. *Biochemistry,* 35**,** 12629-12639.

ANTUNES, T. C., YAMASHITA, K. M., BARBARO, K. C., SAIKI, M. & SANTORO, M. L. 2010. Comparative analysis of newborn and adult *Bothrops jararaca* snake venoms. *Toxicon,* 56**,** 1443–1458.

ATODA, H., ISHIKAWA, M., MIZUNO, H. & MORITA, T. 1998. Coagulation Factor X-Binding Protein from *Deinagkistrodon acutus* Venom Is a Gla Domain-Binding Protein. *Biochemistry,* 37**,** 17361-17370.

ATODA, H., YOSHIDA, N., ISHIKAWA, M. & MORITA, T. 1994. Binding Properties of the Coagulation Factor IX/factor X-binding Protein Isolated from the Venom of *Trimeresurus flavoviridis*. *European Journal of Biochemistry,* 224**,** 703-708.

BARAMOVA, E. N., SHANNON, J. D., BJARNASON, J. B. & FOX, J. W. 1989. Degradation of extracellular matrix proteins by hemorrhagic metalloproteinases. *Archives of Biochemistry and Biophysics,* 275**,** 63-71.

BARLOW, A., POOK, C. E., HARRISON, R. A. & WUSTER, W. 2009. Coevolution of diet and prey-specific venom activity supports the role of selection in snake venom evolution. *Proceedings of the Royal Society of Biological Sciences,* 276**,** 2443-2449.

BAZAA, A., MARRAKCHI, N., EL AYEB, M., SANZ, L. & CALVETE, J. J. 2005. Snake venomics: Comparative analysis of the venom proteomes of the Tunisian snakes *Cerastes cerastes*, *Cerastes vipera* and *Macrovipera lebetina*. *Proteomics,* 5**,** 4223-4235.

BECKER, C., HAMMERLE-FICKINGER, A., RIEDMAIER, I. & PFAFFL, M. W. 2010. mRNA and microRNA quality control for RT-qPCR analysis. *Methods,* 50**,** 237-243.

BENDTSEN, J. D., NIELSEN, H., VON HEIJNE, G. & BRUNAK, S. 2004. Improved prediction of signal peptides: SignalP 3.0. *Journal of Molecular Biology,* 340**,** 783-795.

BERNARD, P. S. & WITTWER, C. T. 2002. Real-Time PCR Technology for Cancer Diagnostics. *Clinical Chemistry,* 48**,** 1178-1185.

BIEMONT, C. & VIEIRA, C. 2006. Genetics: Junk DNA as an evolutionary force. *Nature,* 443**,** 521-524.

BLACK, A. R., DONEGAN, C. M., DENNY, B. J. & DOLLY, J. O. 1988. Solubilization and physical characterization of acceptors for dendrotoxin and beta-bungarotoxin from synaptic membranes of rat brain. *Biochemistry,* 27**,** 6814-6820.

BLOOM, D. A., BURNETT, J. W. & ALDERSLADE, P. 1998. Partial purification of box jellyfish (*Chironex fleckeri*) nematocyst venom isolated at the beachside. *Toxicon,* 36**,** 1075-1085.

BUSTIN, S., BENES, V., GARSON, J., HELLEMANS, J., HUGGETT, J., KUBISTA, M., MUELLER, R., NOLAN, T., PFAFFL, M., SHIPLEY, G., VANDESOMPELE, J. & WITTWER, C. 2009. The MIQE Guidelines: Minimum Information for Publication of Quantitative Real-Time PCR Experiments. *Clinical Chemistry,* 55**,** 611-622.

BUSTIN, S. A. 2000. Absolute quantification of mRNA using real-time reverse transcription polymerase chain reaction assays. *J Mol Endocrinol,* 25**,** 169=193.

BUSTIN, S. A., BENES, V., NOLAN, T. & PFAFFL, M. W. 2005. Quantitative real-time RT-PCR – a perspective. *Journal of Molecular Endocrinology,* 34**,** 597-601.

CALVETE, J., ESCOLANO, J. & SANZ, L. 2007a. Snake Venomics of *Bitis* Species Reveals Large Intragenus Venom Toxin Composition Variation: Application to Taxonomy of Congeneric Taxa. *Journal of Proteome Research,* 6**,** 2732-2745.

CALVETE, J. J. 2005. Structure-Function Correlations of Snake Venom Disintegrins. *Current Pharmaceutical Design,* 11**,** 829-835.

CALVETE, J. J., MARCINKIEWICZ, C., MONLEÓN, D., ESTEVE, V., CELDA, B., JUÁREZ, P. & SANZ, L. 2005. Snake venom disintegrins: evolution of structure and function. *Toxicon,* 45**,** 1063-1074.

CALVETE, J. J., MARCINKIEWICZ, C. & SANZ, L. 2007b. Snake venomics of *Bitis gabonica gabonica*. Protein family composition, subunit organization of

venom toxins and characterization of dimeric disintegrins Bitisgabonin-1 and Bitisgabonin-2. *Journal of Proteome Research,* 6**,** 326-336.

CALVETE, J. J., MORENO-MURCIANO, M. P., THEAKSTON, R. D., KISIEL, D. G. & MARCINKIEWICZ, C. 2003. Snake venom disintegrins: novel dimeric disintegrins and structural diversification by disulphide bond engineering. *Biochemical Journal,* 372**,** 725-34.

CARNEIRO, S., FERNANDES, W., SANT'ANNA, S. & YAMANOUYE, N. 2007. Microvesicles in the venom of *Crotalus durissus terrificus* (Serpentes, Viperidae). *Toxicon,* 49**,** 106-110.

CARNEIRO, S. M., ASSAKURA, M. T., BARRENCE, F. A. C., CARDOSO, S. R. T., CAMARGO, A. C. & SESSO, A. 2002. Immunolocalization of venom metalloproteases in venom glands of adult and of newborn snakes of *Bothrops jararaca*. *Tissue&Cell,* 34**,** 381-389.

CASEWELL, N., HARRISON, R., WUSTER, W. & WAGSTAFF, S. 2009. Comparative venom gland transcriptome surveys of the saw-scaled vipers (Viperidae: Echis) reveal substantial intra-family gene diversity and novel venom transcripts. *Bmc Genomics,* 10**,** 564.

CASEWELL, N. R., WAGSTAFF, S. C., HARRISON, R. A., RENJIFO, C. & WUSTER, W. 2011a. Domain loss facilitates accelerated evolution and neofunctionalization of duplicate snake venom metalloproteinase toxin genes. *Molecular Biology and Evolution,* 28**,** 2637-49.

CASEWELL, N. R., WAGSTAFF, S. C., HARRISON, R. A. & WUSTER, W. 2011b. Gene tree parsimony of multilocus snake venom protein families reveals species tree conflict as a result of multiple parallel gene loss. *Molecular Biology and Evolution,* 28**,** 1157-72.

CASTOE, T., DE KONING, A. J., HALL, K., YOKOYAMA, K., GU, W., SMITH, E., FESCHOTTE, C., UETZ, P., RAY, D., DOBRY, J., BOGDEN, R., MACKESSY, S., BRONIKOWSKI, A., WARREN, W., SECOR, S. & POLLOCK, D. 2011. Sequencing the genome of the Burmese python (*Python molurus bivittatus*) as a model for studying extreme adaptations in snakes. *Genome Biology,* 12**,** 406.

CHANG, L.-S., CHUNG, C., WU, B.-N. & YANG, C.-C. 2002. Characterization and Gene Organization of Taiwan Banded Krait (*Bungarus multicinctus*) γ-Bungarotoxin. *Journal of Protein Chemistry,* 21**,** 223-229.

CHANG, L.-S., LIN, J., CHOU, Y.-C. & HONG, E. 1997. Genomic Structures of Cardiotoxin 4 and Cobrotoxin from *Naja Naja Atra* (Taiwan Cobra). *Biochemical and Biophysical Research Communications,* 239**,** 756-762.

CHEN, T., BJOURSON, A., MCCLEAN, S., ORR, D., O'KANE, E., RAO, P. & SHAW, C. 2003a. Cloning of maximakinin precursor cDNAs from Chinese toad, *Bombina maxima*, venom. *Peptides,* 24**,** 853-861.

CHEN, T., BJOURSON, A., ORR, D., KWOK, H., RAO, P., IVANYI, C. & SHAW, C. 2002. Unmasking venom gland transcriptomes in reptile venoms. *Analytical Biochemistry,* 311**,** 152-156.

CHEN, T., FOLAN, R., KWOK, H., O'KANE, E., BJOURSON, A. & SHAW, C. 2003b. Isolation of scorpion (*Androctonus amoreux*i) putative alpha neurotoxins and parallel cloning of their respective cDNAs from a single sample of venom. *Regulatory Peptides,* 115**,** 115-121.

CHEN, T., KWOK, H., IVANYI, C. & SHAW, C. 2006. Isolation and cloning of exendin precursor cDNAs from single samples of venom from the Mexican

beaded lizard (*Heloderma horridum*) and the Gila monster (*Heloderma suspectum*). *Toxicon,* 47**,** 288-295.

CHEN, T. & SHAW, C. 2003. Identification and molecular cloning of novel trypsin inhibitor analogs from the dermal venom of the Oriental fire-bellied toad (*Bombina orientalis*) and the European yellow-bellied toad (*Bombina variegata*). *Peptides,* 24**,** 873-880.

CHEN, T., XUE, Y., ZHOU, M. & SHAW, C. 2005. Molecular cloning of mRNA from toad granular gland secretion and lyophilized skin: identification of Bo8--a novel prokineticin from *Bombina orientalis*. *Peptides,* 26**,** 377-383.

CHEN, Y.-L. & TSAI, I.-H. 1996. Functional and Sequence Characterization of Coagulation Factor IX/Factor X-Binding Protein from the Venom of *Echis carinatus leucogaster*. *Biochemistry,* 35**,** 5264-5271.

CHEN, Y. L. & TSAI, I. H. 1995. Functional and Sequence Characterization of Agkicetin, a New Glycoprotein IB Antagonist Isolated from *Agkistrodon acutus* Venom. *Biochemical and Biophysical Research Communications,* 210**,** 472-477.

CHENG, X., QIAN, Y., LIU, Q., LI, B. X. Y., ZHANG, M. & LIU, J. 1999. Purification, Characterization, and cDNA Cloning of a New Fibrinogenlytic Venom Protein, Agkisacutacin, from *Agkistrodon acutus* Venom. *Biochemical and Biophysical Research Communications,* 265**,** 530-535.

CHIJIWA, T., TOKUNAGA, E., IKEDA, R., TERADA, K., OGAWA, T., ODA-UEDA, N., HATTORI, S., NOZAKI, M. & OHNO, M. 2006. Discovery of novel [Arg49] phospholipase A2 isozymes from *Protobothrops elegans* venom and regional evolution of Crotalinae snake venom phospholipase A2 isozymes in the southwestern islands of Japan and Taiwan. *Toxicon,* 48**,** 672-682.

CHIPPAUX, J. P. 2011. Estimate of the burden of snakebites in sub-Saharan Africa: A meta-analytic approach. *Toxicon,* 57**,** 586-599.

CHIPPAUX, J. P., WILLIAMS, V. & WHITE, J. 1991. Snake venom variability: methods of study, results and interpretation. *Toxicon,* 29**,** 1279-1303.

CIDADE, D. A. P., SIMÃO, T. A., DÁVILA, A. M. R., WAGNER, G., DE L.M. JUNQUEIRA-DE-AZEVEDO, I., LEE HO, P., BON, C., ZINGALI, R. B. & ALBANO, R. M. 2006. *Bothrops jararaca* venom gland transcriptome: Analysis of the gene expression pattern. *Toxicon,* 48**,** 437-461.

COBURN, G. A. & MACKIE, G. A. 1999. Degradation of mRNA in *Escherichia coli*: an old problem with some new twists. *Prog Nucleic Acid Res Mol Biol,* 62**,** 55-108.

COHEN, S. & LEVI-MONTALCINI, R. 1956. A Nerve Growth-Stimulating Factor isolated from Snake venom. *Proc Natl Acad Sci U S A,* 42**,** 571–574.

COOK, D. A. N., OWEN, T., WAGSTAFF, S. C., KINNE, J., WERNERY, U. & HARRISON, R. A. 2010a. Analysis of camelid antibodies for antivenom development: Neutralisation of venom-induced pathology. *Toxicon,* 56**,** 373-380.

COOK, D. A. N., OWEN, T., WAGSTAFF, S. C., KINNE, J., WERNERY, U. & HARRISON, R. A. 2010b. Analysis of camelid IgG for antivenom development: Serological responses of venom-immunised camels to prepare either monospecific or polyspecific antivenoms for West Africa. *Toxicon,* 56**,** 363-372.

COOK, D. A. N., SAMARASEKARA, C. L., WAGSTAFF, S. C., KINNE, J., WERNERY, U. & HARRISON, R. A. 2010c. Analysis of camelid IgG for antivenom development: Immunoreactivity and preclinical neutralisation of venom-induced pathology by IgG subclasses, and the effect of heat treatment. *Toxicon,* 56**,** 596-603.

CORRÊA-NETTO, C., JUNQUEIRA-DE-AZEVEDO, I. D. L. M., SILVA, D. A., HO, P. L., LEITÃO-DE-ARAÚJO, M., ALVES, M. L. M., SANZ, L., FOGUEL, D., ZINGALI, R. B. & CALVETE, J. J. 2011. Snake venomics and venom gland transcriptomic analysis of Brazilian coral snakes, *Micrurus altirostris* and *M. corallinus*. *Journal of Proteomics,* 74**,** 1795-1809.

COUSIN, X. & BON, C. 1997. Acetylcholinesterase from snake venom. *C R Seances Soc Biol Fil.,* 191**,** 381-400.

CURRIER, R., HARRISON, R., ROWLEY, P., LAING, G. & WAGSTAFF, S. 2010. Intra-specific variation in venom of the African Puff Adder (*Bitis arietans*): Differential expression and activity of snake venom metalloproteinases (SVMPs). *Toxicon,* 55**,** 864-873.

CURRIER, R. B., CALVETE, J. J., SANZ, L., HARRISON, R. A., ROWLEY, P. D. & WAGSTAFF, S. C. 2012. Unusual Stability of Messenger RNA in Snake Venom Reveals Gene Expression Dynamics of Venom Replenishment. *Plos One,* 7**,** e41888.

DALTRY, J. C., PONNUDURAI, G., SHIN, C. K., TAN, N. H., THORPE, R. S. & WUSTER, W. 1996a. Electrophoretic profiles and Biological activities: Intraspecific variation in the venom of the Malayan Pitviper (*Calloselasma rhodostoma*). *Toxicon,* 34**,** 67-79.

DALTRY, J. C., WUSTER, W. & THORPE, R. S. 1996b. Diet and snake venom evolution. *Nature,* 379**,** 537-540.

DE AZEVEDO, I. D. L. M. J., FARSKY, S. H. P., OLIVEIRA, M. L. S. & HO, P. L. 2001. Molecular Cloning and Expression of a Functional Snake Venom Vascular Endothelium Growth Factor (VEGF) from the *Bothrops insularis* Pit Viper: A

new member of the VEGF family of proteins. *Journal of Biological Chemistry,* 276**,** 39836-39842.

DE CARVALHO, D. D., SCHMITMEIER, S., NOVELLO, J. C. & MARKLAND, F. S. 2001. Effect of BJcuL (a lectin from the venom of the snake *Bothrops jararacussu*) on adhesion and growth of tumor and endothelial cells. *Toxicon,* 39**,** 1471-1476.

DHANANJAYA, B. & D'SOUZA, C. 2010. An overview on nucleases (DNase, RNase, and phosphodiesterase) in snake venoms. *Biochemistry (Mosc),* 75**,** 1-6.

DHANANJAYA, B. L., NATARAJU, A., RAJESH, R., RAGHAVENDRA GOWDA, C. D., SHARATH, B. K., VISHWANATH, B. S. & D'SOUZA, C. J. M. 2006. Anticoagulant effect of *Naja naja* venom 5′nucleotidase: Demonstration through the use of novel specific inhibitor, vanillic acid. *Toxicon,* 48**,** 411-421.

DOLEY, R., MACKESSY, S. & KINI, R. M. 2009. Role of accelerated segment switch in exons to alter targeting (ASSET) in the molecular evolution of snake venom proteins. *Bmc Evolutionary Biology,* 9**,** 146.

DOLEY, R., PAHARI, S., MACKESSY, S. & KINI, R. M. 2008. Accelerated exchange of exon segments in Viperid three-finger toxin genes (*Sistrurus catenatus edwardsii*; Desert Massasauga). *Bmc Evolutionary Biology,* 8**,** 196.

DREYFUS, M. & RÉGNIER, P. 2002. The Poly(A) Tail of mRNAs: Bodyguard in Eukaryotes, Scavenger in Bacteria. *Cell,* 111**,** 611-613.

DU, X.-Y., CLEMETSON, J. M., NAVDAEV, A., MAGNENAT, E. M., WELLS, T. N. C. & CLEMETSON, K. J. 2002. Ophioluxin, a Convulxin-like C-type Lectin from *Ophiophagus hannah* (King Cobra) Is a Powerful Platelet Activator via Glycoprotein VI. *Journal of Biological Chemistry,* 277**,** 35124-35132.

DUNWIDDIE, T. V. & WORTH, T. 1982. Sedative and anticonvulsant effects of adenosine analogs in mouse and rat. *Journal of Pharmacology and Experimental Therapeutics,* 220**,** 70-76.

EICHEL, H. J., CONGER, N. & CHERNICK, W. S. 1964. Acid and alkaline ribonucleases of human parotid, submaxillary, and whole saliva. *Archives of Biochemistry and Biophysics,* 107**,** 197-208.

ESCALANTE, T., SHANNON, J., MOURA-DA-SILVA, A. M., GUTIERREZ, J. M. & FOX, J. W. 2006. Novel insights into capillary vessel basement membrane damage by snake venom metalloproteinases: a biochemical and immunohistochemical study. *Archives of Biochemistry and Biophysics,* 455**,** 144-153.

ESCOUBAS, P., SOLLOD, B. & KING, G. F. 2006. Venom landscapes: Mining the complexity of spider venoms via a combined cDNA and mass spectrometric approach. *Toxicon,* 47**,** 650-663.

FAN, M. & JAMAL MUSTAFA, S. 2006. Role of adenosine in airway inflammation in an allergic mouse model of asthma. *International Immunopharmacology,* 6**,** 36-45.

FERREIRA, S. H., BARTELT, D. C. & GREENE, L. J. 1970a. Isolation of bradykinin-potentiating peptides from *Bothrops jararaca* venom. *Biochemistry.,* 9**,** 2583-2593.

FERREIRA, S. H., GREENE, L. J., ALABASTER, V. A., BAKHLE, Y. S. & VANE, J. R. 1970b. Activity of various fractions of bradykinin-potentiating factor against angiotensin I converting enzyme. *Nature,* 225**,** 379-380.

FLEIGE, S. & PFAFFL, M. W. 2006. RNA integrity and the effect on the real-time qRT-PCR performance. *Molecular Aspects of Medicine,* 27**,** 126-139.

FOX, J. W. & SERRANO, S. M. T. 2005. Structural considerations of the snake venom metalloproteinases, key members of the M12 reprolysin family of metalloproteinases. *Toxicon,* 45**,** 969-985.

FOX, J. W. & SERRANO, S. M. T. 2008. Insights into and speculations about snake venom metalloproteinase (SVMP) synthesis, folding and disulfide bond formation and their contribution to venom complexity. *FEBS Journal,* 275**,** 3016-3030.

FRANCESCHI, A., RUCAVADO, A., MORA, N. & GUTIERREZ, J. M. 2000. Purification and characterizationof BaH4, a haemorrhagic metalloproteinase from the venom of the snake *Bothrops asper*. *Toxicon,* 38**,** 62-77.

FRANCIS, B. & KAISER, I. I. 1993. Inhibition of Metalloproteinases in *Bothrops asper* Venom by Endogenouse Peptides. *Toxicon,* 31**,** 889-899.

FRANCIS, B., SEEBART, C. & KAISER, I. 1992. Citrate is an endogenous inhibitor of snake venom enzymes by metal ion chelation. *Toxicon,* 30**,** 1239-1246.

FRANCISCHETTI, I. M. B., MY-PHAM, V., HARRISON, J., GARFIELD, M. K. & RIBEIRO, J. M. C. 2004. *Bitis gabonica* (Gaboon viper) snake venom gland: toward a catalog for the full-length transcripts (cDNA) and proteins. *Gene,* 337**,** 55-69.

FRIETAS, M., GENO, P., SUMNER, L., COOKE, M., HUDIBURG, S., OWNBY, C., KAISER, I. & ODELL, G. 1992. Citrate is a Major Component of Snake Venoms. *Toxicon,* 30**,** 461-464.

FROBERT, Y., CRÉMINON, C., COUSIN, X., RÉMY, M.-H., CHATEL, J.-M., BON, S., BON, C. & GRASSI, J. 1997. Acetylcholinesterases from Elapidae snake venoms: biochemical, immunological and enzymatic characterization.

Biochimica et Biophysica Acta (BBA) - Protein Structure and Molecular Enzymology, 1339**,** 253-267.

FRY, B. 2005. From genome to "venome": Molecular origin and evolution of the snake venom proteome inferred from phylogenetic analysis of toxin sequences and related body proteins. *Genome Research***,** 403-420.

FRY, B. G., SCHEIB, H., VAN DER WEERD, L., YOUNG, B., MCNAUGHTAN, J., RAMJAN, S. F. R., VIDAL, N., POELMANN, R. E. & NORMAN, J. A. 2008. Evolution of an Arsenal: Structural and functional diversification of the venom system in the advanced snakes. *Molecular & Cellular Proteomics,* 7**,** 215-246.

FRY, B. G., VIDAL, N., NORMAN, J. A., VONK, F. J., SCHEIB, H., RAMJAN, S. F. R., KURUPPU, S., FUNG, K., HEDGES, S. B., RICHARDSON, M. K., HODGSON, W. C., IGNJATOVIC, V., SUMMERHAYES, R. & KOCHVA, E. 2006. Early evolution of the venom system in lizards and snakes. *Nature,* 439**,** 584-588.

FRY, B. G., VIDAL, N., VAN DER WEERD, L., KOCHVA, E. & RENJIFO, C. 2009. Evolution and diversification of the Toxicofera reptile venom system. *Journal of Proteomics,* 72**,** 127-136.

FRY, B. G., WUSTER, W., KINI, R. M., BRUSIC, V., KHAN, A., VENKATARAMAN, D. & ROONEY, A. P. 2003. Molecular evolution and phylogeny of elapid snake venom three-finger toxins. *Journal of Molecular Evolution,* 57**,** 110-129.

FUJIMI, T. J., NAKAJYO, T., NISHIMURA, E., OGURA, E., TSUCHIYA, T. & TAMIYA, T. 2003. Molecular evolution and diversification of snake toxin genes, revealed by analysis of intron sequences. *Gene,* 313**,** 111-118.

FURTADO, M. F. D., MARUYAMA, M., KANIGUTI, A. S. & ANTONIO, L. C. 1991. Comparative study of nine *Bothrops* snake venoms from adult female snakes and their offspring. *Toxicon,* 29**,** 219-226.

FURTADO, M. F. D., TRAVAGLIA-CARDOSO, S. R. & ROCHA, M. M. T. 2006. Sexual dimorphism in venom of *Bothrops jararaca* (Serpentes: Viperidae). *Toxicon,* 48**,** 401-410.

GALLIE, D. R. 1991. The cap and poly(A) tail function syntergistically to regulate mRNA translational efficiency. *Genes and Development,* 5**,** 2108-2116.

GAO, J. F., QU, Y. F., ZHANG, X. Q. & JI, X. 2011. Within-clutch variation in venoms from hatchlings of *Deinagkistrodon acutus* (Viperidae). *Toxicon,* 57**,** 970–977.

GEORGATSOS, J. G. & LASKOWSKI, M. 1962. Purification of an Endonuclease from the Venom of *Bothrops atrox*. *Biochemistry,* 1**,** 288-295.

GIBBS, H. L., SANZ, L., CHIUCCHI, J. E., FARRELL, T. M. & CALVETE, J. J. 2011. Proteomic analysis of ontogenetic and diet-related changes in venom composition of juvenile and adult Dusky Pigmy rattlesnakes (*Sistrurus miliarius barbouri*). *Journal of Proteomics,* 74**,** 2169–2179.

GIRISH, K. S. & KEMPARAJU, K. 2006. Inhibition of *Naja naja* venom hyaluronidase: Role in the management of poisonous bite. *Life Sciences,* 78**,** 1433-1440.

GIRISH, K. S., MOHANAKUMARI, H. P., NAGARAJU, S., VISHWANATH, B. S. & KEMPARAJU, K. 2004. Hyaluronidase and protease activities from Indian snake venoms: neutralization by *Mimosa pudica* root extract. *Fitoterapia,* 75**,** 378-380.

GOPALAKRISHNAKONE, P., DEMPSTER, D. W., HAWGOOD, B. J. & ELDER, H. Y. 1984. Cellular and mitochondrial changes induced in the structure of murine skeletal muscle by crotoxin, a neurotoxic phospholipase A2 complex. *Toxicon,* 22**,** 85-98.

GUHANIYOGI, J. & BREWER, G. 2001. Regulation of mRNA stability in mammalian cells. *Gene,* 265**,** 11-23.

GUO, A. Y., ZHU, Q. H., CHEN, X. & LUO, J. C. 2007. GSDS: a gene structure display server. *Yi Chuan,* 29**,** 1023-1026.

GUO, Y.-W., CHANG, T.-Y., LIN, K.-T., LIU, H.-W., SHIH, K.-C. & CHENG, S.-H. 2001. Cloning and Functional Expression of the Mucrosobin Protein, a β-Fibrinogenase of *Trimeresurus mucrosquamatus* (Taiwan Habu). *Protein Expression and Purification,* 23**,** 483-490.

GUTIÉRREZ, J. M., LOMONTE, B., LEÓN, G., ALAPE-GIRÓN, A., FLORES-DÍAZ, M., SANZ, L., ANGULOA, Y. & CALVETE, J. J. 2009. Snake venomics and antivenomics: Proteomics tools in the design and control of antivenoms for the treatment of snakebite envenoming. *Journal of Proteomics,* 72**,** 165-182.

GUTIÉRREZ, J. M., ROJAS, E., QUESADA, L., LEON, G., NUNEZ, J., LAING, G. D., SASA, M., RENJIFO, J. M., NASIDI, A., WARRELL, D. A., THEAKSTON, R. D. G. & ROJAS, G. 2005a. Pan-African Polyspecific antivenom produced by caprylic acid purification of horse IgG: an alternative to the antivenom crisis is Africa. *Transactions of the Royal Society of Tropical Medicine and Hygiene,* 99**,** 468-475.

GUTIÉRREZ, J. M. & RUCAVADO, A. 2000. Snake venom metalloproteinases: Their role in the pathogenesis of local tissue damage. *Biochemistry,* 82**,** 841-850.

GUTIÉRREZ, J. M., RUCAVADO, A., ESCALANTE, T. & DÍAZ, C. 2005b. Hemorrhage induced by snake venom metalloproteinases: biochemical and biophysical mechanisms involved in microvessel damage. *Toxicon,* 45**,** 997-1011.

HAMAKO, J., MATSUI, T., SUZUKI, M., ITO, M., MAKITA, K., FUJIMURA, Y., OZEKI, Y. & TITANI, K. 1996. Purification and Characterization of Bitiscetin, a Novel von Willebrand Factor Modulator Protein from *Bitis arietans* Snake Venom. *Biochemical and Biophysical Research Communications,* 226**,** 273-279.

HARRISON, R. A., COOK, D. A., RENJIFO, C., CASEWELL, N. R., CURRIER, R. B. & WAGSTAFF, S. C. 2011. Research strategies to improve snakebite treatment: Challenges and progress. *Journal of Proteomics,* 74**,** 1768-1780.

HARRISON, R. A., HARGREAVES, A., WAGSTAFF, S. C., FARAGHER, B. & LALLOO, D. G. 2009. Snake Envenoming: A Disease of Poverty. *PLoS Neglected Tropical Diseases,* 3**,** e569.

HARRISON, R. A., IBISON, F., WILBRAHAM, D. & WAGSTAFF, S. C. 2007. Identification of cDNAs encoding viper venom hyaluronidases: Cross-generic sequence conservation of full-length and unusually short variant transcripts. *Gene,* 392**,** 22-33.

HARVEY, A. L. & KARLSSON, E. 1980. Dendrotoxin from the venom of the green mamba, *Dendroaspis angusticeps*. *Naunyn-Schmiedeberg's Archives of Pharmacology,* 312**,** 1-6.

HAYASHI, M. A. F. & CAMARGO, A. C. M. 2005. The Bradykinin-potentiating peptides from venom gland and brain of *Bothrops jararaca* contain highly site specific inhibitors of the somatic angiotensin-converting enzyme. *Toxicon,* 45**,** 1163-1170.

HAYTER, J. R., ROBERTSON, D. H. L., GASKELL, S. J. & BEYNON, R. J. 2003. Proteome Analysis of Intact Proteins in Complex Mixtures. *Molecular and Cellular Proteomics,* 2**,** 85-95.

HEINTZMAN, N. & REN, B. 2007. The gateway to transcription: identifying, characterizing and understanding promoters in the eukaryotic genome. *Cellular and Molecular Life Sciences,* 64**,** 386-400.

HERRERA, M., LEÓN, G., SEGURA, A., MENESES, F., LOMONTE, B., CHIPPAUX, J. P. & GUTIÉRREZ, J. M. 2005. Factors associated with adverse reactions induced by caprylic acid-fractionated whole IgG preparations: comparison between horse, sheep and camel IgGs. *Toxicon,* 46**,** 775-781.

HERRICK, D., PARKER, R. & JACOBSON, A. 1990. Identification and comparison of stable and unstable mRNAs in *Saccharomyces cerevisiae*. *Molecular and cellular biology,* 10**,** 2269-2284.

HILL, R. E. & MACKESSY, S. P. 2000. Characterization of venom (Duvernoy's secretion) from twelve species of colubrid snakes and partial sequence of four venom proteins. *Toxicon,* 38**,** 1663-1687.

HOGUE-ANGELETTI, R. A., FRAZIER, W. A., JACOBS, J. W., NIALL, H. D. & BRADSHAW, R. A. 1976. Purification, characterization, and partial amino acid sequence of nerve growth factor from cobra venom. *Biochemistry,* 15**,** 26-34.

HUANG, T. F., HOLT, J. C., LUKASIEWICZ, H. & NIEWIAROWSKI, S. 1987. Trigramin. A low molecular weight peptide inhibiting fibrinogen interaction with platelet receptors expressed on glycoprotein IIb-IIIa complex. *Journal of Biological Chemistry,* 262**,** 16157-16163.

IBM 2009. PAWS Statistics. *Command Syntax reference.* 18 ed. Chicago.

ITOH, N., TANAKA, N., FUNAKOSHI, I., KAWASAKI, T., MIHASHI, S. & YAMASHINA, I. 1988. Organization of the gene for batroxobin, a thrombin-like snake venom enzyme. Homology with the trypsin/kallikrein gene family. *Journal of Biological Chemistry,* 263**,** 7628-7631.

IZIDORO, L. F. M., RIBEIRO, M. C., SOUZA, G. R. L., SANT'ANA, C. D., HAMAGUCHI, A., HOMSI-BRANDEBURGO, M. I., GOULART, L. R., BELEBONI, R. O., NOMIZO, A., SAMPAIO, S. V., SOARES, A. M. & RODRIGUES, V. M. 2006. Biochemical and functional characterization of an l-amino acid oxidase isolated from *Bothrops pirajai* snake venom. *Bioorganic & Medicinal Chemistry,* 14**,** 7034-7043.

JACKSON, K. 2002. How Tubular Venom-Conducting Fangs Are Formed. *Journal of Morphology,* 252**,** 291-297.

JACKSON, K. 2003. The evolution of venom-delivery systems in snakes. *Zoological Journal of the Linnean Society,* 137**,** 337–354.

JACKSON, K. 2007. The evolution of venom-conducting fangs: Insights from developmental biology. *Toxicon,* 49**,** 975-981.

JIANG, Y., LI, Y., LEE, W., XU, X., ZHANG, Y., ZHAO, R., ZHANG, Y. & WANG, W. 2011. Venom gland transcriptomes of two elapid snakes (*Bungarus multicinctus* and *Naja atra*) and evolution of toxin genes. *Bmc Genomics,* 12**,** 1.

JUÁREZ, P., WAGSTAFF, S., OLIVER, J., SANZ, L., HARRISON, R. & CALVETE, J. 2006. Molecular Cloning of Disintegrin-like Transcript BA-5A from a *Bitis arietans* Venom Gland cDNA Library: A Putative Intermediate in the Evolution of the Long-Chain Disintegrin Bitistatin. *Journal of Molecular Evolution,* 63**,** 142-152.

KAMIGUTI, A. S., HAY, C. R. M., THEAKSTON, R. D. G. & ZUZEL, M. 1996. Insights into the mechanisms of haemorrhage caused by snake venom metalloproteinases. *Toxicon,* 34**,** 627-642.

KAPSOGEORGOU, E. K., ABU-HELU, R. F., MOUTSOPOULOS, H. M. & MANOUSSAKIS, M. N. 2005. Salivary gland epithelial cell exosomes: A source of autoantigenic ribonucleoproteins. *Arthritis & Rheumatism,* 52**,** 1517-1521.

KARDONG, K. V. 1980. Evolutionary Patterns in Advanced Snakes. *American Zoologist,* 20**,** 269-282.

KARLSSON, E., MBUGUA, P. M. & RODRIGUEZ-ITHURRALDE, D. 1984. Fasciculins, anticholinesterase toxins from the venom of the green mamba *Dendroaspis angusticeps*. *Journal de physiologie,* 79**,** 232-40.

KASHIMA, S., ROBERTO, P. G., SOARES, A. M., ASTOLFI-FILHO, S., PEREIRA, J. O., GIULIATI, S., JR, M. F., XAVIER, M. A. S., FONTES, M. R. M., GIGLIO, J. R. & FRANÇA, S. C. 2004. Analysis of *Bothrops jararacussu* venomous gland transcriptome focusing on structural and functional aspects: I—gene expression profile of highly expressed phospholipases A2. *Biochimie,* 86**,** 211-219.

KASTURIRATNE, A., WICKREMASINGHE, A. R., DE SILVA, N., GUNAWARDENA, N. K., PATHMESWARAN, A., PREMARATNA, R., SAVIOLI, L., LALLOO, D. G. & JANAKA DE SILVA, H. 2008. The Global Burden of Snakebite: A Literature Analysis and Modelling Based on Regional Estimates of Envenoming and Deaths. *Public Library of Science-Medicine,* 5.

KINI, R. M. 2003. Excitement ahead: structure, function and mechanism of snake venom phospholipase A_2 enzymes. *Toxicon,* 42**,** 827-840.

KINI, R. M. 2006. Structure-function relationships and mechanism of anticoagulant phospholipase A_2 enzymes from snake venoms. *Toxicon,* 45**,** 1147-1161.

KINI, R. M. & GOUDA, T. V. 1982a. Studies on snake venom enzymes: Part I. Purification of ATPase, a toxic component of *Naja naja* venom & its inhibition by potassium gymnemate. *Indian Journal of Biochemistry and Biophysics,* 2**,** 152-154.

KINI, R. M. & GOUDA, T. V. 1982b. Studies on snake venom enzymes: Part II--Partial characterization of ATPases from Russell's viper (*Vipera russelli*) venom & their interaction with potassium gymnemate. *Indian Journal of Biochemistry and Biophysics,* 5**,** 342-346.

KIRKPATRICK, L. L., MATZUK, M. M., DODDS, D. N. C. & PERIN, M. S. 2000. Biochemical Interactions of the Neuronal Pentraxins: Neuronal pentraxin (NP) receptor binds to taipoxin and taipoxin-associated calcium-binding protein 49 via NP1 and NP2. *Journal of Biological Chemistry,* 275**,** 17786-17792.

KOCHVA, E. 1987. The Origin of Snakes and Evolution of the Venom Apparatus. *Toxicon,* 25**,** 65-106.

KOMORI, Y., NIKAI, T., TANIGUCHI, K., MASUDA, K. & SUGIHARA, H. 1999. Vascular Endothelial Growth Factor VEGF-like Heparin-Binding Protein from the Venom of *Vipera aspis aspis* (Aspic Viper). *Biochemistry,* 38**,** 11796-11803.

KOO, B.-H., SOHN, Y.-D., HWANG, K.-C., JANG, Y., KIM, D.-S. & CHUNG, K.-H. 2002. Characterization and cDNA cloning of halyxin, a heterogeneous three-chain anticoagulant protein from the venom of *Agkistrodon halys brevicaudus*. *Toxicon,* 40**,** 947-957.

KORDIŠ, D. & GUBENŠEK, F. 2000. Adaptive evolution of animal toxin multigene families. *Gene,* 261**,** 43-52.

KORDIŠ, D., KRIZAJ, I. & GUBENSEK, F. 2002. Functional Diversification of Animal Toxins by Adaptive Evolution. *In:* MENEZ, A. (ed.) *Perspectives in Molecular Toxinology.* John Wiley and Sons Ltd.

KOSTIZA, T. & MEIER, J. 1996. Nerve Growth Factors from Snake venoms: Chemical Properties, Mode of Action and Biological Significance. *Toxicon,* 34**,** 787-806.

KOYAMA, J., INOUE, S. & HAYASHI, K. 1992. Purification and amino-acid sequence of a nerve growth factor from the venom of *Vipera russelli russelli*. *Biochimica et Biophysica Acta (BBA) - Protein Structure and Molecular Enzymology,* 1160**,** 287-292.

KOZAK, M. 1986. Bifunctional messenger RNAs in eukaryotes. *Cell,* 47**,** 481-483.

KREIL, G. 1995. Hyaluronidases-A group of neglected enzymes. *Protein Science,* 4**,** 1666-1669.

KRIŽAJ, I., ROWAN, E. G. & GUBENŠEK, F. 1995. Ammodytoxin A acceptor in bovine brain synaptic membranes. *Toxicon,* 33**,** 437-449.

KUBISTA, M., ANDRADE, J. M., BENGTSSON, M., FOROOTAN, A., JONÁK, J., LIND, K., SINDELKA, R., SJÖBACK, R., SJÖGREEN, B., STRÖMBOM, L., STÅHLBERG, A. & ZORIC, N. 2006. The real-time polymerase chain reaction. *Molecular Aspects of Medicine,* 27**,** 95-125.

KUDO, K. & TU, A. T. 2001. Characterization of Hyaluronidase Isolated from *Agkistrodon contortrix contortrix* (Southern Copperhead) Venom. *Archives of Biochemistry and Biophysics,* 386**,** 154-162.

KWOK, H., CHEN, T., IVANYI, C. & SHAW, C. 2008. DNA in Amphibian and Reptile Venom Permits Access to Genomes Without Specimen Sacrifice. *Genomic Insights,* 1**,** 17-24.

LACHUMANAN, R., ARMUGAM, A., TAN, C.-H. & KANDIAH, J. 1998. Structure and organization of the cardiotoxin genes in *Naja naja sputatrix*. *FEBS Letters,* 433**,** 119-124.

LALLOO, D. G. & THEAKSTON, R. D. G. 2003. Snake Antivenoms. *Journal of Toxicology Clinical Toxicology* 41**,** 277-290.

LAWSON, R., SLOWINSKI, J. B., CROTHER, B. I. & BURBRINK, F. T. 2005. Phylogeny of the Colubroidea (Serpentes): New evidence from mitochondrial and nuclear genes. *Molecular Phylogenetics and Evolution,* 37**,** 581-601.

LEE, T. I. & YOUNG, R. A. 2000. Transcription of Eukaryotic protein-coding genes. *Annual Review of Genetics,* 34**,** 77-137.

LEONI, C., GALLERANI, R. & CECI, L. R. 2008. A genome walking strategy for the identification of eukaryotic nucleotide sequences adjacent to known regions. *Biotechniques,* 44**,** 232-235.

LI, S., WANG, J., ZHANG, X., REN, Y., WANG, N., ZHAO, K., CHEN, X., ZHAO, C., LI, X., SHAO, J., YIN, J., WEST, M. B., XU, N. & LIU, S. 2004a. Proteomic characterization of two snake venoms: *Naja naja atra* and *Agkistrodon halys*. *Journal of Biochemistry,* 384**,** 119-127.

LI, Y., ST. JOHN, M. A. R., ZHOU, X., KIM, Y., SINHA, U., JORDAN, R. C. K., EISELE, D., ABEMAYOR, E., ELASHOFF, D., PARK, N.-H. & WONG, D. T. 2004b. Salivary Transcriptome Diagnostics for Oral Cancer Detection. *Clinical Cancer Research,* 10**,** 8442-8450.

LOPEZ-LOZANO, J. L., DE SOUSA, M. V., RICART, C. A. O., CHAVEZ-OLORTEGUI, C., SANCHEZ, E. F., MUNIZ, E. G., BUHRNHEIM, P. F. & MORHY, L. 2002. Ontogenetic variation of metalloproteinases and plasma coagulant activity in venoms of wild *Bothrops atrox* specimens from Amazonian rain forest. *Toxicon,* 40**,** 977-1006.

MACKAY, I. M. 2004. Real-time PCR in the microbiology laboratory. *Clinical Microbiology and Infection,* 10**,** 190-212.

MACKAY, I. M., ARDEN, K. E. & NITSCHE, A. 2002. Real-time PCR in virology. *Nucleic Acids Research,* 30**,** 1292-1305.

MACKESSY, S. 1991. Morphology and Ultrastructure of the Venom Glands of the Northern Pacific RattIesnake *Crotalus viridis oreganus*. *Journal of Morphology,* 208**,** 109-128.

MACKESSY, S. P. 2002. Biochemistry and Pharmacology of Colubrid snake venoms. *Journal of Toxicology Toxin Reviews,* 21**,** 43-83.

MACKESSY, S. P. & BAXTER, L. M. 2006. Bioweapons synthesis and storage: The venom gland of front-fanged snakes. *Zoologischer Anzeiger* 245**,** 147-159.

MACKESSY, S. P., SIXBERRY, N. M., HEYBORNE, W. H. & FRITTS, T. 2006. Venom of the Brown Treesnake, *Boiga irregularis*: Ontogenetic shifts and taxa-specific toxicity. *Toxicon,* 47**,** 537–548.

MAHALAKSHMI, Y. V., JAGANNADHAM, M. V. & PANDIT, M. W. 2000. Ribonuclease from Cobra Snake Venom: Purification by Affinity Chromatography and Further Characterization. *IUBMB Life,* 49**,** 309-316.

MAHALAKSHMI, Y. V. & PANDIT, M. W. 1987. A new ribonuclease from cobra venom (*Naja naja*) showing specificity towards cytidylic acid. *Biochemical and Biophysical Research Communications,* 145**,** 740-748.

MANIATIS, T. & REED, R. 2002. An extensive network of coupling among gene expression machines. *Nature,* 416**,** 499-506.

MARAGANORE, J. M. & HEINRIKSON, R. L. 1985. The role of lysyl residues of phospholipases A2 in the formation of the catalytic complex. *Biochemical and Biophysical Research Communications,* 131**,** 129-138.

MARAGANORE, J. M., MERUTKA, G., CHO, W., WELCHES, W., KÉZDY, F. J. & HEINRIKSON, R. L. 1984. A new class of phospholipases A2 with lysine in place of aspartate 49. Functional consequences for calcium and substrate binding. *Journal of Biological Chemistry,* 259**,** 13839-43.

MARKLAND, F. S. 1976. [19] Crotalase. *In:* LASZLO, L. (ed.) *Methods in Enzymology*. Academic Press.

MARKLAND, F. S. 1998. Snake venoms and the Haemostatic System. *Toxicon,* 36**,** 1749-1800.

MATSUI, T., FUJIMURA, Y. & TITANI, K. 2000. Snake venom proteases affecting hemostasis and thrombosis. *Biochimica et Biophysica Acta (BBA) - Protein Structure and Molecular Enzymology,* 1477**,** 146-156.

MATSUI, T., SAKURAI, Y., FUJIMURA, Y., HAYASHI, I., OH-ISHI, S., SUZUKI, M., HAMAKO, J., YAMAMOTO, Y., YAMAZAKI, J., KINOSHITA, M. & TITANI, K. 1998. Purification and amino acid sequence of halystase from snake venom of *Agkistrodon halys blomhoffii*, a serine protease that cleaves specifically fibrinogen and kininogen. *European Journal of Biochemistry,* 252**,** 569-575.

MEBS, D. & OWNBY, C. L. 1990. Myotoxic components of snake venoms: Their biochemical and biological activities. *Pharmacology & Therapeutics,* 48**,** 223-236.

MENEZES, M. C., FURTADO, M. F., TRAVAGLIA-CARDOSO, S. R., CAMARGO, A. C. M. & SERRANO, S. M. T. 2006. Sex-based individual variation of snake venom proteome among eighteen *Bothrops jararaca* siblings. *Toxicon,* 47**,** 304-312.

MEYER, S., TEMME, C. & WAHLE, E. 2004. Messenger RNA turnover in eukaryotes: pathways and enzymes. *Crit Rev Biochem Mol Biol,* 39**,** 197-216.

MILNE, T. J., ABBENANTE, G., TYNDALL, J. D., HALLIDAY, J. & LEWIS, R. J. 2003. Isolation and characterization of a cone snail protease with homology to CRISP proteins of the pathogenesis-related protein superfamily. *The Journal of Biological Chemistry,* 278**,** 31105-10.

MOCHCA-MORALES, J., MARTIN, B. M. & POSSANI, L. D. 1990. Isolation and characterization of Helothermine, a novel toxin from *Heloderma horridum horridum* (Mexican beaded lizard) venom. *Toxicon,* 28**,** 299-309.

MONTECUCCO, C., GUTIERREZ, J. M. & LOMONTE, B. 2008. Review: Cellular pathology induced by snake venom phospholipase A_2 myotoxins and neurotoxins: common aspects of their mechanisms of action. *Cellular and Molecular Life Sciences,* 65**,** 2897-2912.

MORITA, T. 2005. Structures and functions of snake venom CLPs (C-type lectin-like proteins) with anticoagulant-, procoagulant-, and platelet-modulating activities. *Toxicon,* 45**,** 1099-1114.

MORITA, T., NIWATA, Y., OHGI, K., OGAWA, M. & IRIE, M. 1986. Distribution of Two Urinary Ribonuclease-Like Enzymes in Human Organs and Body Fluids. *The Journal of Biochemistry,* 99**,** 17-25.

MOTT, R. 1997. EST_GENOME: a program to align spliced DNA sequences to unspliced genomic DNA. *Computer Applications in the Biosciences (CABIOS),* 13**,** 477-478.

NAWARAK, J., SINCHAIKUL, S., WU, C.-Y., LIAU, M.-Y., PHUTRAKUL, S. & CHEN, S.-T. 2003. Proteomics of snake venoms from Elapidae and Viperidae families by multidimensional chromatographic methods. *Electrophoresis,* 24**,** 2838-2854.

NCBI. 2012a. *BLAST (Basic Local Alignment Search Tool)* [Online]. Available: http://blast.ncbi.nlm.nih.gov/Blast.cgi [Accessed 15 February 2012].

NCBI. 2012b. *ORF Finder (Open Reading Frame Finder)* [Online]. Available: http://www.ncbi.nlm.nih.gov/gorf/gorf.html [Accessed 15 February 2012].

NCBI. 2012c. *Wise2 - Intelligent algorithms for DNA searches* [Online]. Available: http://www.ebi.ac.uk/Tools/Wise2/index.html [Accessed 12 March 2012].

NEI, M., GU, X. & SITNIKOVA, T. 1997. Evolution by the birth-and-death process in multigene families of the vertebrate immune system. *Proceedings of the National Academy of Sciences,* 94**,** 7799-7806.

NEIVA, M., ARRAES, F. B. M., DE SOUZA, J. V., RÁDIS-BAPTISTA, G., PRIETO DA SILVA, Á. R. B., WALTER, M. E. M. T., BRIGIDO, M. D. M., YAMANE, T., LÓPEZ-LOZANO, J. L. & ASTOLFI-FILHO, S. 2009. Transcriptome analysis of the Amazonian viper *Bothrops atrox* venom gland using expressed sequence tags (ESTs). *Toxicon,* 53**,** 427-436.

NESTERENKO, M., TILLEY, M. & UPTON, S. 1994. A simple modification of Blum's silver stain method allows for 30 minute detection of proteins in polyacrylamide gels. *Journal of Biochemistry and Biophysics Methods,* 28**,** 239-242.

NOBILE, M., MAGNELLI, V., LAGOSTENA, L., MOCHCA-MORALES, J., POSSANI, L. D. & PRESTIPINO, G. 1994. The toxin helothermine affects potassium currents in newborn rat cerebellar granule cells. *Journal of Membrane Biology,* 139**,** 49-55.

NOBILE, M., NOCETI, F., PRESTIPINO, G. & POSSANI, L. D. 1996. Helothermine, a lizard venom toxin, inhibits calcium current in cerebellar granules. *Experimental Brain Research,* 110**,** 15-20.

O'SHEA, M. 2005. Venomous Snake Diversity and Distribution. *In:* JUDET, C. (ed.) *Venomous Snakes of the World.* New Holland Publishers.

ODELL, G., FERRY, P., VICK, L., FENTON, A., DECKER, L., COWELL, R., OWNBY, C. & GUTIERREZ, J. 1998. Citrate inhibition of snake venom proteases. *Toxicon,* 36**,** 1801-1806.

OGAWA, T., CHIJIWA, T., ODA-UEDA, N. & OHNO, M. 2005. Molecular diversity and accelerated evolution of C-type lectin-like proteins from snake venom. *Toxicon,* 45**,** 1-14.

OHBAYASHI, T., SCHMIDT, E. E., MAKINO, Y., KISHIMOTO, T., NABESHIMA, Y.-I., MURAMATSU, M. & TAMURA, T.-A. 1996. Promoter Structure of the Mouse TATA-Binding Protein (TBP) Gene. *Biochemical and Biophysical Research Communications,* 225**,** 275-280.

OLIVERA, B., IMPERIAL, J. & BULAJ, G. 2002. Cone snails and conotoxins: evolving sophisticated neuropharmacology. *In:* MENEZ, A. (ed.) *Perspectives in Molecular Toxinology.* John Wiley and Sons Ltd.

OLSSON, A.-K., DIMBERG, A., KREUGER, J. & CLAESSON-WELSH, L. 2006. VEGF receptor signalling? in control of vascular function. *Nat Rev Mol Cell Biol,* 7**,** 359-371.

ORON, U. & BDOLAH, A. 1973. Regulation of Protein Synthesis in the Venom Gland of Viperid Snakes. *The Journal of Cell Biology,* 56**,** 177-190.

ORON, U. & BDOLAH, A. 1978. Intracellular Transport of Proteins in Active and Resting Secretory Cells of the Venom gland of *Vipera Palaestinae*. *The Journal of Cell Biology***,** 488-502.

ORON, U., KINAMON, S. & BDOLAH, A. 1978. Asynchrony in the Synthesis of Secretory Proteins in the Venom Gland of the Snake *Vipera palaestinae*. *Journal of Biochemistry,* 174**,** 733-739.

OUYANG, C. & HUANG, T.-F. 1983. Inhibition of platelet aggregation by 5′-nucleotidase purified from *Trimeresurus gramineus* snake venom. *Toxicon,* 21**,** 491-501.

OUYANG, C. & HUANG, T.-F. 1986. Platelet aggregation inhibitors from *Agkistrodon acutus* snake venom. *Toxicon,* 24**,** 1099-1106.

PAHARI, S., MACKESSY, S. & KINI, R. M. 2007. The venom gland transcriptome of the Desert Massasauga Rattlesnake (*Sistrurus catenatus edwardsii*): towards an understanding of venom composition among advanced snakes (Superfamily Colubroidea). *Bmc Molecular Biology,* 8**,** 115.

PAINE, M., DESMOND, H., THEAKSTON, R. & CRAMPTON, J. 1992. Gene expression in *Echis carinatus* (Carpet Viper) venom glands following milking. *Toxicon,* 30**,** 379-386.

PALANISAMY, V., SHARMA, S., DESHPANDE, A., ZHOU, H., GIMZEWSKI, J. & WONG, D. T. 2010. Nanostructural and Transcriptomic Analyses of Human Saliva Derived Exosomes. *Plos One,* 5**,** e8577.

PARK, N. J., LI, Y., YU, T., BRINKMAN, B. M. N. & WONG, D. T. 2006. Characterization of RNA in Saliva. *Clinical Chemistry,* 52**,** 988-994.

PAWLAK, J. & KINI, R. M. 2008. Unique gene organization of colubrid three-finger toxins: Complete cDNA and gene sequences of denmotoxin, a bird-specific toxin from colubrid snake *Boiga dendrophila* (Mangrove Catsnake). *Biochimie,* 90**,** 868-877.

PEDERSEN, A. G., BALDI, P., CHAUVIN, Y. & BRUNAK, S. 1999. The biology of eukaryotic promoter prediction—a review. *Computers & Chemistry*, 23**,** 191-207.

PENG, M., LU, W., BEVIGLIA, L., NIEWIAROWSKI, S. & KIRBY, E. P. 1993. Echicetin: a snake venom protein that inhibits binding of von Willebrand factor and alboaggregins to platelet glycoprotein Ib. *Blood,* 81**,** 2321-2328.

PERKINS, D. N., PAPPIN, D. J. C., CREASY, D. M. & COTTRELL, J. S. 1999. Probability-based protein identification by searching sequence databases using mass spectrometry data. *Electrophoresis*, 20**,** 3551-3567.

PFAFFL, M. 2001. A new mathematical model for relative quantification in real-time RT-PCR. *Nucleic Acids Research,* 29**,** 2002-2007.

PIMENTA, D. C., PREZOTO, B. C., KONNO, K., MELO, R. L., FURTADO, M. F., CAMARGO, A. C. M. & SERRANO, S. M. T. 2007. Mass spectrometric analysis of the individual variability of *Bothrops jararaca* venom peptide fraction. Evidence for sex-based variation among the bradykinin-potentiating peptides. *Rapid Communications in Mass Spectrometry* 21**,** 1034–1042.

PIRKLE, H. 1998. Thrombin-like Enzymes from Snake Venoms: An Updated Inventory. *Thrombosis and Haemostasis*, 79**,** 675-683.

POLGÁR, J., CLEMETSON, J. M., KEHREL, B. E., WIEDEMANN, M., MAGNENAT, E. M., WELLS, T. N. C. & CLEMETSON, K. J. 1997. Platelet Activation and Signal Transduction by Convulxin, a C-type Lectin from

Crotalus durissus terrificus (Tropical Rattlesnake) Venom via the p62/GPVI Collagen Receptor. *Journal of Biological Chemistry,* 272**,** 13576-13583.

POLGÁR, J., MAGNENAT, E. M., PEITSCH, M. C., WELLS, T. N. & CLEMETSON, K. J. 1996. Asp-49 is not an absolute prerequisite for the enzymic activity of low-Mr phospholipases A2: Purification, characterization and computer modelling of an enzymically active Ser-49 phospholipase A2, ecarpholin S, from the venom of *Echis carinatus sochureki* (saw-scaled viper). *J Biochem,* 319**,** 961-968.

PONNUDURAI, G., CHUNG, M. C. M. & TAN, N. H. 1994. Purification and Properties of the L-Amino Acid Oxidase from Malayan Pit Viper (*Calloselasma rhodostoma*) Venom. *Archives of Biochemistry and Biophysics,* 313**,** 373-378.

POOK, C. E. & MCEWING, R. 2005. Mitochondrial DNA sequences from dried snake venom: a DNA barcoding approach to the identification of venom samples. *Toxicon,* 46**,** 711-715.

PUKRITTAYAKAMEE, S., WARRELL, D. A., DESAKORN, V., MCMICHAEL, A. J., WHITE, N. J. & BUNNAG, D. 1988. The hyaluronidase activities of some Southeast Asian snake venoms. *Toxicon,* 26**,** 629-637.

RAMKUMAR, V., STILES, G. L., BEAVEN, M. A. & ALI, H. 1993. The A3 adenosine receptor is the unique adenosine receptor which facilitates release of allergic mediators in mast cells. *Journal of Biological Chemistry,* 268**,** 16887-90.

READ, M., SMITH, S., LAMB, M. & BRINKHOUS, K. 1989. Role of botrocetin in platelet agglutination: formation of an activated complex of botrocetin and von Willebrand factor. *Blood,* 74**,** 1031-1035.

REID, H. A. & THEAKSTON, R. D. G. 1978. Changes in coagulation effects by venoms of *Crotalus atrox* as snakes age. *American Journal of Tropical Medicine and Hygiene,* 27**,** 1053-1057.

REZA, M. A., SWARUP, S. & KINI, R. M. 2007. Structure of two genes encoding parallel prothrombin activators in *Tropidechis carinatus* snake: gene duplication and recruitment of factor X gene to the venom gland. *Journal of Thrombosis and Haemostasis,* 5**,** 117-126.

RISHI, A. S., NELSON, N. D. & GOYAL, A. 2004. Genome walking of large fragments: an improved method. *Journal of Biotechnology,* 111**,** 9-15.

ROSS, J. 1995. mRNA stability in mammalian cells. *Microbiol Rev,* 59**,** 423-50.

RUCAVADO, A., NUNEZ, J. & GUTIERREZ, J. M. 1998. Blister formation and skin damage induced by BaP1, a haemorrhagic metalloproteinase from the venom of the snake *Bothrops asper*. *International Journal of Experimental Pathology,* 79**,** 245-254.

SACHS, A. 1993. Messenger RNA degradation in eukaryotes. *Cell,* 74**,** 413-21.

SAINI, K. S., SUMMERHAYES, I. C. & THOMAS, P. 1990. Molecular events regulating messenger RNA stability in eukaryotes. *Molecular and Cellular Biochemistry,* 96**,** 15-23.

SAITOH, M., NAGAI, K., NAKAGAWA, K., YAMAMURA, T., YAMAMOTO, S. & NISHIZAKI, T. 2004. Adenosine induces apoptosis in the human gastric cancer cells via an intrinsic pathway relevant to activation of AMP-activated protein kinase. *Biochemical Pharmacology,* 67**,** 2005-2011.

SAKURAI, Y., FUJIMURA, Y., KOKUBO, T., IMAMURA, K., KAWASAKI, T., HANDA, M., SUZUKI, M., MATSUI, T., TITANI, K. & YOSHIOKA, A. 1998. The cDNA Cloning and Molecular Characterization of a Snake Venom

Platelet Glycoprotein Ib-binding Protein, Mamushigin, from *Agkistrodon halys blomhoffii* Venom. *Thromb Haemost,* 79**,** 1199-1207.

SALDARRIAGA, M. M., OTEROA, R., NUNEZ, V., TOROA, M. F., DıAZ, A. & GUTIERREZ, J. M. 2003. Ontogenetic variability of *Bothrops atrox* and *Bothrops asper* snake venoms from Colombia. *Toxicon,* 42**,** 405-411.

SALES, P. B. V. & SANTORO, M. L. 2008. Nucleotidase and DNase activities in Brazilian snake venoms. *Comparative Biochemistry and Physiology Part C: Toxicology & Pharmacology,* 147**,** 85-95.

SANZ, L., ESCOLANO, J., FERRETTI, M., BISCOGLIO, M. J., RIVERA, E., CRESCENTI, E. J., ANGULO, Y., LOMONTE, B., GUTIÉRREZ, J. M. & CALVETE, J. J. 2008. Snake venomics of the South and Central American Bushmasters. Comparison of the toxin composition of *Lachesis muta* gathered from proteomic versus transcriptomic analysis. *Journal of Proteomics,* 71**,** 46-60.

SANZ, L., GIBBS, H. L., MACKESSY, S. P. & CALVETE, J. 2006. Venom Proteomes of Closely Related *Sistrurus* Rattlesnakes with Divergent Diets. *Journal of Proteome Research,* 5**,** 2098-2112.

SANZ, L., HARRISON, R. A. & CALVETE, J. J. 2012. First draft of the genomic organization of a PIII-SVMP gene. *Toxicon,* 60**,** 455-469.

SCOTT, D., WHITE, S., OTWINOWSKI, Z., YUAN, W., GELB, M. & SIGLER, P. 1990. Interfacial catalysis: the mechanism of phospholipase A2. *Science,* 250**,** 1541-1546.

SEGURA, Á., VILLALTA, M., HERRERA, M., LEÓN, G., HARRISON, R., DURFA, N., NASIDI, A., CALVETE, J. J., THEAKSTON, R. D. G., WARRELL, D. A. & GUTIÉRREZ, J. M. 2010. Preclinical assessment of the

efficacy of a new antivenom (EchiTAb-Plus-ICP®) for the treatment of viper envenoming in sub-Saharan Africa. *Toxicon,* 55**,** 369-374.

SEKIYA, F., ATODA, H. & MORITA, T. 1993. Isolation and characterization of an anticoagulant protein homologous to botrocetin from the venom of *Bothrops jararaca*. *Biochemistry,* 32**,** 6892-6897.

SERRANO, S. M. T., SHANNON, J. D., WANG, D., CAMARGO, A. C. M. & FOX, J. W. 2005. A multifaceted analysis of viperid snake venoms by two-dimensional gel electrophoresis: An approach to understanding venom proteomics. *Proteomics,* 5**,** 501-510.

SHEBUSKI, R. J., RAMJIT, D. R., BENCEN, G. H. & POLOKOFF, M. A. 1989. Characterisation and platelet inhibitory activity of Bitistatin, a potent arginine-glycine-aspartic acid-containing peptide from the venom of the viper *Bitis arietans*. *The Journal of Biological Chemistry,* 264**,** 21550-21556.

SHEINESS, D., PUCKETT, L. & DARNELL, J. E. 1975. Possible relationship of poly(A) shortening to mRNA turnover. *Proc Natl Acad Sci U S A,* 72**,** 1077-1081.

SHIN, Y. & MORITA, T. 1998. Rhodocytin, a Functional Novel Platelet Agonist Belonging to the Heterodimeric C-Type Lectin Family, Induces Platelet Aggregation Independently of Glycoprotein Ib. *Biochemical and Biophysical Research Communications,* 245**,** 741-745.

SHYU, A. B., GREENBERG, M. E. & BELASCO, J. G. 1989. The c-fos transcript is targeted for rapid decay by two distinct mRNA degradation pathways. *Genes Dev,* 3**,** 60-72.

SIANG, A., DOLEY, R., VONK, F. & KINI, R. M. 2010. Transcriptomic analysis of the venom gland of the red-headed krait (*Bungarus flaviceps*) using expressed sequence tags. *Bmc Molecular Biology,* 11**,** 24.

SIEBERT, P. D., CHENCHIK, A., KELLOGG, D. E., LUKYANOV, K. A. & LUKYANOV, S. A. 1995. An improved PCR method for walking in uncloned genomic DNA. *Nucleic Acids Research,* 23**,** 1087-1088.

SIIGUR, E., AASPÕLLU, A. & SIIGUR, J. 1999. Molecular Cloning and Sequence Analysis of a cDNA for Factor V Activating Enzyme, a Coagulant Protein from *Vipera lebetina* Snake Venom. *Biochemical and Biophysical Research Communications,* 262**,** 328-332.

SIIGUR, E., NEUMAN, T., JÄRVE, V., TARA, A. & SIIGUR, J. 1985. Isolation and characterization of nerve growth factor from *Vipera lebetina* (snake) venom. *Comp Biochem Physiol B Biochem,* 81**,** 211-215.

SIIGUR, J., ARUMÄE, U., NEUMAN, T., SAMEL, M., SIIGUR, E. & SAARMA, M. 1986. Isolation and characterization of nerve growth factor from *Vipera berus* (common viper) venom. *Comparative Biochemistry and Physiology Part B: Comparative Biochemistry,* 83**,** 621-625.

SIIGUR, J., ARUMÄE, U., NEUMAN, T., SIIGUR, E. & SAARMA, M. 1987. Monoclonal antibody immunoaffinity chromatography of the nerve growth factor from snake venoms. *Comparative Biochemistry and Physiology Part B: Comparative Biochemistry,* 87**,** 329-334.

SINGH, V. K. & KUMAR, A. 2001. PCR Primer Design. *Molecular Biology Today,* 2**,** 27-32.

SMITH, L. A., LAFAYE, P. J., LAPENOTIERE, H. F., SPAIN, T. & DOLLY, J. O. 1993. Cloning and functional expression of dendrotoxin K from black mamba, a potassium channel blocker. *Biochemistry,* 32**,** 5692-5697.

SOBOL BROWN, R., BROWN, M., BDOLAH, A. & KOCHVA, E. 1975. Accumulation of some secretory enzymes in venom glands of *Vipera palaestinae*. *American Journal of Physiology,* 229**,** 1675-1679.

SOUSA, J., MONTEIRO, R., CASTRO, H. & ZINGALI, R. 2001. Proteolytic action of *Bothrops jararaca* venom upon its own constituents. *Toxicon,* 39**,** 787-792.

STÁBELI, R. G., MARCUSSI, S., CARLOS, G. B., PIETRO, R. C. L. R., SELISTRE-DE-ARAÚJO, H. S., GIGLIO, J. R., OLIVEIRA, E. B. & SOARES, A. M. 2004. Platelet aggregation and antibacterial effects of an l-amino acid oxidase purified from *Bothrops alternatus* snake venom. *Bioorganic & Medicinal Chemistry,* 12**,** 2881-2886.

STERN, R. & JEDRZEJAS, M. J. 2006. Hyaluronidases: Their Genomics, Structures, Mechanisms of Action. *Chemical Reviews,* 106**,** 818-839.

STILES, B. G., SEXTON, F. W. & WEINSTEIN, S. A. 1991. Antibacterial effects of different snake venoms: Purification and characterization of antibacterial proteins from *Pseudechis australis* (Australian king brown or mulga snake) venom. *Toxicon,* 29**,** 1129-1141.

TAKAHASHI, H., HATTORI, S., IWAMATSU, A., TAKIZAWA, H. & SHIBUYA, M. 2004. A Novel Snake Venom Vascular Endothelial Growth Factor (VEGF) Predominantly Induces Vascular Permeability through Preferential Signaling via VEGF Receptor-1. *Journal of Biological Chemistry,* 279**,** 46304-46314.

TAKATSUKA, H., SAKURAI, Y., YOSHIOKA, A., KOKUBO, T., USAMI, Y., SUZUKI, M., MATSUI, T., TITANI, K., YAGI, H., MATSUMOTO, M. & FUJIMURA, Y. 2001. Molecular characterization of l-amino acid oxidase from *Agkistrodon halys blomhoffii* with special reference to platelet aggregation. *Biochimica et Biophysica Acta (BBA) - Protein Structure and Molecular Enzymology*, 1544**,** 267-277.

TAKEDA, S., TAKEYA, H. & IWANAGA, S. 2012. Snake venom metalloproteinases: Structure, function and relevance to the mammalian ADAM/ADAMTS family proteins. *Biochimica et Biophysica Acta (BBA) - Proteins and Proteomics*, 1824**,** 164-176.

TAN, N.-H. & SWAMINATHAN, S. 1992. Purification and properties of the l-amino acid oxidase from monocellate cobra (*Naja naja kaouthia*) venom. *International Journal of Biochemistry*, 24**,** 967-973.

TAN, N. H. & SAIFUDDIN, M. N. 1989. Isolation and characterization of an unusual form of L-amino acid oxidase from King cobra (*Ophiophagus hannah*) venom. *Biochemistry International*, 19**,** 937-944.

TANAKA, Y., YOSHIHARA, K., TSUYUKI, M. & KAMIYA, T. 1994. Apoptosis Induced by Adenosine in Human Leukemia HL-60 Cells. *Experimental Cell Research*, 213**,** 242-252.

TAYLOR, D., IDDON, D., SELLS, P., SEMOFF, S. & THEAKSTON, R. D. G. 1986. An Investigation of Venom Secretion by the Venom Glands Cells of the Carpet Viper (*Echis carinatus*). *Toxicon*, 24**,** 651-659.

THEAKSTON, R. D. & REID, H. A. 1983. Development of simple standard assay procedures for the characterization of snake venoms. *Bulletin of the World Health Organisation*, 61**,** 949-956.

TOUGU, V. 2001. Acetylcholinesterase: Mechanism of Catalysis and Inhibition. *Current Medicinal Chemistry -Central Nervous System Agents,* 1**,** 155-170.

TSAI, I.-H., WANG, Y.-M., CHEN, Y.-H., TSAI, T.-S. & TU, M.-C. 2004. Venom phospholipases A2 of bamboo viper (*Trimeresurus stejnegeri*): molecular characterization, geographic variations and evidence of multiple ancestries. *J Biochem,* 377**,** 215-223.

VANDESOMPELE, J., DE PRETER, K., PATTYN, F., POPPE, B., VAN ROY, N., DE PAEPE, A. & SPELEMAN, F. 2002. Accurate normalization of real-time quantitative RT-PCR data by geometric averaging of multiple internal control genes. *Genome Biology,* 3**,** 0034.1–0034.11.

VASILENKO, S. K. & RYTE, V. C. 1975. Isolation of highly purified ribonuclease from cobra (*Naja oxiana*) venom. *Biokhimiia,* 40**,** 578-583.

VENTERS, B. J. & PUGH, B. F. 2009. How eukaryotic genes are transcribed. *Crit Rev Biochem Mol Biol,* 44**,** 117-141.

VIDAL, N., DELMAS, A.-S., DAVID, P., CRUAUD, C., COULOUX, A. & HEDGES, S. B. 2007. The phylogeny and classification of caenophidian snakes inferred from seven nuclear protein-coding genes. *Comptes Rendus Biologies,* 330**,** 182-187.

VILJOEN, C. & BOTES, D. 1979. Influence of pH on the kinetic and spectral properties of phospholipase A_2 from *Bitis gabonica* (Gaboon Adder) snake venom. *Toxicon,* 17**,** 77-87.

WAGSTAFF, S., FAVREAU, P., CHENEVAL, O., LAING, G., WILKINSON, M., MILLER, R., STOCKLIN, R. & HARRISON, R. 2008. Molecular characterisation of endogenous snake venom metalloproteinase inhibitors. *Biochemical and Biophysical Research Communications,* 365**,** 650–656.

WAGSTAFF, S. & HARRISON, R. 2006. Venom gland EST analysis of the saw-scaled viper, *Echis ocellatus*, reveals novel α9β1 integrin-binding motifs in venom metalloproteinases and a new group of putative toxins, renin-like aspartic proteases. *Gene,* 377**,** 21-32.

WAGSTAFF, S. C., LAING, G. D., THEAKSTON, R. D. G., PAPASPYRIDIS, C. & HARRISON, R. A. 2006. Bioinformatics and Multiepitope DNA Immunization to Design Rational Snake Antivenom. *PLoS Med,* 3**,** e184.

WAGSTAFF, S. C., SANZ, L., JUÁREZ, P., HARRISON, R. A. & CALVETE, J. 2009. Combined snake venomics and venom gland transcriptomic analysis of the ocellated carpet viper, *Echis ocellatus*. *Journal of Proteomics,* 71**,** 609-623.

WALKER, B. A., JACOBSON, M. A., KNIGHT, D. A., SALVATORE, C. A., WEIR, T., ZHOU, D. & BAI, T. R. 1997. Adenosine A3 receptor expression and function in eosinophils. *American journal of respiratory cell and molecular biology,* 16**,** 531-7.

WANG, J., SHEN, B., GUO, M., LOU, X., DUAN, Y., CHENG, X. P., TENG, M., NIU, L., LIU, Q., HUANG, Q. & HAO, Q. 2005. Blocking Effect and Crystal Structure of Natrin Toxin, a Cysteine-Rich Secretory Protein from *Naja atra* Venom that Targets the BKCa Channel. *Biochemistry,* 44**,** 10145-10152.

WANG, Y., LIU, C. L., STOREY, J. D., TIBSHIRANI, R. J., HERSCHLAG, D. & BROWN, P. O. 2002. Precision and functional specificity in mRNA decay. *Proc Natl Acad Sci U S A,* 99**,** 5860-5.

WARRELL, D. A. 2010. Snake bite. *The Lancet,* 375**,** 77-88.

WARRELL, D. A., ORMEROD, L. D. & DAVIDSON, N. M. 1975. Bites by Puff Adder (*Bitis arietans*) in Nigeria, and value of antivenom. *British Medical Journal*, 4**,** 697-700.

WEINSTEIN, S. A., SMITH, T. L. & KARDONG, K. V. 2010. Reptile Venom Glands. *In:* MACKESSY, S. P. (ed.) *Handbook of Venom and Toxins of Reptiles.* Taylor and Francis Group, LLC.

WEIS, W. I., TAYLOR, M. E. & DRICKAMER, K. 1998. The C-type lectin superfamily in the immune system. *Immunological Reviews,* 163**,** 19-34.

WHITTINGTON, C. M., KOH, J. M. S., WARREN, W. C., PAPENFUSS, A. T., TORRES, A. M., KUCHEL, P. W. & BELOV, K. 2009. Understanding and utilising mammalian venom via a platypus venom transcriptome. *Journal of Proteomics,* 72**,** 155-164.

WILLIAMS, D., GUTIÉRREZ, J. M., HARRISON, R., WARRELL, D. A., WHITE, J., WINKEL, K. D. & GOPALAKRISHNAKONE, P. 2010. The Global Snake Bite Initiative: an antidote for snake bite. *The Lancet,* 375**,** 89-91.

WILLIAMS, D. J., GUTIÉRREZ, J.-M., CALVETE, J. J., WÜSTER, W., RATANABANANGKOON, K., PAIVA, O., BROWN, N. I., CASEWELL, N. R., HARRISON, R. A., ROWLEY, P. D., O'SHEA, M., JENSEN, S. D., WINKEL, K. D. & WARRELL, D. A. 2011. Ending the drought: New strategies for improving the flow of affordable, effective antivenoms in Asia and Africa. *Journal of Proteomics,* 74**,** 1735-1767.

WINKSY, L. & HARVEY, J. A. 1986. Retardation of associative learning in the rabbit by an adenosine analog as measured by classical conditioning of the nictitating membrane response. *Journal of Neuroscience,* 9**,** 2684-2690.

XU, X., WANG, X., XI, X., LIU, J., HUANG, J. & LU, Z. 1982. Purification and partial characterization of hyaluronidase from five pace snake (*Agkistrodon acutus*) venom. *Toxicon,* 20**,** 973-981.

YAMAZAKI, Y., BROWN, R. L. & MORITA, T. 2002a. Purification and Cloning of Toxins from Elapid Venoms that Target Cyclic Nucleotide-Gated Ion Channels. *Biochemistry,* 41**,** 11331-11337.

YAMAZAKI, Y., KOIKE, H., SUGIYAMA, Y., MOTOYOSHI, K., WADA, T., HISHINUMA, S., MITA, M. & MORITA, T. 2002b. Cloning and characterization of novel snake venom proteins that block smooth muscle contraction. *European Journal of Biochemistry,* 269**,** 2708-2715.

YAMAZAKI, Y., MATSUNAGA, Y., NAKANO, Y. & MORITA, T. 2005. Identification of Vascular Endothelial Growth Factor Receptor-binding Protein in the Venom of Eastern Cottonmouth. *Journal of Biological Chemistry,* 280**,** 29989-29992.

YAMAZAKI, Y., MATSUNAGA, Y., TOKUNAGA, Y., OBAYASHI, S., SAITO, M. & MORITA, T. 2009. Snake Venom Vascular Endothelial Growth Factors (VEGF-Fs) Exclusively Vary Their Structures and Functions among Species. *The Journal of Biological Chemistry,* 284**,** 9885–9891.

YAMAZAKI, Y. & MORITA, T. 2004. Structure and function of snake venom cysteine-rich secretory proteins. *Toxicon,* 44**,** 227-231.

YAMAZAKI, Y. & MORITA, T. 2006. Molecular and functional diversity of vascular endothelial growth factors. *Molecular Diversity,* 10**,** 515-527.

YATES, J., ENG, J., CLAUSER, K. & BURLINGAME, A. 1996. Search of sequence databases with uninterpreted high-energy collision-induced dissociation spectra of peptides. *Journal of The American Society for Mass Spectrometry,* 7**,** 1089-1098.

YINGPRASERTCHAI, S., BUNYASRISAWAT, S. & RATANABANANGKOON, K. 2003. Hyaluronidase inhibitors (sodium cromoglycate and sodium auro-

thiomalate) reduce the local tissue damage and prolong the survival time of mice injected with *Naja kaouthia* and *Calloselasma rhodostoma* venoms. *Toxicon,* 42**,** 635-646.

ZELANIS, A., DE SOUZA VENTURA, J., CHUDZINSKI-TAVASSI, A. M. & DE FATIMA DOMINGUES FURTADO, M. 2007. Variability in expression of *Bothrops insularis* snake venom proteases: an ontogenetic approach. *Comparative biochemistry and physiology. Toxicology & pharmacology : CBP,* 145**,** 601-9.

ZHANG, B., LIU, Q., YIN, W., ZHANG, X., HUANG, Y., LUO, Y., QIU, P., SU, X., YU, J., HU, S. & YAN, G. 2006. Transcriptome analysis of *Deinagkistrodon acutus* venomous gland focusing on cellular structure and functional aspects using expressed sequence tags. *Bmc Genomics,* 7**,** 152.

ZHANG, C. & GOPALAKRISHNAKONE, P. 1999. Histopathological studies of the acute inflammation in synovial tissue of rat knee joint following intra-articular injection of PLA_2 from Chinese Cobra (*Naja naja atra*) venom. *Toxicon,* 37**,** 783-799.

ZULIANI, J. P., GUTIERREZ, J. M., SILVA, L., S.C., S., LOMONTE, B. & TEIXEIRA, C. 2005. Activation of cellular functions in macrophages by venom secretory Asp-49 and Lys-49 phospholipases A_2. *Toxicon,* 46**,** 523-532.

ŽUPUNSKI, V., KORDIŠ, D. & GUBENŠEK, F. 2003. Adaptive evolution in the snake venom Kunitz/BPTI protein family. *FEBS Letters,* 547**,** 131-136.